Circadian Orchestration of the Cellular Proteome

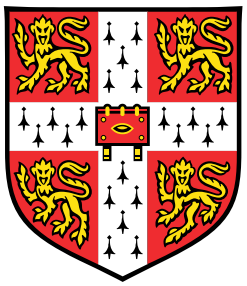

David Chuen Soong Wong

MRC Laboratory of Molecular Biology
University of Cambridge

This dissertation is submitted for the degree of
Doctor of Philosophy

Trinity College

November 2019

I dedicate this thesis to my parents, who have tirelessly supported me every step of the way.

Declaration

I hereby declare that this thesis is the result of my own work and includes nothing which is the outcome of work done in collaboration except as declared in the Acknowledgements and specified in the text.

It is not substantially the same as any that I have submitted, or, is being concurrently submitted for a degree or diploma or other qualification at the University of Cambridge or any other University or similar institution except as declared in the Acknowledgements and specified in the text. I further state that no substantial part of my dissertation has already been submitted, or, is being concurrently submitted for any such degree, diploma or other qualification at the University of Cambridge or any other University or similar institution except as declared in the Acknowledgements and specified in the text

It does not exceed the prescribed word limit for the relevant Degree Committee.

David Chuen Soong Wong
November 2019

Acknowledgements

The incredible journey leading to this thesis would not have been possible without the efforts of many people. First and foremost I would like to thank my supervisor John O'Neill for his excellent guidance throughout my PhD and for curating the most amazing collaborative, discursive and fun environment in the lab every day. He is the most creative and resourceful scientist I have had the pleasure to meet and it has been an honour to work together.

I would like to thank all the current and past members of the lab for providing practical and moral support over the years. In particular Marrit Putker and Ned Hoyle taught me all that they know, and together they shaped my thinking and skillset as a scientist and as a cyclist. Marrit Putker and Estere Seinkmane did a huge amount of work which I built upon throughout my PhD, and Alessandra Stangherlin also worked closely together, particularly with the many mammoth time-course experiments that we did. Daniel Fernando also helped with a time-course experiment during his summer project. Thanks are also due to Andrew Beale, Priya Crosby, Nina Rzechorzek, Aiwei Zeng and Silvia Barbiero for their support, debates, fun lab retreats and great snacks.

I am very grateful for all the collaborations that were possible thanks to the unique LMB community. In particular, the core facilities have been instrumental in my work. My utmost thanks go to Sew Peak Chew, who worked tirelessly for weeks on end processing my mass-spectrometry samples, and also to Jason Day who performed ICP-MS for thousands of my samples. Biomedical services, Ares and the genotyping service have been incredible at taking care of our mouse colonies and helping me with my experiments; particular thanks to Claire Knox, Liam Bray, Martin Reed, Carolyn Perriment, Jo Chesham and Marisa Coetzee. Credit is also due to a huge number of people behind the scenes, and a non-exhaustive list includes glass-wash services for providing reagents and autoclaving, IT for technological support and development of exciting projects, electronics and workshop for making bespoke equipment for us, reception for their friendliness and sorting out a huge range of things for us, security for keeping us safe and providing company during the lonely hours of the early morning during time-course experiments, domestic services for keeping things clean, health and safety for keeping us healthy and safe, and of course the canteen for keeping me healthy and fed.

Thanks also to Tim Stevens for teaching me about machine learning, Python, and helping me with the kinase recognition motif analysis. On a similar note, Arun Prasad helped me

configure and use the D2P2 database for prediction of intrinsic disorder. I also acknowledge Marco Sciacovelli and Christian Frezza for training and helping me with Seahorse metabolic assays. Thanks also to Manu Derivery for collaboration and to Joe Watson for helping with the quantum dot experiments, numerous great chats and top notch performances in the cryptic pub quiz at The Mill.

The School of Clinical Medicine has of course enabled me to undertake my PhD, and I would like to thank the MB/PhD programme for setting up this opportunity. Particular thanks go to Lesley Flood, Rob Semple, Hannah Dennis and Stefan Marciniak for administrating the programme and providing excellent support and events. I would also like to thank the MRC Doctoral Training Programme, the Rouse Ball Fund and the Strauss Bursary for financial support.

My academic support network has also been invaluable to me in my PhD journey. I would like to thank Trinity College for providing me with a roof over my head for so many years as well as an incredible academic environment. Particular thanks go to the fellows including David Baulcombe, Andrew Crawford and Alan Weeds for the graduate biologist seminars and dinners, and to Rebecca Fitzgerald and Catherine Aiken for pastoral support on the medical side. Thanks also to my university supervisor James Locke and my second supervisor Manu Hegde who has listened and supported me since the very beginning, providing life and scientific advice. This thesis was compiled using LaTeX software, and thanks are due to Krishna Kumar for providing the PhD thesis template for all Cambridge students, and to Tim Beach who showed me how to work the software.

My most heartfelt thanks go to my family and friends who have been there for me every step of the way, through the hard times and the high times. Finally, special thanks to my parents Dorothy and Geoffrey for their tireless moral and culinary support, and to Olivia Knutson for her patience and understanding – I would not have been able to get to this point without them.

Abstract

Circadian rhythms are biological oscillations with a period length of roughly 24 hours. They confer an adaptive advantage as they enable the prediction of the regular environmental changes caused by the rotation of the Earth, and so they are highly conserved. Circadian coordination of biology is an important feature not only across kingdoms, but also at multiple levels of biological scale, from behaviour to physiology and cell biology. On the cellular level it is thought that mammalian circadian rhythms are driven by a delayed feedback loop, involving the transcription and translation of a core set of 'clock proteins'. This cellular timekeeping system is remarkably precise and robust to perturbations.

In the first chapter of this thesis I explored the mechanism of action of picrotoxin, a drug that shortens circadian period through unknown means. I uncovered features that are not readily explained by the canonical transcriptional-translational-feedback loop (TTFL) model of circadian rhythm generation. In the second part of this thesis I used mass spectrometry-based proteomics to characterise the cellular circadian proteome, and I uncovered the reciprocal, rhythmic regulation of protein and ion concentrations in cultured cells. Strikingly, by using a genetic knock-out of the CRYPTOCHROME (CRY) proteins I found that the generation of these rhythms was not dependent upon the TTFL, strongly supporting an alternative model of circadian rhythm generation – the post-translational oscillator (PTO) model. In the next chapter I explored the circadian regulation of the PERIOD 2 (PER2) protein in CRY-deficient cells, suggesting that a key determinant of PER2 behaviour in the absence of the TTFL may be cellular protein and ion concentrations. In the final chapter I investigated the functional consequences of CRY knock-out. I found that CRY-deficient cells and animals have disrupted proteostasis and metabolism, and found that impaired proteostasis attenuates circadian rhythmicity at the cellular and organism levels.

Altogether, the work presented in this thesis provides evidence for a PTO model of circadian rhythm generation. I have uncovered circadian regulation of the cellular proteome even in the absence of the canonical TTFL. I propose that rather than driving circadian rhythms, the TTFL confers robustness to cellular timekeeping and facilitates proteostasis.

Table of contents

List of figures

List of tables

Nomenclature

Acronyms / Abbreviations

ATP	Adenosine triphosphate
cAMP	Cyclic adenosine monophosphate
CCG	Clock-controlled gene
CK1	Casein kinase 1
CKO	CRY1/CRY2 double knockout
Cry	*Cryptochrome* gene
CRY	CRYPTOCHROME protein
DBP	D-box binding protein
DMSO	Dimethylsulfoxide
DNA	Deoxyribonucleic acid
eIF2α	Eukaryotic initiation factor 2 alpha
FRQ	FREQUENCY protein
GSK3	Glycogen synthase kinase 3
ICP-MS	Inductively coupled plasma mass spectrometry
IDP	Intrinsically disordered protein
IDR	Intrinsically disordered region
IMAC	Immobilised metal ion affinity chromatography
ISR	Integrated stress response
iTRAQ	Isobaric tag for relative and absolute quantitation
KCC1	Potassium-chloride cotransporter 1

LC-MS/MS	Liquid chromatography with tandem mass spectrometry
MOAC	Metal oxide affinity chromatography
NEM	N-ethylmaleimide
NKCC1	Sodium-potassium-chloride cotransporter 1
OSR1	Oxidative stress-responsive kinase 1
PER2::LUC	PER2::LUCIFERASE fusion protein
Per	*Period* gene
PER	PERIOD protein
PQC	Protein quality control
PTM	Post-translational modification
PTO	Post-translational oscillator
PTX	Picrotoxin
RNA	Ribonucleic acid
ROR	RAR-related orphan receptor
SCN	Suprachiasmatic nucleus of the hypothalamus
SILAC	Stable isotope labelling with amino acids in cell culture
TMT	Tandem mass tag
TRX	Thioredoxin
TTFL	Transcriptional-translational feedback loop
WNK1	With no lysine (K) kinase 1

Chapter 1

General introduction

1.1 Circadian rhythms

1.1.1 Definitions

The circadian field is extremely broad, from the study of bird migration [1] to the structural investigations of proteins in cyanobacteria [2]. Therefore there is a unique richness to the literature, involving many disciplines from mathematics to field biology to the clinic. Unfortunately, a result of this richness and cross-talk between levels of biological scale is that the use of language can be somewhat contradictory, confusing and convoluted. Clear expression of meaning is crucial for scientific endeavour, and so I will begin this thesis by setting out some definitions that carry for the rest of the work. These definitions are based on the context in which the terms are most commonly used, as well as canonical definitions set out by the forefathers of the circadian field, who used this language to describe their careful and ground-breaking observations almost 60 years ago [3–6].

The word "circadian" is rooted in the Latin words *circa* (roughly) and *dies* (day). Circadian rhythms are endogenous biological oscillations that have a period length of roughly 24 hours in constant environmental conditions. The period length is "temperature compensated". This means that period length is maintained roughly constant over a wide range of temperatures. Whereas most enzymatic reactions double with every 10°C increase in temperature (Q_{10} = 2-3) [7], circadian period length changes much less (Q_{10} = 0.8-1.4) [8]. This is a functional prerequisite of a useful clock, since they need to be precise despite changes in weather or climate [5]. Finally, they can be entrained to exogenous stimuli, i.e. environmental parameters that show 24h oscillations due to the rotation of the Earth – these environmental parameters are called "zeitgebers". These are the fundamental "Empirical Generalisations" that were set out by Pittendrigh based on the collection of careful observations and experimentation presented

at the Cold Spring Harbour Symposium of 1960 [4]. The term "circadian" first came into use around this time, and it was formally defined at this seminal meeting to facilitate understanding of myriad observations of endogenous biological rhythms that approximated 24 hours, and to guide subsequent research into them [4]. This definition of "circadian" is important because it is often used in error when describing experiments. If an experiment is conducted in the presence of a zeitgeber (e.g. light-dark cycles), then these conditions are referred to as "diurnal".

Key measurable parameters of oscillations are period length, phase and amplitude (Figure 1.1). Period length is the length of time taken to complete a full cycle of an oscillation. Amplitude is the difference between the peak and the mean value of the signal. Relative amplitude is the peak-to-trough difference, divided by the mean value of the signal. Damping is the rate of change of the amplitude over time. Phase is the progress of an oscillator through its cycle, and a phase shift refers to a displacement of this along the time axis, either delaying or advancing. Recordings of an oscillation are often detrended using a 24-hour moving average, thus removing the baseline and allowing these parameters to be measured more precisely, usually by non-linear regression (see Chapter 2 for more details).

An "oscillator" is a process that can generate rhythms. The period length of a circadian oscillator is roughly 24 hours, thus approximating the rotation of the Earth.

A "clock" is an oscillator that is self-sustaining and does not damp over time. Note that damping in cell culture experiments at the population level is caused by loss of synchrony between cells that individually do not damp [9]. I will use "circadian clock" to refer to the hypothetical minimum set of components that are necessary and sufficient to sustain a circadian rhythm.

A "clock gene" is a gene whose product is then translated to a protein (also referred to as "clock protein") that subsequently directly or indirectly feeds back to inhibit its own transcription in a rhythmic manner. The fidelity of circadian timekeeping is also regulated by the expression of the clock genes. Examples are *Bmal1*, *Per* and *Cry* genes.

"Entrainment" is the synchronisation of a clock to a zeitgeber – an extrinsic signal that itself oscillates with a 24-hour rhythm because of the rotation of the Earth (e.g. temperature cycles).

"Synchronisation" is the alignment of the phases of two or more oscillators. This is often synonymous with entrainment but can also be applied to one-off perturbations (as opposed to continually oscillating ones) that align the phases of multiple clocks (e.g. serum shock).

A "state variable" is a molecule whose abundance and/or post-translational modification state determines the phase of the cellular clock.

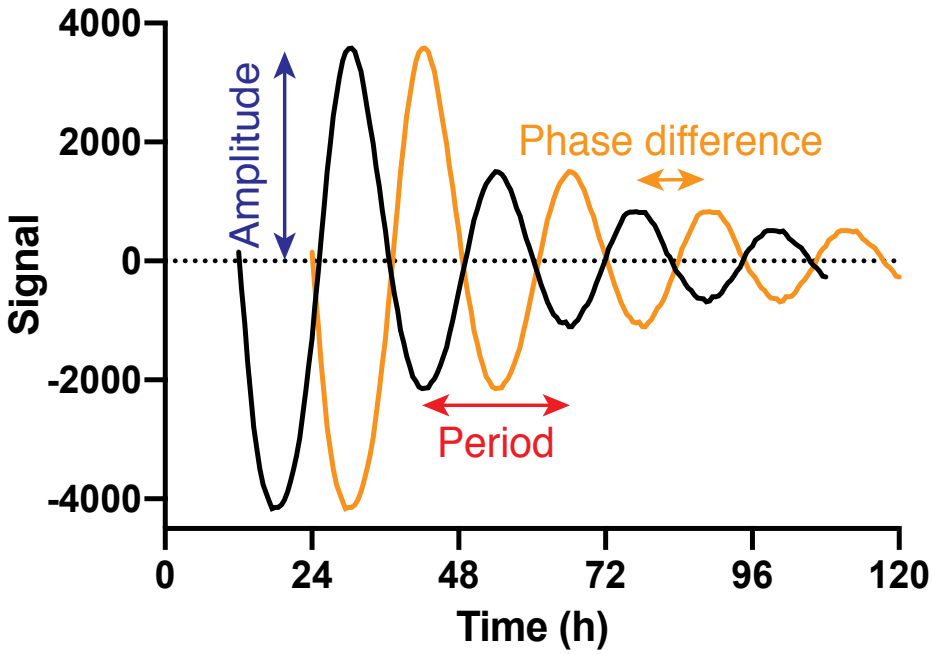

Figure 1.1 Features of Oscillations. Oscillations have measurable parameters. Amplitude is the deviation of the signal from the baseline. When amplitude changes over time, the rate of change is known as damping rate. Period length is the length of time taken to complete an oscillation. Phase refers to the stage of the cycle that the system is in at any particular point in time, and this is usually considered in the context of phase shifts or differences between datasets.

1.1.2 Circadian timekeeping at multiple levels of biological scale

Life may have existed on Earth over 3 billion years ago [10]. Throughout this time, organisms have had to find ways to adapt to an environment that changes due to the rotation of the Earth. This rotation causes daily variation in food availability, temperature and light. Endogenous timing mechanisms allow organisms to predict these changes and adapt their behaviour and physiology to the external cycles. This has been shown in bacteria, plants and mammals to confer evolutionary advantage over organisms that do not have this internal timekeeping [11–17].

The first recorded observation of a circadian rhythm was made in 1729 by Jean-Jacques de Mairan [5]: the daily opening and closing of the leaves of *Mimosa pudica*. De Mairan observed that this persisted in constant darkness, showing that this behaviour is endogenously controlled by a circadian timekeeping mechanism. Such rhythmicity has been observed at all levels of biological scale, from the macroscopic behaviour of flies and humans to the activity of single cells and even protein complexes. These oscillations are remarkable for their persistence and precision – rhythms in behaviour can persist for over 2 years in some rodents, and the standard deviation of the average period length of a mouse rhythm is around one minute [5].

In mammals, the suprachiasmatic nucleus (SCN) in the hypothalamus imparts circadian coordination upon behaviour, physiology and cellular function through neuronal and hormonal signalling [18–24]. However, since circadian regulation of cellular activity and gene expression

persist *ex vivo* in almost all mammalian cell types tested [25–28], it is clear that the fundamental unit of circadian timekeeping is the cell. An interesting exception is the mouse testis, where PER1 protein and mRNA (see the next section for details about PER) were not found to be rhythmic [29], although this does not rule out the presence of a circadian clock involving different molecular components.

1.1.3 Rhythmic gene expression is coordinated by transcription/translation feedback

Over 40% of protein-encoding genes are subject to circadian regulation in at least one tissue in healthy young wild-type adult mice [30], with a similar proportion of the human genome under diurnal regulation in healthy individuals [31]. Delayed transcriptional feedback repression of clock genes has been proposed to drive rhythmic gene expression in mammals as well as other eukaryotes; the clock gene circuitry behind these transcriptional-translational feedback loops (TTFLs) has been described for several model organisms [32–34]. The cycling of clock protein activity is the means by which cellular clocks organise most daily biological functions, and this is supported by the strong phenotypes of clock gene mutants [35].

In mammalian cells, CLOCK and BMAL1 are basic helix-loop-helix (bHLH) – PER-ARNT-SIM (PAS) transcription factors. CLOCK is semi-redundant with NPAS2, but recruitment of BMAL1-containing complexes to the promoter regions of *Period* and *Cryptochrome* genes is essential for their differential expression over the daily cycle (Figure 1.2). PER and CRY proteins mediate the negative limb of the feedback loop by forming large macromolecular complexes which bind and inhibit the transcriptional activity of BMAL1-containing complexes [36–39]. Thus transcription of many clock-controlled genes is repressed along with genomic loci for PER and CRY themselves [40, 41]. These activating and repressing complexes function together with enhancer elements in a tissue-specific manner to differentially recruit various histone and chromatin remodelling complexes, resulting in large-scale changes in chromatin accessibility and compaction [42, 40, 43, 34, 44]. This is the core TTFL in mammals, and the prevailing dogma in the field (I will refer to it as the "TTFL model") is that it is responsible for the generation of cellular circadian rhythms [34].

Given the dynamic regulation of chromatin structure by TTFL components as described above, it would be reasonable to suspect that there may be an interaction between the circadian clock and the cell cycle, which also involves a great deal of chromatin remodelling. These two cycles are indeed intertwined, and current competing theories posit that the circadian clock in mammals may 'gate' cell cycle progression such that specific checkpoints are more likely to proceed at certain times of day [45], or that there may be more complex coupling between the cell cycle and the TTFL [46]. However, little is known about the molecular mechanisms linking these processes.

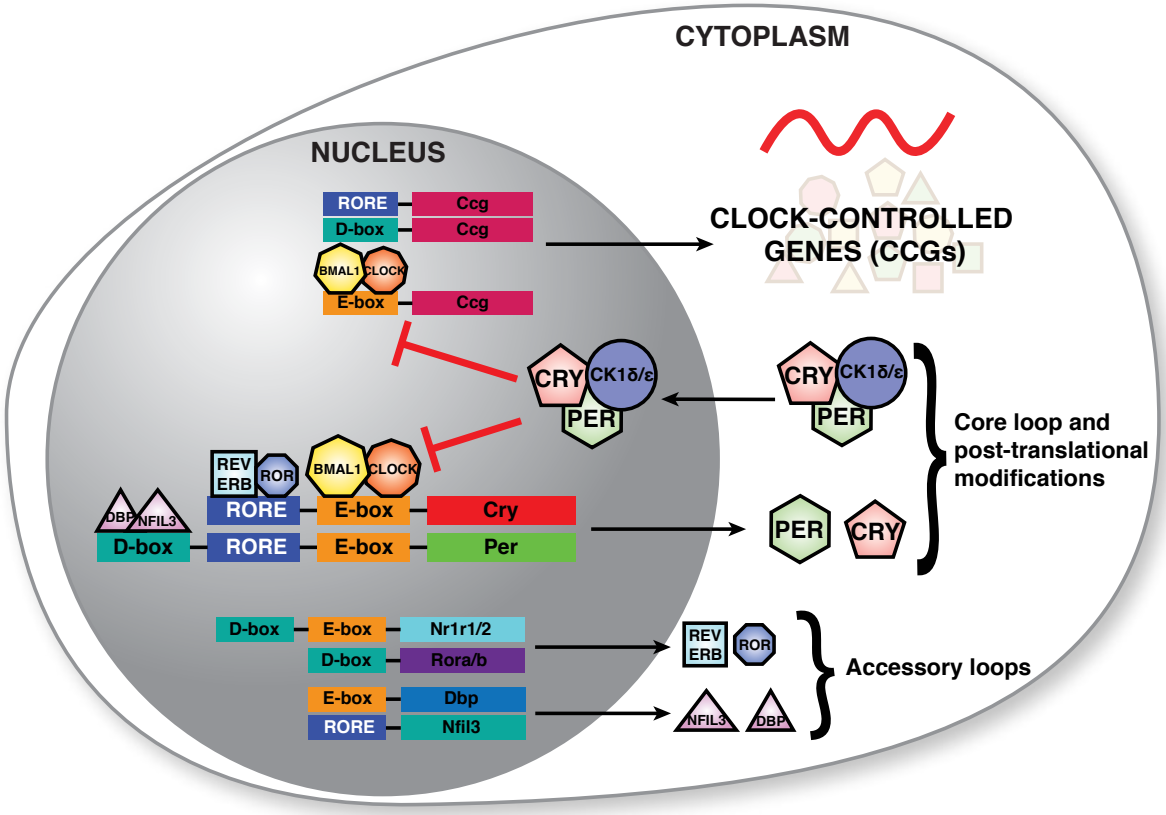

Figure 1.2 The mammalian TTFL coordinates the rhythmic transcription of the clock-controlled genes (CCGs). The transcription factors BMAL1 and CLOCK activate the transcription of the CCGs. Period (PER) and cryptochrome (CRY) proteins form a complex with regulatory factors such as casein kinase 1 (CK1). Cryptochrome proteins license the nuclear translocation of this complex, which goes on to inhibit the activity of BMAL1-containing complexes. Since *Per* and *Cry* genes are also under the control of BMAL1-containing complexes, PER and CRY proteins inhibit their own transcription. This negative feedback loop forms the core of the TTFL. The accessory loops modulate the expression of CCGs, and are not essential for TTFL function. See text for details.

Several auxiliary feedback loops supplement this core TTFL, and their relative contributions to cellular clock function varies between tissues [47, 48]. The best characterised auxiliary loops involve the REV-ERB nuclear receptors and the transcription factor DBP (D-box binding protein). The transcription of REV-ERBα (*Nr1d1*) and REV-ERBβ (*Nr1d2*) is activated by CLOCK/BMAL1 complexes, and this results in the feedback repression of *Bmal1* and other targets that have ROR-binding promoter elements [49]. The rhythmic transcription of DBP is also dependent on CLOCK/BMAL1 activity [50, 51]. DBP binds to D-box promoter elements, and is antagonised by NFIL3 (nuclear factor, interleukin-3 regulated), which is itself regulated by the activity of the REV-ERB-ROR loop activity [52, 53]. These auxiliary feedback loops modify the rhythmic expression of clock controlled genes [54], but they are not essential for basic TTFL function [48].

The processes described above are indispensable for the circadian coordination of gene expression in mammalian cells. However, the explicit molecular mechanism for 24-hour period determination is not fully understood. TTFLs are in fact commonly used in cell biology to terminate a signalling process and return to baseline. The fundamental concept is the negative feedback of gene products that simultaneously induce gene expression changes and directly or indirectly lead to their own degradation [55]. This is the basis for the oscillations in the developmental segmentation clock (roughly 2 hour period) [56, 57], the ERK signalling pathway (roughly 3 hour period) [58, 59] and the NFκB pathway (roughly 4 hour period) [60]. The period length in these cases reflect the time delays caused by RNA processing and translation, and the oscillations damp after several cycles. This is fundamentally different to circadian oscillations [61, 27]; the time constants are insufficient to account for the long time delay of 24 hours between transcriptional activation of *Per* and *Cry*, and the degradation of their repressive complexes. For this reason, post-translational regulation of clock protein activity by enzymes such as casein kinases [62–68] is thought to be the basis for the lengthy delay (Figure 1.3A).

Post-transcriptional regulation of RNA processing and RNA silencing by small interfering RNAs have been implicated in circadian control and the regulation of protein synthesis [69–80]. However, to my knowledge there has been no demonstration that their rhythmic regulation is required for circadian timekeeping.

1.1.4 Problems with the TTFL model

The precise molecular mechanism for circadian period determination at the cellular level remains unknown, despite the popularity of the TTFL model. In this section I will discuss some of the findings in the literature which are not readily explained by the TTFL model. These discrepancies suggest that circadian rhythm generation (and therefore period determination) may not in fact require the TTFL.

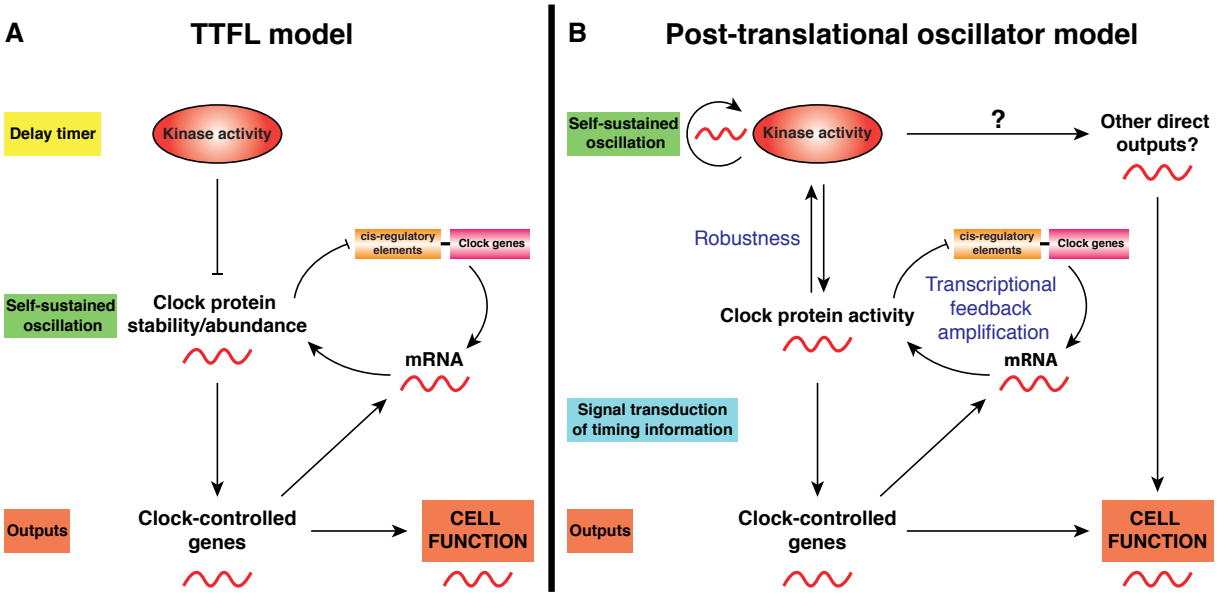

Figure 1.3 Two models for cellular circadian rhythm generation. A) The TTFL model. The mechanism that generates the rhythms is the TTFL. Enzymes that mediate post-translational modification of the clock proteins are invoked to give rise to the long 24-hour time delay. These enzymes include casein kinases and glycogen synthase kinase. The output of this self-sustained oscillation is the rhythmic expression of clock-controlled genes (CCGs) and therefore cellular function. Some CCGs such as PER and CRY feed back to the TTFL to regulate its activity as described in the text. **B)** The post-translational oscillator (PTO) model. In this alternative model, there is a post-translational mechanism that is sufficient to generate circadian oscillations – this PTO is self-sustaining. The TTFL is not necessary for circadian rhythm generation, but it confers robustness and amplification to the PTO-generated oscillations. The TTFL uses this timing information to control the expression of CCGs and thus cell function. The PTO may also coordinate circadian regulation of cell function directly, independently of the TTFL. This figure is adapted from Wong and O'Neill, 2018 [6].

It has emerged that the rhythmic expression of central TTFL components, or 'clock genes', is not actually essential for the persistence of circadian timekeeping at the cellular level. Rather, all that is required is that the activity of TTFL components should lie within a permissive range [81]. This has been shown for BMAL1 (or its paralog BMAL2) [82], CLOCK (or its paralog NPAS2) [83], PER1 or PER2 [84], and CRY1 or CRY2 [85]. Furthermore, in complementation assays, constitutive expression of BMAL1 or CRY1 or PER2 is sufficient to rescue circadian gene expression rhythms in their respective single or double knockouts [84, 78, 48, 86]. However, if PER2 or CRY1 proteins are overexpressed in knockout backgrounds, rhythmic transcription is impaired [84, 87]. Similarly, in *Drosophila melanogaster*, constitutive expression of the repressive TTFL components (*per* and *tim*) is sufficient for circadian rhythms in behaviour, whilst overexpression or knockout abolishes it [88]. Finally, in the fungus *Neurospora crassa*, circadian rhythms in the activity of FRQ protein (the major TTFL repressor protein in *Neurospora*, functionally analogous to PER) can be decoupled from its stability: deletion of the F-box protein that normally enables its degradation (FWD1) results in FRQ accumulation to constant levels but whilst still maintaining activity rhythms [89]. Together, these findings suggest that rhythmic clock protein activity rather than abundance is important for circadian transcriptional oscillations, and that transcriptional-translational feedback reinforces this oscillation rather than generates it. Moreover, these elegant genetic complementation experiments indicate that the critical TTFL proteins only need to expressed within a permissive range for rhythms in their activity to be observed. Put simply, rhythmic regulation of protein expression is not required for circadian coordination of physiology, and rhythmic activity through post-translational modifications may be sufficient.

In fact, proteomics studies have shown that the circadian transcription of DNA to mRNA correlates very poorly with circadian rhythms in the abundance of the encoded proteins. Around 50% of rhythmic proteins in mouse liver and SCN have no corresponding cycling mRNA [90, 91]. In addition, it was found in mouse liver that half of the cycling proteome showed a phase delay of more than 6 hours relative to their corresponding mRNA and that 20% of the cycling proteome had no cycling transcript at all [92], with similar findings under diurnal conditions [93]. In cultured *Drosophila* S2 (Schneider 2) cells only 7% of rhythmic proteins detected had corresponding rhythmic mRNAs [94], and in *Neurospora crassa* 41% of rhythmic proteins did not arise from rhythmic mRNAs [95], suggesting that this discrepancy may be common between many eukaryotes. Moreover, proteomics studies have revealed time-of-day variations in the post-translational modification of FRQ in *Neurospora crassa* [96] and in the mouse liver phosphoproteome and acetylome [97, 98]. These studies suggest that post-translational regulation of proteins is critical for the circadian coordination of cell function, whereas circadian rhythms in transcription may be insufficient to account for the full range of circadian coordination of cellular function.

The most important problem for the TTFL model is that circadian rhythms have been observed in eukaryotic cells in the absence of transcription in multiple independent scenarios. A

TTFL-based model would predict that circadian period be sensitive to changes in transcription rate. However, period length and temperature compensation in cultured NIH3T3 fibroblasts is robust against inhibition of RNA polymerase II [99]. Furthermore, circadian rhythms have been observed in isolated red blood cells (which do not have organelles and therefore no capacity for transcription) from both mice and humans in the following parameters: oxidised peroxiredoxin (PRX-$SO_{2/3}$) abundance, membrane physiology and NAD(P)H concentration [100–103]. In fact, rhythms in the absence of transcription were observed almost 60 years ago in a macroscopic alga, *Acetabularia mediterranea* [104, 105], where circadian rhythms in chloroplast migration persist over many days despite removal of the cell nucleus. Circadian rhythms in phosphorylation also persist in the absence of translation in the red alga *Cyanidioschyzon merolae* [106], and circadian rhythms in the bioluminescence and photosynthesis in *Lingulodinium polyedrum* do not require rhythmic changes in RNA abundance [107]. Finally, circadian rhythms in ion transport and PRX-$SO_{2/3}$ abundance persist in the picoeukaryotic alga *Ostreococcus tauri* even in constant darkness, where all RNA production ceases [108–110]. The oscillators responsible for driving these diverse non-transcriptional eukaryotic circadian rhythms are still unknown, and so it is unclear whether these represent unusual cellular specialisations to specific niches, or whether they result from the same post-translational mechanism that drives circadian rhythmicity in other cellular contexts. In the next section I will explore the evidence for the latter possibility.

1.1.5 An alternative model: the post-translational oscillator (PTO)

In light of the problems noted above, an alternative model is that a post-translational mechanism is responsible for circadian rhythm generation, and this does not require transcriptional-translational feedback loops (Figure 1.3B) [111–114, 6]. First, I will describe the precedent for this PTO model, which is set by the entirely post-translational clock that has been elucidated in the cyanobacterium *Synechococcus elongatus*. I will then discuss some candidates for mammalian PTO components.

In *S. elongatus* there is a circadian rhythm in KaiC protein phosphorylation and complex formation with KaiA/B that is temperature compensated, and this may be reconstituted in vitro with just the purified recombinant proteins (KaiA, B and C) together with Mg.ATP [115]. There are some similarities between this oscillator and mammalian post-translational timekeeping mechanisms. First, KaiC is a slow Ser/Thr phosphotransferase, with turnover rate (k_{cat}) in the order of hours [116]; in parallel, CK1δ also has a slow k_{cat} in the phosphorylation of PER peptide substrates, in the order of minutes [117]. In comparison, most cellular kinases are roughly a hundred-fold faster (10 s^{-1}) [118–120]. Secondly, this KaiA/B/C post-translational oscillator is sufficient to generate circadian rhythms in gene expression, whereas the cyanobacterial TTFL alone cannot [121]. However, when the capacity for transcriptional feedback is removed, the gene expression rhythms are less robust, suggesting that the TTFL in cyanobacteria stabilises the PTO [121]. Finally, KaiC is primarily in large macromolecular complexes with many substrate

effectors [122], where the dynamic exchange of subunits is key for timekeeping competence [123, 124]. By comparison, CK1 also has multiple substrates and functions, and is a component of large cytosolic macromolecular complexes with PER and CRY proteins [36]. The elucidation of the cyanobacterial PTO and its conceptual similarities with post-translational processes regulating mammalian timekeeping raises the possibility that a similar PTO may also exist in mammals.

Many post-translational mechanisms have been implicated as regulating and being regulated by circadian timekeeping, including acetylation, sumoylation, glycosylation, cysteine oxidation and phosphorylation [125–130]. In addition, countless other essential cellular processes have been identified as exhibiting circadian regulation, with many also feeding back to affect the phase, amplitude or period of clock gene expression. Some examples include global protein synthesis rates [131, 75], ion transport [132], cAMP/Ca^{2+} signalling [133], redox balance [134, 135], mitochondrial metabolism [136] and the actin cytoskeleton [137]. It is perhaps unsurprising that pharmacological or genetic perturbation of many cellular processes can affect circadian gene expression. In particular, the activity of these processes may be permissive for the observed circadian rhythms, without being involved in rhythm generation itself. An essential timekeeping mechanism is a cellular process that contributes to rhythm generation and/or period determination, and its rhythmic regulation is necessary for any circadian rhythm to be observed [6]. Therefore, an appropriate test for essentiality involves clamping the activity of a process at a level equal to its average over the course of a circadian cycle. If the process is essential to circadian timekeeping, then circadian rhythmicity would cease. If the process is non-essential for circadian timekeeping, then circadian rhythmicity would persist. Such experiments have ruled out redox balance [135] and BMAL1 abundance [48, 138] as essential variables of the timekeeping mechanism.

With this definition of essentiality in mind, the list of possible components of the mammalian PTO is greatly simplified. Not all post-translational processes have been equally scrutinised, but the candidates I will list have been reported multiple times, pharmacologically and genetically, to directly affect the temporal activity of clock protein transcription factors. These important candidates include: the proteasomal degradation machinery [139–143, 51, 144], casein kinase I (CK1) [145, 64, 146, 66, 147], casein kinase II (CK2) [148–150], glycogen synthase kinase 3 (GSK3) [151–153, 67, 154–156], and protein phosphatase 1 (PP1) [63, 157, 146, 158].

The enzymes listed above are proposed to contribute to cellular timekeeping by effecting the site-specific phosphorylation of clock proteins. Phosphorylation has many consequences for clock proteins depending on the context, including promoting nuclear entry [159, 152, 160, 161], regulation of transcriptional activity [162–165, 78, 166–168] and promoting hyperphosphorylation leading to ubiquitin-mediated proteasomal degradation [169, 170, 144]. In addition, it has recently been shown that the period length of the circadian rhythms in membrane electrophysiology in red blood cells is sensitive to CK1 and CK2 inhibition [100]. In the same paper, it was found that CK1 activity was necessary for temperature compensation in the red blood cells.

Finally, it is worth noting that the rate of CK1 enzymatic activity is intrinsically temperature compensated for clock protein substrates [171, 172], indicating that CK1 activity may be critical for this fundamental feature of circadian rhythms. Together, these remarkable findings suggest strongly that phosphorylation is an important PTO candidate, particularly involving CK1 activity.

1.1.6 Implications for the evolution of circadian rhythms

The TTFL model and the PTO model have different implications for the evolution of circadian rhythms in eukaryotes [6]. The TTFL model suggests that circadian rhythms are likely to have evolved at least thrice in eukaryotes, in each case retaining the fundamental concept of transcriptional feedback repression generating oscillations whilst recruiting the same set of post-translational regulatory mechanisms as a delay timer to achieve 24-hour periodicity. In this convergent evolution TTFL model, all the examples of circadian rhythms in the absence of transcriptional feedback repression (such as in red blood cells) represent specific and recent adaptations to environmental and physiological niches. In contrast, the PTO model suggests a divergent evolutionary history: an evolutionarily ancient post-translational mechanism for generating circadian timekeeping was present in the last common eukaryotic ancestor. Over time, organism- and cell-type specific transcriptional effectors ("clock proteins") were recruited as multicellular organisms and different phyla arose. The resultant transcriptional feedback loops were evolutionarily advantageous as they confer robustness to timekeeping by the PTO.

1.2 Quantitative proteomics

1.2.1 An introduction to proteomics

Cells are complex systems crowded with macromolecular machines that are primarily composed of proteins, and these effect biological processes [173]. Traditional methods of studying proteins have been mainly antibody-based and biased towards small subsets for which high-quality assays have been available [174]. Recently the simultaneous identification and quantification of thousands of proteins in biological samples has become possible with mass-spectrometry (MS)-based methods [175–177]. Hence MS-based proteomics has become an invaluable tool to quantitatively measure the biochemical state of cells and tissues.

The experimental workflow for the proteomics presented in this thesis is described in detail in Chapter 2, but I will outline the basic concepts here to provide context for my results. Biological samples containing proteins are typically digested with trypsin, thus liberating short peptides. For complex samples such as cell lysates, biochemical fractionation of these peptides is usually performed to aid analysis [178]. The fractions are then separated by liquid chromatography (LC),

and as they elute they are subjected to electrospray ionisation [179] before being directly sprayed into the mass spectrometer.

The mass spectrometer performs two levels of measurement in tandem [178]. The first level is referred to as "MS1", and this is a measurement of the mass-to-charge ratio (m/z) of peptide molecular ions. The molecular ions are then fragmented. The second level is referred to as "MS2", and this is a measurement of the m/z values of the fragment ions of a specific peptide ion. This workflow is therefore referred to as "LC-MS/MS". The fragment ion pattern information is combined with the MS1 measurement to enable confident identification of peptides and subsequent mapping to proteins [180]. The signal intensities of the peptides or fragment ions are used to estimate relative changes in abundance across samples.

LC-MS/MS involves many steps, and technical variability may be introduced at several stages. Strategies have been developed to improve the reliability of quantification, and these are based on isotopic labelling, which includes chemical isotopic labelling, metabolic isotopic labelling and isobaric tagging [181, 175]. Recently label-free approaches have become more popular due to simpler experimental design and sample preparation [182, 183]. However, label-free quantification requires multiple runs, which requires more material and reduces throughput compared to isotopic labelling [176]. Another disadvantage is that the measurement precision is comparatively poor [184].

1.2.2 Quantification methods

A common method for isotopic labelling in cell culture studies is to add heavy-labelled amino acids ("SILAC", stable isotope labelling with amino acids in cell culture) to the culture medium so that the labelled amino acids are eventually incorporated into all proteins. This allows samples to be labelled with different isotopes and then combined for MS analysis. Therefore relative quantification is achieved in a single run, resulting in high measurement precision. A major limitation is that the complexity of the MS1 spectrum is greatly increased with the number of samples because each label has a different mass. This limits confidence of peptide identification, and so only 2 or 3 samples can be compared in a single experiment.

Another method is known as isobaric tagging, and this has some advantages over isotopic labelling. Isobaric tags covalently modify peptides, and so they do not require long periods of incubation for amino acid incorporation since they are applied to the lysate. They use the distribution of heavy isotopes in the tag to encode different conditions. Thus each tag has an identical total mass, and so MS1 spectrum complexity is unaffected by the number of samples. Therefore the number of conditions that can be compared in an isobaric tag experiment far exceeds that of SILAC.

The most commonly used isobaric tags are TMT (tandem mass tag) [185] and iTRAQ (isobaric tag for relative and absolute quantitation) [186]. TMT is available with up to 11-plex reagents, whereas iTRAQ is only available with up to 8-plex. Therefore TMT allows the comparison of more samples simultaneously, and is therefore most ideal for circadian experiments that generate many samples across several timepoints.

1.2.3 Post-translational modifications

Advances in MS have made it possible to identify and quantify post-translational modifications (PTMs) of proteins [187]. A wide range of PTMs including phosphorylation, acetylation and several others have been implicated in the control of circadian rhythm [125–130]. A common feature of most of these PTMs is their rhythmicity, and so the study of dynamic changes in PTMs across time is desirable for understanding their relationship with the circadian clock. One of the most common PTMs of clock proteins is phosphorylation, and this is essential for circadian rhythm generation in multiple species [96, 188]. Phosphorylation is also the most common PTM in the cell [189, 190]. Therefore to understand the cell-autonomous circadian coordination of the proteome, a phosphoproteomics approach is valuable.

Due to the low stoichiometric amount of phosphorylated proteins in the proteome, enrichment of phosphopeptides prior to LC-MS/MS is carried out [191]. Many approaches have been developed [192], including IMAC (immobilised metal ion affinity chromatography) and MOAC (metal oxide affinity chromatography). IMAC uses the electrostatic interactions between immobilised positive metal ions such as Fe^{3+} and negatively charged phosphate groups to capture phosphopeptides [193]. Similarly, MOAC uses the affinity of metals within metal oxide particles such as TiO_2 to retain the phosphopeptides [194]. Non-specific binding is reduced using washes that are described in Chapter 2. In my experimental workflow, both IMAC and MOAC are used to maximise the efficiency of phosphopeptide enrichment.

1.3 Protein homeostasis

1.3.1 Introduction to protein homeostasis

All cells must regulate synthesis, folding and degradation of thousands of proteins to maintain their abundances at the levels necessary for proper cellular function. This regulation is known as protein homeostasis, and this is often shortened to “proteostasis”. Linguistically this is problematic because “proteostasis” implies a static population of proteins, whereas protein homeostasis more correctly describes the dynamic equilibrium of maintaining protein abundance and function. Protein homeostasis is achieved through a wide range of cellular pathways

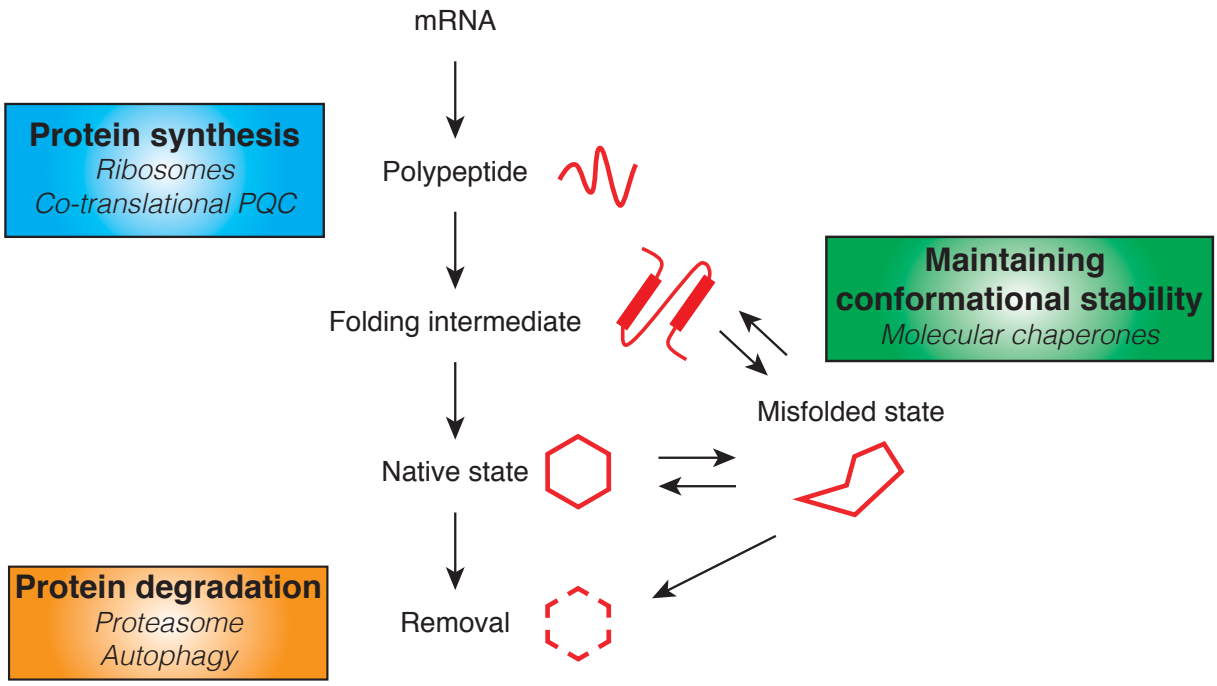

Figure 1.4 The proteostasis network. The abundance of thousands of proteins must be maintained at levels necessary for proper cellular function. In addition, the proteins must be in their 'native state' to be functional, i.e. the correct 3-dimensional structure. The proteostasis network achieves this via a large network of machinery that mediates translation and co-translational protein quality control (PQC), maintaining the conformational stability of proteins using molecular chaperones, and protein degradation via the proteasome or autophagy pathways. See text for details.

that monitor and regulate protein expression, folding, assembly, localisation and degradation [195, 196].

Imbalance can be caused by having too much or too little protein or having proteins that are incorrectly folded and therefore non-functional. In a general sense, excessive imbalance is considered a form of cellular stress. The cell contains a range of sensors that detect such stresses and initiate signalling cascades aimed at restoring protein homeostasis. The main outputs of stress sensors typically involve a reduction in the rate of translation (to minimise exacerbation of the imbalance) and increased protein degradation and protein maturation capacities. The result of these activities is a return to equilibrium, or the establishment of a new set point of equilibrium.

1.3.2 The proteostasis network

The cellular machinery for ensuring a balanced proteome as described above can be broadly divided into three linked processes: protein synthesis, maintaining conformational stability and protein degradation (Figure 1.4) [195].

A key step in protein synthesis is the translation of messenger RNA (mRNA) into an amino acid sequence. This process is performed by ribosomes, which are large complexes formed of

RNA and protein. Within this enzyme, transfer RNA (tRNA) base-pairs with mRNA which results in the formation of a peptide bond between the growing nascent polypeptide and the incoming amino acid carried by the tRNA [197]. In mammalian cells, around 3 million ribosomes work to synthesise the proteome, consuming up to 75% of the cellular energy resource in the form of ATP [198]. This demonstrates the importance of translation, as it is a significant energetic investment for the cell.

For the most part, newly synthesised proteins must form defined 3D structures to function correctly. An important exception to this rule is proteins that have intrinsically disordered regions (IDRs), which lack a stable tertiary structure unless they interact with partner molecules [199, 200]. The folded (or native) state of proteins is thermodynamically favourable, but to achieve this efficiently and to avoid forming kinetically stable but biologically unfavourable intermediates many proteins require molecular chaperones to aid with the folding process [201, 202]. It is important to remember that the cell is a highly complex environment crowded with macromolecules, and this increases the effective concentrations of proteins, thus increasing effective association constants by several orders of magnitude relative to dilute solutions [203]. In addition, translating ribosomes are organised in polysomes (multiple ribosomes translating in tandem on one mRNA molecule), and therefore many nascent polypeptides are often in close proximity. A consequence of this is that many nascent polypeptides require co-translational recruitment of chaperones such as Hsp70 to stabilise them [204]. These molecular chaperones promote folding by ATP-dependent and ATP-independent processes, consisting of sequential binding to and release from proteins at exposed hydrophobic amino acid residues [205].

Molecular chaperones also participate in the maintenance of conformational stability of proteins after synthesis is complete. Many chaperones are constitutively expressed in the cell, including members of the HSP70 and HSP90 families [206, 207]. These maintain proteins in solution and reverse unfolding to preserve functional structures. Some chaperones such as clusterin and haptoglobin even operate in the extracellular space to maintain conformational stability of secreted proteins [208].

Protein degradation is important for adjusting the abundance of functional proteins during normal cellular processes such as cell division and responding to environmental changes [195]. Two main pathways are responsible for protein degradation: the ubiquitin-proteasome system (UPS) and the autophagosomal-lysosomal pathway. The UPS is primary degradation route for proteins with short half-life, whereas autophagy is the primary route for proteins with a long half-life [209].

1.3.3 The integrated stress response (ISR)

In response to imbalances in the proteome, the proteostasis network is used to restore homeostasis. Several pathways have been described, that are triggered as a result of sensors detecting cellular

stress. These include the heat shock response in the cytoplasm [210], the unfolded protein response in the endoplasmic reticulum [211], stress responses in the mitochondria, Golgi and lysosomes [212, 213], and the integrated stress response, which is a common pathway activated in response to a wide range of stress stimuli [214].

I will provide a brief overview of the integrated stress response (ISR), since this is of relevance to the work in the later chapters. In this response, 4 kinases act as sensors that detect a range of physiological changes that may disrupt cellular homeostasis. These kinases phosphorylate eukaryotic translation initiation factor 2 alpha (eIF2α), which leads to a global inhibition of translation, with a simultaneous induction of the transcription of specific genes that restore homeostasis, including activating transcription factor 4 (ATF4) [214] (Figure 1.5).

The four eIF2α kinases are PERK (PKR-like ER kinase), PKR (double-stranded RNA-dependent protein kinase), HRI (haeme-regulated eIF2α kinase), and GCN2 (general control non-derepressible 2). Each one is activated by distinct physiological or environmental parameters, which trigger dimerization and autophosphorylation of the kinase (Figure 1.5) [215]. This signal is switched off by dephosphorylation, mediated by a protein phosphatase 1 (PP1) complex. Crucially, GADD34 (also known as PPP1R15A) regulates the phosphatase activity of this complex by targeting the enzyme to eIF2α [216]. GADD34 expression is induced by ATF4 downstream of eIF2α phosphorylation, thus forming a negative-feedback loop to restore protein homeostasis [216].

eIF2α is at the core of the ISR. It is the main regulatory subunit of the eIF2 complex because it contains both the RNA-binding and phosphorylation sites. This is part of the larger pre-initiation complex (PIC) that licenses the initiation of translation, by recognising and recruiting the 5'methylguanine cap of mRNA before migrating to the AUG start codon [217, 218]. Thus eIF2 is central in the process of cap-dependent translation of mRNA. ISR activation leads to the phosphorylation of eIF2α, which blocks the formation of the PIC. Hence there is a global attenuation of cap-dependent translation. Paradoxically, a small subset of mRNAs including ATF4 and GADD34 are preferentially translated because they do not require cap recognition, but instead have alternative mechanisms for translation initiation involving re-initiation using alternative AUG start codons or directly recruiting ribosomes to internal ribosome entry sites [219, 217, 220].

ATF4 is the best understood effector of the ISR [214]. In addition to its role during the ISR it has an important role in many processes across different tissues, such as development [221], lipid metabolism and thermoregulation [222, 223]. The increased translation of ATF4 mRNA during ISR activation leads to the transcriptional upregulation of stress-responsive genes. The identities of the stress-responsive genes that are upregulated is context-dependent, and the cell modulates this response by transcriptional, translational and post-translational regulation of ATF4 expression, as well as through a large number of interacting partners [224, 214]. Hence the ultimate outcome of the ISR is dependent on the nature of the stress, its duration and severity,

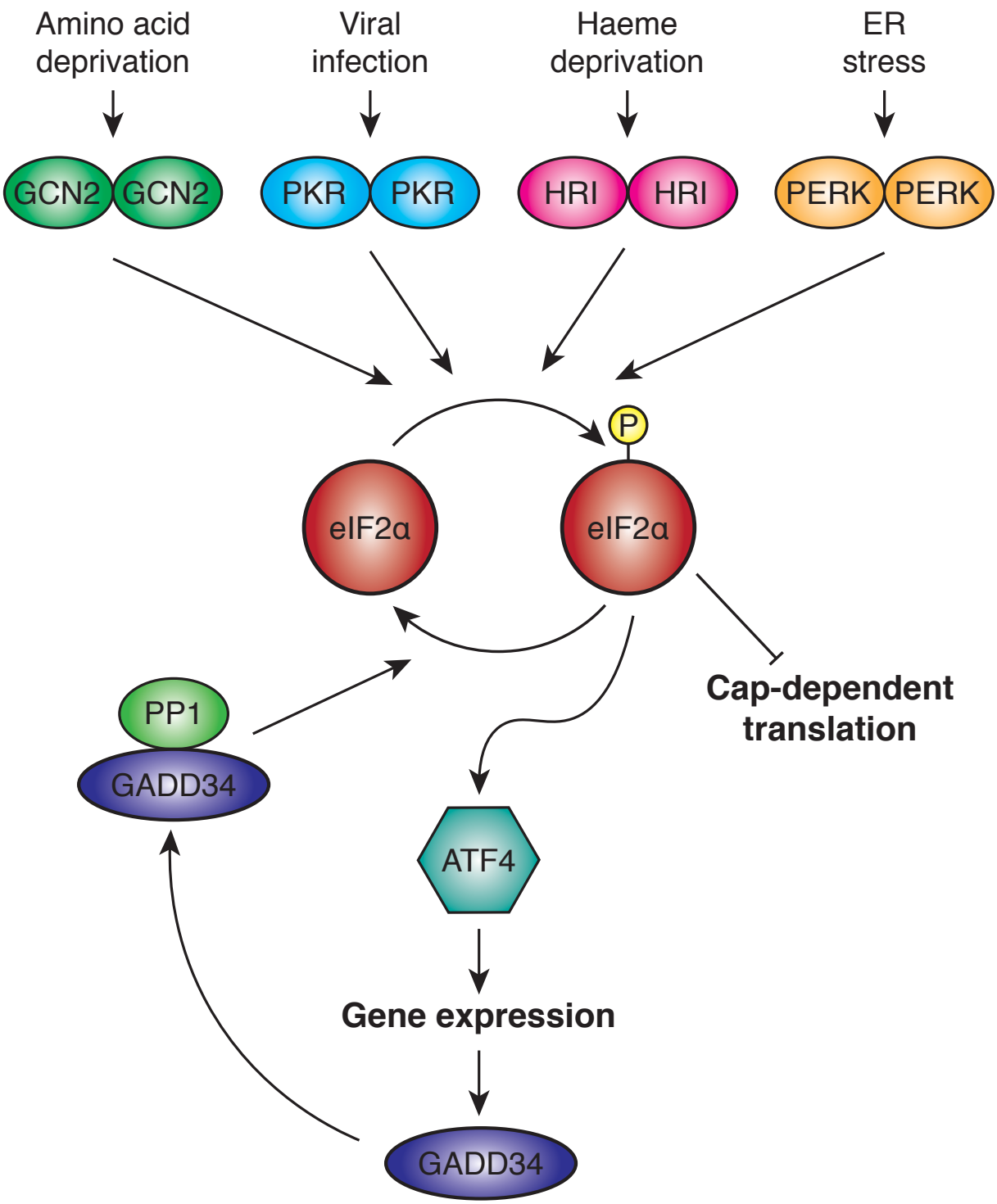

Figure 1.5 The integrated stress response. The integrated stress response (ISR) is a common pathway that is activated in response to a wide range of stress stimuli. 4 kinases sense different physiological changes; upon activation they dimerise and phosphorylate eIF2α. This leads to the attenuation of cap-dependent translation, and the simultaneous upregulation of cap-independent translation of mRNAs including ATF4 and GADD34. ATF4 is a transcription factor that activates the transcription of many stress-responsive genes. GADD34 expression is also induced by the transcriptional activity of ATF4, and in complex with PP1 it facilitates the dephosphorylation of phospho-eIF2α, thus forming a negative feedback loop to turn off the pathway. See text for details.

the extent of eIF2α phosphorylation and ATF4 translation, as well as the expression of other transcription factors. Moreover, a short-lived ISR is associated with the restoration of protein homeostasis, whilst a prolonged ISR can lead to a cellular adaptation or a death response [225].

In summary, the proteostasis network primarily functions to regulate protein synthesis, folding and degradation under normal conditions. Sensors expressed by the cell detect stress stimuli and recruit certain components of the proteostasis network to re-establish homeostasis after acute non-physiological perturbation. This is self-limiting: negative feedback is used to turn the stress response off. In cases of low-level chronic stress induction, cells are still able to achieve protein homeostasis, albeit with a different set point, for example by increasing the capacity for folding and protein degradation [209, 225].

1.4 Overview of the thesis

The overall goal of this thesis was to investigate the cellular mechanism for circadian rhythm generation and how it regulates the proteome. To achieve this I primarily used cell culture, employing biochemical, pharmacological and mass-spectrometry techniques. I extracted the fibroblasts from mice expressing the PER2 protein endogenously fused to firefly luciferase (PER2::LUC) [28], allowing real-time reporting of circadian rhythms in cell culture. As described above, the fundamental unit of circadian timekeeping is the cell. At the organism level, mice show daily rhythms in feeding even when housed in constant darkness, and this has been demonstrated to drive rhythmic gene expression through endocrine signalling [226–229]. Therefore cell culture systems were appropriate for my purposes, since they enable exposure to truly constant conditions at the cellular level.

In Chapter 3 I used this experimental system to assess the effects of a drug called picrotoxin. This drug shortens circadian period length via an unknown mechanism, and the goal of this chapter was to improve understanding of TTFL function through the characterisation of the mechanism of drug action. My experiments revealed that picrotoxin has profound effects on the TTFL as a strong synchronising factor.

In the remaining chapters I used cells from CRY1$^{-/-}$; CRY2$^{-/-}$ mice [230]. This double knockout is used to genetically abolish TTFL function. In Chapter 4 I performed proteomics and phosphoproteomics to explore the circadian regulation of the proteome and how the absence of a TTFL impacts upon this. Surprisingly I found that circadian regulation of the proteome persists without a TTFL, thus supporting the PTO model of circadian rhythm generation. I went on to explore some specific predictions made by this big data approach, revealing antiphasic rhythmic regulation of cellular protein and ion concentrations.

In Chapter 5 I explored the rhythmic regulation of PER2 activity in CRY1$^{-/-}$; CRY2$^{-/-}$ cells using the PER2::LUC reporter. The PTO model predicts that this should persist in the absence of a TTFL, and I presented a number of experimental manipulations suggesting that the ability to observe this phenomenon may be dependent on the state of the proteostasis network in these cells. In addition, I hypothesised that a major function of CRY is to maintain protein homeostasis. In Chapter 6 I took these observations further, examining the role of CRY in cellular proteostasis. I found that in the absence of CRY, cellular protein homeostasis was disrupted, and this also has consequences to the health of the organism as a whole. Furthermore, I explored the link between circadian rhythmicity and disruption of protein homeostasis. In the final chapter I discussed how my findings change our understanding of circadian rhythms through the characterisation of the cell-autonomous circadian regulation of the proteome, and support of the PTO model for circadian rhythm generation. Moreover, I propose a new interpretation of the role of the TTFL in cellular timekeeping and protein homeostasis generally.

Chapter 2

Materials and Methods

2.1 Mammalian cell culture

All animal work was licensed by the Home Office under the Animals (Scientific Procedures) Act 1986, with Local Ethical Review by the Medical Research Council and the University of Cambridge, UK. Fibroblasts homozygous for PER2::LUCIFERASE [28] were extracted from adult mouse lung tissue and and then serial passage was used as described previously to induce spontaneous immortalisation [62, 231]. Fibroblasts were cultured in Dulbecco's Modified Eagle Medium (DMEM), supplemented with 100 units/ml penicillin, 100 µg/ml streptomycin (Gibco) and 10% FetalClone III serum (HyClone, Thermo Fisher). All cells were confirmed to be free of Mycoplasma. Unless stated otherwise, confluent cell cultures were used during experiments to abolish any effects of cell division, since these cells display contact inhibition.

2.2 General statistics

P values are annotated in figures with asterisks, where the number of asterisks indicates the significance (Table 2.1). Technical replicates are denoted as "n" in the figures or figure legends (e.g. n=3), and biological replicates are denoted as "N".

Table 2.1 P value representation with asterisks.

Symbol	P value
Ns.	$P > 0.05$
*	$P \leq 0.05$
**	$P \leq 0.01$
***	$P \leq 0.001$
****	$P \leq 0.0001$

2.3 Longitudinal bioluminescent reporter experiments

Cellular bioluminescence assays were carried out in "air medium" as described below, and modifications are reported in the text. Air medium was based on DMEM without glucose, L-glutamine, phenol red, sodium pyruvate and sodium bicarbonate (Sigma). The following were added: 0.35 g/L sodium bicarbonate (Sigma), 5 g/L glucose (Sigma), 20 mM MOPS (VWR), penicillin/streptomycin solution (as above), Glutamax (Thermo Fisher), B27 (Thermo Fisher), 1 mM potassium luciferin solution (Biosyth), 1% FetalClone III serum. The medium was adjusted to pH 7.6 at room temperature, and osmolality adjusted to 350-360 mOsm/kg using sodium chloride. Temperature cycles (12 hours 37°C – 12 hours 32°C) were used for at least 3 days to synchronise the cells before being changed from normal culture medium (supplemented with 0.3 mM Luciferin) into air medium. Longitudinal recordings of bioluminescence were obtained using a Lumicycle (Actimetrics), LB962 plate reader (Berthold technologies) or an ALLIGATOR (Cairn Research). Bioluminescence was recorded as counts per second (cps) in the Lumicycle and plate reader, and ALLIGATOR measurements were reported as relative luminescence units (RLU).

Data from longitudinal bioluminescence recordings were analysed using Prism Graphpad 8 (San Diego, Ca). A 24-hour moving average was used to detrend data, and so circa-24 hour rhythms can more easily be observed and measured. Detrending in this way removes changes in baseline that occur on a timescale greater than a day, and so circadian changes are not detected, and no new 24-hour rhythms are introduced by this method. Then a circadian damped cosine wave was fitted by least-squares to determine period, phase and amplitude. The formula is as follows:

$$y = (mx + c) + ae^{-kx}cos(\frac{2\pi x - r}{p}) \tag{2.1}$$

Where m is the baseline gradient, c is the displacement in the y-axis, k is the damping rate, a is the amplitude, r is the phase and p is the period. The first 24 hours of each recording were omitted because this represents the transient effects of medium change on clock gene expression. In Chapter 5, rhythmicity of bioluminescence recordings was assessed by comparing the fit of this equation to the null hypothesis of a straight line using the Extra sum-of-squares F test in Prism Graphpad 8 (San Diego, CA). If fitting to the damped cosine was preferred ($p \leq 0.05$) then the recording was deemed "rhythmic".

"Robustness" is a measure of the strength of rhythmicity, which is proportional to the relative amplitude, and inversely proportional to the damping rate. I calculated this as follows:

$$robustness = \frac{relative\ amplitude}{|k|} \tag{2.2}$$

k is the damping rate from the cosine fitting. In some cases, rhythms increased in amplitude over time, and so the absolute value of *k* is used in this calculation. Relative amplitude is the value of *a* from the cosine fitting, normalised for the average baseline over the time period used for the fitting.

2.4 Luciferase assays after picrotoxin treatment

Cells cultured in DMEM with 10% FetalClone III serum and 0.3 mM luciferin were exposed to temperature cycles for at least 3 days before medium was changed and they were shifted to constant 37°C. Parallel longitudinal bioluminescence recordings were taken to determine the phase of drug addition. Cells were lysed at 4-hour intervals after drug treatment using the same buffer as described in Section 2.13, but with 1% TX-100 instead of digitonin. Samples were then flash frozen and stored at -20°C until the end of the collection period. After thawing, 10 µl of the samples were plated in triplicate with 80 µl assay buffer as described in Section 2.13, omitting luciferin. Luciferase assays were initiated by automated injection of 10 µl luciferin solution, and bioluminescence immediately recorded.

2.5 Biochemical characterisation of picrotoxin activity

1 µg thioredoxin (TRX) was empirically determined to be the optimal amount to run on SDS PAGE (data not shown). Reaction volume was set as 10 µL, and pH-adjusted phosphate-buffered saline was used to dilute reagents. First, 8.55 µM TRX was reduced by incubation with 1 mM TCEP at room temperature for 30 minutes. The samples were then run through a desalting column before the reactions with 100 µM N-ethylmaleimide (NEM) were carried out at room temperature for 60 minutes. Picrotoxin was then incubated with the appropriate samples overnight at 70°C. Reaction products were boiled in LDS sample buffer before running on NuPAGE^{TM} Novex^{TM} 4-12% Bis-Tris Protein Gels (Thermo Fisher), and stained with Colloidal Coomassie Blue Stain (Severn Biotech).

2.6 Proteomics and phosphoproteomics

Dr Sew Peak Chew performed the enzymatic digestion, TMT labelling, HPLC fractionation, enrichment of phosphopeptides, LC-MS/MS and peptide/protein identification.

2.6.1 Sample preparation

A timecourse was carried out as described below in section 2.9. At each timepoint cells were washed twice in ice cold PBS and then lysed at room temperature in 100 µL lysis buffer (8 M urea, 20 mM Tris, pH 8) for 20 minutes. The lysis buffer was prepared the day before sampling began, and frozen in 1 mL aliquots. At each timepoint, one aliquot was defrosted at room temperature (23°C) whilst shaking at 700 rpm for 5 minutes. After lysis the cells were scraped and technical replicates were combined before flash freezing in liquid nitrogen and storage at -80°C.

After defrosting the samples were sonicated for 2 minutes and the protein concentration was measured using a BCA assay (Pierce). 12 pooled samples were created by combining a portion of each experimental sample such that each sample/pool contained an equal amount of protein. All samples were then flash frozen in liquid nitrogen and stored at -80°C.

2.6.2 Enzymatic Digestion

Each sample (256 µg) was reduced with 5 mM DTT at 56°C for 30 minutes and then alkylated with 10 mM iodoacetamide in the dark at room temperature for 30 minutes. They were then digested with mass spectrometry grade Lys-C (Promega) at a protein:Lys-C ratio of 100:1 (w/w) for 4 hours at 25°C. Next, the samples were diluted to 1.5 M urea using 20 mM HEPES (pH 8.5) and digested at 30°C overnight with trypsin (Promega) at a ratio of 70:1 (w/w). Digestion was quenched by the addition of trifluoroacetic acid (TFA) to a final concentration of 1%. Any precipitates were removed by centrifugation at 13000g for 15 minutes. The supernatants were desalted using homemade C18 stage tips containing 3M Empore extraction disks (Sigma) and 5 mg of Poros R3 resin (Applied Biosystems). Bound peptides were eluted with 30-80% acetonitrile (MeCN) in 0.1% TFA and lyophilized.

2.6.3 TMT (Tandem mass tag) peptide labelling

The lyophilized peptides from each sample were resuspended in 100 µl of 2.5% MeCN, 250 mM triethylammonium bicarbonate. According to manufacturer's instructions, 0.8 mg of each TMT 10plex reagent (Thermo) was reconstituted in 41 µl of anhydrous MeCN. The peptides from each time point were labelled with a distinct TMT tag for 75 minutes at room temperature. The labelling reaction was quenched by incubation with 8 µl 5% hydroxylamine for 30 min. The labelled peptides from all time points per experiment were combined into a single sample and partially dried to remove MeCN in a SpeedVac (Thermo Scientific). After this, the sample was desalted as before and the eluted peptides were lyophilized.

2.6.4 Basic pH Reverse-Phase HPLC fractionation

The TMT labelled peptides were subjected to off-line High Performance Liquid Chromatography (HPLC) fractionation, using an XBridge BEH130 C18, 3.5 µm, 4.6 mm x 250 mm column with an XBridge BEH C18 3.5 µm Van Guard cartridge (Waters), connected to an Ultimate 3000 Nano/Capillary LC System (Dionex). Peptide mixtures were resolubilized in solvent A (5% MeCN, 95% 10 mM ammonium bicarbonate, pH 8) and separated with a gradient of 1-90% solvent B (90% MeCN, 10% 10 mM ammonium bicarbonate, pH 8) over 60 minutes at a flow rate of 500 µl/min. A total of 60 fractions were collected. They were combined into 20 fractions and lyophilized and desalted as before. 5% of the total eluate from each fraction was taken out for proteome LC-MS/MS analysis and the rest was used for phosphopeptide enrichment.

2.6.5 Enrichment of phosphopeptides

All 20 fractions of peptide mixture were enriched first using PHOS-Select iron affinity gel, an Iron (III) Immobilised Metal Chelate Affinity Chromatography (IMAC) resin (Sigma). Desalted peptides were resuspended in 30% MeCN, 0.25 M acetic acid (loading solution) and 30 µl of IMAC beads, previously equilibrated with the loading solution, was added. After 60 minutes incubation at room temperature, beads were transferred to a homemade C8 (3M Empore) stage tip and washed 3 times with loading solution. Phosphopeptides were eluted sequentially with 0.4 M NH_3, 30% MeCN, 0.4 M NH_3 and 20 µl of 50% MeCN, 0.1% TFA. The flow-through from the C8 stage tips was collected and combined into 10 fractions, and used for titanium dioxide (TiO_2) phosphopeptide enrichment. For this, the total volume of flow-through was made up to 50% MeCN, 2 M lactic acid (loading buffer) and incubated with 1-2 mg TiO_2 beads (Titansphere, GL Sciences, Japan) at room temperature for 1 hour. The beads were transferred into C8 stage tips, washed in the tip twice with the loading buffer and once with 50% MeCN, 0.1% TFA. Phosphopeptides were then eluted sequentially with 50 mM K_2HPO_4 (pH 10) followed by 50% MeCN, 50 mM K_2HPO_4 (pH 10) and 50% MeCN, 0.1% TFA.

The first 10 fractions of IMAC and the 10 fractions of TiO_2 enriched phosphopeptides were combined, and the other 10 fractions from IMAC enrichment were combined into 5 fractions, thus making a total of 15 fractions for phosphoproteomics analysis. Phosphopeptide solution from these fractions were acidified, partially dried, and desalted with a C18 Stage tip that contained 1.5 µl of Poros R3 resin. These were then partially dried again and thus ready for mass spectrometry analysis.

2.6.6 LC MS/MS

The fractionated peptides were analysed by LC-MS/MS using a fully automated Ultimate 3000 RSLC nano System (Thermo) fitted with a 100 µm x 2 cm PepMap100 C18 nano trap column and a 75 µm × 25 cm reverse phase C18 nano column (Aclaim PepMap, Thermo). Samples were separated using a binary gradient consisting of buffer A (2% MeCN, 0.1% formic acid) and buffer B (80% MeCN, 0.1% formic acid), and eluted at 300 nL/min with an acetonitrile gradient. The outlet of the nano column was directly interfaced via a nanospray ion source to a Q Exactive Plus mass spectrometer (Thermo). The mass spectrometer was operated in standard data-dependent mode, performing a MS full-scan in the m/z range of 350-1600, with a resolution of 70000. This was followed by MS2 acquisitions of the 15 most intense ions with a resolution of 35000 and Normalised Collision Energy (NCE) of 33%. MS target values of 3e6 and MS2 target values of 1e5 were used. The isolation window of precursor ion was set at 0.7 Da and sequenced peptides were excluded for 40 seconds.

2.6.7 Spectral processing and peptide and protein identification

The acquired raw files from LC-MS/MS were processed using MaxQuant (Cox and Mann) with the integrated Andromeda search engine (v1.6.3.3). MS/MS spectra were quantified with reporter ion MS2 from TMT 10plex experiments and searched against the *Mus musculus* UniProt Fasta database (Dec 2016). Carbamidomethylation of cysteines was set as fixed modification, while methionine oxidation, N-terminal acetylation and phosphorylation (STY) (for phosphoproteomics group only) were set as variable modifications. Protein quantification requirements were set at 1 unique and razor peptide. In the identification tab, second peptides and match between runs were not selected. Other parameters in MaxQuant were set to default values.

The MaxQuant output file was then processed with Perseus (v1.6.2.3). Reporter ion intensities were uploaded to Perseus. The data was filtered: identifications from the reverse database were removed, only identified by site, potential contaminants were removed and we only considered proteins with $\geq$1 unique and razor peptide. Then all columns with an intensity "less or equal to zero" were converted to "NAN" and exported as a .txt file.

The MaxQuant output file with phosphor (STY) sites table was also processed with Perseus software (v1.6.2.3). The data was filtered: identifications from the reverse database were removed, only identified by site, potential contaminants were removed and we only considered phosphopeptides with localization probability $\geq$0.75. Then all columns with intensity "less or equal to zero" were converted to "NAN" and exported as a .txt file.

2.6.8 Bioinformatics

All data handling was done using R v3.5.1. Only proteins present in all of the samples and pools were included for analysis, and since the sample for timepoint 12 was missing for CRY1$^{-/-}$; CRY2$^{-/-}$, abundance values were inferred for each protein by taking the mean of the two neighbouring timepoints. Sample loading normalisation was carried out by taking the sum of all intensities for each time point and normalising to the mean of these, since an equal amount of protein was used for each TMT labelling reaction. This was followed by internal reference scaling (IRS) to allow for comparisons between TMT experiments [232]: for each TMT 10plex experiment the arithmetic mean abundance for each protein in both pools was calculated. Then the mean of these means was calculated and used to normalise the values for each protein for all the samples.

Rhythmicity was tested using the RAIN (Rhythmicity Analysis Incorporating Non-parametric methods) algorithm [233], and multiple testing was corrected for using the adaptive Benjamini-Hochberg method. Proteins with a corrected $p \leq 0.05$ were deemed significant. Relative amplitude of rhythmic proteins was calculated by detrending the data using a 24-hour moving average and dividing the resultant range by the average normalised protein abundance. To include only proteins with a biologically relevant level of oscillation, only those with relative amplitude $\geq 10\%$ were taken for further analysis (See Chapter 4 for details). Metacycle is a package written in R combining 3 statistical methods of rhythm analysis [234]: ARSER, JTK_CYCLE, and Lomb-Scargle methods. Within this package I used the meta2d function to analyse my data, and compared the outputs in Chapter 4.

Phosphoproteomics data were handled in the same way, except that normalised phosphopeptide abundances were adjusted according to the changes in abundance of the corresponding protein from the normalised total proteome data. Hence changes in phosphorylation were decoupled from changes in the total amount of protein. These adjusted values were then used for rhythmicity analysis.

Gene ontology analysis was performed using online tools (www.geneontology.org), and functional annotation clustering was performed using the Database for Annotation, Visualization and Integrated Discovery (DAVID) v6.8. All functional annotation was performed using the list of all proteins detected in our experiment as the background. Kinase recognition motifs were screened using a custom script written in Python v2.7 by Dr Tim Stevens.

2.7 Cell volume measurements

Cell volume measurements were performed by Dr Alessandra Stangherlin. WT cardiac fibroblasts were transfected with pCDNA3.1 tdTomato and diluted 1:2 with control cells (transfected with

no DNA). Cell mixtures were then seeded in μslides (IBIDI, 80826), grown to confluence and entrained by temperature cycles. 24 hours before recording began, medium was changed to air medium supplemented with 1% Hyclone III and the plates were sealed. Z-stacks were acquired every hour for 2.5-3 days using a Leica SP8 confocal microscope. Imaris software (Oxford instruments) was used for 3D reconstruction, tracking and determination of cell volume. Comparison of fit was done using GraphPad Prism 8 as described above (Chapter 2.3).

2.8 Western blotting

For Western blots, proteins were run on NuPAGE^{TM} Novex^{TM} 4-12% Bis-Tris Protein Gels (Thermo Fisher) before transferring to nitrocellulose membranes. For transfer, the iBlot system (Thermo Fisher) was used. Membranes were blocked using 5% milk powder (Marvel) or 0.125% BSA (Sigma) and 0.125% milk powder (Marvel) in TBS containing 0.1% Tween-20 (TBST) for 30 minutes at room temperature then incubated with primary antibody at 4°C overnight. HRP-conjugated secondary antibodies (Thermo Fisher) diluted 1:10000 in blocking buffer were incubated with the blots for 1 hour at room temperature. Chemiluminescence was detected in a Biorad chemidoc using Immobilon reagent (Millipore). Protein loading was checked by staining gels with Colloidal Coomassie Blue Stain (Severn Biotech). Densitometric analysis was carried out using Image Lab 4.1 (Biorad Laboratories 2012).

2.9 Timecourse experiments: general structure

Cells were plated at a near-confluent density (roughly 27,000 cells per cm^2) and cultured in DMEM with 10% FetalClone III serum for one week in a temperature-controlled incubator that was programmed to oscillate between 32°C and 37°C, with transitions every 12 hours. The cells received a medium change at the transition between 37°C and 32°C after 4 days. After another 3 days the cells received another medium change at the same transition time into medium containing either 10% or 1% serum, and the incubator was programmed to remain at 37°C constantly. At this time, a subset of cells received medium containing 1 mM luciferin, and these were placed into an ALLIGATOR for bioluminescent recording. After 24 hours, sampling began, with 3 hour intervals, and continuing for 3 days. The nature of the sampling varied according to the specific experiment, and details will be discussed in separate sections. Timecourse experiments were performed in 12-hour shifts with Dr Alessandra Stangherlin or Estere Seinkmane.

2.10 Measurement of cellular protein content

Confluent monolayers of cells were washed twice with ice-cold PBS. Cells were then incubated with 200 µL digitonin lysis buffer (50 mM Tris pH 7.4, 0.01% digitonin, 5 mM EDTA, 150 mM NaCl, 1 U/mL Benzonase, protease and phosphatase inhibitors) on ice for 15 minutes. After this, lysates were collected, and then the cells were incubated with 200 µL RIPA buffer (50 mM Tris pH 7.4, 1% SDS, 5 mM EDTA, 150 mM NaCl, 1 U/mL Benzonase, protease and phosphatase inhibitors), on ice for 15 minutes. Cells lysates were then scraped and collected and all samples were flash frozen in liquid nitrogen. Protein concentration was measured for all the samples at once after thawing. RIPA lysates were sonicated at high power for 10 seconds at 4°C to shear genomic DNA. RIPA lysates and digitonin lysates were clarified by centrifugation at 21,000 g for 15 minutes at 4°C.

To measure protein concentration using intrinsic tryptophan fluorescence, 10 µL of each sample was transferred into a UV-transparent 384 well plate (Corning 4681) in triplicate or quadruplicate. After brief centrifugation of the plate, quantification was carried out using a Tecan Spark 10M microplate reader, with excitation at 280 nm and emission at 350 nm. Protein concentration of 10 µL lysate was also measured in 96-well plates using the bicinchoninic acid assay (BCA assay, Pierce), according to the manufacturer's instructions. For both assays, standards were made using bovine serum albumin (Fisher Scientific), dissolved using the same lysis buffer as the lysates being measured. Standard curves were fitted to a quadratic curve using Prism Graphpad 8 (San Diego, Ca), and protein concentrations were interpolated. Coomassie staining was also used to measure relative changes in protein content. Lysates were run on NuPAGE^{TM} Novex^{TM} 4-12% Bis-Tris Protein Gels (Thermo Fisher) and stained with Colloidal Coomassie Blue Stain (Severn Biotech). Using ImageJ, regions of interest were drawn over whole lanes and average intensity was measured.

Each technique has its advantages and disadvantages. The BCA assay (Thermo) may be confounded by reducing metabolites that are able to induce a colour change by reducing copper II to copper I. Intrinsic tryptophan fluorescence may be confounded by free tryptophan and folding state. Coomassie staining on a gel is difficult to quantify and binds in a similar way to the BCA reagent. In terms of advantages, BCA is reliable, samples can be recovered after intrinsic tryptophan fluorescence, and Coomassie is easy to visualise. After the first experiment I only used BCA assay and intrinsic tryptophan fluorescence due to their reliability, independent modes of measurement, and limited sample sizes.

2.11 Measurement of the effective diffusion coefficient of quantum dots

Quantum dot synthesis was carried out by Thomas Pons, and conjugation was carried out by Joseph (hitherto referred to as Joe) Watson. I carried out dilution of quantum dots and application to cell cultures. Joe Watson then performed image acquisition, effective diffusion coefficient calculation and the preparation of images for presentation.

CdSe/CdS/ZnS core/shell quantum dots (QDs) were synthesised using a high temperature reaction of metal carboxylates and sulphur and selenium precursors in octadecene as described previously [235], and then conjugated to streptavidin followed by incubation with biotinylated Cell Penetrating Poly Disulphides (CPD) [236] overnight at 4°C. On the day of the experiments, QD-CPD conjugates were diluted to a final 1 nM concentration in growth medium without serum, and then added onto cells in a time-course experiment.

WT and CRY1$^{-/-}$; CRY2$^{-/-}$ fibroblasts were seeded in 35 mm dishes (WPI) and grown to confluence, differentially entrained using temperature cycles. QD motion was imaged at predicted troughs and peaks of protein oscillations: 24, 36, 48 and 60 hours after medium change (normal growth medium as described above but with 1% serum and supplemented with 10 mM HEPES). Cells were incubated with 1 nM QDs for 1 hour, washed twice with PBS then imaged at 37°C at atmospheric conditions, maintained using a temperature-controlled chamber (Digital Pixel). All treatments were performed at 37°C and using the conditioned medium from the same dishes to prevent any perturbations caused by medium change. For each time point, several time-lapse recordings from 4 replicate dishes were acquired, and these were then pooled for analysis.

Imaging was performed by Joe Watson using spinning disk confocal microscopy on a setup custom-built by Dr Emmanuel Derivery. This was based on a Nikon Ti stand, 100X PLAN APO NA 1.45 oil immersion objective, a Yokogawa CSUX1 spinning disk head followed by 1.2X relay optics and a Photometrics Prime 95B back-illuminated sCMOS camera operated by Metamorph (Molecular Devices). To maximise sensitivity, the camera was configured in 12 bit dynamic range mode (gain 1), and the camera was synchronised with the spinning disc wheel and operated in pseudo global shutter mode where lasers only switched on when all lines were exposing – this avoided imaging artefacts. To prevent focus drift during fast acquisitions, the stand was equipped with hardware autofocus. QDs were excited by a 488 nm laser (150 mW OBIS mounted in a Cairn laser launch) and single band emission filters mounted in a fast Cairn Optospin filter wheel were used - Chroma 595/50 for QDs. Each acquisition consisted of 1000 frames acquired at 62.5 Hz (10 ms exposure, 6 ms readout).

Estimation of the effective diffusion coefficient of QDs was performed in Fiji and Matlab 2017b (Mathworks) using custom codes written by Dr Emmanuel Derivery. In brief, QD

position was determined using 2D Gaussian fitting, and QD trajectories were tracked using code originally developed by David Grier, John Crocker and Eric Weeks in Matlab 2017b (http://site.physics.georgetown.edu/matlab/index.html). For each track, the mean square displacement (MSD) of segments of increasing duration was then computed and fitted to a subdiffusion model captured by the function $MSD(t) = 4Dt^{\alpha}$ where D is the effective diffusion coefficient. MSD curves were filtered to retain only those with a good fit ($R^2 > 0.9$) and with $\alpha > 0.5$ in order to exclude immobile particles. Effective diffusion of these filtered tracks was then accurately estimated by fitting the first 50 points of their MSD curve by the function $MSD(t) = 4Dt$. The effective diffusion coefficient D was then averaged across all filtered tracks to give an estimate of the effective diffusion coefficient for a given field of view (average number of filtered tracks per field of view was 1125 ± 42). The effective diffusion coefficients per field of view were then averaged for each timepoint of the circadian time-course (between 84-135 fields of view across 4 cell culture dishes for each genotype at each time point).

2.12 Measurement of intracellular ion content

Sample dilution was performed by Dr Alessandra Stangherlin and ICP-MS was performed by Dr Jason Day.

Confluent monolayers of cells were washed on ice with iso-osmotic buffer A (300 mM sucrose, 10 mM Tris base, 1 mM EDTA, pH 7.4 adjusted with phosphoric acid, 330-340 mOsm adjusted with sucrose/HPLC water), followed by iso-osmotic buffer B (300 mM sucrose, 10 mM Tris base, 1 mM EDTA, pH 7.4 adjusted with acetic acid, 330-340 mOsm adjusted with sucrose/HPLC water). This osmolarity was chosen to match the culture medium. Iso-osmotic buffer A contains phosphoric acid which displaces lipid bound ions. Iso-osmotic buffer B contains acetic acid which removes traces of phosphates. Cells were then incubated for 30 minutes at room temperature in 200 µL ICP-MS cell lysis buffer (65% nitric acid, 0.1 mg/mL (100 ppb) cerium). Lysates were then collected and stored at -80°C. All samples were thawed simultaneously and diluted using HPLC water to a final concentration of 5% nitric acid. Diluted samples were analysed by inductively-coupled plasma mass spectrometry (ICP-MS) using the NexION 350D ICP-MS (PerkinElmer Inc.).

2.13 Luciferase folding assays

Cells cultured in DMEM with 10% FetalClone III serum and 0.3 mM luciferin were exposed to temperature cycles for at least 3 days before they were shifted to constant 37°C. At desired timepoints cell plasma membranes were permeabilised to extract cytosol using the following buffer: 100 mM potassium phosphate buffer pH 7.8, 10 mM $MgSO_4$, 1 mM ATP, 1 mM EDTA, 100

mM 2-mercaptoethanol, 0.01% Digitonin (Sigma), 10% glycerol, 1 mM NaF, 1 mM Na_3VO_4, and protease inhibitors. After incubation at 4°C for 20 minutes, the lysate was either used immediately or flash frozen in liquid nitrogen. Boiled lysate controls were obtained by heating lysate samples at 95°C for 10 minutes.

Recombinant luciferase (Promega) was denatured by heating at 45°C for 35 mins (see Chapter 6 for details), before being returned to 4°C. A final concentration of 10 nM was used, except when non-denatured luciferase was used as a positive control, where 100 pM was used. Luciferase assays in solution were carried out as previously described [132], with modifications as follows. On ice, cytosol extract was mixed with recombinant luciferase at a volume ratio of 9:1 and incubated at 37°C for one hour for folding to occur, before 10 µl in triplicate was plated into individual wells of a 96-well plate. 90 µl of luciferase assay buffer was added to each well by automated injection (Tecan Spark 10M microplate reader) and bioluminescence immediately recorded in counts per second. The luciferase assay buffer consisted of 10 mM $MgSO_4$, 30 mM Hepes, 300 µM Luciferin, 1 mM ATP, 10 mM 2-mercaptoethanol, 1 mg/ml BSA. In addition, a control assay was carried out before incubation for refolding. Denatured luciferase incubated with lysis buffer was used as a control for residual activity and spontaneous refolding; the average activity was subtracted from the values recorded from cytosol/luciferase mixes. Then, the values recorded from the samples incubated at 37°C were divided by the values recorded from the pre-folding control plate – this fold-change from the control is the folding activity of the cytosol extract.

2.14 Proteasome activity assays

Around 20,000 cells per well were plated in a 96-well plate, and on the following day they were changed into the appropriate experimental medium for 3 hours. 10 µM epoxomicin in the experimental medium was used as negative control.

The ProteasomeGlo Cell-Based Assay (Promega) was used to measure proteasome catalytic activity. Chymotrypsin-like, trypsin-like and caspase-like activities were measured separately using the relevant substrates from Promega (Suc-LLVY-Glo, Z-LRR-Glo, Z-nLPnLD-Glo respectively). Assay reagents were prepared according to the manufacturer's instructions. The 96-well plate was equilibrated to room temperature, and a volume of assay reagent equal to the volume of medium was added to each well before shaking at 700 rpm for 2 minutes. The plate was incubated at room temperature for a further 10 minutes, and then luminescence was measured using the Tecan Spark 10M microplate reader, recording counts for 1 second. The luminescence readings from the epoxomicin controls represent background protease activity, and so this was subtracted from all other recordings. The luminescence readings from cells changed to exactly the same medium as they were plated in represented "baseline" proteasome activity.

Proteasome activity in response to different concentrations of serum and drugs were expressed as fold-changes from this baseline level.

2.15 Measurement of translation rate

For radiolabelling of cells, a 6-well plate containing confluent monolayer cultures was used. 24 hours after plating, the cells were changed into medium containing 1% serum and ^{35}S-methionine at a concentration of 0.1 mCi/mL. After 10 minutes of incubation on a heat pad, the cells were washed with PBS before lysis with RIPA buffer at room temperature. Samples were reduced with LDS sample buffer with 0.25% 2-mercaptoethanol and run on a gel. The gel was stained with Coomassie and vacuum-dried. The dried gel was exposed to a phosphor screen (GE Healthcare) overnight. Phosphor screen autoradiography was performed using a Typhoon FLA 7000 imager (GE Healthcare). Imaging of the Coomassie stain was performed using a Biorad chemidoc and densitometric analysis was performed in Image J.

Metabolic labelling with L-azidohomoalanine (AHA) was also used to measure translation rate. This non-canonical amino acid is incorporated into newly synthesised proteins in place of methionine, giving them the unique chemical properties of the azide group. This allows click chemistry tagging with a reporter containing an alkyne group in a highly specific reaction, so that the abundance of newly synthesised proteins may be quantified [237, 238]. The experiment was carried out according to the manufacturer's instructions (Thermo). Briefly, cells were washed twice in warm PBS and methionine-free and serum-free medium was added, incubating for 1 hour at 37°C. After this, the medium was replaced with methionine-free and serum-free medium containing Click-IT AHA (Thermo) at a final concentration of 100 μM before incubation for 2 hours at 37°C. Cells were then washed thrice with ice cold PBS and lysed with RIPA buffer on ice. Lysates were collected by scraping then flash frozen. This protocol was carried out at two separate time points, 12 hours apart. All lysates were defrosted and protein concentration was quantified using BCA assay (Thermo). Click reactions were then performed at the same time according to manufacturer's instructions including the use of proprietary reaction buffers (Thermo). Biotin alkyne (Thermo) was used as the detection reagent at a working concentration of 20 μM, and 17.7 μg protein was used for each reaction. Reduced LDS sample buffer was then added before running the lysates on a gel and Western blotting as described above. Biotin was probed for using streptavidin-HRP (1:2000, Cell Signalling).

2.16 Metabolic profiling of cells in culture

To characterise the metabolic profile of cells in culture I used metabolic assays from Seahorse Biosciences [239, 240] to measure extracellular acidification rate (ECAR) and oxygen consump-

tion rate (OCR) according to manufacturer's instructions (Agilent), and with guidance from Dr Marco Sciacovelli and Dr Christian Frezza for machine operation. 18,000 cells per well were plated in a 24-well cell culture microplate (Agilent) and incubated at 37°C overnight to adhere the cells. Empty wells in positions recommended by the manufacturer were used to assess background. Cells were then changed into warm "Seahorse medium" (DMEM without phenol red or bicarbonate, 4.5 g/L glucose, 1 mM pyruvate, 4 mM glutamine), and incubated for 30 minutes in a CO_2-free incubator at 37°C for equilibration. An Agilent Seahorse XFe24 Analyser was then used to measure OCR and ECAR, with injection of antimycin diluted in Seahorse medium at a working concentration of 1 μM after the assay as a negative control.

2.17 Mouse behaviour experiments

2.17.1 General structure for mouse behavioural recordings

Mouse behavioural experiments were conducted at Ares unless stated otherwise. The following people helped with the laborious weighing protocols and setting up cages: Dr John O'Neill, Dr Andrew Beale, Dr Nina Rzechorzek, and Martin Reed. Jo Chesham kindly provided weighing data from the Hastings Lab CRY1$^{-/-}$; CRY2$^{-/-}$ PER2::LUC mouse colony to supplement my own data. Post-mortems were carried out by many helpful members of the Ares staff, and Dr Marisa Coetzee supervised these activities and authorised histopathology reports, which were provided by Abbey Veterinary Services.

WT PER2::LUC and CRY1$^{-/-}$; CRY2$^{-/-}$ PER2::LUC mice were used, with age ranging from 7-11 weeks, and equal numbers of males and females where possible. Mice were individually housed in a temperature and humidity-controlled circadian cabinet (Phenome Technologies) and locomotor activity was monitored by both wheel-running and infra-red motion detection. Mice were entrained using 12 hour light (400 lux), 12 hour dark (LD) cycles for at least 1 week before being subjected to constant darkness (DD) for at least 2 weeks. Locomotor activity was analysed using ClockLab (Actimetrics).

Throughout the experiments the mice received weekly water bottle and food changes. There were 3 visual checks per week, using night vision goggles where necessary, and daily PC checks remotely. Cage setup was standardised with equal amounts of bedding and the running wheels were maintained regularly to ease movement and reduce noise. Mice were weighed before beginning experiments and during experiments when indicated in specific protocols.

2.17.2 Mouse behaviour experiments with ixazomib treatment

An initial experiment to examine drug tolerance was conducted at the Laboratory of Molecular Biology in the Biomedical Services facility, with help from Dr Marisa Coetzee, Dr John O'Neill and Claire Knox. Mice were individually housed and drinking water was supplemented with 10% blackcurrant and apple squash (Co-operative Foodstores Limited) to mask the taste of the drug. 1 male and one female (treatment group) both received 50 µg/mL ixazomib in the supplemented drinking water (ixazomib stock concentration was 50 mg/mL in DMSO). 1 male and one female (control group) received 0.1% DMSO. Water and food consumption as well as mouse weights were recorded daily. Treatment and control group water was swapped after two days. Two mouse behaviour experiments were carried out as described above, whilst closely monitoring drug-treated mice daily for adverse effects. In these experiments, 35 µg/mL ixazomib was used due to mild weight loss observed in the tolerance experiment. This concentration was tolerated for the duration of the treatment (7 days) with no signs of distress.

2.18 Details of antibodies and drugs

Table 2.2 Antibodies.

Antibody name/target	Host species	Catalogue number	Manufacturer
Anti-mouse-HRP	Goat	A4416	Sigma
Anti-rabbit-HRP	Goat	A6154	Sigma
Anti-rat-HRP	Goat	629520	Thermo
HSP90 non-specific	Mouse	ab13492	Abcam
HSP70 non-specific	Mouse	ab2787	Abcam
Tubulin YL1-2	Rat		in-house
Proteasome 20S α1-7	Mouse	ab22674	Abcam
eIF2α	Mouse	AhO0802	Thermo
Phospho-eIF2α-S51	Rabbit	ab32157	Abcam
Histone H3	Rabbit	ab1791	Abcam

Table 2.3 Drugs.

Reagent	Supplier
Cycloheximide	Sigma
Picrotoxin	Sigma
Bortezomib	Generon
Epoxomicin	APExBIO Technology
Ixazomib	Santa-Cruz Biotechnology
MG132	Sigma
Torin 1	Millipore
KS15	Professor Young-Ger Sug, Seoul National University
Tunicamycin	Insight Biotechnology

Chapter 3

Pharmacological manipulation of a state variable by picrotoxin

3.1 Introduction

3.1.1 Pharmacological screens to interrogate the clock mechanism

Genetic networks comprising transcriptional feedback loops are important for circadian regulation in all organisms. In mammalian cells, Bmal1-containing complexes rhythmically activate the transcription of the clock-controlled genes. These complexes are in turn rhythmically inhibited by complexes containing PER and CRY proteins. Cell-based assays using cultured fibroblasts have been used to screen for pharmacologically active compounds that affect clock function [241, 171]. The advantage of this experimental system is that cultured fibroblasts lack intercellular coupling, and so perturbations may be revealed that would otherwise be masked in a system with robust coupling such as the SCN. Such screens may be useful for discovering biological mechanisms driving and regulating the circadian clock [3].

A recent screen of 1260 pharmacologically active compounds were tested with mouse and human cell lines to find out why the cellular clock is flexible yet robust to environmental changes [171]. Whilst many drugs increased period length, only 4 shortened it: picrotoxin, ketoconazole, amsacrine and SB216763 (a GSK3 inhibitor). Whilst many drugs increased period length, only 4 shortened it: picrotoxin, ketoconazole, amsacrine and SB216763 (a GSK3 inhibitor). Ketoconazole acts through the glucocorticoid receptor [242], and modulation of this is known to affect circadian rhythms in cell culture [243, 244]. Amsacrine is a DNA intercalating agent and topoisomerase inhibitor and thus causes DNA damage. Period shortening upon amsacrine treatment has been observed before [110, 151], and it has been proposed that DNA damage may act as a zeitgeber [245]. GSK3 inhibition is already known to affect circadian period length

[151]. Picrotoxin was of particular interest because of its large effect size and its mysterious mechanism of action on the circadian clock. Picrotoxin is a classic irreversible $GABA_A$ receptor antagonist but it was found that this drug reversibly and dose-dependently shortens period length in several human and mouse tissues, independent of cys-loop receptors [246, 247]. However, the molecular mechanism of action on cellular circadian timekeeping remains unknown.

3.1.2 Aims of this chapter

A better understanding of the mechanism of picrotoxin action may provide insight into important clock regulators and how they may be pharmacologically targeted. More generally, this will give some insight into the robustness of the cell-autonomous circadian timekeeping mechanism. In addition, picrotoxin is often used in neuroscience research for its GABA antagonism property; understanding its role as a circadian clock regulator would clarify any confounding effects drug treatment may have for these experimental uses. Hence the aim of the study in this chapter was to find the molecular target of picrotoxin.

3.2 Results and discussion

3.2.1 Picrotoxin treatment is a strong synchroniser

First I resolved to repeat the observations of Freeman et al. [246] to be confident of the effect of picrotoxin in my own hands. In my cell cultures, picrotoxin treatment caused an acute induction of PER2::LUC activity followed by rapid damping (Figure 3.1A). In addition, there was dose-dependent shortening of period (Figure 3.1B), with the same effect size as previously observed in different tissues [246]. This is a replication of previous findings, so I was confident that my experimental system and technique was appropriate for studying the effects of this drug.

The strong induction of PER2::LUC activity suggested that picrotoxin treatment may be a large perturbation of the cellular clock. Large perturbations such as serum shock or glucocorticoid treatment tend to reset the phase of the clock [248, 243]. Hence I decided to conduct an experiment where cells were treated with 100 μM picrotoxin at various times of day (Figure 3.1C,D). This concentration was chosen because of the clear period shortening effect, whilst avoiding extreme damping that makes quantification of period length unreliable. This experiment allows plotting of a phase-response curve (Figure 3.1D), which shows how much the phase is changed as a function of time of drug treatment. I found that there was “type 0 phase-resetting”, i.e. phase was always reset to the same point no matter what the phase of drug addition (Figure 3.1C, D). This suggests that picrotoxin is a strong synchroniser, capable of resetting the clock

regardless of its original phase. Therefore it is likely that the cellular target of picrotoxin is a state variable of the clock.

3.2.2 Picrotoxin increases PER2::LUC half-life

Next, I reasoned that since picrotoxin had a strong effect on PER2::LUC activity and phase, it was likely that picrotoxin targets PER2. More specifically, an increase in half life could lead to rapid accumulation of PER2::LUC molecules, resulting in the increase in PER2::LUC activity. To test this, I cultured cells in the absence of luciferin in the medium, and collected cell lysates at various times (Figure 3.2A). I then performed luciferase assays on the lysates to measure the amount of PER2::LUC molecules were present relative to control at the time of collection. This is preferable to the longitudinal bioluminescence assays, where luciferase activity is a function of the amount of luciferase enzyme synthesised over the preceding 2 hours [132]. These acute luciferase assays showed that levels of PER2 were higher after picrotoxin treatment compared to vehicle (Figure 3.2A). This suggested that there were indeed more molecules of PER2 in cells that had been treated with picrotoxin.

This finding could be explained by a change in half-life of PER2::LUC. To test this I treated cells with a saturating concentration (10 μM) of the protein synthesis inhibitor cycloheximide (CHX). This resulted in a decay in bioluminescence that was readily fit with an exponential decay model. This technique showed that PER2::LUC half-life was increased by a small (roughly 12 minutes) but significant amount (Figure 3.2C).

These results suggest that picrotoxin may affect the circadian clock either directly or indirectly through the stabilisation of PER2.

3.2.3 Picrotoxin has some irreversible effects

During my experiments I observed an unexpected phenomenon that was not reported previously. Upon wash-off, the effect of period shortening was reversible as seen before (Figure 3.3A, B), although there was a dose-dependent irreversible phase advance and increase in amplitude relative to controls (Figure 3.3B, C). The reference point used to calculate relative phase was the time of the second peak after the wash, in the vehicle-treated condition (Figure 3.3A, top green arrow). This residual effect of picrotoxin suggested that the drug may bind to its target covalently or with very high affinity, and that the target is long-lived in the cell.

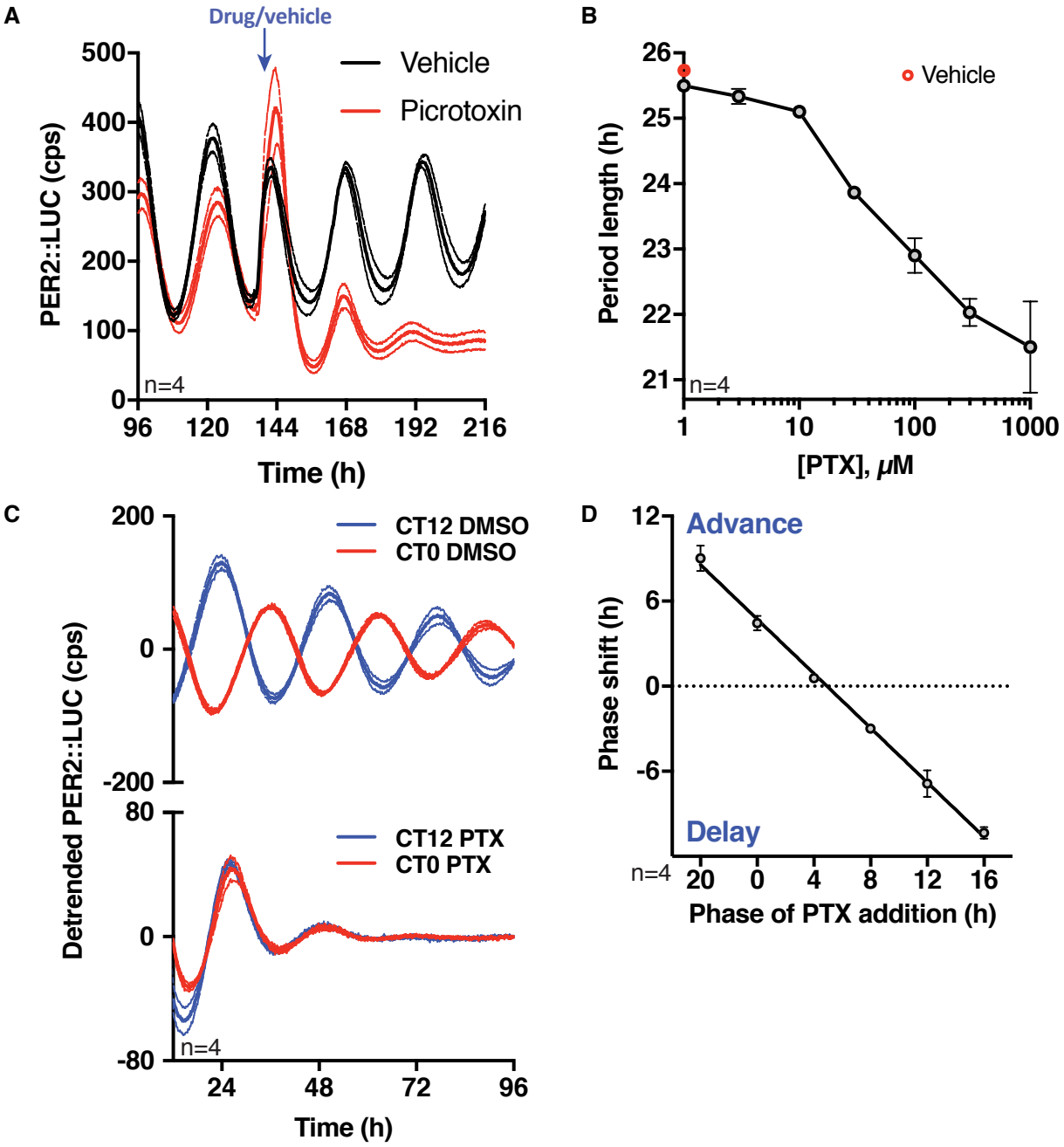

Figure 3.1 Picrotoxin shortens period length and resets circadian phase. A) Longitudinal bioluminescence recordings of fibroblasts treated with 100 μM picrotoxin or DMSO vehicle at the time indicated by the blue arrow. Mean±SEM, representative of N=3. **B)** Dose-response curve showing period-shortening effect of picrotoxin. The period length of the vehicle condition (i.e. 0 μM) is annotated in red. P<0.0001, one-way ANOVA, mean±SD. **C)** Examples of detrended bioluminescence traces showing that phase is set to the same point irrespective of time of 100 μM picrotoxin addition. Mean±SD. This experiment was performed with the help of Daniel Fernando, who carried out some of the time points and performed the initial analysis. **D)** Phase-response curve showing type 0 resetting. Mean±SD.

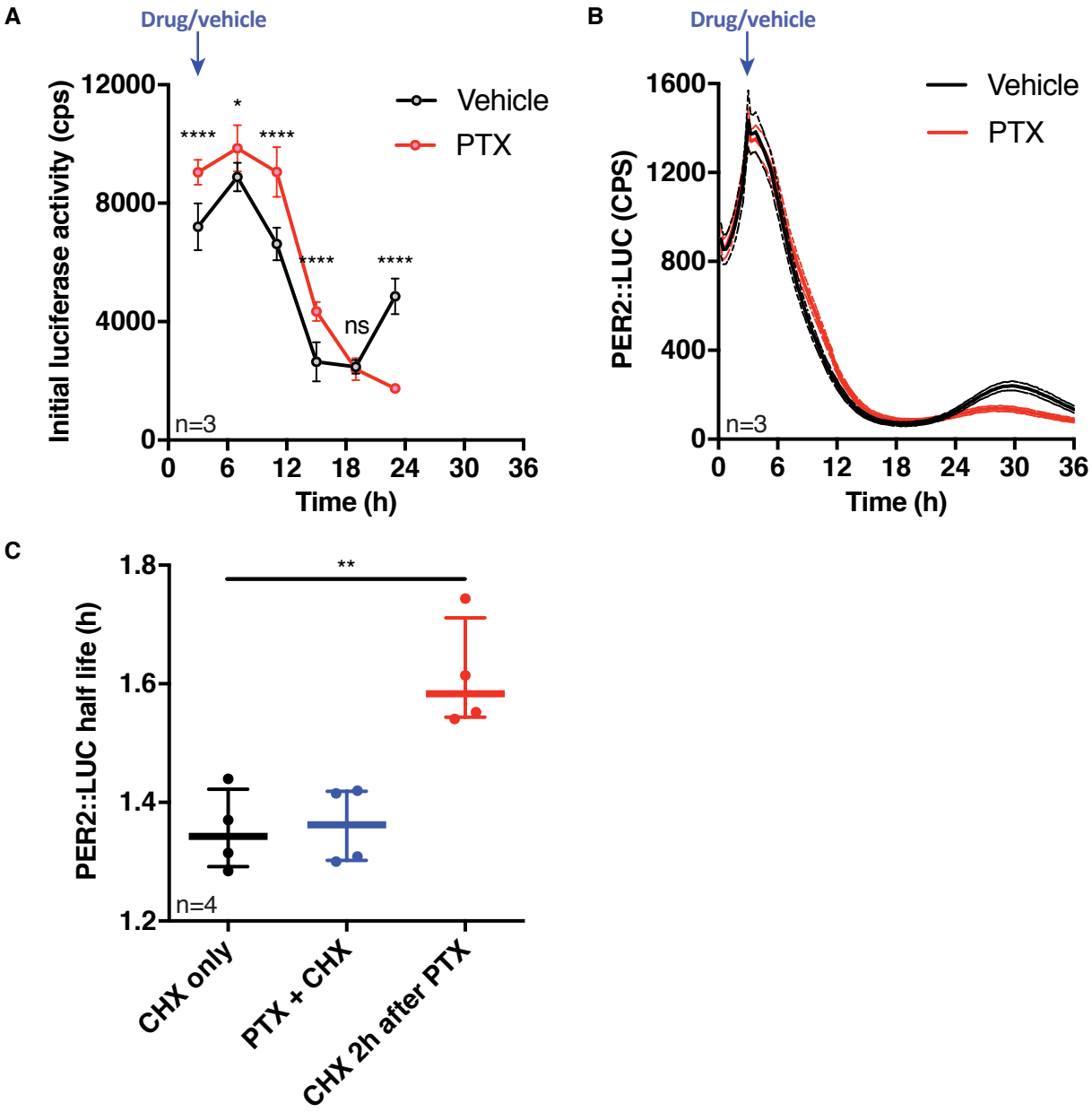

Figure 3.2 Picrotoxin increases the stability of PER2::LUC. A) Acute luciferase activity assays showing increased PER2::LUC levels. X-axis is time after medium change. Drug/vehicle was added at T=3h. P<0.0001, 2-way ANOVA, Holm-Sidak post-test. Mean±SD. **B)** Longitudinal bioluminescence recording performed in parallel to A) for reference. Mean±SEM. **C)** PER2::LUC half-life measured from exponential decay curves generated by addition of 10 µM cycloheximide on its own ("CHX only"), at the same time as ("PTX + CHX"), or 2 hours after ("CHX 2h after PTX"), addition of picrotoxin, Student's t test, n=4, representative data shown of N=2.

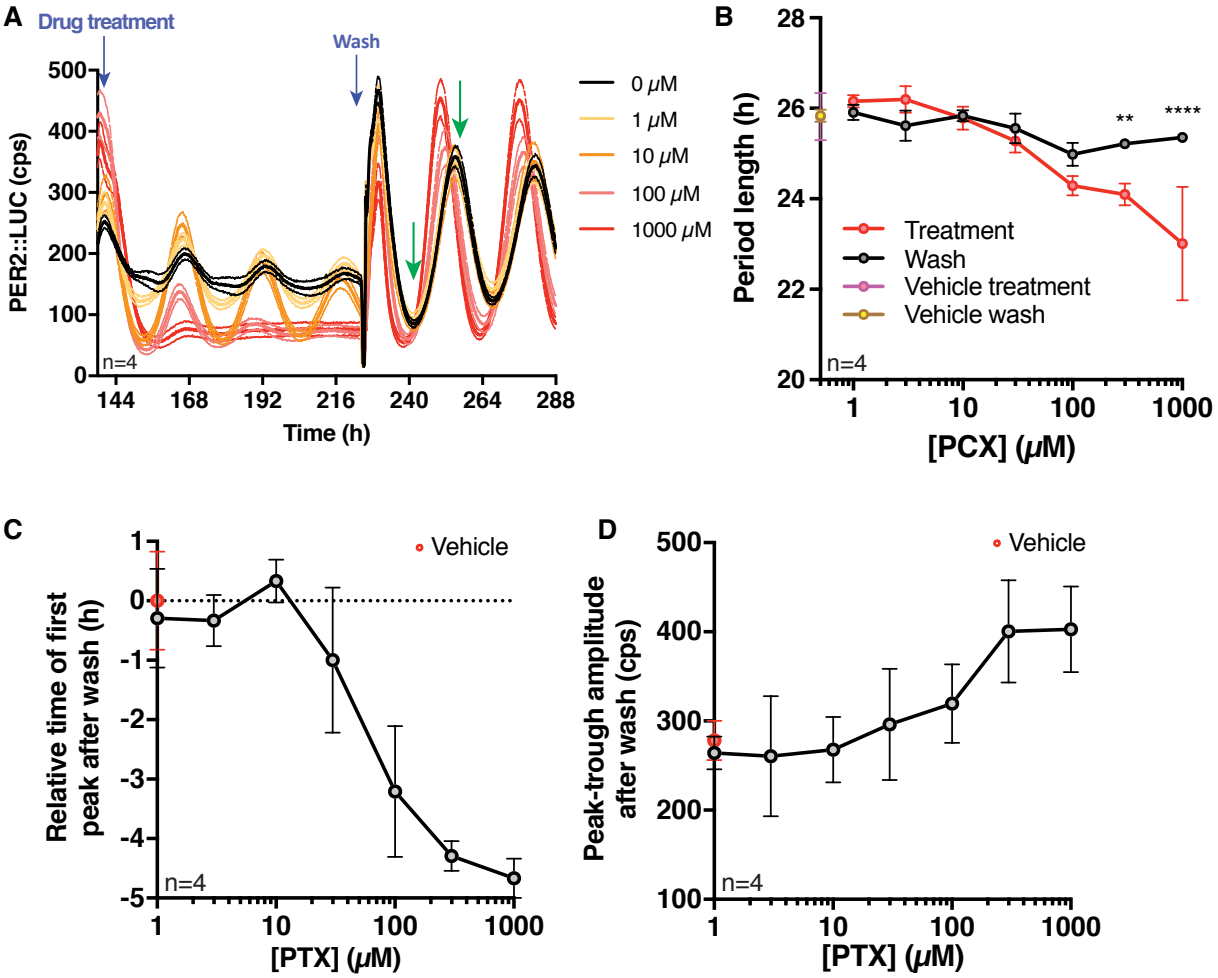

Figure 3.3 The irreversible effects of picrotoxin. A) Longitudinal bioluminescence showing the wash-off after drug treatment. Mean±SEM. Green arrows show the features used to manually measure phase and amplitude. **B)** Quantification of period length in A), comparing drug treatment (red) and wash-off (black). The period lengths for the vehicle treatment and subsequent wash are annotated in magenta and brown respectively on the *y*-axis. Two-way ANOVA, Sidak's multiple comparisons test, mean±SD. **C)** There is a dose-dependent phase advance after picrotoxin wash-off ($p<0.0001$, one-way ANOVA, mean±SD). **D)** There is also a dose-dependent increase in amplitude after picrotoxin wash-off ($p<0.001$, one-way ANOVA, mean±SD).

3.2.4 Removal of Picrotoxin is a strong synchroniser

The formulation of "air medium" is described in Chapter 2. It contains factors that act as strong synchronising cues, including B27 and serum. When these factors are added to cells, they induce PER2 expression, thus synchronising the cellular clocks. B27 and serum have different strengths of synchronisation, so when they are added separately the cells are synchronised to different phases (Figure 3.4A). Given the finding that picrotoxin has effects even upon wash-off, I sought to test whether this was dependent on the synchronising cues in the medium.

The relaxation of the picrotoxin effect caused by the wash abolished the differential response to B27 and serum, instead acting as a very strong resetting signal itself (Figure 3.4B). This indicates that picrotoxin must be targeting a state variable of the clock.

3.2.5 Picrotoxin biochemical characterisation

Picrotoxin is in fact an equimolar mixture of two different compounds: picrotin and picrotoxinin (Figure 3.5A). Both have similar functional groups, and I hypothesised that the epoxide group may be the reactive moiety responsible for covalently binding to thiol groups on its protein target. To test this, I used recombinant human thioredoxin (TRX) as a model protein, since it contains two cysteines that would be accessible to picrotoxin. Ideally this would allow me to analyse the picrotoxin-bound protein by mass spectrometry, thus generating a "fingerprint" that could be used to search the proteome of treated cells for picrotoxin binding.

I designed three reactions that would test my hypothesis (Figure 3.5B). Reaction 1 was the reaction between TRX and picrotoxin. Reaction 2 was the well characterised alkylation of thiol groups by N-ethylmaleimide (NEM), which results in a near-irreversible modification. Reaction 3 is the incubation of the product of reaction 2 with picrotoxin; picrotoxin should not be able to bind to the modified TRX. I hoped to observe these reaction products on a gel, with the product of reaction 1 shifted up by 600 Da due to the added mass from picrotoxin modification, and the products of reactions 1 and 3 both shifted by only 250 Da (due to alkylation by NEM), confirming that picrotoxin was indeed reacting to the thiol groups rather than another part of the protein.

A representative image of the reaction products is shown in Figure 3.5C. There was an upwards shift relative to control associated with the reactions in which NEM was present (reactions 2 and 3), suggesting that this reaction worked. However, there was no shift when incubated with picrotoxin (reaction 1), and no difference between reactions 2 and 3, suggesting that picrotoxin was not binding to thioredoxin. I tested several different pH conditions, reaction times and different temperatures, but all showed the same pattern. I also tried using BSA and

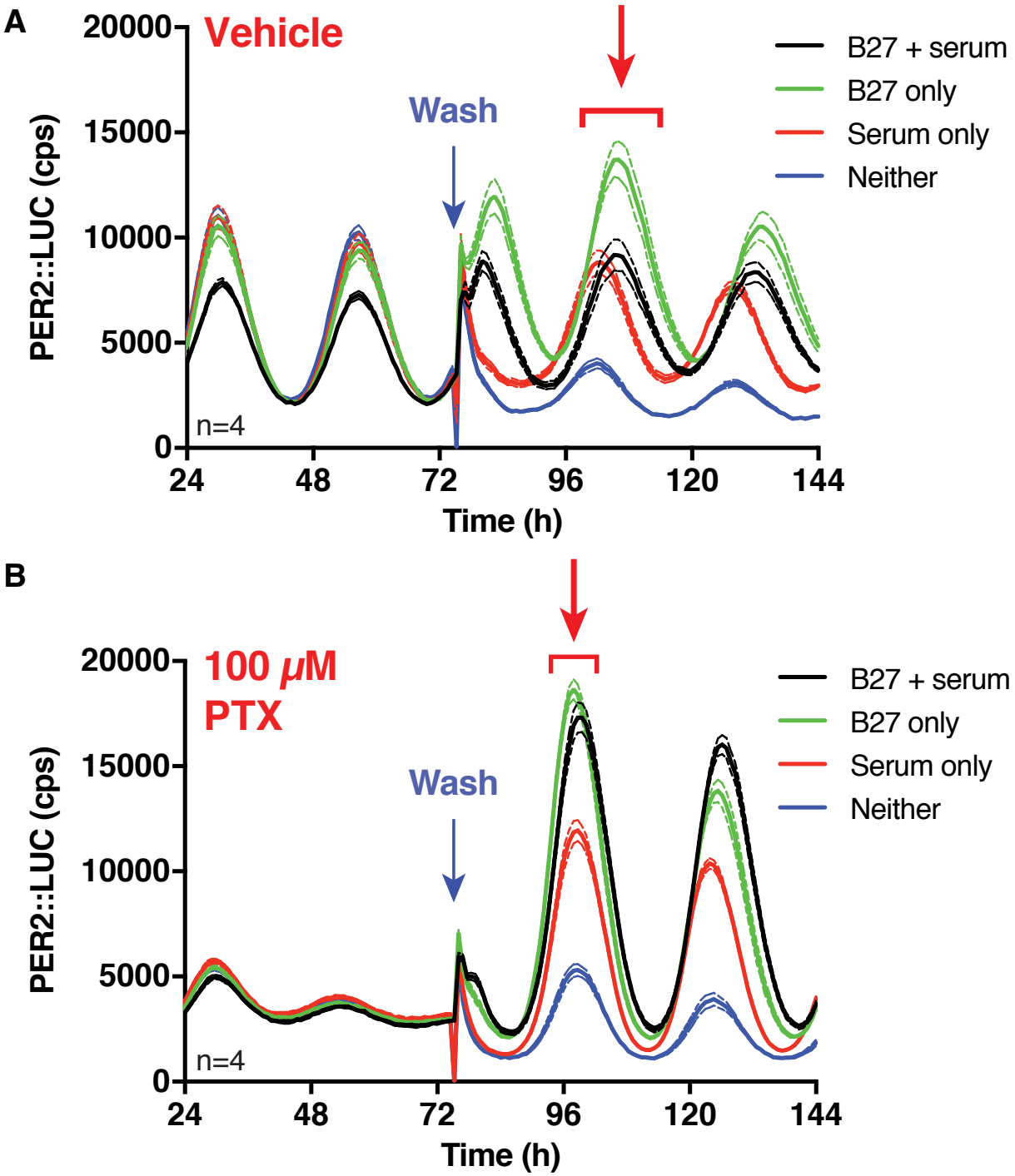

Figure 3.4 Picrotoxin removal is a strong zeitgeber. A) Bioluminescence recordings of cells all treated with DMSO (control) diluted in air medium containing B27 and serum. Where indicated by the blue arrow, cells were washed with medium containing various combinations of B27 and serum or neither. The red arrow indicates phase variation after the wash. Mean±SEM. Relative to control (B27 + serum), the phase ranged between -3.5 h (phase delay) and +13.1 h (phase advance). **B)** Bioluminescence recordings of cells treated with 100 µM picrotoxin dissolved in air medium containing B27 and serum. Where indicated by the blue arrow, cells were washed with medium containing various combinations of B27 and serum or neither. The red arrow indicates phase alignment after the wash. Mean±SEM. Relative to control (B27 + serum), the phase ranged between -2.8 h and +4.8 h.

lysozyme as model proteins as they have more cysteine groups so a larger shift would be seen, but no effect was seen (data not shown).

3.3 Conclusions

3.3.1 Summary of findings

The primary aim of this study was not met, since I did not find the target of picrotoxin. I have confirmed previous observations [246] that picrotoxin reversibly shortens period length. In addition I have found evidence that picrotoxin treatment stabilises the repressive PER2 complex, explaining the initial PER2::LUC induction and rapid damping. There is also evidence for residual effects of picrotoxin following wash-off, suggesting that the mechanism of binding to its target could be covalent or very high affinity, although chemical characterisation has so far been inconclusive.

The current model of the TTFL predicts that processes that stabilise clock proteins would slow turnover and thus lengthen period [249]. In agreement with this, the drug KL001 stabilises CRY and lengthens period [250]. However contradictory findings have been reported. For example, recently synthesised KL001 derivatives stabilise CRY1 and shorten period [251]. In addition it has been found that CRY1 can determine circadian period independently of degradation rate and that the combinatorial phosphorylation of several sites may be more important for period determination [117]. The complex relationship between protein stability and period length is not unique to mammals. For example it has previously been noted that stability of FRQ in *Neurospora crassa*, which has a function in the fungal clock analogous to that of PER2, can be uncoupled from period determination [89]. Thus the observation that picrotoxin shortens period despite stabilising PER2 contradicts the standard model, but similar observations have been made before.

I propose that picrotoxin may stabilise PER2 protein, thus increasing its half-life and resulting in period shortening. The initial induction of PER2::LUC activity may be associated with synchronisation of phase between individual cells – this would need to be tested using single cell bioluminescence imaging in the future. The small increase of half-life of roughly 12 minutes may be enough to shorten period by more than 2 hours, but mathematical modelling would be needed in the future to test this. Picrotoxin likely binds to its target via high affinity interactions, and this could either directly or indirectly result in the effect on PER2 protein. For example, picrotoxin may inhibit CK1, a kinase that targets PER2 for degradation, thus indirectly affecting half-life. Different approaches to finding the target of picrotoxin are needed to explore these possibilities further.

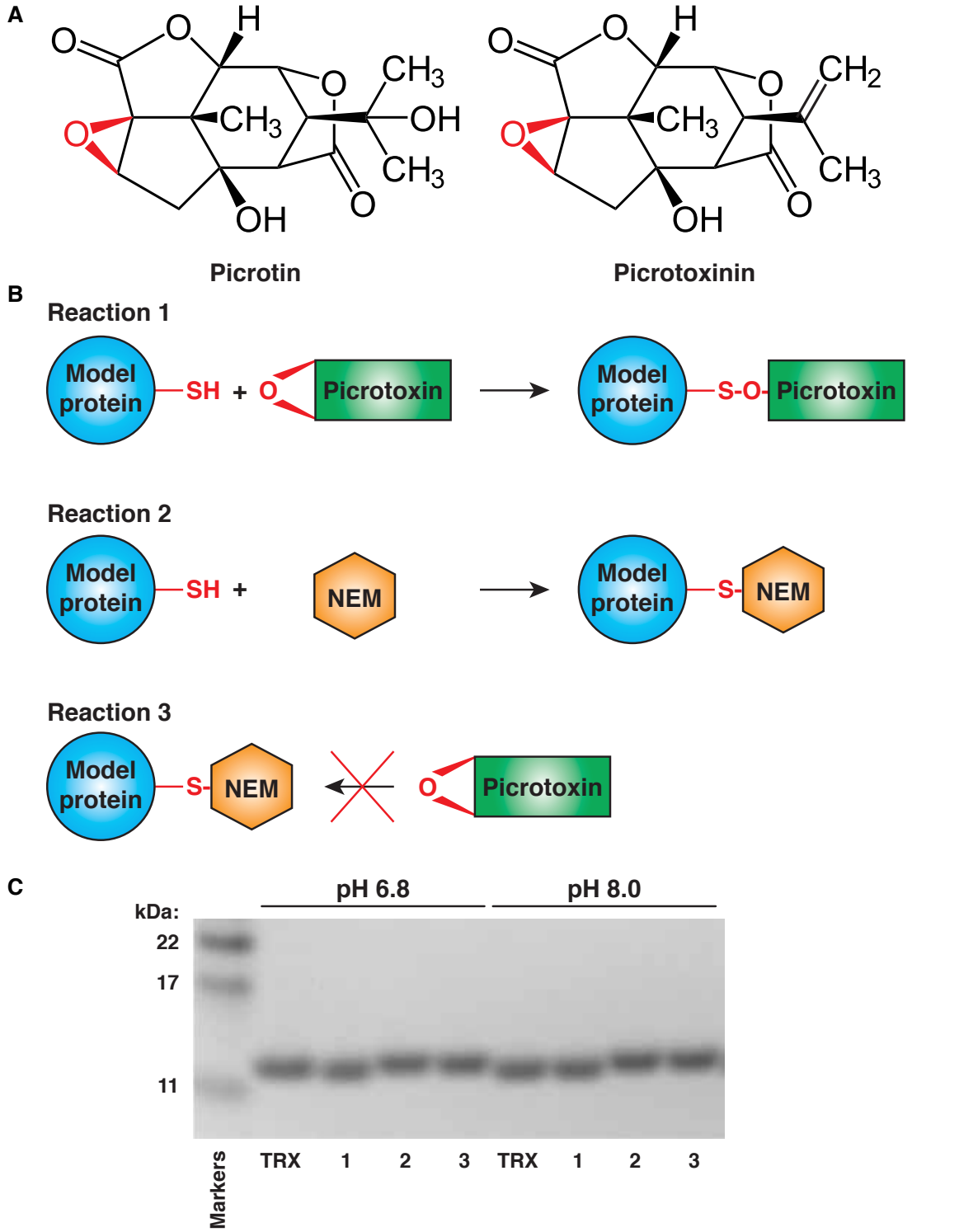

Figure 3.5 Assaying the biochemical properties of picrotoxin. A) Picrotoxin is an equimolar mixture of picrotin ($C_{15}H_{18}O_7$) and picrotoxinin ($C_{15}H_{16}O_6$). Epoxide groups are highlighted in red. **B)** Schematic diagrams of 3 reactions used to test the biochemical properties of picrotoxin. Reaction 1 is the hypothesised reaction between a thiol group on a protein and the epoxide group on the picrotoxin molecule. Reaction 2 is the known irreversible alkylation of thiol groups by N-ethylmaleimide (NEM). Reaction 3 represents the alkylated thiol group being unreactive to picrotoxin. **C)** The reactions in B) were performed using thioredoxin (TRX) as the model protein, and the products were run on a gel, along with TRX alone as a control. A representative image of such a gel is shown, where reactions took place on ice for 90 mins at different pH values. TRX has a molecular weight of 11.7 kDa, picrotoxinin 292 Da, picrotin 310 Da and NEM 125 Da.

3.3.2 Future strategies to find the target of picrotoxin

To test the chemical reactivity of picrotoxin with a functional assay, I would incubate the drug with various hypothetical targets prior to treatment. For example, picrotoxin may be incubated with thioredoxin and then applied to cells. If there is attenuation of the period shortening effect of picrotoxin, that would suggest that thioredoxin has bound and inactivated the drug.

It would be informative to explore the structural effects of picrotoxin on the PER2 complex. PER2 is targeted for degradation through multi-site phosphorylation by CK1 [252, 253]. Assessing the phosphorylation status of PER2 after picrotoxin treatment by immunoprecipitation of tagged PER2 and western blot would be useful for this.

Another useful technique is drug affinity responsive target stability (DARTS) [254, 255]. This involves adding the drug to a cell lysate, resulting in target protein binding to the drug, thus reducing its susceptibility to proteolysis. When the samples are then run on a gel with uncut controls, targets should remain visible upon protein staining with Coomassie blue. These bands can then be cut out and proteins identified by mass spectrometry.

These three approaches together would shed light upon the target of the drug as well as its mechanism of action upon the circadian clock.

Chapter 4

Circadian proteomics and phosphoproteomics

4.1 Introduction

4.1.1 Current understanding – circadian proteomics

As described in Chapter 1, quantitative proteomics is a powerful tool for understanding cellular processes at the systems level. Several circadian proteomics studies have been done using mouse tissues *in vivo* [93, 256, 91, 257, 92] and in SCN slices *ex vivo* [90]. Whilst the mice in these studies were kept in constant darkness, they still exhibit daily rhythms in feeding that have been shown to drive rhythmic gene expression in the liver [227–229], and so the results do not represent the output of the cell-autonomous circadian clock. To understand the cell-autonomous circadian proteome, cell culture systems are ideal since they allow for exposure to truly constant conditions at the cellular level. This would result in a better understanding of the cellular clock rather than the processes involved in responding to feeding cues and light conditions.

To my knowledge, the only published study addressing cell-autonomous circadian regulation of the mammalian cellular proteome was performed using cultured fibroblasts *in vitro* by our laboratory using SILAC and mass spectrometry [137]. In this study, 1608 proteins were identified across the time course, and 237 of these showed a circadian rhythm in abundance. This is far fewer than previous studies of the circadian proteome using SILAC (3132 in Robles and Mann 2014 [92], 5827 in Mauvoisin et al. 2014 [93]). The protein extraction method is the most likely reason for this discrepancy.

The first *in vivo* circadian phosphoproteome was characterised in mouse liver, and revealed the importance of circadian regulation in many signalling pathways [98]. This has since been carried out for mouse hippocampus, and this study showed the importance of circadian regulation

of phosphorylation in synaptic and cytoskeletal processes [258]. Together, these studies suggest that the circadian regulation of phosphorylation is important in the physiology of multiple tissues in mammals. The circadian phosphoproteome has also been characterised in *Arabidopsis* [259] and *Neurospora* [95], suggesting that the physiological importance of the rhythmic regulation of phosphorylation at the proteome level may be conserved among eukaryotic species. To my knowledge, the circadian phosphoproteome has not hitherto been characterised at the cellular level in mammals, and so the cell-autonomous contribution to the circadian control of the phosphoproteome is unknown.

4.1.2 Aims for this chapter

Cells have evolved elaborate mechanisms to regulate the function of proteins in time and space. Whilst the spatial control of cell biology is relatively well understood [260] we are only beginning to appreciate the temporal control of cellular function. To improve understanding of this, I sought to characterise the cell-autonomous circadian control of the cellular proteome and phosphoproteome. More specifically, I wished to assess the contribution of the TTFL to the temporal control of the proteome, and so I compared wild type (WT) cells to CRY1$^{-/-}$; CRY2$^{-/-}$ (CKO) cells. As described in Chapter 1, CKO cells have no functional TTFL, and so they represent a negative control in this experiment.

4.2 Results and discussion

4.2.1 Experimental design

A time course experiment was carried out as described in Chapter 2. Once confluent, cells were entrained for 7 days in temperature cycles. Following this, the medium was changed and the cells were put into constant 37°C, and sample collection began 24 hours later. The experiment was designed so that there were 3 technical replicates per time point, i.e. 3 wells in a 6-well plate per genotype. Detection of the total proteome required very little protein – in the order of 2 µg, but technical replicates were pooled to maximise the amount of protein for phosphopeptide enrichment. Sample preparation is described in detail in Chapter 2, but I will outline the key points here (Figure 4.1). Briefly, the aim was to create several pool samples including all time points of both genotypes to enable comparisons between TMT runs. As a result, each 10-plex TMT experiment included 8 experimental samples and 2 pools. Enzymatic digestion, TMT labelling and fractionation were performed by Dr Sew Peak Chew.

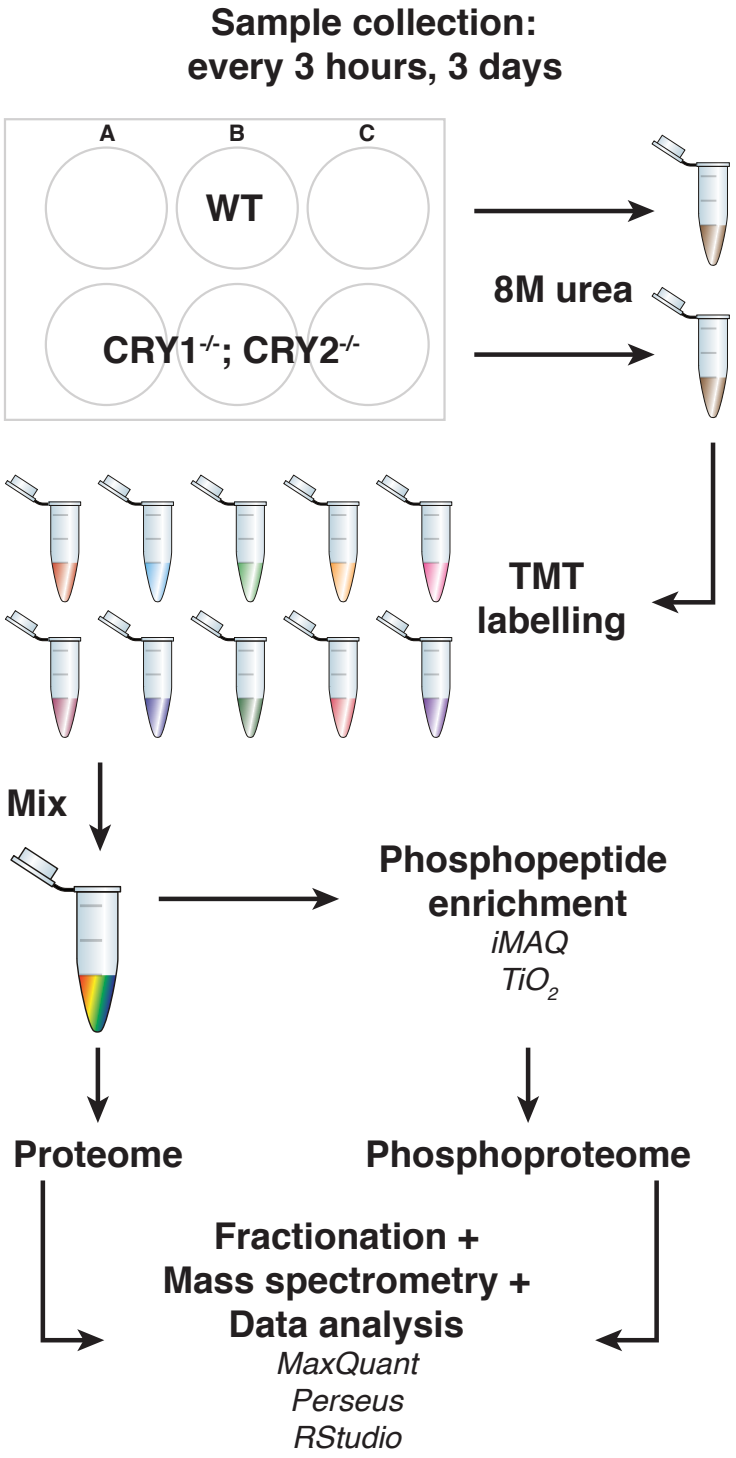

Figure 4.1 Proteomics and phosphoproteomics experimental workflow. At 3-hour intervals over 3 days, confluent monolayers of primary fibroblasts cultured at constant 37°C were lysed in 8 M urea. For both genotypes, 3 technical replicates were combined into one sample. 12 pooled samples were created, and all samples were adjusted to the same protein concentration for trypsin digestion. Peptides were labelled using 10-plex TMT: each set was comprised of 8 time-course samples and two pooled samples. The 10 labelled samples were mixed and split into proteomics and phosphoproteomics workflows. This was repeated for each set of TMT reagents, hence 6 sets in total were used. Peptide and protein identification was performed in MaxQuant, and the data was cleaned using Perseus. The resulting quantitative data was normalized and analysed using statistical tools in RStudio.

4.2.2 Data analysis

Peptide and protein identification were also performed by Dr Sew Peak Chew using Maxquant and Perseus software applications as described in Chapter 2. I used the R programming language for subsequent bioinformatic analysis due to the extensive statistical libraries available. The sample loading normalisation required proteins to be present in all samples and pools because this method assumes that an equal amount of protein was loaded into the mass spectrometer for each sample. Internal reference scaling (IRS) permits the comparison of protein levels between TMT experiments because all the pools theoretically contain the same amount of every protein. This technique was first described by Phillip A. Wilmarth [232].

Several statistical tests have been developed for the analysis of rhythmicity. Non-parametric methods do not make assumptions related to experimental noise and the nature of the underlying model, by analysing the ranks of values rather than the measured values themselves. The JTK_CYCLE programme uses this type of method for rhythm detection, but it is not suitable for detecting waveforms that are not sinusoidal in shape. The RAIN (Rhythmicity Analysis Incorporating Non-parametric methods) algorithm was created to address this problem, and it was shown to out-perform JTK_CYCLE in sensitivity [233]. I therefore chose to use the RAIN algorithm and compared it against Metacycle, which is a programme that combines 3 different methods of rhythm detection for reliability: JTK_CYCLE, ARSER (ARS) and Lomb-Scargle (LS) [234].

I used the WT dataset to compare Metacycle with RAIN. Metacycle found 135 rhythmic proteins, and 76% of these were also detected as rhythmic by RAIN (Figure 4.2A). RAIN found 589 rhythmic proteins, 487 of which were not detected by Metacycle. This is in line with the increased sensitivity, particularly for non-sinusoidal waveforms, reported by Thaben and Westermark in their original publication [233]. For this reason I decided to use the RAIN algorithm for the rest of my analyses.

The presence of rhythmicity does not guarantee biological relevance; if a protein shows very small changes in abundance over the circadian cycle, this is unlikely to be functionally relevant. I sought a statistical method to generate a threshold for this. The distribution of relative amplitudes of rhythmic proteins in WT cells was used to decide an inclusion threshold for proteins that varied in abundance significantly. The cumulative distribution function of relative amplitude is shown in Figure 4.2B, with the median and quartiles annotated. The 25% quartile was situated at a relative amplitude of approximately 0.1, and I set this as my threshold. Hence the bottom quartile of each dataset was considered functionally arrhythmic.

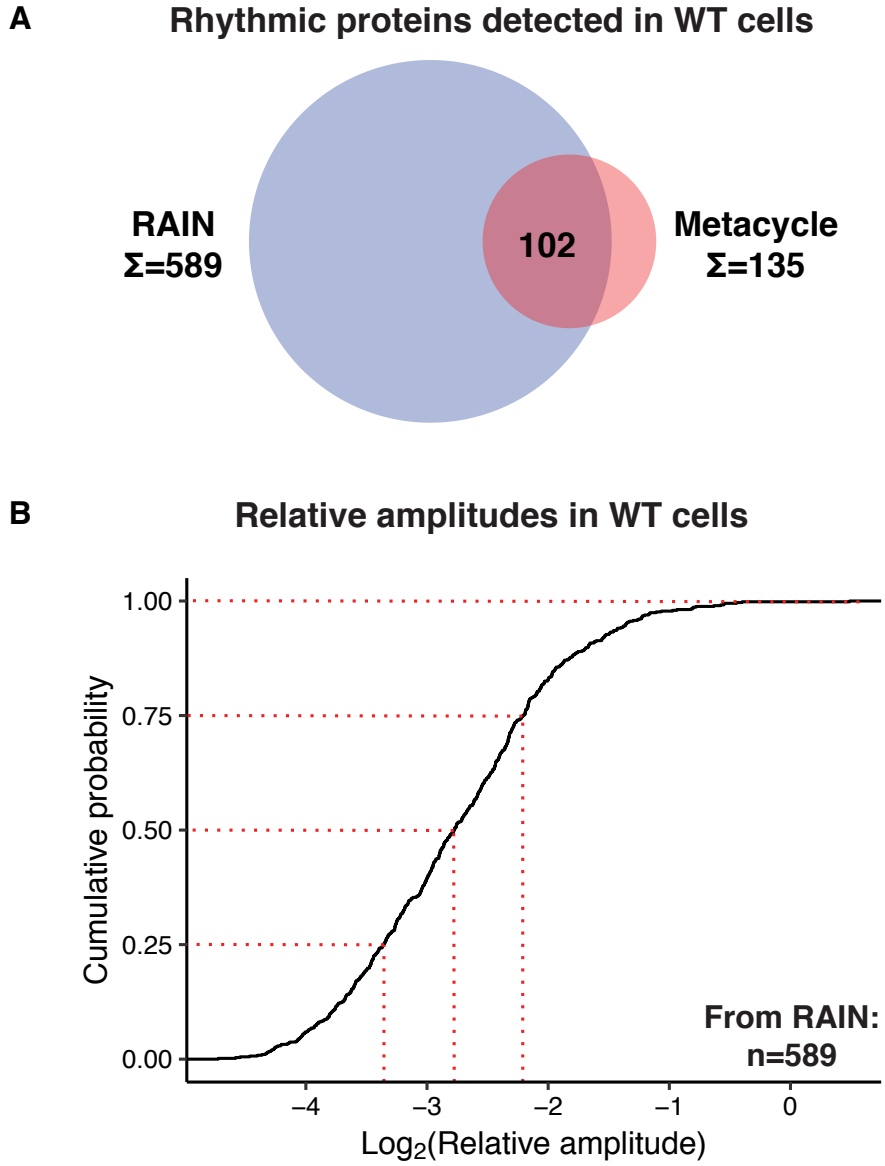

Figure 4.2 Definitions of rhythmicity – statistical and functional. A) In the WT dataset, the RAIN algorithm detected 589 rhythmic proteins. Metacycle detected 135 rhythmic proteins, and 102 of these were also detected by RAIN. Given this overlap and the known advantages of RAIN (see text), this algorithm was used as a statistical definition of rhythmicity. **B)** Relative amplitudes of the proteins detected as rhythmic by RAIN were calculated. They are plotted here as a cumulative distribution function, with the 25%, 50%, 75% and 100% quartiles annotated. Proteins with relative amplitude below the 25% quartile were deemed functionally arrhythmic. This corresponded to a relative amplitude of 10%, and so this was the threshold used in the analysis of the rest of the dataset.

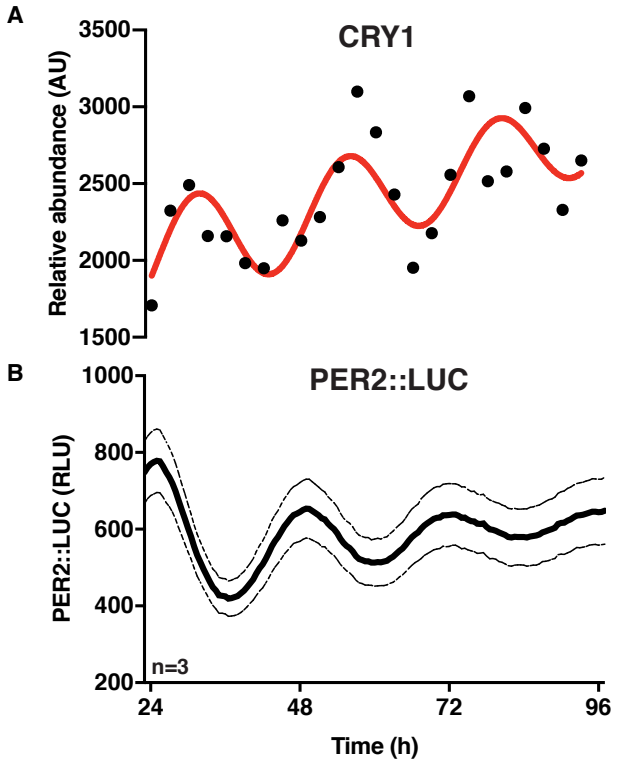

Figure 4.3 Benchmarking using CRY1. **A)** The relative abundance of CRY1 detected in the WT dataset is plotted. It was not found statistically rhythmic by RAIN (p=0.07), but it was fit by a damped cosine wave in preference to a straight line (Extra sum-of-squares F test, p=0.01). The damped cosine is plotted in red. **B)** Longitudinal bioluminescence recording of WT PER2::LUC fibroblasts, performed simultaneously with the proteomics experiment as a phase marker. Mean±SEM.

4.2.3 Validation with clock proteins

I used the WT dataset to confirm whether my bioinformatic processing hitherto had been appropriate or if I had made mathematical errors. To do this I sought out known clock proteins to examine the circadian profile. CRY1 was the only clock protein detected in all the WT samples (it was not detected in the CKO samples at all) (Figure 4.3A). CRY1 abundance was rhythmic with a phase slightly delayed relative to the parallel PER2::LUC recording (Figure 4.3B). CRY1 protein rhythms at the cell autonomous level have not been reported before, but it is known that the phase of its mRNA is similarly delayed relative to that of Per2 mRNA [34]. Since this agreed with expectations, I was confident that my normalisation and analysis method was appropriate.

4.2.4 Coverage

My data analysis included 5718 proteins that were present in all samples and pools. For phosphoproteomics, this number was 3164 phosphopeptides. 7% of the wild-type proteome was rhythmic with a relative amplitude of $\geq$10% (Figure 4.4A). The previous proteomics study from our lab using cells in culture found that roughly 15% were rhythmic [137] and the discrepancy

is likely due to the large difference in overall coverage. However, the figure of 15% is similar to studies using mouse tissues in vivo [93, 256, 91, 257, 92]. Studies using mouse tissues are not examining temporal coordination by the endogenous cellular clock because of the presence of physiological zeitgebers like feeding rhythms resulting in daily rhythms of insulin which is known to entrain the TTFL and drive rhythmic gene expression [226, 227]. Hence previous studies are likely to have over-estimated the proportion of the proteome under cell-autonomous circadian control. Furthermore, none of those studies filtered out proteins with low relative amplitude. Indeed, in a study using SCN slices ex vivo the authors estimate between 6-13% of the proteome being under rhythmic control [90].

3164 phosphopeptides were detected in all the samples, of which 8.8% were rhythmic with a relative amplitude $\geq$10% in wild-type cells (Figure 4.4B). There have been no similar experiments in cell culture, although a study with mouse liver gave a figure of 25% of detected phosphopeptides being under circadian control [98] with a large amplitude as defined by fold-change. This study had a much larger coverage, with over 20,000 phosphopeptides detected, probably due to the large amount of material available in livers. The same caveat regarding non-cell autonomous control of the proteome as described above applies here. Strikingly a larger proportion of the detected proteome (18.2%) and phosphoproteome (17.9%) was rhythmic in CKO relative to WT cells (Figure 4.4B).

The findings here are not compatible with the current paradigm for timekeeping mechanism within the circadian field as described in Chapter 1, that the TTFL is required for the generation of circadian rhythms in mammalian cells (i.e. the TTFL model). If the post-translational oscillator (PTO) model is correct, a naïve assumption might be that whilst some proteins may be rhythmic in CKO cells, the number would be far fewer since there is no signal amplification by the TTFL. The fact that a *larger* proportion of the proteome and phosphoproteome is under rhythmic control means that something more interesting may be afoot. More specifically, the TTFL could be *suppressing* rhythms instead of generating them. To find out more, I explored the identities of the rhythmic proteins and phosphopeptides.

4.2.5 Rhythms in cellular ion content

I inspected the proteins and phosphopeptides that were rhythmic in both genotypes, since these represent direct outputs of TTFL-independent timekeeping, and may even include components of the clock mechanism itself. There were 156 proteins and 65 phosphopeptides that were rhythmic in both genotypes (Figure 4.5A, Appendix Table 1, Appendix Table 2). The 156 rhythmic proteins were highly enriched for transmembrane ion transporters (Figure 4.5B). The electroneutral co-transporter Na-K-Cl (NKCC1, *Slc12a2*) was rhythmic in abundance (Figure 4.5D, Appendix Table 1), suggesting that rhythmic ion fluxes may be driven by these oscillations. Circadian regulation in the abundance and activity of these ion channels has also been seen in

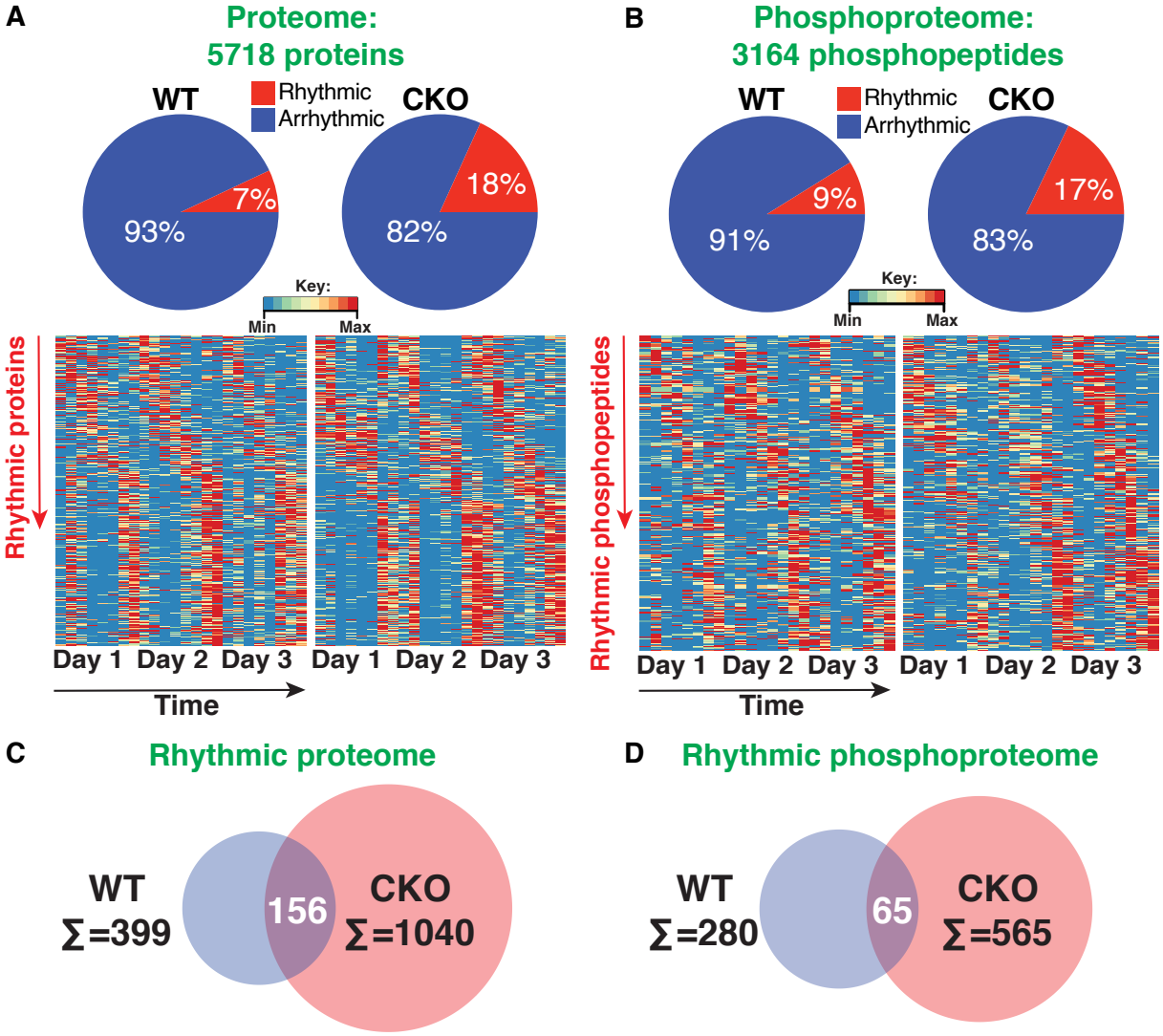

Figure 4.4 Global features of the circadian proteome and phosphoproteome. A) 5718 proteins were detected in all samples and pools. Of these, 7% were rhythmic in WT and 18% in CKO. The heatmaps show min-max normalized plots for all the rhythmic proteins in WT (left) and CKO (right) as a visual representation of the efficacy of the data processing method. Each row is a protein (sorted by phase), and each column is a time point from the time-course experiment (3h intervals over 3 days). **B)** 3164 phosphopeptides were detected in all the samples and pools. Of these, 9% were rhythmic in WT and 17% in CKO. The corresponding heatmaps also show the efficacy of the data processing. Each row is a phosphopeptide (sorted by phase), and each column is a time point from the time-course experiment (3h intervals over 3 days). **C), D)** Venn diagrams showing the numbers of rhythmic proteins and phosphopeptides for WT and CKO cells, with the overlaps annotated.

other studies *in vivo* [261] and *in vitro* [262]. Working with Dr Alessandra Stangherlin and Dr Jason Day, we found that ion concentrations were under rhythmic control, including sodium and potassium (Figure 4.5C). Other ions such as iron were not rhythmic in WT (p=0.06, RAIN) but rhythmic in CKO (p<0.001, RAIN). Sodium and potassium were rhythmic in both WT and CKO (p<0.0001, RAIN). Rhythms in magnesium and potassium have been observed before [109], and my results supplement this by expanding the number of ions measured.

Oxidative Stress Response 1 (OSR1, *Osxr1*), is a kinase that interacts with [263] and regulates NKCC1 activity [264]. OSR1 exists in a complex with the protein kinase WNK1 (With No Lysine [K]), and this complex is required for NKCC1 function [265]. In my phosphoproteomics dataset, phosphosite S339 in OSR1 was rhythmic in both WT and CKO (Figure 4.5E, Appendix Table 2). The relative amplitude of this oscillation was around 20%, suggesting that it may be physiologically significant. Together, these findings suggest that rhythmic ion flux may be driven by rhythmic OSR1 activity. In the future, this result will be validated by western blot against this phosphosite. In addition, genetic and pharmacological inhibition would be useful to test the contribution of this pathway in the circadian regulation of intracellular ion content.

Since such changes in ion concentrations would likely result in a change in osmolarity of the intracellular environment if unbuffered, we decided to test for circadian changes in cell volume. Dr Alessandra Stangherlin found that the majority of WT cells showed no circadian rhythm in cell volume (Figure 4.5F). Whilst 16% of cells did exhibit a circadian change in cell volume, this cannot explain the magnitude of ion rhythms at the population level, which was in the order of 50% relative amplitude (Figure 4.8A, B). Given the nature of the protocol when establishing primary cell lines (Chapter 2), it is plausible that there may be some heterogeneity in the cell culture, resulting in this phenomenon. It may be that the cells that do have circadian variation in volume may have a different process regulating this, and in the future cell sorting may be a way to assess this if a suitable biomarker is found.

In summary, the observed rhythms in intracellular ion concentrations were likely to be generated by rhythms in plasma membrane transporter activity. Furthermore, I hypothesised that since intracellular osmolarity must be defended [266], another process must be responsible for compensating for the changes in ion concentration. Almost 25% of the cell by weight is protein [203] so I explored the proteomics dataset to find out whether changes in global protein content could contribute to this compensation.

4.2.6 Rhythms in cytosolic protein concentration

It seemed feasible that the protein content of the cell may change to compensate for the rhythmic variations in intracellular ion concentration to maintain osmostasis. Circadian rhythms in translation have been reported before [267–269], and OSR1 is phosphorylated by the mammalian target of rapamycin complex 2 (mTORC2) [270]. mTORC2 has many functions including the

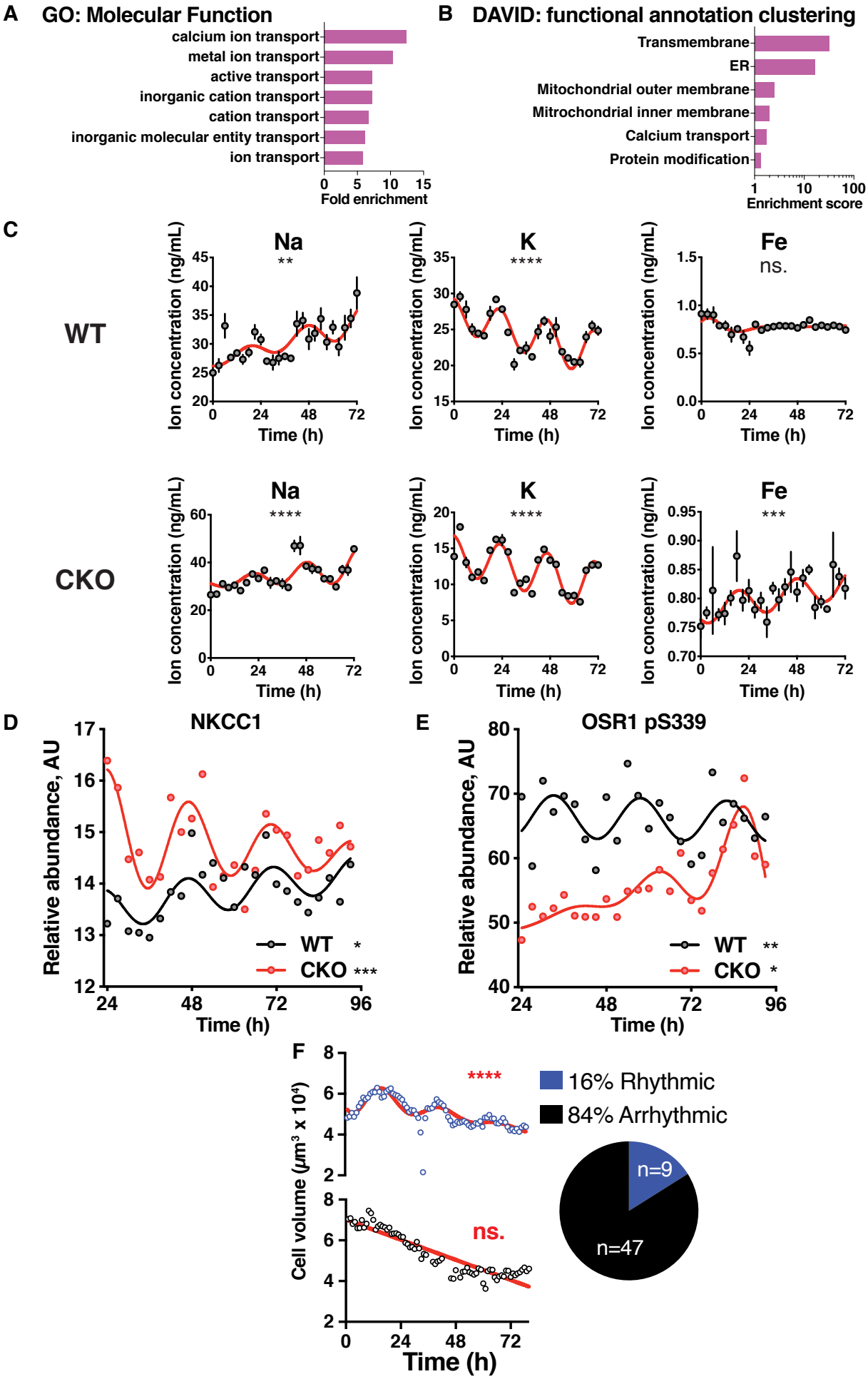
A
GO: Molecular Function
calcium ion transport
metal ion transport
active transport
inorganic cation transport
cation transport
inorganic molecular entity transport
ion transport
0 5 10 15
Fold enrichment
B
DAVID: functional annotation clustering
Transmembrane
ER
Mitochondrial outer membrane
Mitrochondrial inner membrane
Calcium transport
Protein modification
1 10 100
Enrichment score
C
WT
CKO
Na
K
Fe
ns.
Ion concentration (ng/mL)
Time (h)
D
NKCC1
Relative abundance, AU
WT *
CKO ***
Time (h)
E
OSR1 pS339
Relative abundance, AU
WT **
CKO *
Time (h)
F
Cell volume (μm³ x 10⁴)
16% Rhythmic
84% Arrhythmic
n=9
n=47
Time (h)

Figure 4.5 Circadian regulation of cellular ion content. A), B) GO analysis and DAVID functional annotation of the proteins that were rhythmic in both genotypes. **C)** ICP-MS was used to measure concentrations of various ions in a time-course conducted under the same conditions as the proteomics experiment, representative of 3 timecourse experiments that were carried out (N=3). Sodium (Na), potassium (K) and iron (Fe) are plotted here. The top row is WT data, the bottom row is CKO. Benjamini-Hochberg-corrected p-values were generated by the RAIN algorithm and annotated using asterisk symbols. Red lines are damped cosines fit to the data for illustration only. Mean±SEM, n=4 throughout. **D)** NKCC1 protein (*Slc12a2*) relative abundance is plotted here, obtained from the quantitative proteomics dataset. Damped cosine fitting is also plotted for visualisation only. RAIN-generated corrected p-values are annotated as asterisks: p=0.049 for WT, p=0.002 for CKO. **E)** OSR1 pS339 phosphosite relative abundance is plotted here, obtained from the quantitative proteomics dataset. Damped cosine fitting is also plotted for visualisation only. RAIN-generated corrected p-values are annotated as asterisks: p=0.001 for WT, p=0.03 for CKO. **F)** WT cell volume data collected by Dr Alessandra Stangherlin across a 3-day time-course, with 1 hour resolution. P-values are annotated symbolically with asterisks, generated by the extra sum-of-squares F test comparing a circadian damped cosine and straight line. Damped cosine and straight line fits are plotted along with time-course data from representative rhythmic (blue) and non-rhythmic (grey) cells.

regulation of translation [271]. I therefore hypothesised that circadian rhythms in translation and ion flux may be linked. To test this I first interrogated the proteomics dataset to look for evidence of phase clustering amongst the rhythmic proteins.

To do this, I used the phase information from the RAIN algorithm estimation – this is the time at which the oscillation of any given protein is at its peak. The phase is reported as number between 3 hours and 24 hours, in 3-hour intervals. Since a rhythm is cyclical, the maximum value for phase is 24 hours. These values correspond to "experimental time", i.e. the time point at which a sample was collected. For example, if the peak abundance of a protein occurred at "experimental time 24 hours", this means that the peaks occur in samples taken at the very beginning of the experiment, 24 hours later, or 72 hours later. I plotted a histogram of these values in a circular form to visually aid the assessment of phase distribution (Figure 4.6). The phase distribution of rhythmic proteins in wild-type cells was clustered at experimental time T24 (Figure 4.6A), and relative to this, the distribution of rhythmic phosphopeptides is more spread out (Figure 4.6B). This phase clustering also occurs in CKO cells, suggesting that this temporal organisation is independent of the TTFL. The main disadvantage of this analysis is that it does not take into account the absolute abundance of proteins or the relative amplitude of oscillation. However, it is a useful indicator of temporal organisation of protein abundance globally.

Phase clustering of proteins has been observed in proteomics studies in other laboratories [95, 98], so this may be a conserved phenomenon. Given this phase clustering, I hypothesised that there may be rhythms in the protein content of the cell. I reasoned that whole cell lysates may contain many structural proteins with long half-lives that would not show circadian rhythmicity, and this could mask the ability to observe rhythms in the abundance of soluble, free proteins in the cytosol.

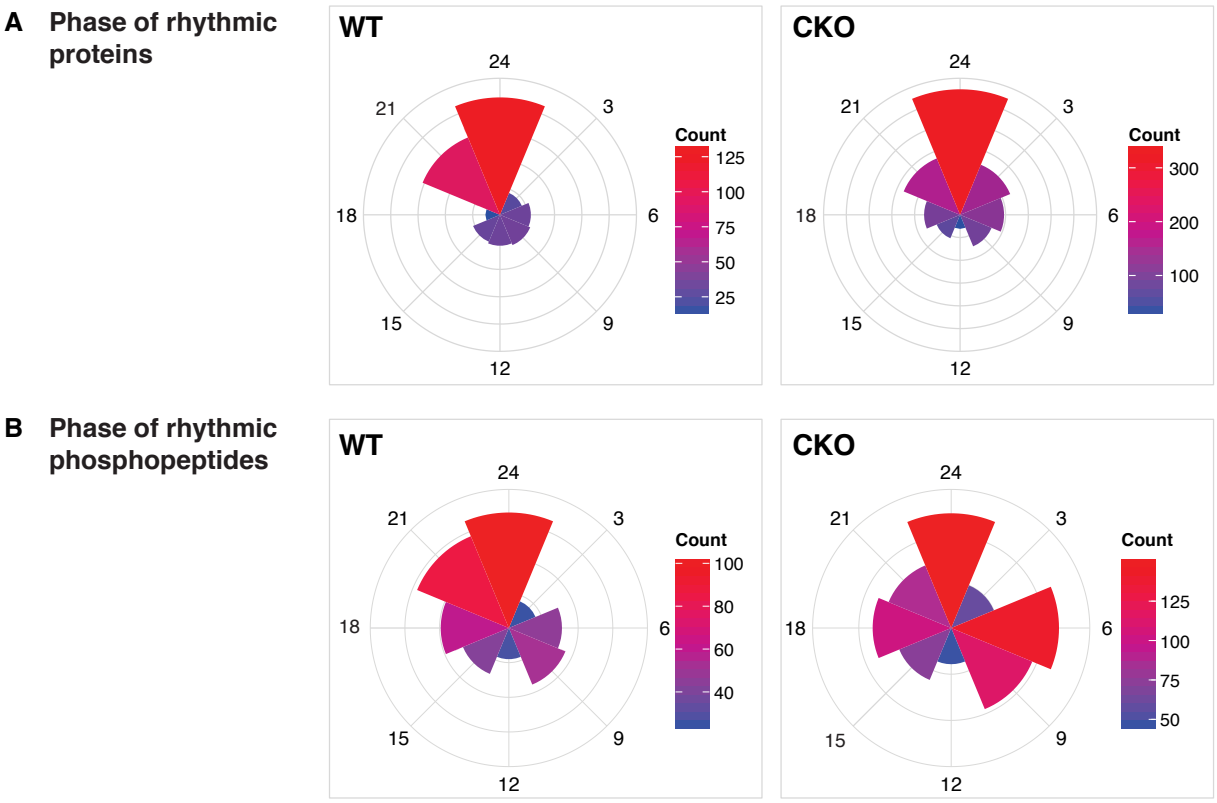

Figure 4.6 Phase clustering of rhythmic proteins and phosphopeptides. **A)** Circular histograms were plotted, taking phase information from the RAIN algorithm output for each protein. Concentric circles represent the counts scale, with the outermost circle marking the upper end of the counts. The time scale between 3-24h is annotated as the spokes in the circle. **B)** Phase diagrams were also plotted for the rhythmic phosphopeptides.

To test this, I used a lysis buffer based on 0.01% digitonin to extract cytosolic proteins. Digitonin is a plant glycoside that permeabilises membranes by forming complexes with membrane cholesterol. Because of this, digitonin selectively disrupts the plasma membrane, since other intracellular membranes such as those of the mitochondria and endoplasmic reticulum have relatively little cholesterol [272–274]. Upon complex formation with cholesterol, pores are formed that allow the passage of molecules with molecular weights of at least 200 kDa [274]. The concentration of digitonin determines the amount of protein extracted, and between 0.01-0.08% (w/v) only soluble cytosolic proteins are released [275]. The process of cytosolic protein extraction is complete after just 2 minutes of incubation with digitonin at 0°C [275], so this is a fast and convenient method compared to other methods such as subcellular fractionation [276].

Using this method I carried out a timecourse experiment, simultaneously performing ICP-MS to measure ion concentration. I found that there were rhythms in cytosolic protein concentration in antiphase to the rhythms in potassium content, and this was also recapitulated in CKO cells (Figure 4.7A). I chose the concentration of digitonin to be 0.01% as this the lower end of the range described above for cytosolic extraction. It would be informative to test a range of concentrations to investigate the extent of cytosolic extraction in my cell type – it is plausible that only the most labile proteins are released using this concentration. In comparison the total protein extracted using RIPA buffer was not rhythmic (Figure 4.7A), but gradually decreasing over time – this may be due to increased protein degradation as a function of time in culture, and this could be tested in future using autophagy markers.

I resolved to validate this finding using an independent method of measurement. The cytoplasm is a crowded environment, and proteins contribute a significant amount to this [203]. The diffusion of macromolecules in such an environment is inversely proportional to their concentration, so I predicted that the rate of diffusion of large particles in the cytoplasm would be higher at the nadir of cytosolic protein concentration. To test this, I collaborated with Joe Watson and Dr Emmanuel Derivery to measure the diffusion of inert quantum dots (QDs). These are nanoparticles roughly 18 nm in diameter that are taken up into the cytoplasm, and they are fluorescent so they may be imaged using confocal microscopy (see Chapter 2 for details of synthesis, imaging and quantification). A similar technique has been used in a recent study that demonstrated the control of biophysical properties of the cytoplasm by mTORC1, likely through ribosomal biogenesis [277]. If my hypothesis was correct, then these quantum dots would show greater diffusion at the trough of cytosolic protein concentration, and less diffusion at the peak of cytosolic protein concentration. Measurements were taken at 12-hour intervals and diffusion coefficient was calculated at each time point (Figure 4.7B, C). Figure 4.7B shows examples of images with software tracking overlaid, illustrating the types of movements displayed by the QDs.

In both genotypes there was a time-of-day difference in diffusion coefficient, but this may be due to the lower diffusion coefficient seen in the last time point – Sidak's multiple comparisons

post-hoc test found no statistically significant difference between 36 hours after the start of the experiment compared to 24 hours (Figure 4.7C). However, there was a trend, with a decrease of 3% between 24h and 36h, and an increase of 8% between 36h and 48h in WT cells, and differences of 5% and 20% respectively in CKO cells. Thus the lower diffusion coefficient corresponds to the peak of the cytosolic protein concentration illustrated in Figure 4.7A. The reason for the small effect size is likely related to the fact that macromolecules other than proteins also contribute to molecular crowding in the cytoplasm. Further biological replicates are needed to confirm this result, particularly whether the measurements at 60h were real, or a technical artefact. This is a functionally relevant experiment, because even small changes in macromolecular crowding affects protein function, as will be explored later. Finally, there were statistically significant differences between WT and CKO cells at 3 of the 4 timepoints, with an effect size of around 16% throughout. This suggests that there is a substantial difference in cytoplasmic crowding between the genotypes, which may have important consequences for the protein homeostasis network. This is explored in more detail in Chapter 6.

These findings suggest that the rhythmic abundance of labile cytosolic proteins may be buffering the changes in osmolarity caused by the rhythms in ion concentrations reported above. An alternative interpretation is that the causal effects are in the other direction, i.e. the rhythms in protein cause the rhythms in ions to buffer osmolarity. Since it is a cyclical process the causality is difficult to unravel. Dr Alessandra Stangherlin has taken this aspect of the project further (Stangherlin et al., in review), and more detailed discussion is beyond the scope of this chapter.

4.2.7 Regulation of protein:ion ratio

Colloidal solutes have greater relative osmotic potential compared with small ionic solutes [278], and so small changes in soluble protein concentration require stoichiometrically larger changes in ion concentration to maintain osmotic homeostasis. I was intrigued to find out if this was reflected in my dataset, so I measured the relative amplitudes of the protein and ion oscillations. The relative amplitudes for both protein concentration and ion content were greater in CKO cells compared to WT (Figure 4.8A, B). Potassium is the most abundant intracellular cation, so I used potassium concentration as a proxy for "ion content". This is consistent with the greater relative osmotic potential of proteins relative to ions.

Because of this I then calculated protein:ion ratio for each timepoint. This is an indicator of the contribution of colloidal and ionic solutes to cytoplasmic osmolarity. For each time point I calculated the average protein concentration between technical replicates, and divided this by the potassium ion concentration. I found that protein:ion ratio was not constant, but rhythmic in WT cells (Figure 4.8C). Notably, CKO cells had a higher average protein:ion ratio (Figure 4.8D) as well as greater relative amplitude (Figure 4.8E), suggesting that these cells may be less able to maintain osmotic homeostasis compared to WT. Maintaining cellular osmotic homeostasis is

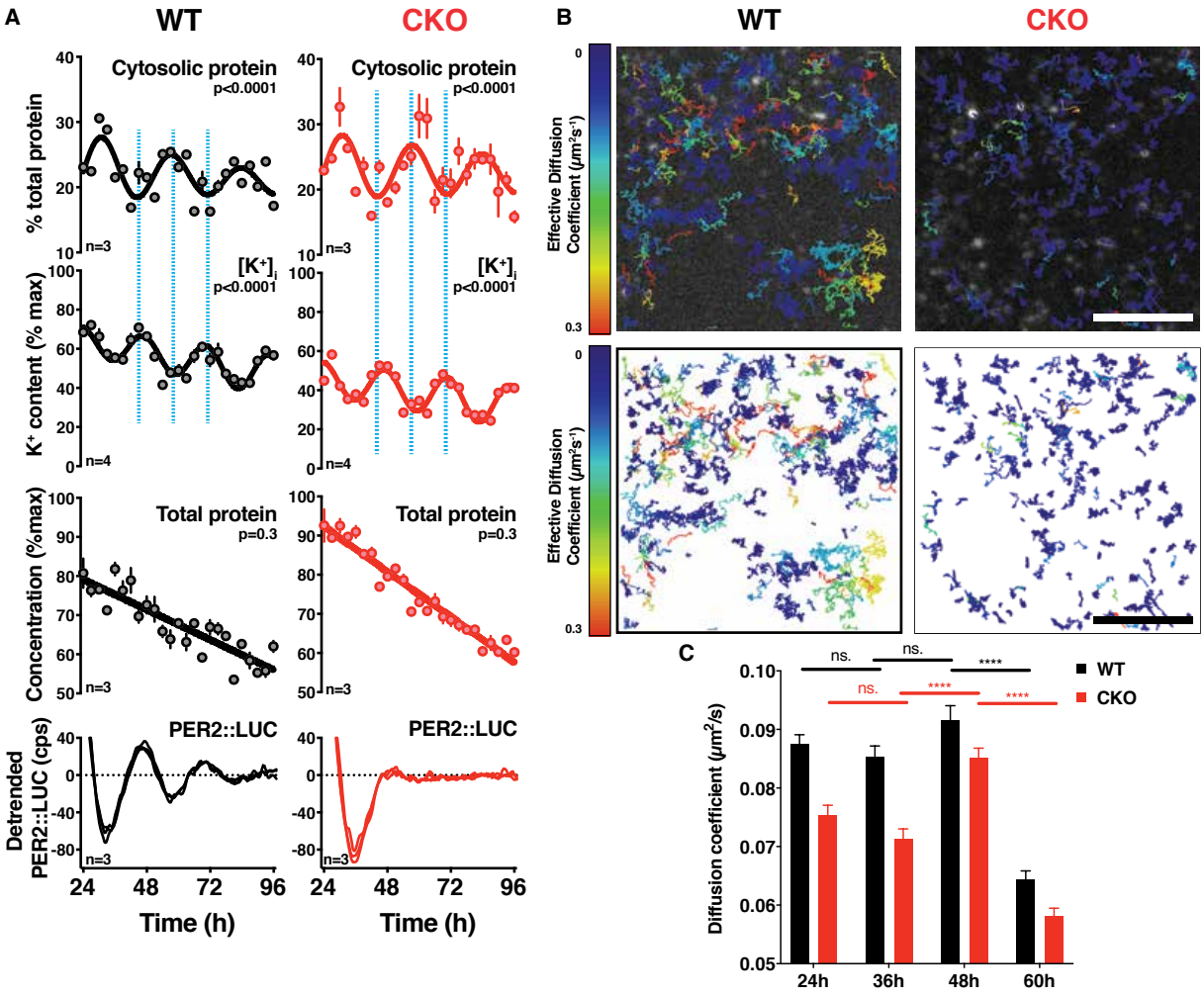

Figure 4.7 Cytosolic protein concentration is rhythmic in antiphase to ions. A) From one time-course experiment, ions, cytosolic proteins and total protein were extracted in parallel samples. The presented experiment is representative of 3 timecourse experiments that were carried out (N=3). Parallel PER2::LUC recordings were also performed and plotted below as a phase marker. Blue lines indicate the antiphasic oscillations in cytosolic protein and potassium concentration. Mean±SEM, p values from RAIN, red lines are fits by a damped cosine or a straight line. **B)** Above: representative images of quantum dots (QD) with diffusion paths annotated. Below: The same images, just showing the diffusion paths. Scale bar 5 μm. The quantum dot synthesis, imaging, image analysis and figure preparation was performed by Joe Watson, and I cultured the cells and loaded them with the quantum dots at each time point. **C)** Diffusion coefficient was plotted for each timepoint for both genotypes. There was time-of-day variation in both genotypes (2-way ANOVA with Sidak's multiple comparisons test, p<0.0001 for time effect, mean±SEM). N=84-135 fields of view across 4 separate dishes of cells at each time point.

important for regulating protein function [266], and so the findings here suggest that CKO cells may have impaired protein homeostasis. This will be explored further in Chapter 6.

The greater relative amplitude of cytosolic protein concentration oscillations in CKO cells could be achieved in two ways: more proteins being under rhythmic control relative to WT or increased amplitude of proteins that are also rhythmic in WT. I plotted probability density histograms from the proteomics dataset to test the distribution of relative amplitude amongst the rhythmic proteins. I found that rhythmic proteins in CKO cells had a higher relative amplitude but there was only a 1% difference, and so this is unlikely to account for the greater relative amplitude of cytosolic protein concentration (Figure 4.8F). This suggests that the greater relative amplitude of oscillations of protein concentration is primarily due to the fact that more proteins are rhythmic in CKO cells compared to WT.

4.2.8 Insights into the clock mechanism

To gain more insight into the mechanism driving these rhythms, I turned to the rhythmic phosphoproteome. Dr Tim Stevens kindly wrote a script using the Python programming language for the identification of kinase recognition motifs amongst the phosphopeptide sequences in my dataset. GSK3 and CK1 are kinases that have been widely implicated in period determination of the circadian clock [139, 146, 113, 149]. They have also been implicated in PTO models of the circadian clock [100, 6], and so I expected these kinases to be highly represented in the rhythmic phosphoproteome.

I used this script to analyse the sequences of phosphopeptides found to be rhythmic in both WT and CKO. I used the set of all phosphopeptides in my dataset as the background, i.e. including non-rhythmic phosphopeptides. Thus I could detect and count kinase recognition motifs in both sets of phosphopeptides. Compared to the background, I found that kinases typically associated with period determination (e.g. GSK3 and CK1) were not over-represented (Figure 4.9). However, these kinases have some of the largest number of motifs in the background dataset. It may be that altering their function by genetic or pharmacological means may have a major effect on period length due to non-TTFL-specific perturbation of cellular physiology. Kinases whose recognition motifs that were over-represented in the rhythmic pool were CAMK2, CHK1, CHK2, NEK-1, PKA, PKB, PKC and PKD. It is possible that some these kinases are therefore instrumental in rhythm generation.

If phosphorylation is crucial to circadian rhythm generation, the specific identities of the phosphopeptides that are rhythmic in both genotypes may give insight into the mechanism. For example, beta-catenin and Ppp1 regulatory subunit 12A were interesting hits. Beta-catenin is a target of GSK3 in the Wnt signalling [279], suggesting that the pathway is under rhythmic regulation as a direct output of the post-translational oscillator. Ppp1 regulatory subunit 12A is a regulator of protein phosphatase 1. Protein phosphatases have been implicated in circadian

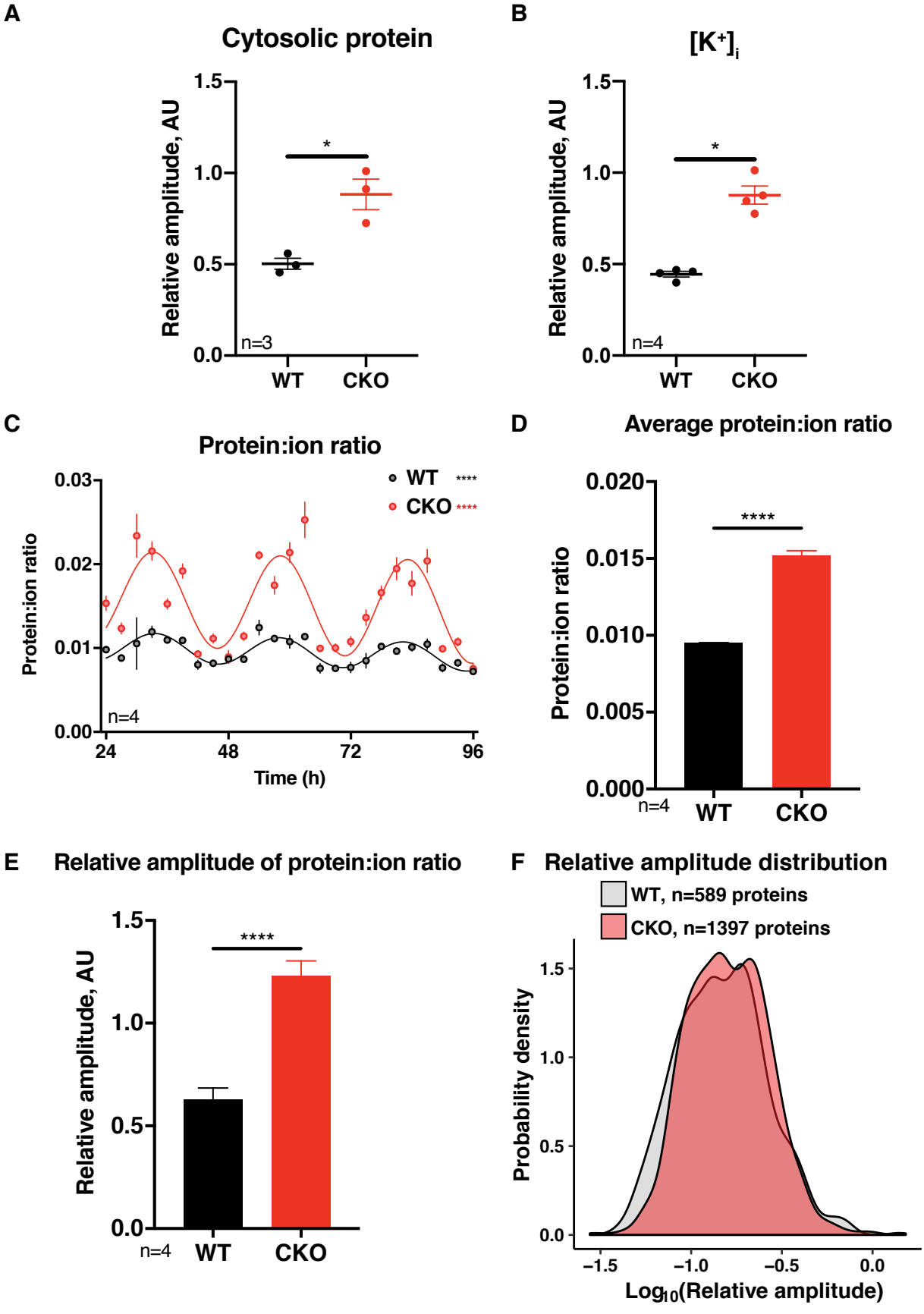
A
Cytosolic protein
Relative amplitude, AU
1.5
1.0
0.5
0.0
*
n=3
WT
CKO
B
[K+]i
Relative amplitude, AU
1.5
1.0
0.5
0.0
*
n=4
WT
CKO
C
Protein:ion ratio
Protein:ion ratio
0.03
0.02
0.01
0.00
WT ****
CKO ****
n=4
24
48
72
96
Time (h)
D
Average protein:ion ratio
Protein:ion ratio
0.020
0.015
0.010
0.005
0.000
****
n=4
WT
CKO
E
Relative amplitude of protein:ion ratio
Relative amplitude, AU
1.5
1.0
0.5
0.0
****
n=4
WT
CKO
F
Relative amplitude distribution
WT, n=589 proteins
CKO, n=1397 proteins
Probability density
1.5
1.0
0.5
0.0
−1.5
−1.0
−0.5
0.0
Log10(Relative amplitude)

Figure 4.8 Protein:ion ratio is dysregulated in the absence of CRY. A) Relative amplitude of cytosolic protein oscillations from Figure 4.7 is greater in CKO compared to WT (Student's t test with Welch correction, mean±SEM). **B)** Relative amplitude of potassium concentration oscillations from Figure 4.7 is greater in CKO compared to WT (Student's t test with Welch correction, mean±SEM). **C)** Protein:ion ratio was calculated from the cytosolic protein and potassium concentrations in Figure 4.7. For each time point, the average cytosolic protein concentration was divided by the potassium concentration of each biological replicate. Mean±SD. P were values calculated by RAIN and annotated using asterisks in the legend. **D)** Average protein:ion ratio was greater in CKO compared to WT (Student's t test with Welch correction, mean±SEM). **E)** Relative amplitude of protein:ion ratio was also greater in CKO compared to WT (Student's t test with Welch correction, mean±SEM). **F)** Distributions of relative amplitudes of rhythmic proteins from the proteomics dataset (WT and CKO analysed separately). Probability density is plotted on the y-axis to make it easier to compare WT (grey) and CKO (red). One-sided Kolmogorov-Smirnov test for alternative hypothesis CKO is greater than WT, p=0.003. WT median = 0.15, CKO median = 0.16.

regulation in the context of dephosphorylation of TTFL components [146, 113, 188]. In general, their activity and specificity are poorly understood relative to kinases, and this antagonistic role may in fact turn out to be crucial for circadian timekeeping.

4.3 Conclusions

4.3.1 Summary of findings

Using proteomics and phosphoproteomics approaches I have characterised the circadian coordination of the proteome, and subsequently uncovered reciprocal regulation of intracellular ion and soluble protein concentration. Furthermore, this is independent of the TTFL, and there are some rhythmic hits from the phosphoproteomics data that will be interesting to follow-up on in the future as potential clock components. Due to limitations of time, experimental validation of targets by western blot was not achieved, and this is an important next step. Furthermore, proteomic study of the proteins liberated by digitonin lysis is needed to confirm the identity of the proteins referred to as 'cytosolic' here, and this should be tested by alternative methods of cytosol extraction, such as differential centrifugation.

4.3.2 Evidence for a post-translational oscillator

The presence of rhythms in CKO cells lends evidence to the post-translational oscillator (PTO) model described in Chapter 1. Moreover, some direct outputs of the PTO exist, for example the antiphasic rhythms in cellular ion content and cytosolic protein concentration, and potentially the Wnt signalling pathway. The mechanism behind this remains unknown, but from my data

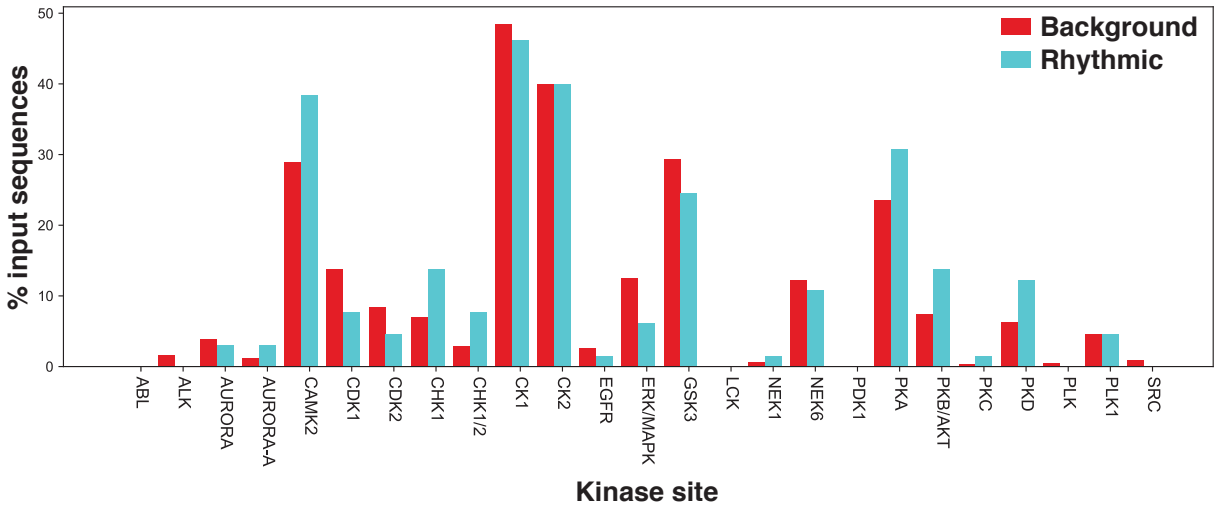

Figure 4.9 Kinase binding predictions from phosphopeptide sequences. Using the phosphoproteomics dataset, phosphopeptides sequences were analysed, with the number of kinase binding motifs counted for a panel of 25 kinases present in the PHOSIDA database. Phosphopeptides that were rhythmic in both genotypes (blue) were compared to the background of phosphopeptides present in all samples and pools (red).

it seems plausible that a PTO may directly or indirectly rhythmically phosphorylate and/or dephosphorylate OSR1, through rhythmic regulation of kinase and phosphatase activity. A way to test this would be to treat cells with kinase inhibitors and carry out a time-course experiment. If protein and ion rhythms are abolished, this would support the hypothesis that rhythmic regulation of kinase activity is necessary for rhythm generation. However the multiple off-target effects of kinase inhibitors may confound this line of enquiry.

This would give rise to rhythms in the activity of electroneutral ion transporters, subsequently leading to the observed rhythms in ion abundance (Figure 4.10). Rhythms in labile cytosolic proteins may be driven by rhythms in translation or degradation of proteins. This may be tested in future by measuring translation and degradation rate using radiolabelled methionine in pulse-chase experiments. Alternatively, the observed rhythms may represent daily rhythms in digitonin extraction from cells. The amount of protein released by this method could be affected by compartmentalisation of proteins or even the phase-separation of proteins into condensations that may not be able to exit the cell. This should be tested in the future by alternative methods of cytosolic protein extraction such as fractionation by centrifugation. In addition, fluorescently labelling cytosolic proteins known to phase separate would enable testing of whether proteins in condensations are liberated by digitonin.

My results show that protein and ion rhythms are likely direct outputs of the PTO. However, it is possible that these may also be mechanistically related, as depicted by dotted arrows in Figure 4.10. For example, rhythms in translation have been reported before that are driven by rhythmic mTOR activity [78]. mTORC2 is known to phosphorylate OSR1 [270], which may be a way in which rhythms in the control of translation feed in to regulate rhythms in ion flux

simultaneously. In Chapter 5 I examine the post-translational oscillator more closely, and show more evidence of its activity.

4.3.3 Novel roles of the TTFL

The finding that more proteins and phosphopeptides were rhythmic in CKO cells is striking. The data suggest that the TTFL may be supressing the rhythmicity of many proteins, decreasing the amplitude of oscillations of protein:ion ratio, thus maintaining osmostasis. To test if this is truly an effect of the TTFL it would be valuable to carry out proteomics experiments and time-course experiments measuring protein and ion concentrations using different clock gene knockouts, such as *Bmal1*.

Osmotic homeostasis must be maintained to prevent disordered protein aggregation and preserve enzyme function [266, 280]. The cytosol is a crowded environment [203], and proteins constitute up to 26% of the cell by weight depending on cell type [203]. Therefore small changes in protein concentration may result in large changes in osmotic potential unless this is counterbalanced. The fact that the amplitude of oscillations in protein:ion ratio are greater in CKO cells suggests that there may be a dysregulation in protein and osmotic homeostasis in these cells. This will be explored further in Chapter 6.

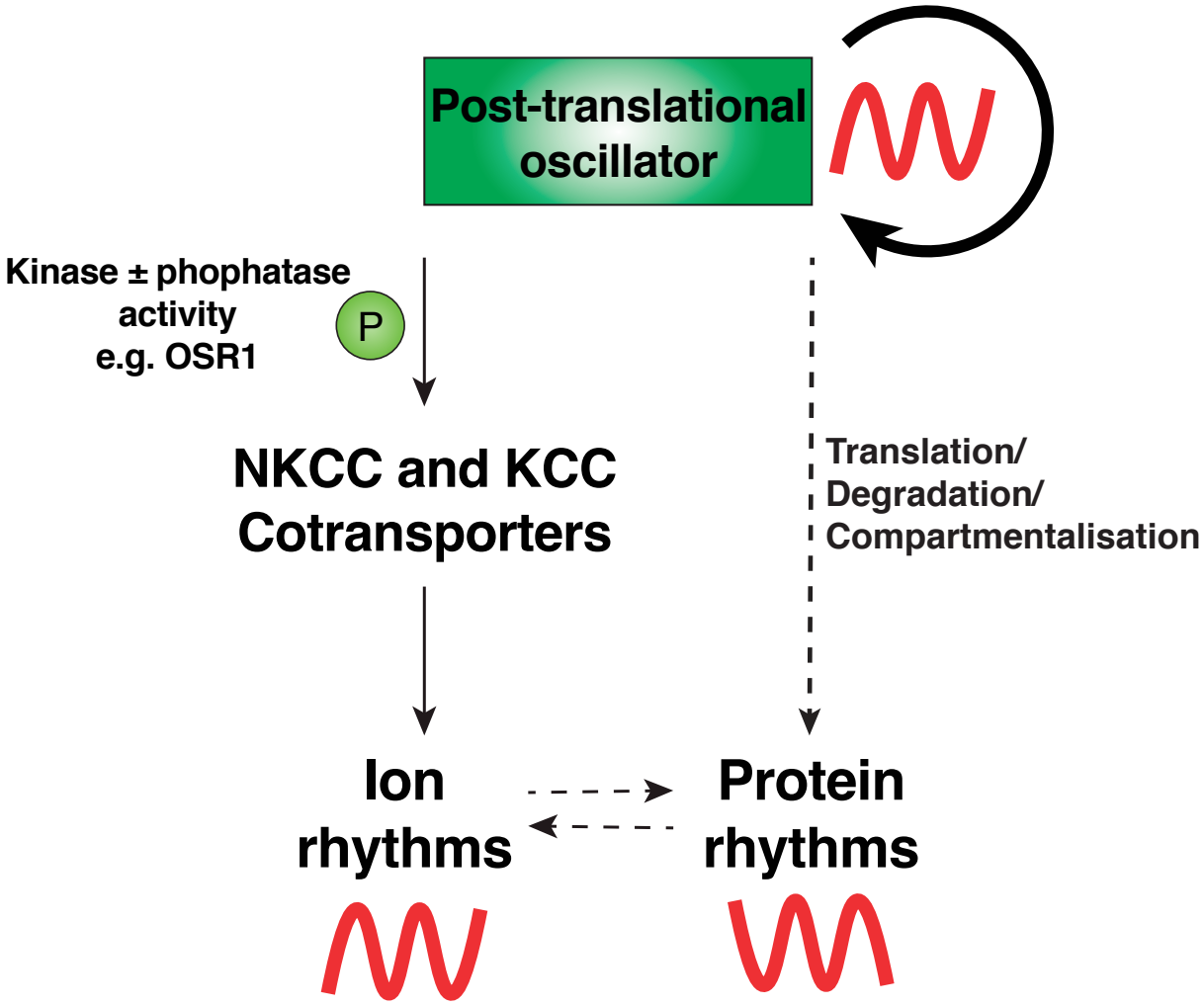

Figure 4.10 Model for the generation of 24-hour rhythms in cytosolic protein concentration and ion content. A self-sustaining post-translational oscillator may have direct outputs including the rhythmic phosphorylation and/or dephosphorylation of OSR1. This would lead to rhythms in sodium-potassium cotransporter activity, resulting in rhythms of intracellular ion content, particularly potassium (the most abundant intracellular cation). In order to maintain osmostasis, the concentration of labile cytosolic proteins must also oscillate but in antiphase to reduce the fluctuations in protein:ratio. These oscillations in labile cytosolic proteins may be driven by rhythmic changes in translation, degradation or compartmentalisation of proteins. The TTFL does not generate these rhythms, but may suppress them, since they are present with greater relative amplitude in CKO cells.

Chapter 5

PER2 links the post-translational oscillator with transcriptional feedback repression

5.1 Introduction

5.1.1 Cellular mechanisms of circadian rhythm generation

As described in Chapter 1, circadian rhythms in transcription in mammalian cells are thought to be driven by the transcriptional translational feedback loop (TTFL). The negative limb of the feedback loop is mediated by complexes containing PER and CRY proteins, which translocate to the nucleus to inhibit transcriptional activity of BMAL1-containing complexes.

When CRY1 and CRY2 are both knocked out in mice, their daily rhythms of locomotor activity observed in 12h:12h light:dark cycles are not sustained under constant conditions [230]. On the cellular level it has been shown that PER and CRY proteins are components of large macromolecular complexes that effect the repressive arm of the feedback loop, directly binding to BMAL1-containing complexes and inhibiting transcriptional activity [36–39]. This occurs at multiple genomic loci including their own, and so their repressive activity is rhythmic [40, 41]. Because CRY activity is essential for the nuclear repression of BMAL1 activity [281–283], CKO mice and cells have no functioning TTFL.

As described in Chapter 1, the TTFL is generally regarded as the process that generates cell-autonomous circadian rhythms. However, central TTFL components such as BMAL1, CLOCK, PER1, PER2, CRY1 or CRY2 do not need to be expressed rhythmically for cellular circadian timekeeping to persist, but rather their activity simply needs to lie within a permissive range [81, 84, 85, 83, 284, 82]. There is also a huge discrepancy between the cycling proteome and corresponding mRNA profiles (See Chapter 1 for more details). Post-transcriptional and post-translational mechanisms are usually invoked to explain these differences.

All major types of post-translational protein modification have been described as regulating or being regulated by the cellular clock [125, 126, 285, 128–130]. Several processes essential for cellular function show circadian regulation *in vitro* and *in vivo*, such as global protein synthesis rates [131, 75], ion transport [109], cAMP/Ca^{2+} signalling [133], mitochondrial metabolism [136], redox balance [134, 135] and the actin cytoskeleton [137]. Many of these clock outputs also feedback to affect the period, phase or amplitude of clock gene expression rhythms. Hence the cell is a highly complex, cyclical system with many interlocking clock outputs and inputs, making it difficult to distinguish cause and consequence when our main experimental reporter is oscillations of clock gene expression.

The observation of circadian rhythms in systems without transcriptional-translational feedback loops (See Chapter 1 for more details) has led to the hypothesis that in eukaryotes a post-translational oscillator (PTO) may be responsible for the generation of cellular circadian timekeeping [111, 6]. In addition, some studies have observed circadian rhythms using the PER2::LUC reporter in SCN slices obtained from CRY1$^{-/-}$; CRY2$^{-/-}$ (CKO) mice [286, 287], and even in mouse behaviour under certain conditions [288]. At the time, these reports were explained by neuronal network effects in the developing mouse brain. This explanation is unsatisfactory however, because it does not provide any cause-effect relationships that can be tested to increase our understanding of the system.

5.1.2 Circadian rhythms in CRY1$^{-/-}$; CRY2$^{-/-}$ fibroblasts

Dr Marrit Putker and others in the lab observed PER2::LUC rhythms in CKO fibroblasts and characterised them before I began my project. I will therefore briefly summarise this substantial body of work to provide context to my own contribution. PER2::LUC rhythms in CKO cells were temperature compensated (Appendix figure 1A), and they could be entrained using temperature cycles (Appendix figure 1B). Hence they are true circadian rhythms as defined in Chapter 1. In agreement with prior literature mentioned above, there was no residual TTFL in these cells or in CKO mouse embryonic fibroblasts, as there was no measurable oscillation in clock gene transcripts, assayed using qPCR and transcriptional reporters (Appendix figure 1C, D).

Moreover, the half-life of PER2::LUC showed time-of-day variation (Appendix figure 2A, B), suggesting that regulation of PER2::LUC half-life may be a mechanism for generating the observed rhythms. This finding also suggests that post-translational modification could be instrumental in rhythm generation, since PER2 degradation is modulated by kinase activity. Strikingly, the CKO period length was sensitive to CK1 inhibition, just as in the WT cells (Appendix figure 2C, D), suggesting that the mechanism for period determination may involve these kinases, and not the TTFL.

Altogether, this provides strong evidence for the presence of a post-translational oscillator (PTO) that is responsible for generating circadian timing in mammalian cells, and that it involves

CK1. However, the ability to observe these rhythms in PER2::LUC activity was variable (Figure 5.1A).

5.1.3 Aims of this chapter

In Chapter 4 I found that many proteins were under circadian regulation in CKO cells. Following this, I showed that cellular ion content and cytosolic protein concentration are under circadian control. This supports the post-translational oscillator (PTO) model, and suggests that there are many direct outputs of the PTO, including the regulation of osmotic homeostasis.

To try and understand how this timekeeping is achieved, I turned to the PER2::LUC reporter. PER2 is subject to many PTMs, and I hypothesised that if the PTO model is true, then there should be detectable rhythmic regulation of PER2 activity in CKO cells. I therefore built upon the experiments described above that were performed by Dr Marrit Putker and others in our laboratory, and in this chapter I explore the variability of the CKO rhythms and discuss possible mechanistic underpinnings.

5.2 Results and discussion

5.2.1 Variability in PER2::LUC rhythms between multiple cell lines

I created 16 independent primary cell lines using the methods described in Chapter 2. Of these, 11 were plated out (5x WT and 6x CKO) around passage 5 in an experiment to record bioluminescence. Of the 6 CKO lines, 4 were significantly rhythmic, i.e. they were better fit with a damped cosine with 24 hour periodicity compared with the null hypothesis as described in Chapter 2.

There were significant differences in circadian period between cell lines (Figure 5.1B), with means between 22.7 and 24.8 hours, but no significant differences in period length between sexes, irrespective of genotype (Figure 5.1C). Therefore, whilst it does not matter from which sex fibroblast cultures are obtained, absolute period measurements must be interpreted with caution, and studies should be carried out using the same cell line throughout if possible. Hence, throughout this thesis cell lines 11 and 12 were used for all experiments.

There was also greater variation in the period measurements from CKO cells compared to wild-type, between technical replicates within experiments (Figure 5.1D). Analysing several experiments performed by myself and by Dr Marrit Putker previously, there was also more variation in period length between experiments (Figure 5.1E). In addition, out of all the experiments performed by myself, 61% of CKO cultures were arrhythmic, and 39% were rhythmic, compared

with 100% of WT cultures. To understand the source of this variability, I attempted to find a set of experimental conditions where rhythms in this reporter were always present.

5.2.2 PER2 has large regions of disorder

The PER2::LUC reporter is a protein fusion, and so its observed behaviour depends on the availability of the mRNA, translation rate, protein folding efficiency, and protein degradation rate, as well as luciferin availability. Folding efficiency and degradation rate may be affected by the presence of intrinsically disordered regions in the protein structure. Clock proteins have been reported to be enriched for disordered regions [289]. To characterise the disorder in mPER2 (*Mus musculus* PER2, Uniprot ID: O54943), I used two independent databases to predict disordered regions. I also used the sequence of firefly luciferase (Uniprot ID: Q27758) appended to the mPER2 sequence, so that I could more accurately assess the behaviour of the PER2::LUC reporter in the context of the experiments reported in this chapter. SPOT-Disorder-Single uses neural networks to predict the disorder of each individual amino acid [290]. In contrast, IUPred2A makes estimations of the strength of interactions between residues in order to predict disorder [291]. By inspection these two mechanistically differing methods agreed with each other, and SPOT labelled 730 amino acids as disordered out of 1806, which is roughly 40% (Figure 5.2A, B, C).

In chapter 4 I showed that the regulation of protein:ion ratio is disrupted in CKO cells. I hypothesised that the high disorder content of PER2 may render its activity susceptible to changes in protein:ion ratio. This is because intrinsically disordered proteins undergo phase-separation upon molecular crowding, and this affects protein function and accessibility to post-translational modification enzymes [292]. Keeping the osmolarity of the medium constant, I varied experimental conditions and applied pharmacological manipulations to metabolically alter cellular protein:ion ratio and assessed its affect on the presence of rhythmicity and its robustness in CKO cultures.

5.2.3 Increased contact inhibition

Primary fibroblasts in culture exhibit contact inhibition – the attenuation of proliferation and locomotion upon cell-cell contact [293]. When a cell stops dividing, there is a proteome-wide modulation of protein degradation, enhancing break-down of long-lived proteins to avoid their accumulation [294]. I hypothesised that given enough time in culture, this transition could alter protein:ion ratio and thus affect the activity of PER2::LUC.

To test this, I carried out two experiments a month apart, using the same cells in the same plates, and between these experiments the cells were kept in entrainment as described in Chapter

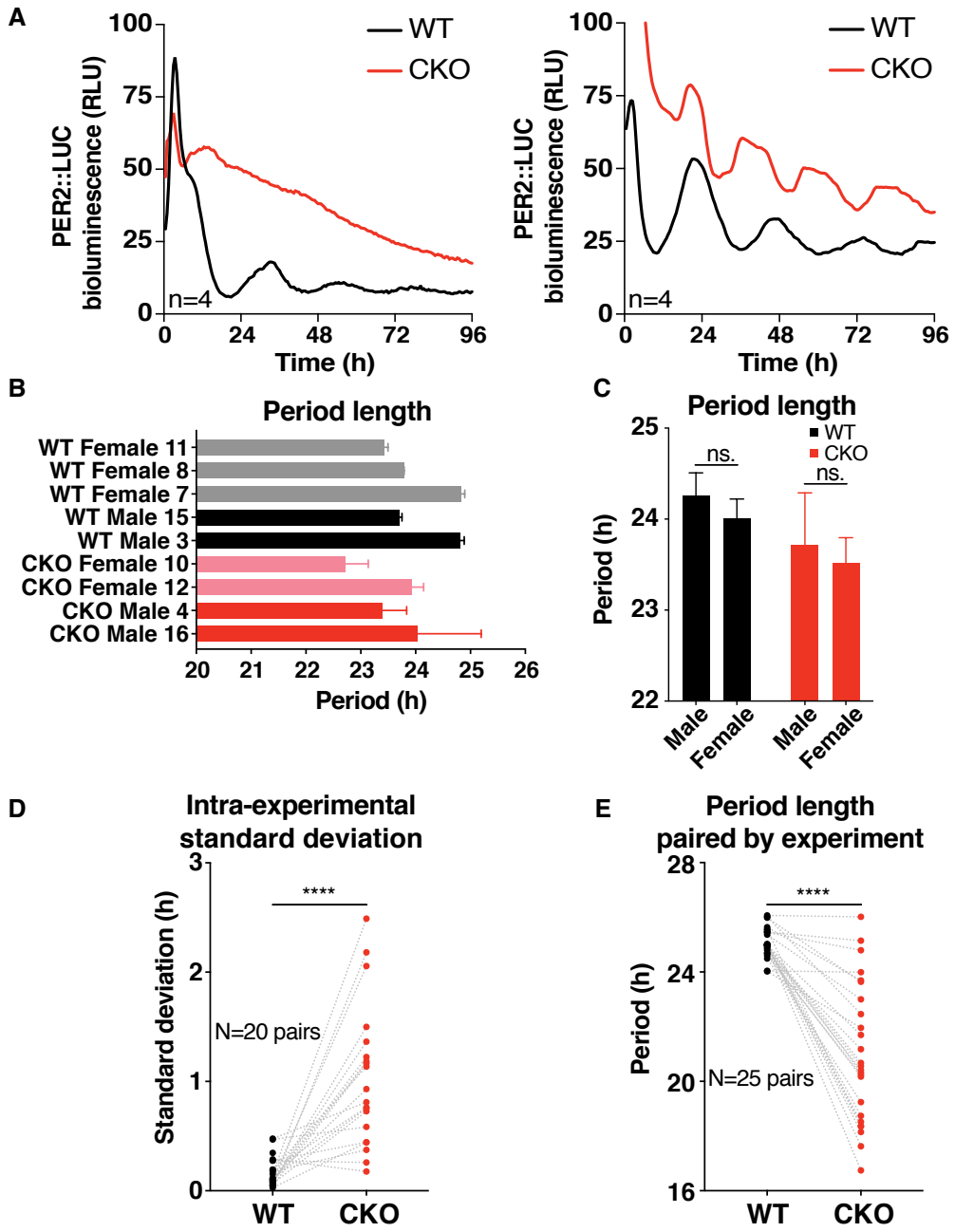

Figure 5.1 Characterisation of PER2::LUC rhythmicity in CKO cells. A) Examples of longitudinal bioluminescence recordings of WT and CKO cells, from two independent experiments and using the same experimental conditions, demonstrating variability. Representative traces shown. **B)** Period measurements from a selection of male and female PER2::LUC cell lines, either WT or CKO. Individual cell lines are identified by number, e.g. cell line 11 is from a female WT mouse, and cell line 4 is from a male CKO mouse. Mean±SEM, n=3. **C)** There are no differences in period length between sexes. Data from A) are grouped by sex, mean±SEM, p=0.996 (WT), p=0.999 (CKO) 2-way ANOVA with Sidak's multiple comparisons test. For males n=6 per genotype, for females n=9 per genotype. **D)** CKO cells display greater intra-experimental variability in period length compared to WT. Standard deviation in period length between technical replicates are plotted, using data from 20 independent longitudinal bioluminescence experiments. The CKO data points are paired with their WT control from their respective experiments. Paired t test. **E)** CKO cells also have greater inter-experimental variability in period length compared to WT. Mean period length was calculated from 25 experiments and WT-CKO pairs plotted. In CKO cells there was greater variance between experiments, as well as shorter period length compared to WT. Paired t test.

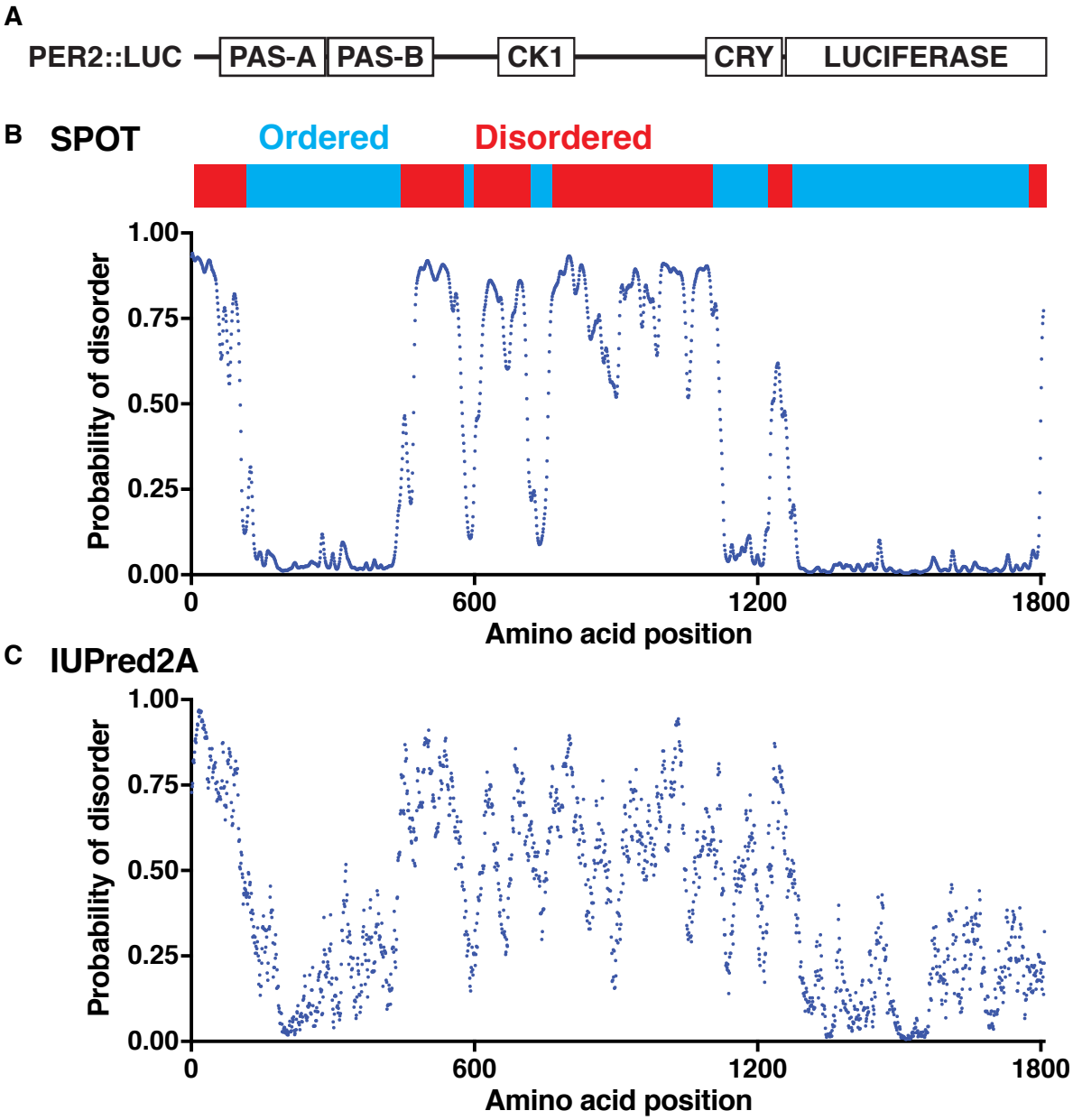

Figure 5.2 The structure of PER2::LUC is around 40% disordered. A) Schematic diagram of the known structural domains of PER2::LUC, including PAS domains, CK1 and CRY binding domains. **B)** Colour-coded disorder classifications predicted by SPOT-Disorder-Single: red = disordered, blue = ordered. Probability of disorder is plotted below for each amino acid as predicted by SPOT-Disorder-Single [290]. **C)** Probability of disorder for each amino acid as predicted by IUPred2A [291].

2, with the medium changed each week. In both experiments I measured the robustness of the PER2::LUC rhythms using the calculation described in Chapter 2.3. Briefly, robustness is the strength of the oscillation, proportional to the relative amplitude and inversely proportional to the damping rate. In other words, a robust oscillation has a large relative amplitude and shows little damping. An oscillation that is not robust shows a very low amplitude and rapid damping.

The robustness of PER2::LUC oscillations was much greater after 1 month of culture in wild-type cells (Figure 5.3A), agreeing with previous observations of increased robustness with confluence [295]. In addition, after 1 month of culture, rhythmicity could be observed in CKO cells that did not show rhythmicity beforehand (Figure 5.3B). The increased time in temperature entrainment may have also contributed to increased robustness due to more synchrony between individual cells. This could be tested in future by varying the amount of time in entrainment, whilst keeping the total amount of time in culture constant.

There is a possibility that the cell cultures are not homogeneous, and are in fact composed of rhythmic and non-rhythmic cells. If a rhythmic subtype outgrows the non-rhythmic cells this could also explain these results. Single cell imaging would be useful to define these populations if present. However, if this hypothesis is true, then one would also expect cells of a higher passage to be more rhythmic since there would be more time for this competition to occur. In fact I found that higher passage cells showed less robust rhythms (Figure 5.3C). This may be due to unpredictable transformation mutations that occur during serial passage, and the attenuation of contact inhibition [293]. Furthermore, CKO cells may be more susceptible to transformation because CRY proteins are involved in a macromolecular complex that targets the oncogene c-myc for degradation [296], as will be discussed further in the next chapter.

5.2.4 Reduced metabolic activity

The glucose concentration in standard tissue culture medium is 4.5 g/L, whereas physiological concentrations are around 1 g/L [297]. Metabolism and translation rate are closely linked [298], and so I hypothesised that changing glucose concentration may affect the translation of PER2::LUC, thus affecting the apparent rhythmicity of this reporter. I measured PER2::LUC rhythmicity in WT and CKO cells across a range of glucose concentrations (Figure 5.4A, B). I found that in CKO cells, robustness of rhythms increased as glucose concentration decreased from 5 g/L to 1 g/L (Figure 5.4D, E). In contrast, WT cells showed increased robustness with the higher glucose concentration (Figure 5.4C, E). It would be informative to measure ATP levels in WT and CKO cells in the different culture conditions to find out whether there is a corresponding difference in metabolic activity.

It seemed plausible that increasing glucose concentration may increase robustness in WT cells by increasing the translation of the PER2::LUC reporter. However, in CKO cells, such an increase in translation may result in disrupted protein homeostasis that may in turn inhibit

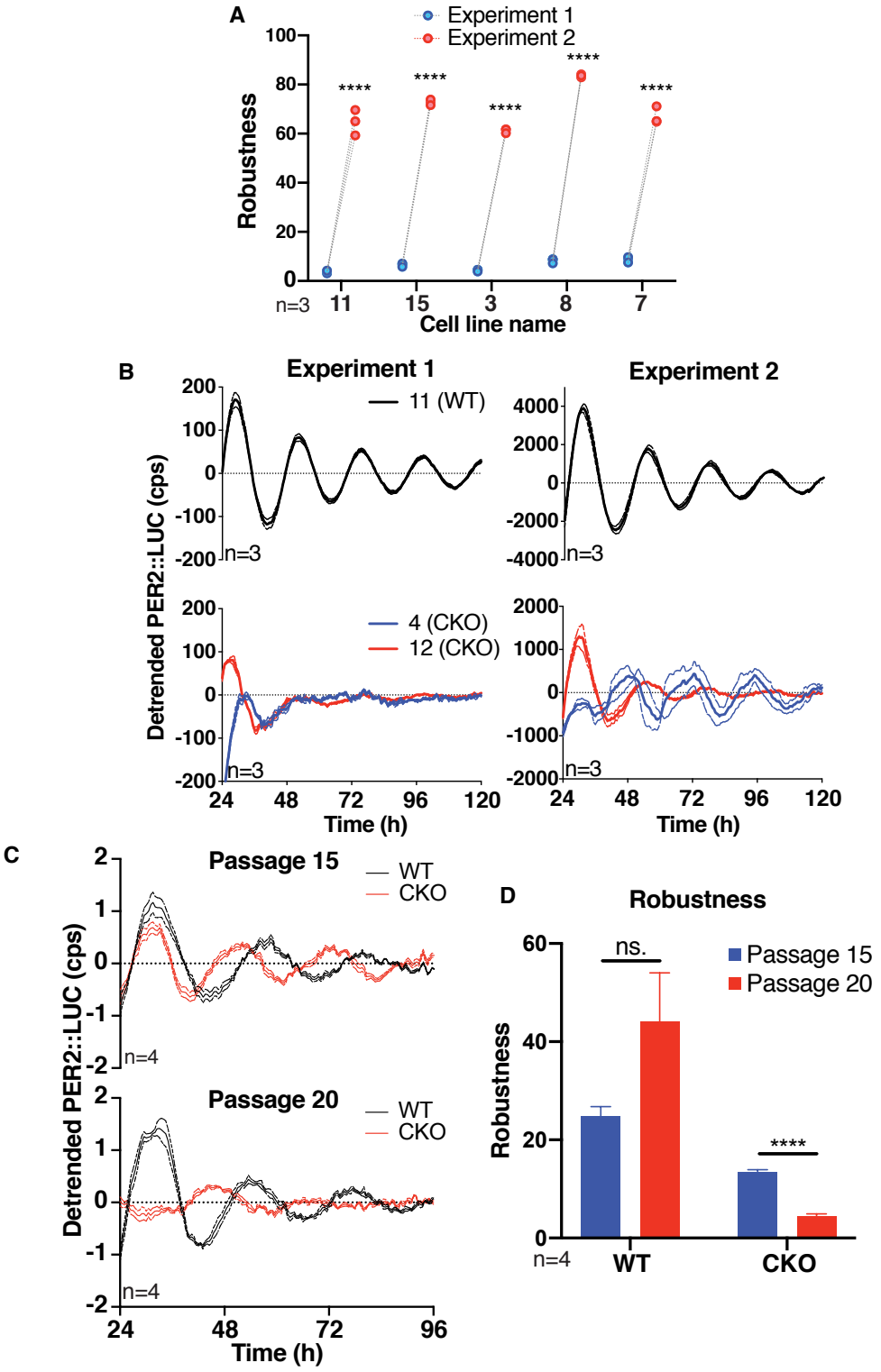

Figure 5.3 Robustness is increased by length of time in culture and passage number. A) Robustness of independent WT cell lines, identified by numbers from Figure 5.1. Experiment 2 was conducted 1 month after Experiment 1, using exactly the same cells in the same dishes. Cell lines are named as for Figure 5.2. Individual replicates are plotted. 2-way ANOVA with Sidak's multiple comparisons test. **B)** Detrended PER2::LUC bioluminescence of WT and CKO lines in Experiment 1 and Experiment 2. WT line number 11 is shown as a reference. CKO lines 4 and 12 are plotted, demonstrating the presence of rhythmicity in Experiment 2. Mean±SEM. **C)** Detrended PER2::LUC bioluminescence of WT and CKO lines, comparing experiments performed with cells of passage 15 (P15) and 20 (P20). Mean±SEM. **D)** Robustness quantifications of the data in C). Mean±SEM, 2-way ANOVA.

PER2::LUC rhythmicity. In the absence of CRY, there is no rhythmic transcription of *Per2* (Appendix Figure 1), and so the abundance of PER2::LUC is more dependent on rates of translation and degradation. In the future a useful experiment would be to measure translation rate in response to changes in glucose concentration acutely to test whether WT and CKO cells are different. In Chapter 6 I explored the metabolic activity and protein homeostasis of CKO cells in more detail under normal culture conditions, and I found that CKO cells were indeed more metabolically active and more sensitive to proteotoxic stress. In the following sections of this chapter I tried different experimental conditions to facilitate protein homeostasis.

5.2.5 Increased protein folding

As described in Chapter 1, protein folding is a key part of protein homeostasis. Misfolded proteins have defective function and trigger cellular stress responses that aim to avoid toxic aggregations [195]. Molecular chaperones play an active role in these responses. Given that reducing metabolic activity increased robustness of PER2::LUC rhythmicity, I hypothesised that a contributing factor may be the reduction of protein aggregation in the cytoplasm subsequent to a decrease in translation rate.

4-phenyl butyrate (4PBA) is a short-chain fatty acid that acts as a 'chemical chaperone' because it prevents misfolding and aggregation of proteins *in vitro* [299]. Chemical chaperones have been shown to increase the amplitude of PER2::LUC oscillations in WT mouse fibroblasts obtained from tail tendon, likely through increasing protein folding capacity in the endoplasmic reticulum [300]. Both WT and CKO cells showed increased robustness with 1 mM 4PBA treatment when they had been pre-incubated with the drug prior to the medium change (Figure 5.5). Whilst at first glance the bioluminescence traces look scarcely rhythmic in the CKO cells, they do fit to a rapidly damping circadian cosine wave in preference to the null hypothesis of a straight line. In fact, these results are likely to be at the limit of detection for PER2::LUC rhythmicity in CKO cells. This highlights the difficulty of observing rhythms in CKO cells using this reporter, and in future studies investigating the generation of rhythms in this experimental model, new reporters are needed. This is discussed at the end of the this chapter. To confirm the effect on protein folding it would be useful to measure the effect of 4PBA treatment on stress markers such as ATF4 and CHOP.

The requirement for pre-incubation with 4-PBA for there to be an effect on rhythmicity suggests that the state of the protein folding machinery at the time of transfer to air medium may be an important factor. The fact that the resulting rhythmicity is not robust but rapidly damped suggests that under these conditions, whilst chaperone activity contributes to PER2::LUC rhythms, it is not an important factor. Instead, I hypothesised that the protein:ion ratio in the cytoplasm at the time of medium change is crucial for the observation of PER2::LUC rhythmicity in CKO cells.

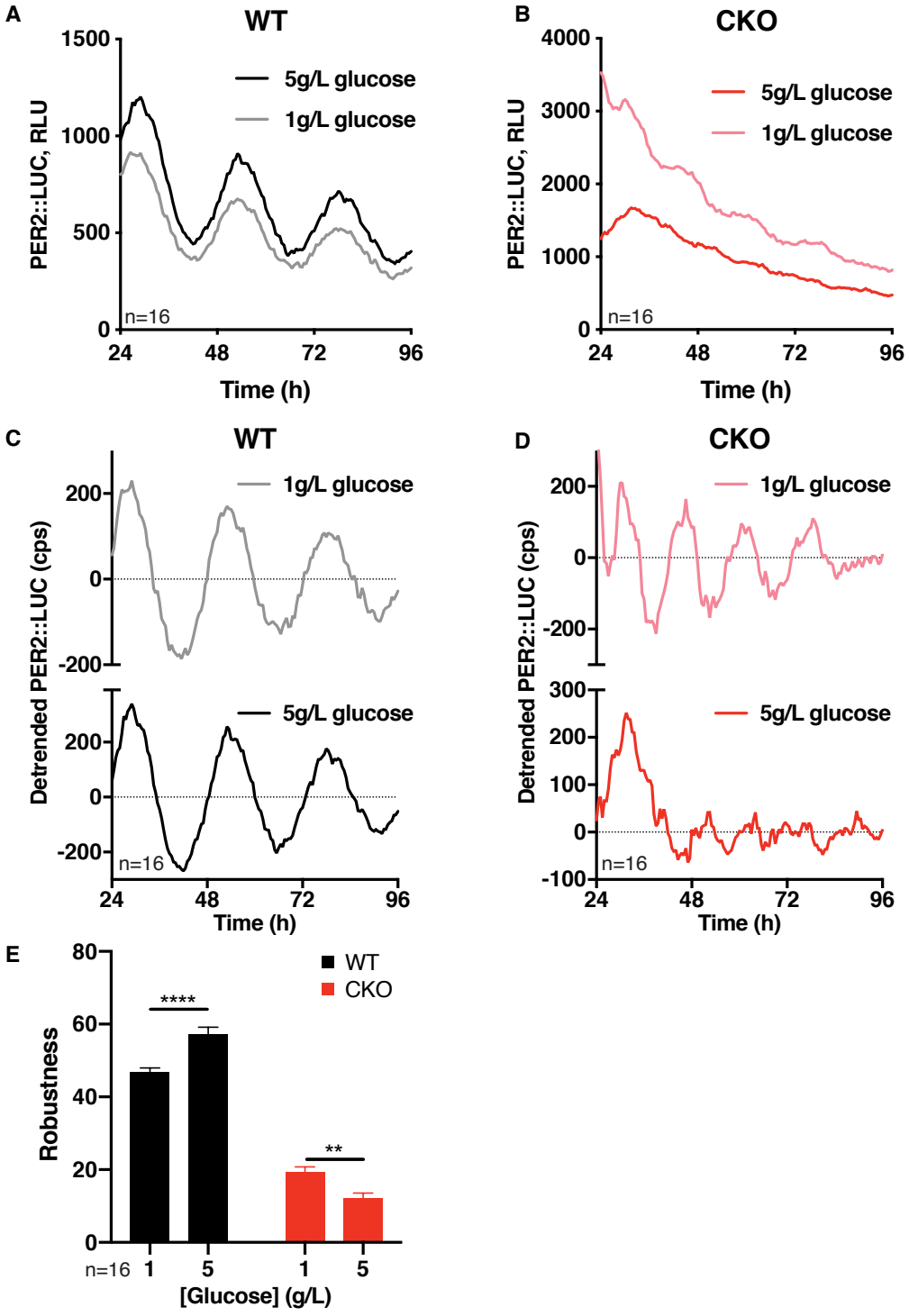

Figure 5.4 Low glucose concentration increases robustness in CKO cells. **A)** Raw PER2::LUC bioluminescence (representative traces shown) of WT cells in either 1 or 5 g/L glucose. **B)** Raw PER2::LUC bioluminescence (representative traces shown) of CKO cells in either 1 or 5 g/L glucose. **C)** Detrended PER2::LUC bioluminescence of WT cells in air medium containing 1g/L (above, grey) or 5g/L (below, black) glucose. **D)** Detrended PER2::LUC bioluminescence of CKO cells in air medium containing 1g/L (above, pink) or 5g/L (below, red) glucose. **E)** Robustness quantifications of the data in A) and B). Mean±SEM, 2-way ANOVA.

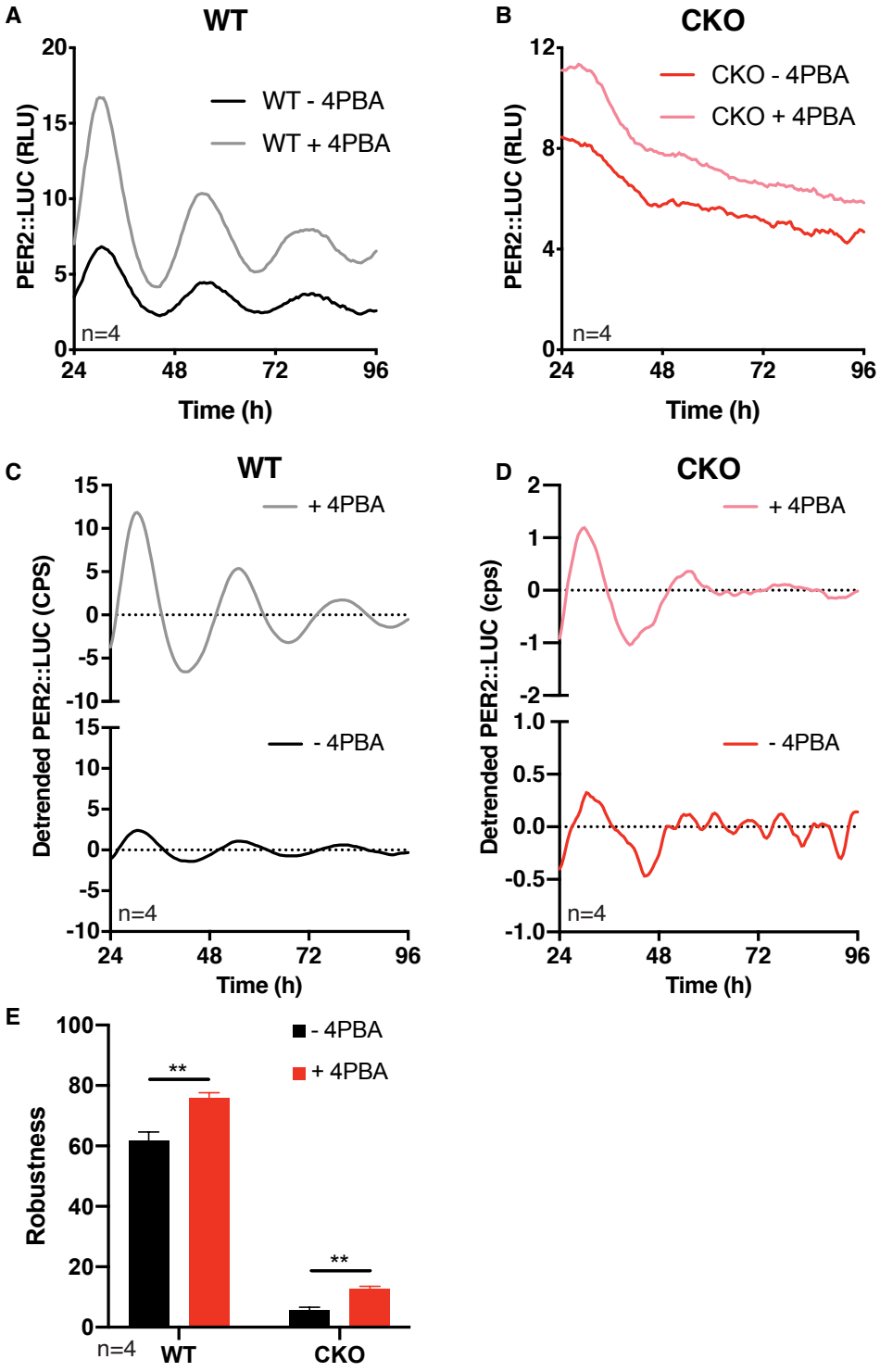

Figure 5.5 Robustness is increased by 4-phenylbutyrate treatment. **A)** Raw PER2::LUC bioluminescence (representative traces shown) of WT cells treated with 1 mM 4PBA or control. **B)** Raw PER2::LUC bioluminescence (representative traces shown) of CKO cells treated with 1 mM 4PBA or control. **C)** Detrended PER2::LUC bioluminescence of WT cells treated with 1 mM 4-PBA (above, grey) or control (below, black). **D)** Detrended PER2::LUC bioluminescence of CKO cells treated with 1 mM 4-PBA (above, pink) or control (below, red). **E)** Robustness quantifications of the data in A) and B). Mean±SEM, 2-way ANOVA.

5.2.6 Decreased synthesis of amino acids

The concentration of amino acids in culture medium has an impact on protein synthesis. I hypothesised that reducing the concentration of amino acids would reduce protein synthesis and thus give more robust PER2::LUC rhythms in CKO cells. Surprisingly, when a range of concentrations of amino acids were used, there was increased robustness with greater amino acid concentrations, although it was not statistically significant (Figure 5.6). Robustness was increased in CKO cells by supplementing ordinary medium with non-essential amino acids alone (Figure 5.7), suggesting that reducing the synthetic load of the cell may be an important factor. These findings also suggest that CKO cells may have reduced proteasome activity, since proteasome inhibition leads to a shortage of intracellular amino acids [301]. This will be explored further in the next chapter.

5.2.7 Manipulations that did not promote rhythmicity

I tested many other variables that did not result in detectable rhythmicity in CKO cultures, and they are listed below:

- Entrainment vs non-entrainment with temperature cycles
- Co-culture with WT cells
- Conditioned medium - WT or CKO donor, WT or CKO acceptor
- pH buffer - MOPS or bicarbonate
- Corticosterone, insulin, B27
- Myc inhibitor 10058-F4
- Rev-erbα inhibitor SR8278
- Inhibition of translation - cycloheximide, rapamycin
- Inhibition of chaperones - cycosporin A, radicicol, VER155008
- Activation of proteasome - PD169316

This list is not exhaustive, as several combinations of conditions were also tested. At the time of testing they seemed to be reasonable variables to explore, although none resulted in the observation of rhythmicity in CKO cells. Due to limitations of space I will not describe in further detail the results of these experiments, but I will briefly summarise the reasoning behind them here. Co-culture and conditioned medium experiments were testing the hypothesis that a secreted

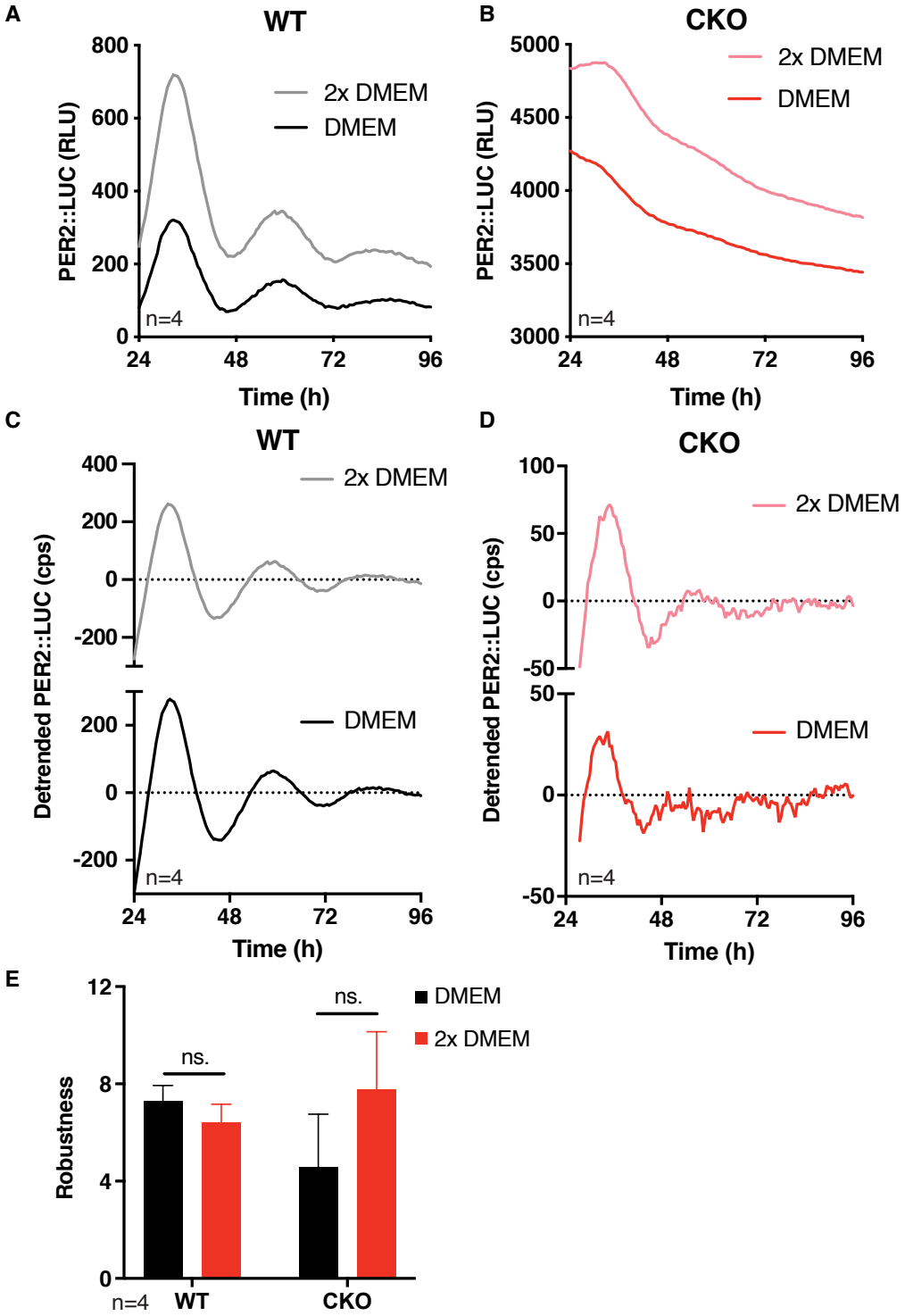

Figure 5.6 Increased amino acid concentration may increase robustness. **A)** Raw PER2::LUC bioluminescence (representative traces shown) of WT cells in air medium containing normal DMEM or DMEM with double the concentration of amino acids (2x DMEM). **B)** Raw PER2::LUC bioluminescence (representative traces shown) of CKO cells in air medium containing normal DMEM or DMEM with double the concentration of amino acids (2x DMEM). **C)** Detrended PER2::LUC bioluminescence of WT cells in air medium containing normal DMEM (below, black) or DMEM with double the concentration of amino acids (2x DMEM, above, grey). **D)** Detrended PER2::LUC bioluminescence of CKO cells in air medium containing normal DMEM (below, black) or DMEM with double the concentration of amino acids (2x DMEM, above, grey). **E)** Robustness quantifications of the data in A) and B). Mean±SEM, 2-way ANOVA, Sidak's multiple comparisons: p = 0.9 for WT and p = 0.4 for CKO.

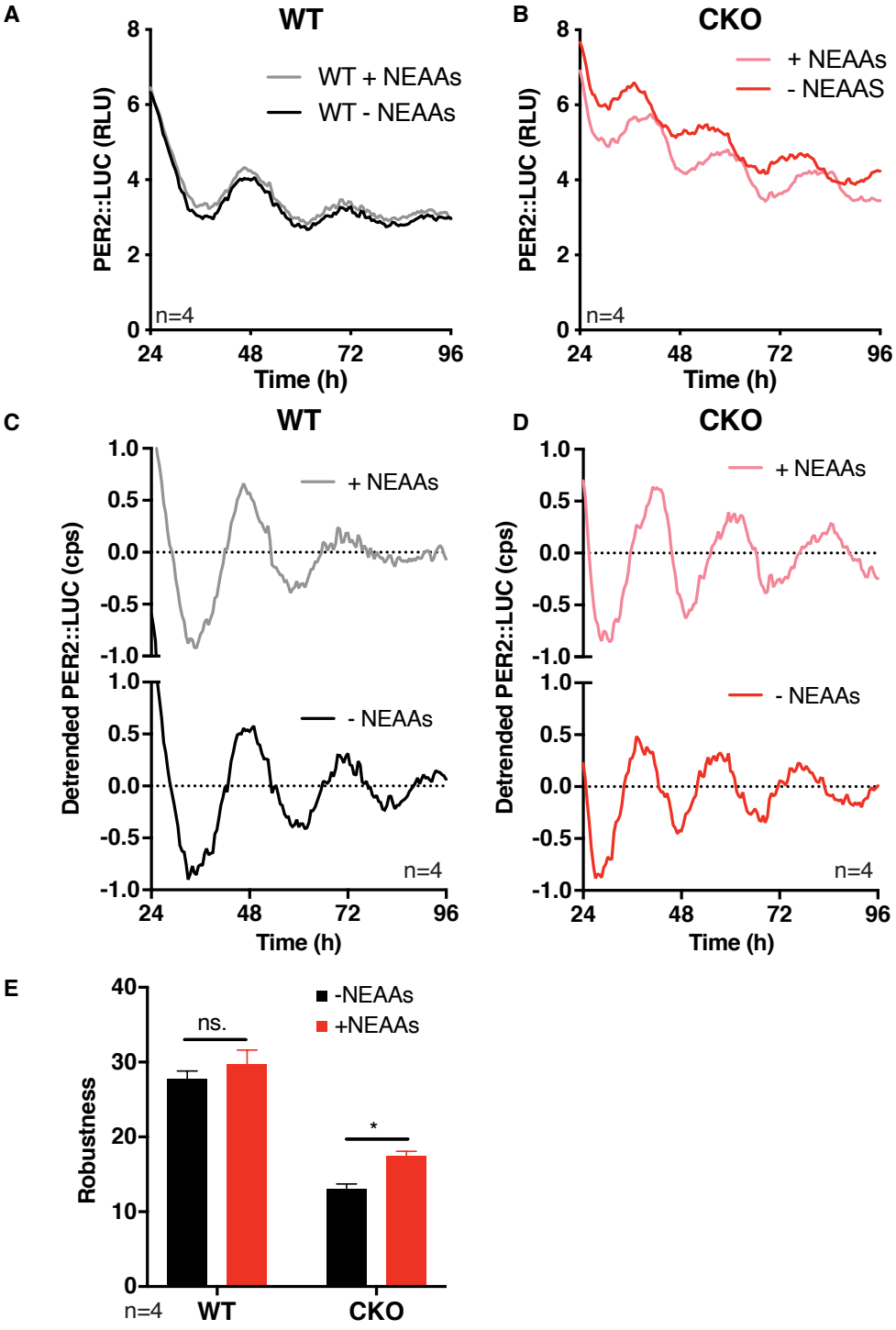

Figure 5.7 Supplementation with non-essential amino acids increases robustness. A) Raw PER2::LUC bioluminescence (representative traces shown) of WT cells in air medium with (+ NEAAs) or without (- NEAAs) non-essential amino acid (NEAA) supplement. **B)** Raw PER2::LUC bioluminescence (representative traces shown) of CKO cells in air medium with (+ NEAAs) or without (- NEAAs) non-essential amino acid (NEAA) supplement. **C)** Detrended PER2::LUC bioluminescence of WT cells in air medium with (above, grey) or without (below, black) non-essential amino acid (NEAA) supplement. **D)** Detrended PER2::LUC bioluminescence of CKO cells in air medium with (above, pink) or without (below, red) non-essential amino acid (NEAA) supplement. **E)** Robustness quantifications of the data in A) and B). Mean±SEM, 2-way ANOVA, Sidak's multiple comparisons.

factor may be critical for observing PER2::LUC rhythmicity, and testing the requirement of entrainment was exploring the role of synchrony between cells in culture. Other pharmacological and metabolic manipulations aimed at exploring the role of protein homeostasis.

The performance of these experiments in the face of such variation required mettle, as more and more variables were discovered to be relevant over time, and to be dependent on the passage of time itself. Whilst I have not tested every possible variable in every possible combination, valuable conclusions and insights may still be drawn from the efforts. Looking back on all the experiments reported in this chapter, the source of variation is likely to be closely related to protein:ion ratio and its effect on the PER2::LUC reporter, and I will discuss this with a broader outlook in the next section.

5.3 Conclusions

5.3.1 Summary of findings

PER2::LUC rhythmicity persists in CKO cells under certain conditions. Taking together all my findings, I hypothesise that culture conditions and pharmacological manipulations that decrease cellular protein content are most likely to result in PER2::LUC rhythmicity. To explain this, I propose that it is the reduction in protein:ion ratio that is permissive for PER2::LUC rhythmicity. As described in section 5.2.2, the protein sequence of PER2 contains large regions of intrinsic disorder, and so it is plausible that PER2 may be rhythmically sequestered and released from biomolecular condensates. This behaviour is likely to be sensitive to macromolecular crowding, which is itself related to intracellular protein:ion ratio. This may in turn render PER2 proteins differentially susceptible to modification by kinases or degradation by the proteasome [302].

Macromolecular crowding is also likely to be affected by osmolarity of culture medium. A recent study showed that increased osmolarity of cell culture medium increased the period length of PER2::LUC rhythms in MEFs through cellular stress signalling [303]. This suggests that intracellular osmolarity is important in clock regulation. However, in this study extremes of osmolarity were used – between 210 mOsm and 480 mOsm, whereas cell culture medium is typically around 300-350 mOsm. In future work it would be valuable to find a way to measure intracellular osmolarity, and to directly observe how physiological changes in cell culture conditions affect this variable, and how this might impact on PER2 protein activity and localisation.

Dr Marrit Putker demonstrated that the half-life of PER2:LUC in CKO cells showed time of day variation, and this is likely to be the basis of the rhythmicity (Appendix Figure 2). She also found that CK1 inhibition lengthened circadian period in CKO cells, just as it did in WT cells, suggesting that CK1 is involved in period determination of the TTFL-independent oscillator

(Appendix Figure 2). This is reminiscent of work done in red blood cells, which do not have a nucleus, but still show circadian rhythmicity in multiple parameters, with period length that is sensitive to the same kinase inhibition [100]. In this context therefore I interpret my findings as observations of circadian rhythms in the post-translational modification of the PER2::LUC reporter that are TTFL-independent, and sensitive to cellular protein:ion ratio. To confirm this experimentally, cellular protein and ion concentrations should be measured in the different culture conditions tested. In addition, it would be useful to measure post-translational modifications of PER2 directly by Western blot to confirm the presence of rhythmicity. Unfortunately PER2 was not detected in my proteomics and phosphoproteomics experiments, likely due to low abundance, below the threshold for detection by mass spectrometry under the conditions of my workflow.

There are alternative interpretations of the work presented in this chapter. Despite exhaustive efforts it was challenging to find out experimental conditions that permitted rhythms in PER2::LUC to be easily observed. In addition, when they were observed, the robustness was often very low. This suggests that the TTFL may be required for robustness of PER2::LUC activity, but another conclusion could be that PER2::LUC was likely to be a poor reporter for the PTO. Instead it would be valuable to create a new reporter, perhaps by targeting a protein with high average abundance and high relative amplitude of oscillation as observed in the proteomics dataset. Such an example is cell cycle progression protein 1 (CCPG1), which I found to be rhythmic in both WT and CKO with relative amplitudes of 27% and 55% respectively (Appendix Table 1). Creating an alternative reporter would be useful in future studies of the PTO as it could enable longitudinal recordings of PTO activity in a TTFL-independent manner. Finally, it would also be informative to use single-cell imaging to test whether the poor rhythmicity at the population level could be explained by individually rhythmic cells that are out of phase.

5.3.2 Disorder amongst TTFL components

The role of intrinsic disorder in clock proteins has been explored in the literature, primarily in the context of the FRQ (Frequency) protein in *Neurospora*, which requires the presence of another "nanny" protein to stabilise its structure and prevent random proteasomal degradation [289, 304, 305]. In mammals, disordered regions of TTFL components have been found to be functionally relevant in regulation of circadian rhythms – for example the disorder in the terminal activation domain of BMAL1 is important for its interaction with CRY1 and period determination [306, 138].

CK1 is an important kinase that mediates both the priming and subsequent processive phosphorylation of PER2, and this process has been proposed to determine period length [252]. For this to work, CK1 must have access to a large number of phosphorylation sites, and it has been proposed that the structural flexibility of PER2 as a result of the disorder permits this (Michael Brunner, personal comm.). Furthermore, FRQ also has structural flexibility that allows

progressive phosphorylation, and so the use of a disordered protein as a molecular timer may be conserved (Michael Brunner, personal comm., unpublished). Finally, PER2 and CRY1 have been reported to form phase-separated nuclear droplets (Michael Brunner, unpublished) and this may be a mechanism for protecting PER2 from degradation.

Hence disorder is functionally relevant in the circadian clock, but the precise identity of the proteins involved does not matter. This very much echoes the discussion in Chapter 1 about the evolution of circadian rhythms in eukaryotes, where similar TTFL network motifs are found between organisms, with different proteins being involved in the TTFLs, but post-translational modification enzymes that determine periodicity are conserved. Therefore evolution may have selected proteins such as PER and FRQ with particular biophysical properties that make them good signal transducers, transmitting temporal information in the form of progressive phosphorylation in a robust manner from the PTO to the gene expression machinery.

In this context, my data suggests that in the absence of CRY, PER2::LUC does not have the supplementary regulation of the TTFL, and so it is subject to the direct outputs of the PTO, which may include regulation of protein:ion ratio as discussed in Chapter 4. This affects the phase-separation of disordered proteins, hence rhythmicity using this reporter can only be observed when the conditions are right, i.e. when the protein:ion ratio permits rhythmic post-translational modification of the disordered PER2::LUC. In the proteomics and phosphoproteomics data presented in Chapter 4, PER2 peptides and phosphopeptides were not detected. However, it would be useful in future analyses of these data to explore in further depth the rhythmic regulation of other intrinsically disordered proteins. For example, fluorescently tagging a rhythmic cytosolic protein with a similar amount of disorder to PER2 would allow observation of whether it is present in aggregations, and whether this behaviour is dependent on changes in protein:ion ratio.

5.3.3 Evidence for the PTO model

The PTO model is supported by my experiments – the rhythmic modification of PER2 may be the primary way in which the PTO provides input to the TTFL in WT cells. As such, PER2 acts as a signalling molecule that transmits timing information from a self-sustaining post-translational oscillation to effect the rhythmic transcription of clock-controlled genes (Figure 5.8). This circuitry could provide amplification of the signal via transcriptional feedback, as well as robustness since the TTFL regulates rhythmic PER2 transcription whilst the PTO regulates rhythmic PER2 post-translational modification [6].

Moreover, without a TTFL to impart autoregulation of transcription, PER2::LUC is not a special protein and it is subject to the global regulation of protein and ion content discussed in Chapter 4. PER2::LUC is an intrinsically disordered protein, and I hypothesise that a high protein:ion ratio may result in sequestration of PER2::LUC molecules in phase separated compartments, thereby inhibiting the rhythmic regulation of PER2::LUC activity (Figure 5.8).

Throughout this chapter I have shown experimental manipulations that result in more robust PER2::LUC rhythms in CKO cells, likely through reduction of cellular protein content. This raises the possibility that CKO cells may have dysregulated protein homeostasis: this will be the subject of the next chapter.

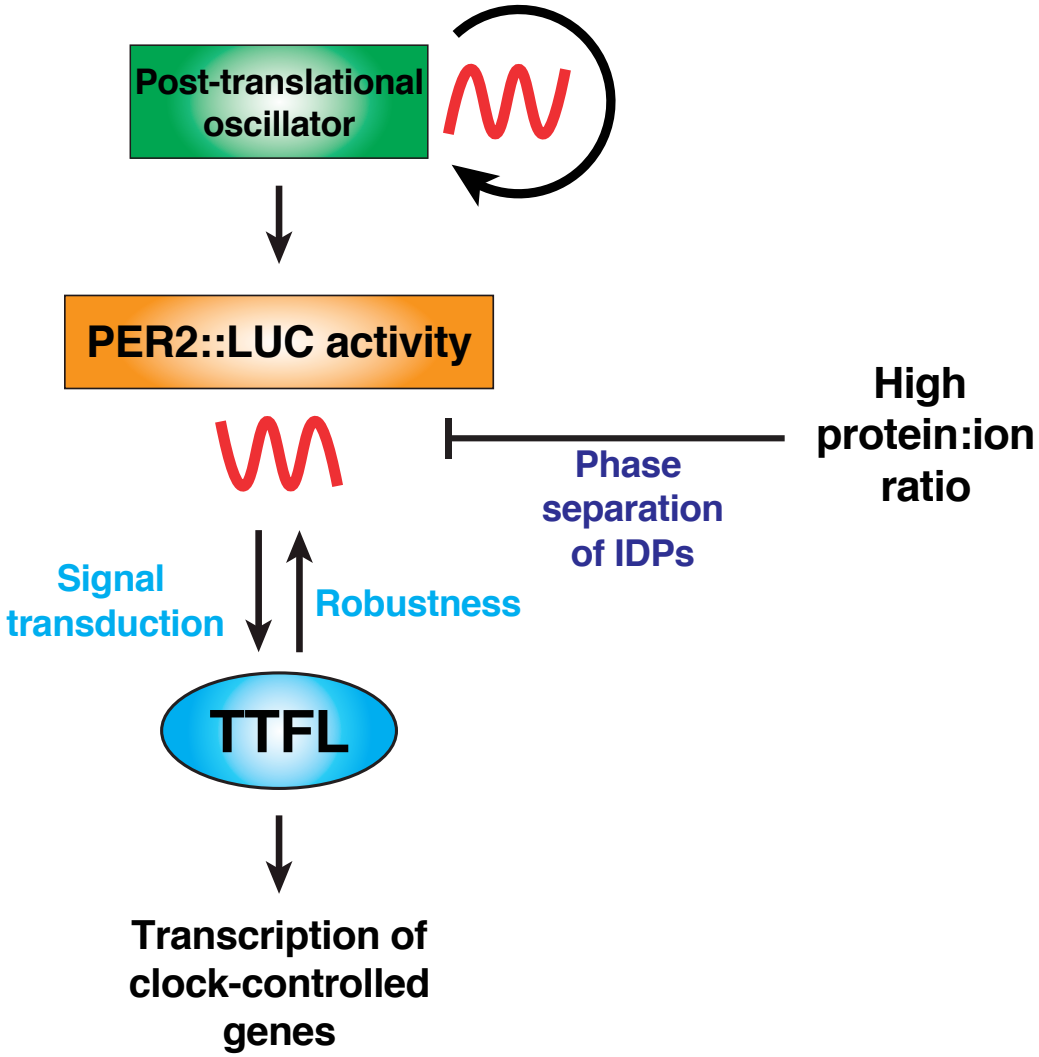

Figure 5.8 Model of PER2::LUC as a temporal signalling factor. PER2:LUC activity is the primary way in which temporal information is conveyed from the post-translational oscillator (PTO) to the transcriptional-translational feedback loop (TTFL), which then rhythmically regulates the transcription of clock-controlled genes. The TTFL imparts robustness to PER2::LUC rhythms in activity through the regulation of PER2::LUC transcription. In CRY-deficient cells, there is no TTFL, but rhythmic post-translational modification of PER2::LUC may be observed indirectly. However, this observation is sensitive to experimental conditions increasing protein:ion ratio. This is because intrinsically disordered proteins (IDPs) like PER2 are sensitive to phase separation when protein concentration is increased. Phase separation alters the activity of proteins, and in this case may inhibit the rhythmic post-translational modification of PER2 by the PTO.

Chapter 6

Cryptochromes regulate cellular proteostasis

6.1 Introduction

6.1.1 Non-timekeeping roles of cryptochromes

Beyond the TTFL, there is evidence that cryptochromes have important functions in cellular protein homeostasis. For example, CRY1 and CRY2 are important components of the E3 ligase complex that recruits c-MYC for degradation: SCF^{FBXL3} (Skp1, Cul1, F-box protein ubiquitin ligase complex) [296]. MYC is an oncoprotein that transcriptionally activates many cellular growth, proliferation and metabolic pathways, and so its levels are tightly controlled by protein degradation [307]. In addition to c-myc, SCF^{FBXL3} has hundreds of potential targets [308], making it an important regulator of protein degradation in the cell. Finally, CRY1 and CRY2 are global transcriptional repressors, either acting directly [40] or indirectly via nuclear hormone receptors [309, 310], suggesting that they regulate the expression of many genes independently of Bmal1-containing complexes. These studies suggest that the loss of CRY1 and CRY2 proteins would result in significant dysregulation of protein homeostasis.

If the loss of CRY1 and CRY2 results in dysregulation of protein homeostasis, it would be reasonable to expect that there would be a phenotype at the organism level [196]. CKO mice are behaviourally arrhythmic, but were originally reported to be otherwise healthy [230]. Since then it has been found that CKO mice have impaired body growth, which is more pronounced in males subsequent to dysregulated growth hormone release [311, 312]. CKO mice also have an altered response to high fat diet, characterised by increased insulin secretion and lipid storage in adipocytes [313]. Finally, female CKO mice have impaired fertility, and this is thought to be age-dependent [314].

6.1.2 Aims of this chapter

In Chapter 4 I showed that the temporal control of protein:ion ratio is dysregulated in CKO cells, suggesting that they have defective protein and osmotic homeostasis. In Chapter 5 I showed that whilst it is possible to observe rhythmic PER2::LUC activity in cells lacking cryptochromes (CRY1$^{-/-}$; CRY2$^{-/-}$, CKO), this was dependent on changes in experimental conditions that may alter cellular protein:ion ratio. These findings suggest that CRYs may be important for cellular proteostasis. In this chapter I present my findings characterising the dysregulated proteostasis in CKO cells and testing some of the consequences of this.

6.2 Results and discussion

6.2.1 CKO cells show defects in protein homeostasis

In Chapter 4 I found that CKO cells have a greater amplitude in oscillation of protein:ion ratio, and that they have a higher protein:ion ratio on average. I hypothesised that this altered set point may affect cellular osmostasis. Adding to this observation, I found that CKO cells have more protein per cell (Figure 6.1A). To test this using an independent method, I turned to the quantum dot (QD) experiment presented in Chapter 4 (Figure 4.7), and found that averaged over time, the diffusion of QDs was reduced in CKO cells (Figure 6.1B). I hypothesised that since CKO cells contain more protein than WT cells, they may be less able to regulate further changes in cytosolic protein content.

To test the sensitivity to changes in protein content, I incubated cells in the absence of serum for 24 hours before treating them with 10% serum. mTORC1 (mammalian target of rapamycin complex 1) is a central node in cellular physiology, sensing a variety of stimuli including growth factors and adjusting processes like protein synthesis and autophagy to increase or decrease cell growth accordingly [315]. I hypothesised that any increase in cytosolic protein concentration in response to such a serum pulse would be mediated by this pathway, and I tested this by inhibiting mTORC1 with Torin 1 [316]. CKO cells showed an increase in cytosolic protein concentration that was mTOR-dependent, since it was blocked by Torin 1 treatment (Figure 6.2). There was no change in WT cells, which seemed to be able to buffer against this perturbation.

6.2.2 CKO cells have reduced proteasomal degradation compared to WT

If cellular protein content increases as a result of a perturbation, cells must degrade them to restore protein homeostasis. I hypothesised that the result in Figure 6.2 may be explained by a reduced capacity for protein degradation, since this would result in an inability to counteract the

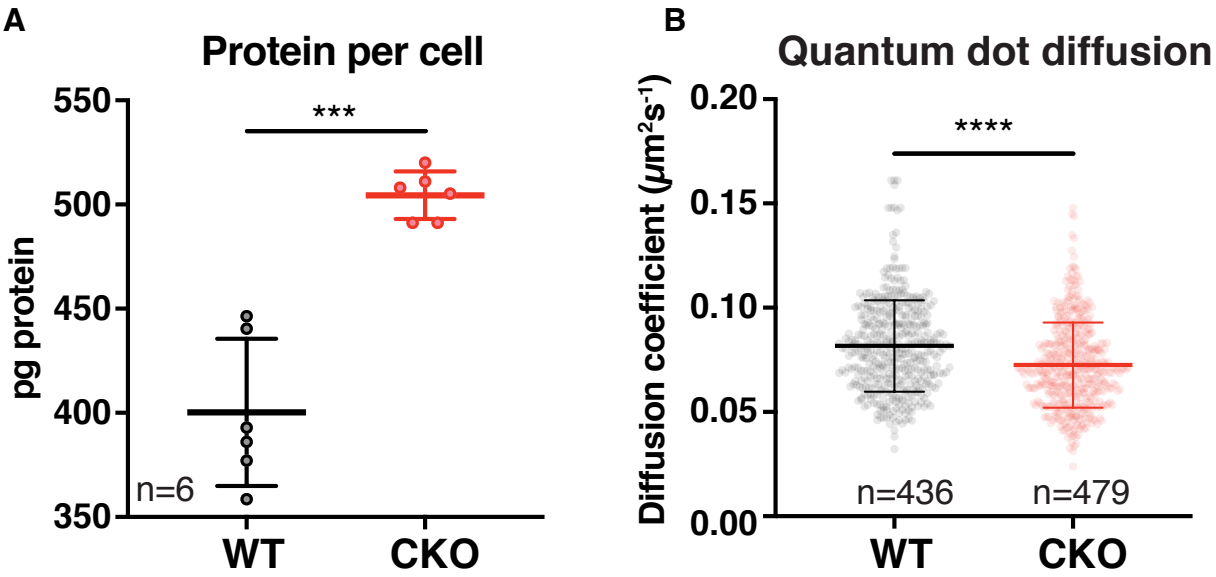

Figure 6.1 CKO cells have more protein in total than WT. A) Total protein mass per cell in confluent WT and CKO cultures. Cells were grown in two 12-well plates; one was used for cell counting and the other was used for lysis in RIPA buffer prior to protein quantification by BCA assay. N = 6 wells. Mean±SEM, Student's t test with Welch correction. **B)** Diffusion coefficient of quantum dots, with data from all time points from the experiment in Figure 4.7 combined. "n" is the number of fields of view pooled together for analysis. Mean±SD.

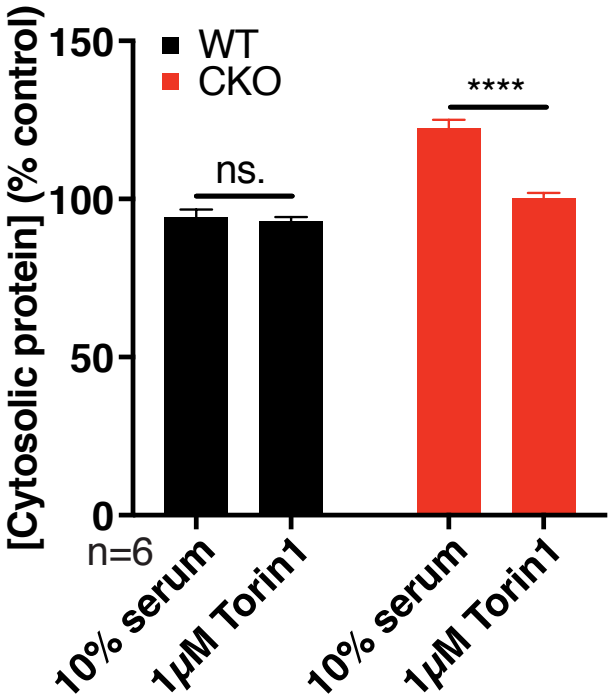

Figure 6.2 CKO cells are more sensitive to serum-induced changes in protein synthesis. Cells were serum-starved for 24 hours before being changed into medium containing 10% serum ± Torin 1. After 4 hours treatment, cytosolic protein was extracted using 0.01% digitonin lysis buffer, and then protein concentration was quantified using BCA assay. Controls were cells changed into serum-free medium. Concentrations are plotted here as a percentage of the controls.

increase in protein concentration after a serum pulse. To test this I searched the proteomics data presented in Chapter 4 for proteasome subunits to test for differences in abundance. Proteasome abundance was around 10% lower in CKO cells as measured by taking average values from the quantitative proteomics reported in Chapter 4 (Figure 6.3A), as well as from western blots of the 20S proteasome (Figure 6.3B).

When examining such cellular processes it is important to assess the functionality as well as the abundance of molecular players. I therefore used the ProteasomeGlo assay to measure proteasome activity. This is described in more detail in Chapter 2.14. Briefly, this is a luciferase-based method to measure the degradation of special substrates that are designed to be cleaved by the proteasome, thus releasing the substrate for luciferase. Substrates are specific to chymotrypsin-like, trypsin-like and caspase-like types of protease activity found in the proteasome. Using this assay, I found that there was a 50% lower activity in all 3 types of proteasomal protease activity (Figure 6.3C). This suggests that in CKO cells the lower abundance of proteasomal catalytic subunits may contribute to lower proteasomal activity, but post-translational regulation is likely to be the main contributor.

The consequence of this finding is that CKO cells may have a lower capacity for protein degradation in response to increases in cellular protein content. Such perturbations may occur after a serum pulse as in the experiment presented in Figure 6.2, or they may be physiological changes such as the rhythms in cytosolic protein concentration presented in Chapter 4. I propose that this may be an important factor contributing to the increased amplitude of oscillations in protein concentration in CKO cells. In addition, the ability to degrade proteins is important in the response to proteotoxic stress, and so one may predict that CKO cells may therefore be more susceptible to stress-inducing stimuli. This hypothesis is explored later in this chapter.

6.2.3 CKO cells do not have altered basal translation rate

Since CKO cells had a reduced proteasome activity relative to WT, I decided to investigate whether translation rate was also different. In order to maintain protein homeostasis, cells need to adjust protein synthesis and protein degradation together in order to avoid accumulation of proteins. In addition, it is plausible that an increased basal translation rate may also contribute to the result in Figure 6.2, since this would present more of a challenge to the proteasomal degradation machinery – hence an increase in translation due to serum pulse would push the cellular protein concentration outside the limit of homeostasis for CKO cells. To measure this I treated cells with ^{35}S-methionine to radiolabel newly synthesised proteins, and I found that there was no difference in translation rate between CKO and WT cells (Figure 6.4A).

I also measured translation rate using a technique based on azidohomoalanine (AHA). AHA is a substitute for methionine, and so it is incorporated into newly synthesised proteins when added to cell culture medium. AHA contains a bio-orthogonal azide moiety, and this may

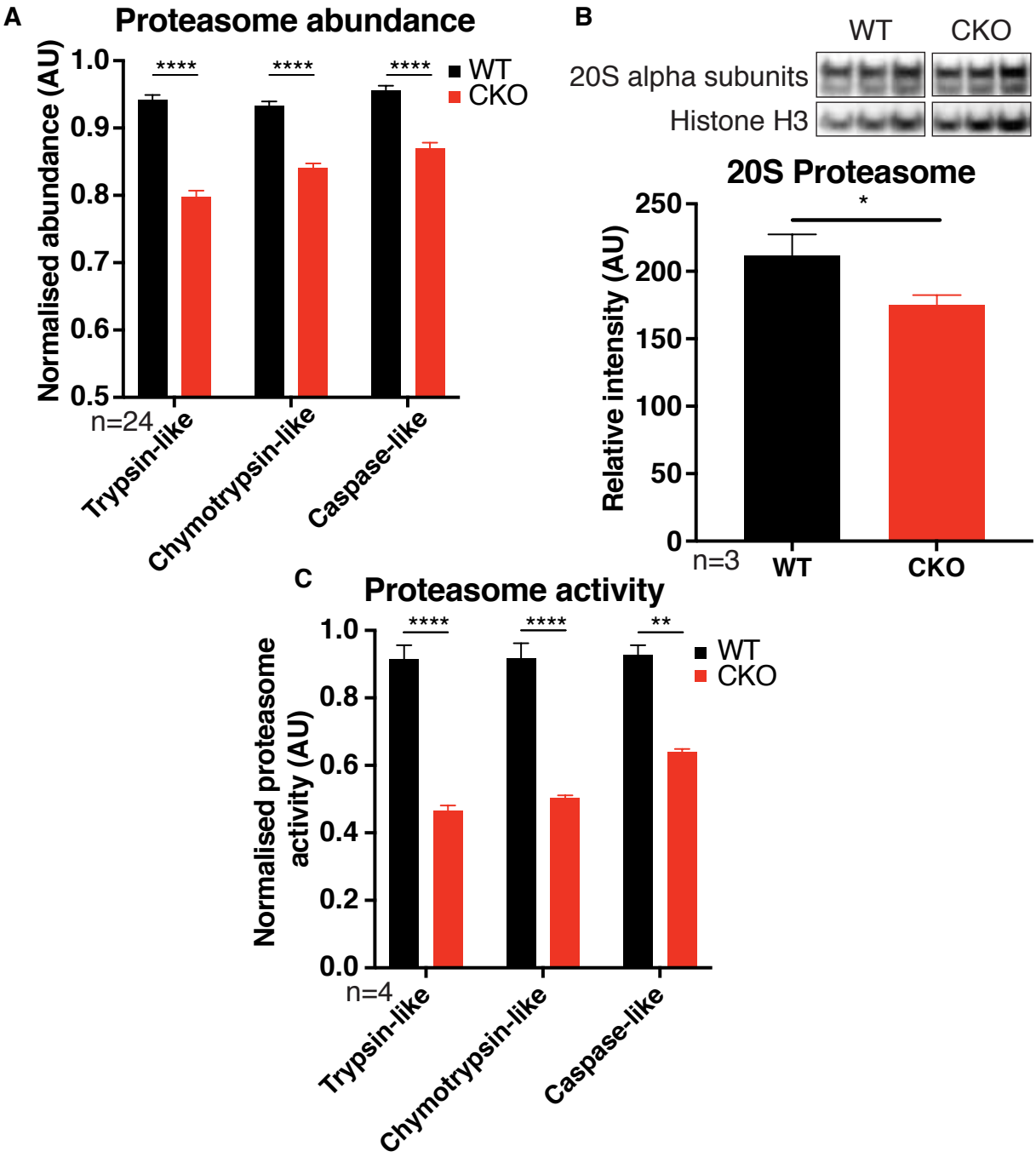

Figure 6.3 CKO cells have reduced proteasome activity. **A)** Relative abundance averaged over time of catalytic proteasome subunits, quantified in the proteomics experiment presented in Chapter 4. Trypsin-like ($\beta 2$), chymotrypsin-like ($\beta 3$) and caspase-like ($\beta 1$) subunits are shown. Mean±SEM, 2-way ANOVA. **B)** Western blots using an antibody that recognises all 7 α-subunits of the 20S proteasome, with anti-histone H3 as loading control. Quantification shown below, mean±SEM, Student's t test with Welch correction. **C)** Proteasome activity measured using ProteasomeGlo Assay (Promega). Trypsin-like, chymotrypsin-like and caspase-like activities were measured separately on the same 96-well plate. Mean±SEM, 2-way ANOVA. Representative experiment shown, N=6.

be chemically labelled with high specificity to an alkyne-containing molecule that acts as the reporter. In my experiment I used biotin-alkyne, which can be detected by Western blot with streptavidin-HRP. I used this method, labelling cells at 2 timepoints in the circadian cycle with AHA. I found that there was no difference between WT and CKO, and there was a trend for increased AHA incorporation at T33 relative to T21 in both genotypes (Figure 6.4B).

For both of these experiments there was only one biological replicate. More replicates would be advisable to confirm that there was no difference in translation between WT and CKO cells. In addition, carrying out measurements at different times of day would be useful for confirming if circadian rhythms in translation also occur in CKO cells – this is known to be the case in WT cells [78]. However, the results shown here suggest that there is no great difference in translation rate – only a small difference would likely be detected by increasing replicate number. Therefore it is reasonable to conclude that CKO cells are likely to have dysregulated protein homeostasis subsequent to unbalanced protein synthesis and degradation – they have the same synthesis rate as WT cells but half the rate of proteasomal degradation. Sequelae of this include the possibility of protein accumulation in the cell (as seen in Figure 6.1), and the subsequent need to prevent protein misfolding and aggregation using molecular chaperones. This is explored next.

6.2.4 Development of a method to measure cytosolic protein folding activity

In addition to regulating synthesis and degradation, protein homeostasis also includes regulation of protein folding. To test the folding activity in cultured cells I developed a luciferase refolding assay based on previous studies investigating chaperone activity [317]. Thermal denaturation of firefly luciferase produces unfolded intermediates that are enzymatically inactive. In the original assay, incubation with rabbit reticulocyte lysate-based buffer results in refolding through ATP-dependent chaperones, and this is detected by the recovery of luciferase enzyme activity [318, 319]. I wished to modify this assay to work with cytosolic extracts from primary fibroblasts, thus measuring the folding activity of the cytosol.

I determined that partial denaturation by heating at 45°C for 35 minutes resulted in the attenuation of luciferase activity, and this was the shortest incubation time required at this temperature, beyond which little difference could be seen (Figure 6.5A). After incubating the denatured luciferase alone at 37°C for 1 hour there was some degree of spontaneous refolding resulting in increased luciferase activity (Figure 6.5B). However, incubation together with cytosolic extract resulted in more efficient refolding, and this was abolished by boiling the cytosolic extract prior to incubation (Figure 6.5B). This suggested that the refolding was dependent on an active enzymatic process.

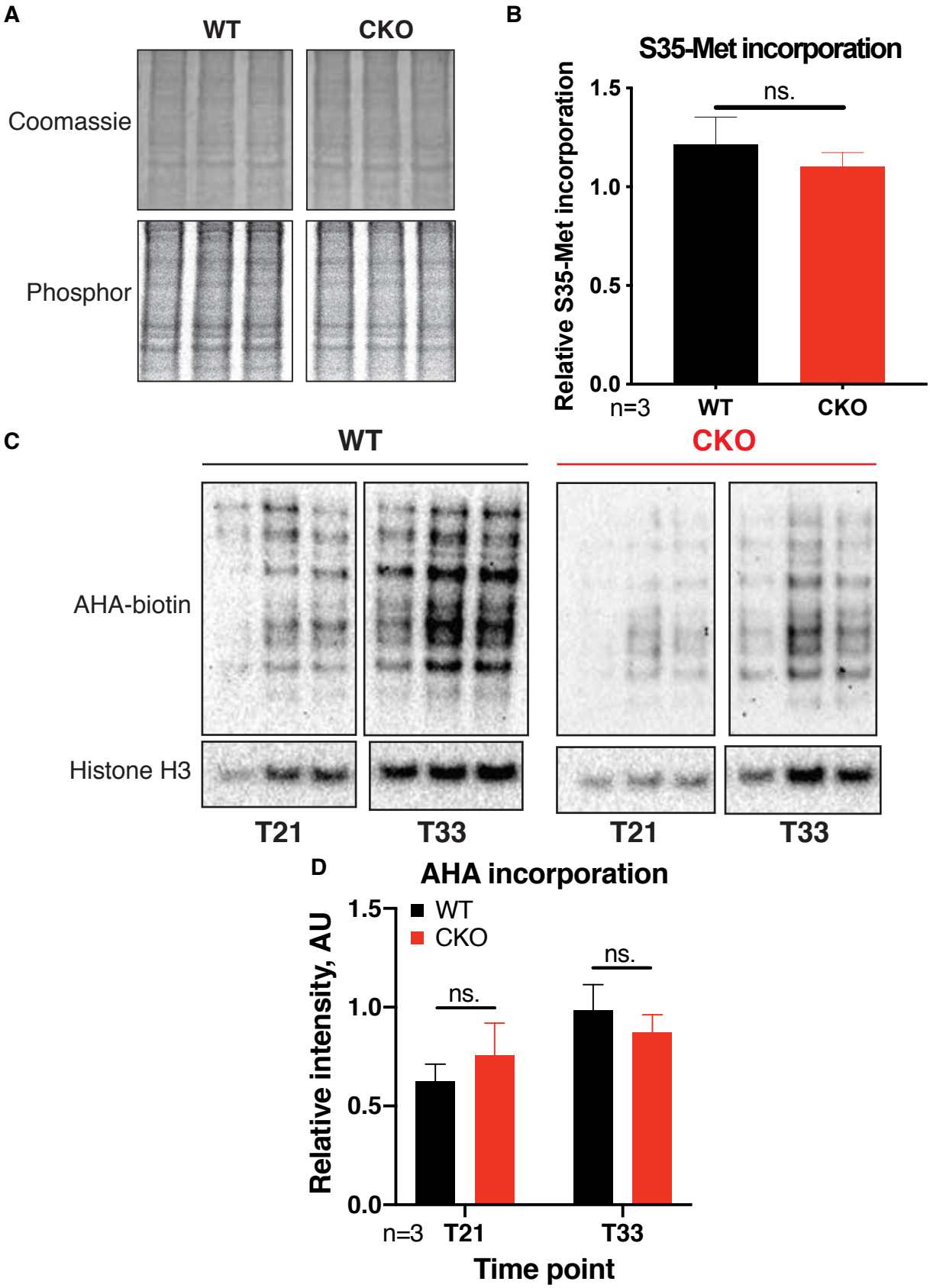

Figure 6.4 CKO cells do not have a different translation rate compared with WT. A) WT and CKO cells were pulsed with 0.1 mCi/mL 35S-methionine to radiolabel newly synthesised proteins. Phosphor screen autoradiographs, with Coomassie image below. **B)** Quantification of A). Mean±SEM, Student's t test with Welch correction. **C)** Representative Western blots showing AHA incorporation by probing against biotin. Histone H3 was the loading control. The two timepoints are referred to as experimental time 21 and 33 (T21 and T33), according to the number of hours after the last medium change. **D)** Quantification of C). Mean±SEM, Student's t test with Welch correction.

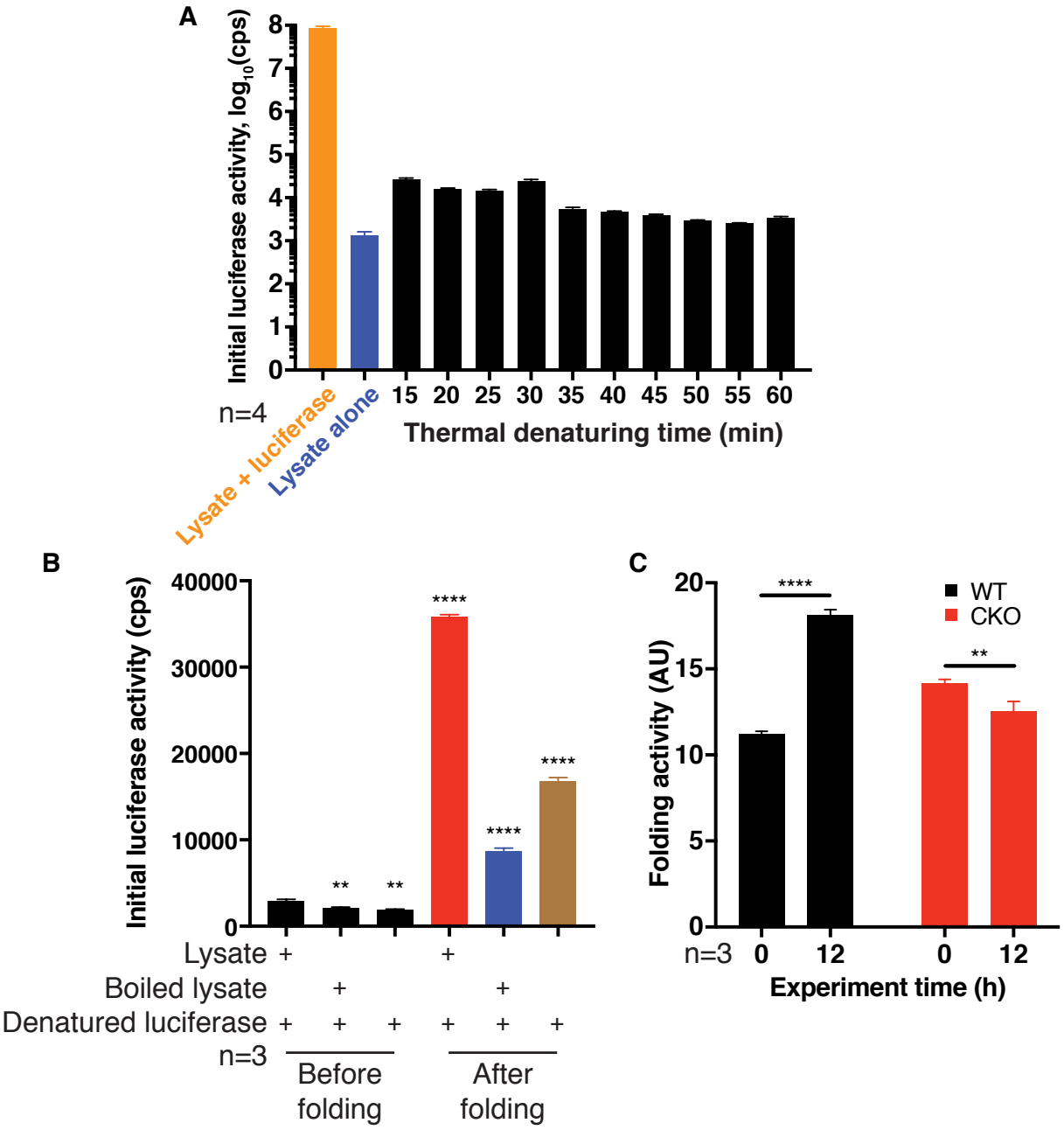

Figure 6.5 Development of a luciferase refolding assay. A) Optimisation showed that heating for 35 minutes was optimal for thermal denaturation of luciferase. Recombinant luciferase was mixed with cell lysate and heated at 45°C for 15-60 mins and bioluminescence was recorded. Positive control (orange) was non-denatured luciferase with cell lysate. Negative control (blue) was cell lysate alone. Mean±SD. **B)** Bioluminescence recordings were done before the incubation for folding as well as afterwards. Thermally denatured luciferase was incubated with cell lysate, boiled cell lysate, or buffer in the absence of cell lysate as a negative control. After folding, there was some spontaneous refolding in the negative control, but much higher luciferase activity in the samples with cell lysate. This was attenuated in samples with boiled cell lysate, suggesting that the refolding is dependent on enzymatic activity. 2-way ANOVA with Dunnett's multiple comparisons test, comparing to control. **C)** Folding activity assays were performed with cell lysates obtained from WT and CKO cells at two timepoints. "Folding activity" is the fold-change of luciferase activity in the samples relative to the pre-assay control (see Chapter 2.12 for details). Both genotypes showed time-of-day variation but the direction of change was opposite in CKO (2-way ANOVA).

By using the modified luciferase refolding assay, I found a time of day difference in folding activity in the WT cells, and a disrupted pattern in CKO cells (Figure 6.5C). More specifically, folding activity increased in WT cells by roughly 60% between the time points whilst folding activity in CKO cells decreased by roughly 10%. Hence both the magnitude and direction of change was different. It would be useful to conduct a time course experiment to test whether there is in fact circadian regulation of folding activity in the cell. This would confirm whether there is a rhythm in chaperone activity in WT and CKO cells, and whether this is disrupted in CKO cells.

I sought to test whether there is a difference in abundance of chaperones in CKO cells relative to WT. First I examined the quantitative proteomics dataset, focussing on the major HSP90 and HSP70 isoforms as these are highly abundant molecular chaperones. I examined the constitutive (*Hsp90ab1*) and inducible (*Hsp90aa1*) forms of HSP90 as well as the constitutive (*Hspa8*) and inducible (*Hspa1b*) forms of HSP70. Constitutive forms are always expressed in the cell, whilst inducible forms are primarily expressed in response to the presence of misfolded proteins. Comparing the average expression across all time points, I found differences in expression level in the constitutive isoform of HSP90 and both constitutive and inducible forms of HSP70 (Figure 6.6A). These differences were less than 10%, apart from the inducible form of HSP70, which was 1.8 times more abundant in CKO cells relative to WT. This suggests that CKO cells have a chronically increased expression of inducible HSP70, consistent with the presence of higher concentrations of proteins that need to be folded.

I then attempted to quantify HSP expression by Western blot. I took samples at two time points, 12 hours apart so that I could measure an average over time. I used primary antibodies that recognised both inducible and constitutive forms of HSP90 and HSP70. This experiment showed an increased expression of HSP90 in CKO cells relative to WT, and decreased expression of HSP70 (Figure 6.6B, C). This does not align with the quantitative mass spectrometry data. However, in future work it would be informative to use antibodies specific to inducible or constitutive forms, and using a different loading control would be different, since there may have been a time of day difference in tubulin abundance (Figure 6.6B). These technical factors may explain the difference in result compared to the quantitative mass spectrometry.

6.2.5 CKO cells are more sensitive to stress

Since CKO cells have impaired protein folding and degradation as well as a higher basal protein content, I hypothesised that they would be more sensitive to proteotoxic stress. The integrated stress response is a cellular response to a diverse range of stimuli including ER stress and amino acid deprivation [214]. The common event from all the stress-inducing stimuli is the phosphorylation of eIF2α which leads to a shutdown of translation globally, whilst promoting the synthesis of factors such as ATF4 to restore proteostasis [320].

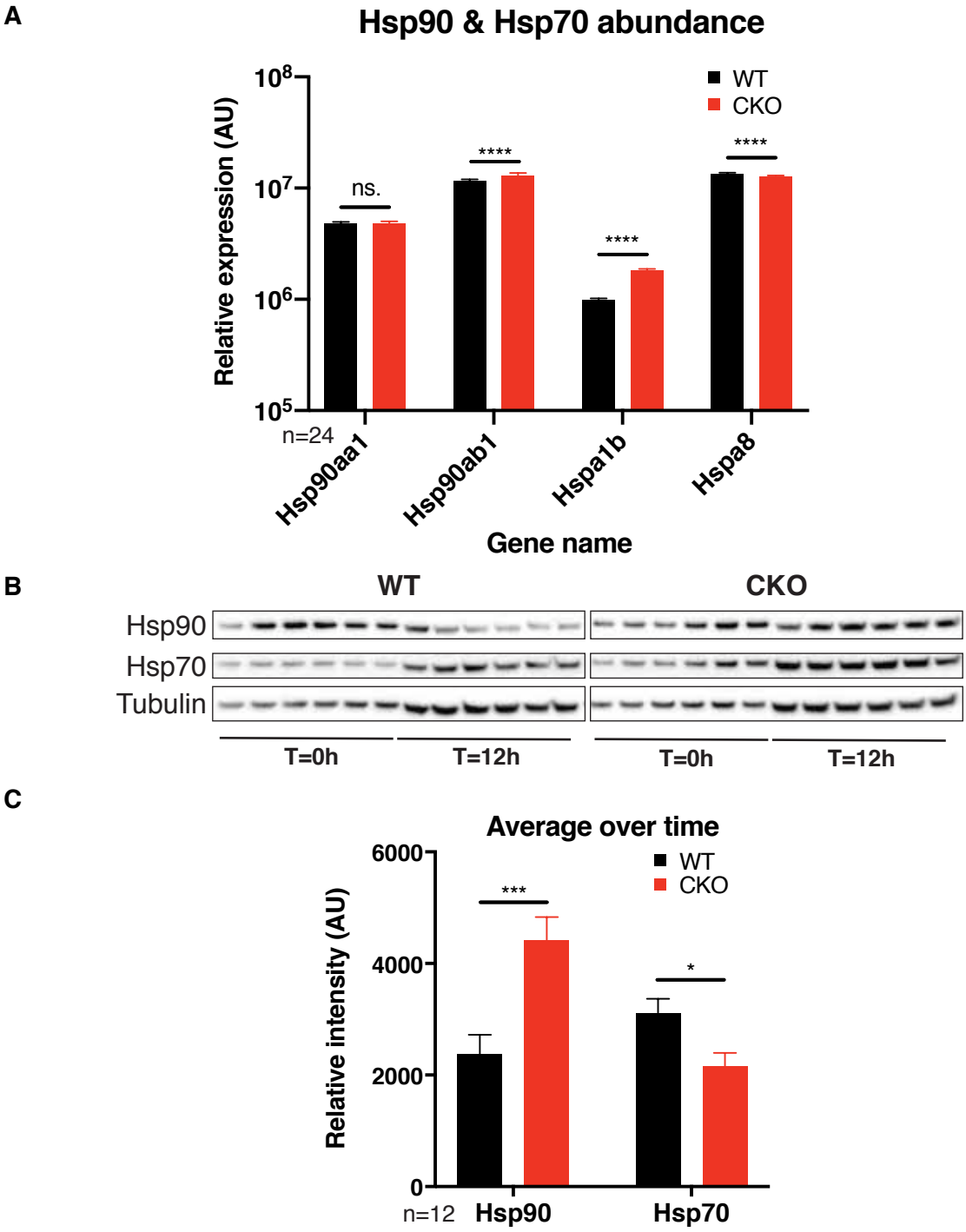

Figure 6.6 Comparison of chaperone abundance in WT and CKO cells. A) Relative abundance averaged over time of HSP90 and HSP70 isoforms, quantified in the proteomics experiment presented in Chapter 4. Gene names are annotated, corresponding to inducible HSP90 (Hsp90aa1), constitutive HSP90 (Hsp90ab1), inducible HSP70 (Hspa1b) and constitutive HSP70 (Hspa8). Mean±SEM, multiple t tests. **B)** Western blots of whole cell lysates collected at 2 time points, 12 hours apart (T=0h, T=12h). Antibodies used in this experiment against HSP90 and HSP70 recognise both inducible and constitutive forms. Tubulin was the loading control. **C)** Quantification of B), mean±SEM, multiple t tests with Holm-Sidak correction.

I performed an experiment to measure the response to physiological stress inducers, using different media as informed by the optimisation experiments described in Chapter 5. I found that even changing into air medium with high glucose (5 g/L) resulted in increased expression of phosphorylated eIF2α relative to WT (Figure 6.7A/B). This was not dependent on the length of time in culture (Figure 6.7A/B). This was surprising since I did not expect the medium change to be a stress-inducing perturbation, but it does suggest that CKO cells may have a greater sensitivity. Under low glucose conditions, the CKO cells were also different to WT (Figure 6.7C). Plotting the same data grouped by genotype, there was a small but significant effect of glucose concentration on WT cells (Figure 6.7D), but not on CKO cells (Figure 6.7E). Altogether, compared to WT, CKO cells expressed higher levels of phosphorylated eIF2α after a medium change regardless of time in culture or glucose concentration. However, the level of phosphorylated eIF2α after medium change decreased as a function of time in culture in both genotypes, suggesting that confluence reduces sensitivity to medium change-induced stress.

To test the response to proteotoxic agents I treated cells with tunicamycin. Tunicamycin inhibits GlcNAc phosphotransferase, which mediates the first step of protein glycosylation in the ER, thus leading to the accumulation of misfolded proteins and induction of the unfolded protein response (UPR) [321, 322]. I also included WT cells treated with KS15 – a drug designed to inhibit both CRY1 and CRY2 [323, 324] to test for recapitulation of the CKO phenotype. CKO cells had higher levels of phosphorylated eIF2α throughout the experiment (Figure 6.8A, B). This suggests that they have an upregulated integrated stress response basally and in response to tunicamycin. WT cells treated with KS15 did not have significantly higher phosphorylated eIF2α levels relative to control, and in fact showed a trend for decreased phosphorylated eIF2α levels (Figure 6.8A, B). This is likely because KS15 is not in fact an effective inhibitor of CRY proteins, as I subsequently discovered – this is discussed later with reference to Figure 6.12, where KS15 did not abolish rhythms, only shortening period by about 1 hour at the maximum concentration permitted by its solubility. Other ways to recapitulate the CKO phenotype in WT cells could be to use inhibitors of phosphatases of eIF2α. Such inhibitors include guanabenz [325] and sephin1 [326], which have been touted as compounds that enhance survival of stressed cells through prolongation of the ISR. Chronic treatment of WT cells with a low dose of these compounds may increase eIF2α phosphorylation – this would be a useful tool to test the effect this has on circadian rhythmicity. However, it would not reveal the mechanism for increased phosphorylated eIF2α in CKO cells, and recent work has suggested that these compounds may not in fact have any effect on the ISR [327].

6.2.6 Cryptochromes limit the rhythmic regulation of intrinsically disordered proteins

Proteins that do not natively adopt a 3D structure are known as intrinsically disordered proteins (IDPs) [200, 328]. IDPs may bind to different targets depending on protein concentration, and so

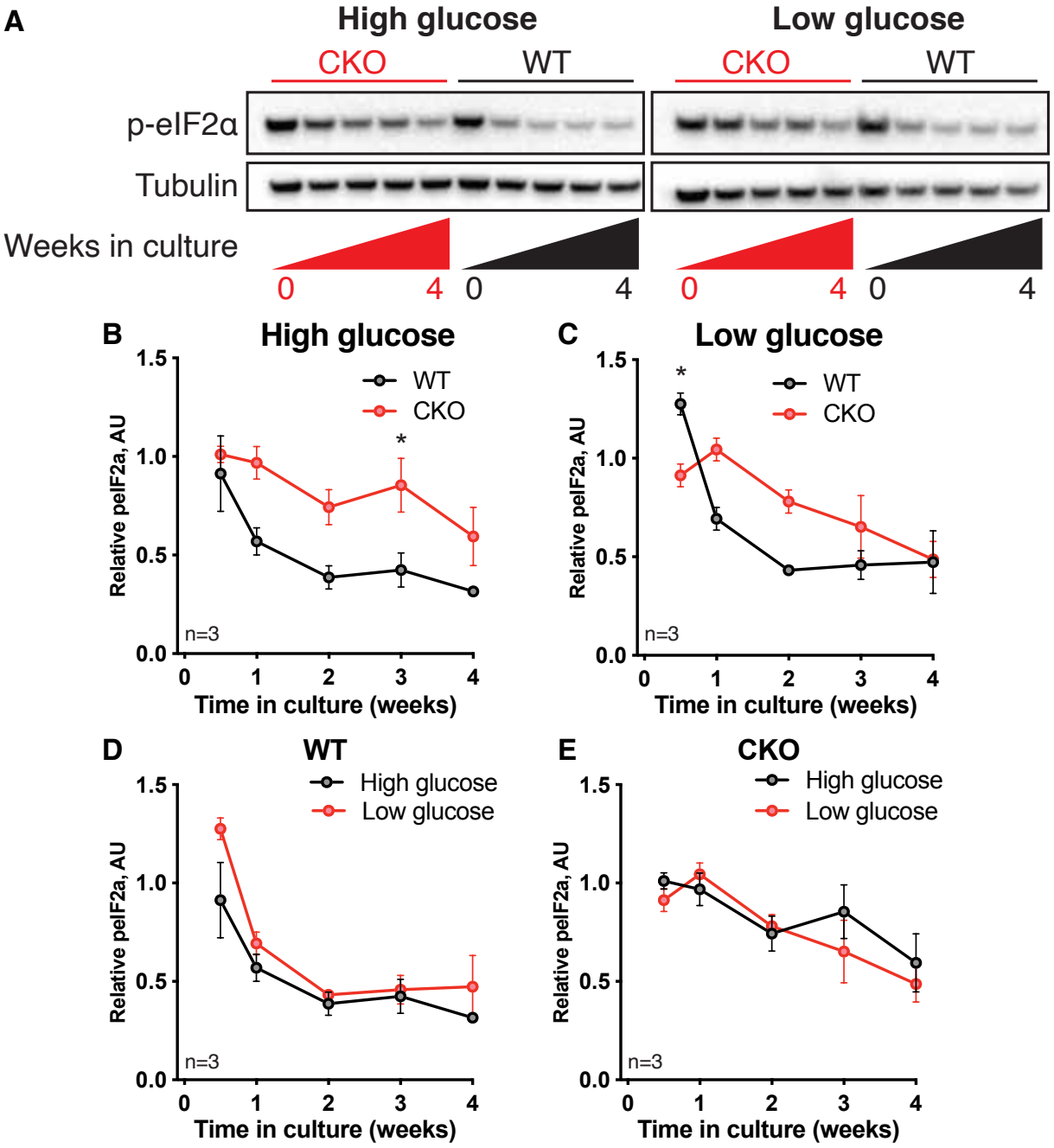

Figure 6.7 CKO cells have a higher expression of phosphorylated eIF2α compared to WT. **A)** Cells cultured for varying amounts of time (between 0 and 4 weeks) were changed into medium containing high (5 g/L) or low (1 g/mL) glucose. 4 hours later they were lysed in RIPA buffer. Representative Western blots shown, probing for phosphorylated eIF2α and tubulin as loading control. **B), C)** Western blot quantifications are plotted here, grouped by glucose concentration to show differences between genotypes. Mean±SEM, 2-way ANOVA. For high glucose, p=0.0001 for genotype effect, for low glucose, p=0.004 for interaction. Asterisks indicate statistically significant differences detected by Sidak's multiple comparisons. **D), E)** The same data is plotted but grouped as genotypes instead to demonstrate that there are no differences between medium glucose concentration. For WT, p=0.03 for glucose effect, for CKO, p=0.37 for glucose effect.

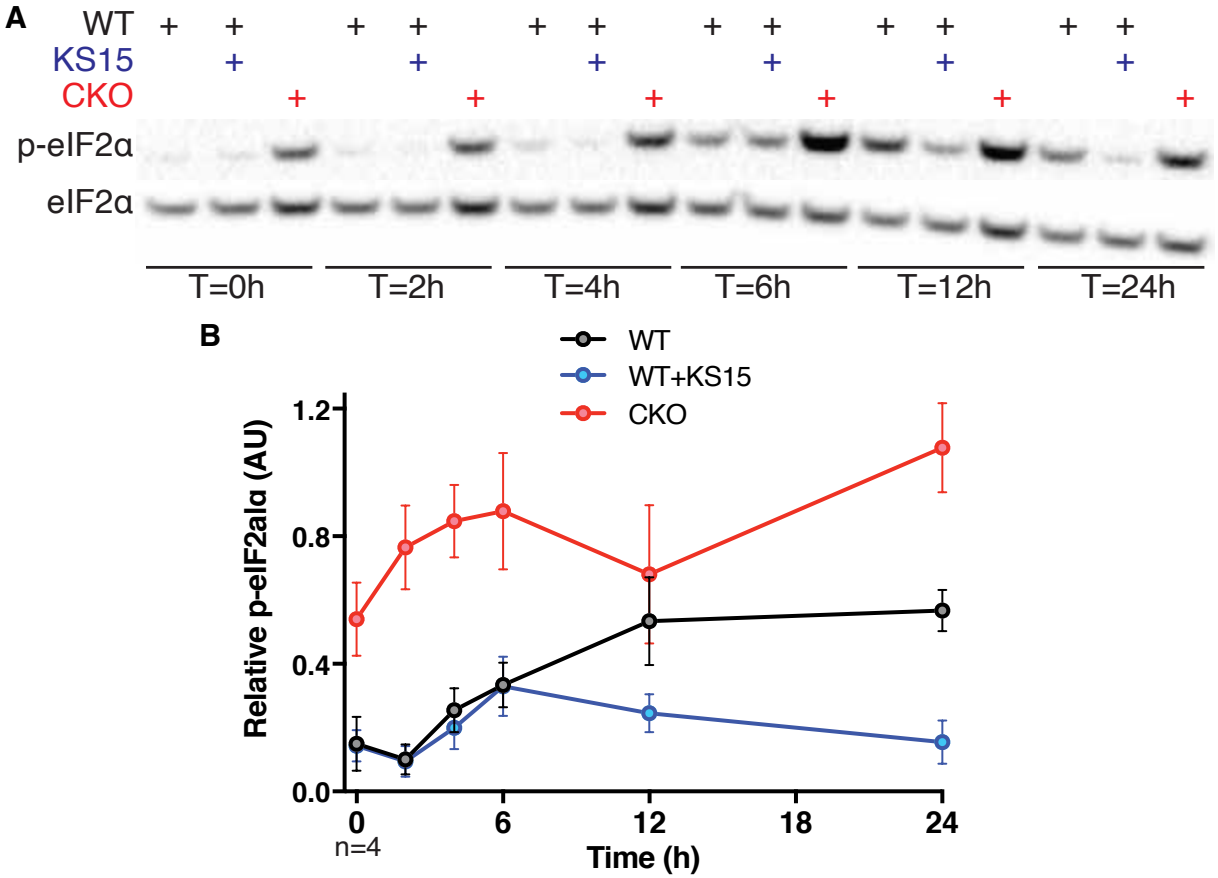

Figure 6.8 The loss of CRY results in increased phosphorylation of eIF2α in response to tunicamycin. A) Cells treated with 500 nM tunicamycin (TUN) were lysed in RIPA buffer at time points from 2-24 hours. WT cells were compared with WT cells treated with 50 µM KS15 (CRY inhibitor) as well as CKO cells. A representative western blot is shown, with probes against phosphorylated (above) and total (below) eIF2α. **B)** Quantification of the western blots in A), including all replicates. Mean±SEM, n=4. 2-way ANOVA showed $p<0.0001$ for genotype effect when comparing WT and CKO, $p=0.03$ for interaction between time and drug treatment when comparing WT and WT with KS15, and $p<0.0001$ for genotype effect when comparing CKO with WT with KS15.

they are tightly regulated in the cell; defects in this lead to disease conditions including cancer and neurodegeneration [329]. In addition, IDPs tend to form aggregates depending on concentration and macromolecular crowding [330, 331]. Macromolecular crowding has a profound effect on reaction rates [332], and so the circadian rhythms in cytosolic protein concentration observed in Chapter 5 may have important functional consequences for IDP aggregation and cellular reaction rates generally.

I hypothesised that if the cellular protein quality control mechanisms are impaired, then levels of IDPs may be dysregulated. I tested this using the proteomics datasets presented in Chapter 4 and sought to assess whether or not rhythmic proteins had higher levels of disorder compared to the background (all proteins in the dataset including rhythmic and non-rhythmic).

I used the meta-predictor D2P2 [333], which draws from 9 independent algorithms to inform predictions of disorder in the amino acid sequences of proteins. Dr Arun Prasad kindly configured the database to allow my searches of several thousand proteins via the web application programming interface, and he also wrote a Python script that enabled me to access the database. I used this script to mine my datasets and create an output containing all the amino acids that are predicted to be in disordered regions by at least 75% of databases. Hence I was able to record the number of disordered amino acids for each protein and each phosphopeptide detected. Using these numbers, I could use statistics to examine the distribution of disordered amino acids in rhythmic proteins and phosphopeptides, comparing them to the background in each case.

In WT cells there was no statistically significant difference in the median number of disordered amino acids among rhythmic proteins compared to background (Figure 6.9A) However, there was a difference in CKO cells, with the median number in rhythmic proteins being lower than in the background (Figure 6.9B). I created probability density plots to enable visual comparison of disorder between rhythmic and background groups in a non-cumulative manner (Figure 6.9C,D). This allowed visualisation of any differences amongst specific ranges of disorder that could be missed in a cumulative distribution function. Inspecting the probability density plots more closely, both WT and CKO cells showed an enrichment in the rhythmic proteins with fewer than 100 disordered amino acids (Figure 6.9C, D). This suggests that the abundance of proteins with some disorder below a threshold of around 100 amino acids is more likely to be under rhythmic control, and this is amplified in the absence of cryptochromes.

Phosphorylation is the most common post-translational modification in the cell [189, 190], and most phosphorylation sites are within intrinsically disordered regions [334]. Due to its double negative charge, phosphorylation is a key regulator of structure and function of IDPs in the cell [335]. Since protein:ion ratio is under circadian control in the cell (Chapter 4), I hypothesised that rhythmic phosphopeptides may be more likely to come from peptides with higher disorder. From my phosphoproteomics dataset, there was no statistical difference in WT cells in the median number disordered amino acids between rhythmic phosphopeptides and background (Figure 6.9E). This was also the case in CKO cells (Figure 6.9F). However,

examining the probability density plots in WT cells, rhythmic phosphopeptides were enriched for parent proteins with more than 500 disordered amino acids (Figure 6.9G). In CKO cells the enrichment was for parent proteins with more than 1000 disordered amino acids (Figure 6.9H).

Together, these findings suggest that rhythmic proteins may be enriched for those with up to 100 disordered amino acids, but rhythmic phosphopeptides may be enriched for those with larger amounts of disorder. These differences were small, but seemed enhanced in CKO cells. Future analyses taking into account protein abundance and specific composition of disordered regions will be necessary to ascertain whether there is functional relevance. In particular, rhythms in protein:ion ratio may affect molecular condensation of proteins, particularly if they have regions of disorder.

6.2.7 CKO cells show a metabolic defect

Another consequence of dysregulated protein quality control in the absence of cryptochromes may be abnormal cellular metabolism and so I hypothesised that CKO cells may have a different metabolic profile to WT cells. To measure this I used the Seahorse assay [239, 240]. This is a commercially available system where the experimenter seeds cells into a provided plate. Once the cells have adhered, the medium is changed into one that lacks a pH buffer. A machine then uses a probe to measure the extracellular pH changes over time to obtain extracellular acidification rate (ECAR). This is a rough measure of glycolysis. Another probe is used to measure changes in dissolved oxygen over time, thus obtaining oxygen consumption rate (OCR). This is a measure of mitochondrial respiration. Experimental details are described in more depth in Chapter 2.16.

Using the Seahorse assay I found that CKO cells had a two-fold higher extracellular acidification rate (ECAR) than WT cells (Figure 6.10A), suggesting that they have a higher rate of glycolysis. Oxygen consumption rate was also increased but to a lesser extent, so mitochondrial respiration was less affected (Figure 6.10B). These observations were passage-dependent, since there was no statistically significant difference when using cells of passage 20, only a trend (Figure 6.10C, D). The passage-dependence suggests that CKO cells may be more sensitive to cellular transformation compared to WT cells.

It has previously been found that CRY1$^{-/-}$; CRY2$^{-/-}$ mouse embryonic fibroblasts (MEFs) have reduced glycolytic gene expression and roughly 20% less lactate production [136]. The experiment in this study was performed under different conditions to mine: MEFs were seeded 8 hours before lactate concentration in the medium was measured. It is plausible that the rate of lactate production changes as a function of time spent in culture, and so the effect that I have observed may only be seen after 24 hours in culture, once the cells have all attached and become confluent.

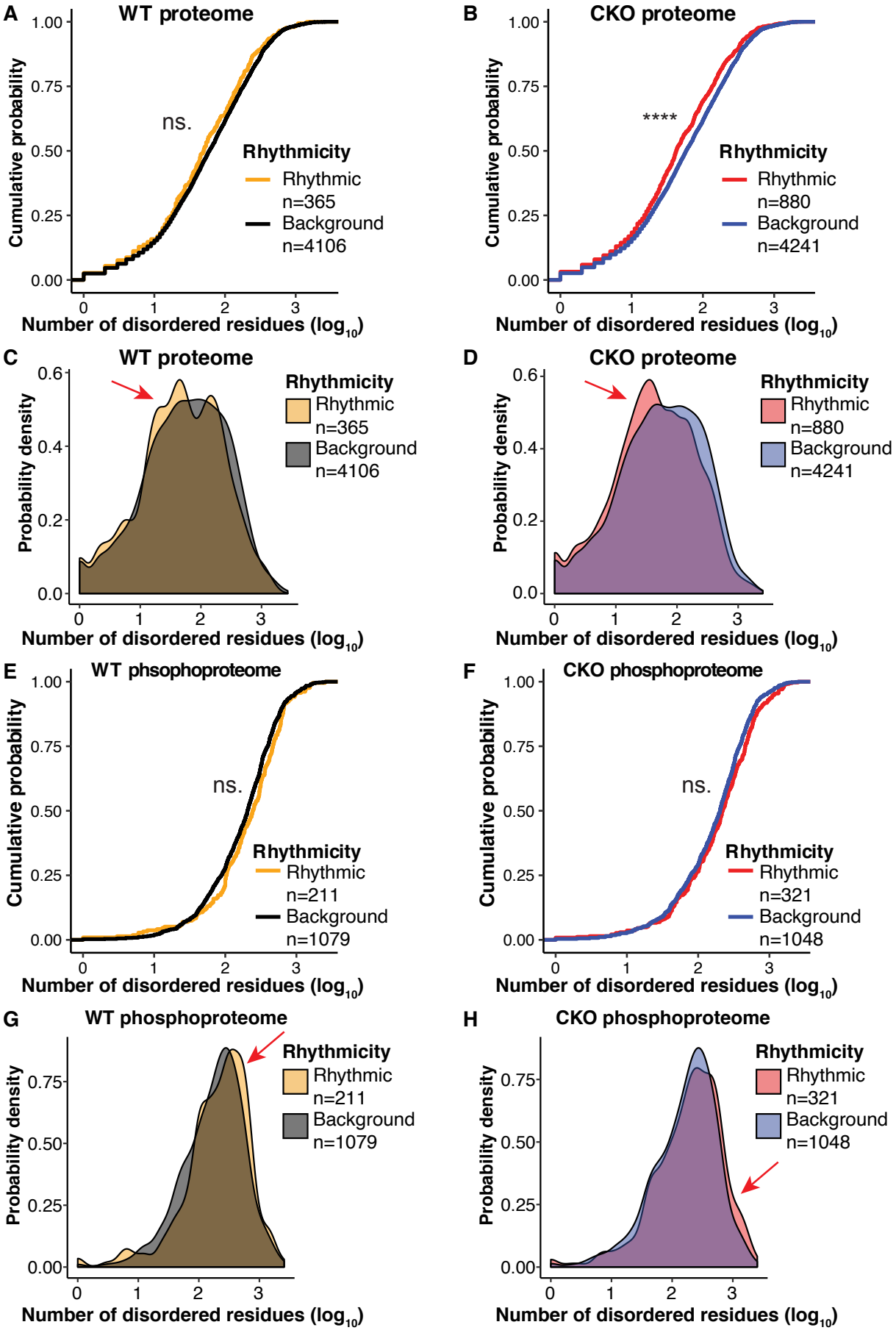
A
WT proteome
Cumulative probability
1.00
0.75
0.50
0.25
0.00
ns.
Rhythmicity
Rhythmic
n=365
Background
n=4106
0
1
2
3
Number of disordered residues (log10)
B
CKO proteome
Cumulative probability
****
Rhythmicity
Rhythmic
n=880
Background
n=4241
Number of disordered residues (log10)
C
WT proteome
Probability density
0.6
0.4
0.2
0.0
Rhythmicity
Rhythmic
n=365
Background
n=4106
Number of disordered residues (log10)
D
CKO proteome
Probability density
Rhythmicity
Rhythmic
n=880
Background
n=4241
Number of disordered residues (log10)
E
WT phsophoproteome
Cumulative probability
ns.
Rhythmicity
Rhythmic
n=211
Background
n=1079
Number of disordered residues (log10)
F
CKO phosphoproteome
Cumulative probability
ns.
Rhythmicity
Rhythmic
n=321
Background
n=1048
Number of disordered residues (log10)
G
WT phosphoproteome
Probability density
0.75
0.50
0.25
0.00
Rhythmicity
Rhythmic
n=211
Background
n=1079
Number of disordered residues (log10)
H
CKO phosphoproteome
Probability density
Rhythmicity
Rhythmic
n=321
Background
n=1048
Number of disordered residues (log10)

Figure 6.9 Disorder in the rhythmic proteome and phosphoproteome in WT and CKO cells. A), B) Cumulative distribution function curves of amount of disorder in rhythmic and background proteins in WT and CKO cells. There was no statistical difference in the median number of disordered amino acids between rhythmic and background proteins in the WT, but there was in CKO (2-sided Kolmogorov-Smirnov test, p=0.178 for WT [median = 50 for rhythmic, 60 for background], p<0.0001 for CKO [median = 42 for rhythmic, 58 for background]). **C), D)** Probability density plots of disorder showing the distribution between rhythmic and background proteins in both genotypes. In both genotypes there were proportionally more proteins in the rhythmic set with less than 100 disordered amino acids (red arrows). **E), F)** Cumulative distribution function curves of amount of disorder in rhythmic and background phosphopeptides in WT and CKO cells. There was no statistical difference in the median number of disordered amino acids between rhythmic and background phosphopeptides in WT or CKO (2- sided Kolmogorov-Smirnov test, p=0.145 for WT [median = 242 for rhythmic, 205 for background], p=0.166 for CKO [median = 215 for rhythmic, 202.5 for background]). **G), H)** Probability density plots of disorder showing the distribution between rhythmic and background phosphopeptides in both genotypes. In both genotypes there were proportionally more proteins in the rhythmic set with more than 300 disordered amino acids (red arrows).

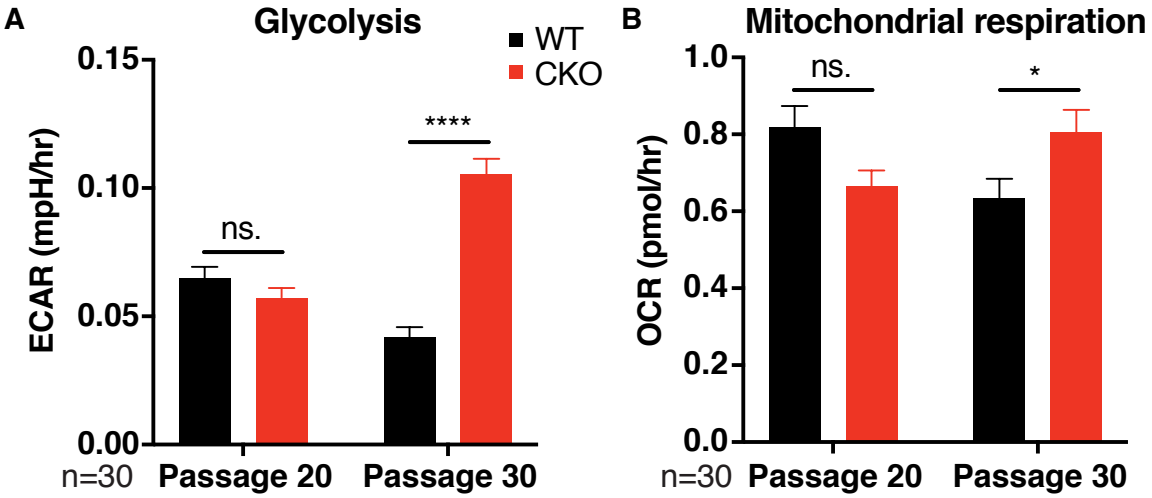

Figure 6.10 CKO cells have a higher rate of glycolysis compared to WT cells. A) Seahorse assays were performed with cells at passage 20 and at passage 30. Extracellular acidification rate (ECAR) is plotted here, mean±SEM. 2-way ANOVA with Sidak's multiple comparisons test. N=3. **B)** Oxygen consumption rate (OCR) measured with Seahorse assays is plotted here, mean±SEM. 2-way ANOVA with Sidak's multiple comparisons test.

Mouse ID	CRY2 genotype	Sex	Age at death (weeks)	Report findings
1	KO	M	3	**EMH**, neutrophilic inflammation in lungs
2	KO	F	0.3	**EMH**, low liver glycogen, bilateral hydronephrosis
3	KO	F	8	**EMH**, bilateral hydronephrosis
4	HET	M	1	**EMH**, bilateral hydronephrosis
5	HET	F	0.6	**EMH**, low liver glycogen
6	KO	F	20	**EMH**, severe lower urinary tract inflammation

Table 6.1 Histopathology of CRY-deficient mice. 6 histopathological examinations were carried out on mice that were moribund and culled as a result. All mice were CRY1$^{-/-}$ and the CRY2 genotype is listed in the second column as homozygous knockout (KO) or heterozygous (HET). Extra-medullary haematopoiesis (EMH) was found in all cases, and kidney pathology was found in two-thirds.

6.2.8 CRY-deficient mice have physiological defects

Given the metabolic defect, I hypothesised that there may be a phenotype at the organism level. By systematically weighing mice weekly, I found that both male and female CKO mice had a smaller mass than wild-types after around 4 weeks, with the phenotype rescued by one copy of CRY2 (Figure 6.11A, B). This agrees with the findings of the study mentioned above [311]. Despite this, CKO mice had a higher rate of food consumption (Figure 6.11C). This suggests that there is inefficient use of energy in CKO mice, which may be related to the increased glycolysis rate I observed at the cellular level. In line with a global cellular defect, I observed a higher spontaneous death rate in adult CKO mice compared to WT controls (Figure 6.11D). CRY1$^{-/-}$; CRY2$^{+/-}$ mice were WT-like. Post-mortem and histopathology examinations were carried out on 7 mice that underwent spontaneous death, and the most common finding was mild extra-medullary haematopoiesis (EMH, a sign of systemic inflammation) (Table 6.1). This lends support to the hypothesis of a generalised cellular defect. The cause of death was not confirmed in the histopathology reports, but several of the mice likely died due to sepsis or electrolyte disturbance secondary to kidney failure.

In the context of the other findings in this chapter, these results suggest that a general defect in cellular protein homeostasis may result in chronically increased energy consumption, and a consequence of this may be the systemic defects observable at the organism level, i.e. reduced growth and systemic inflammation.

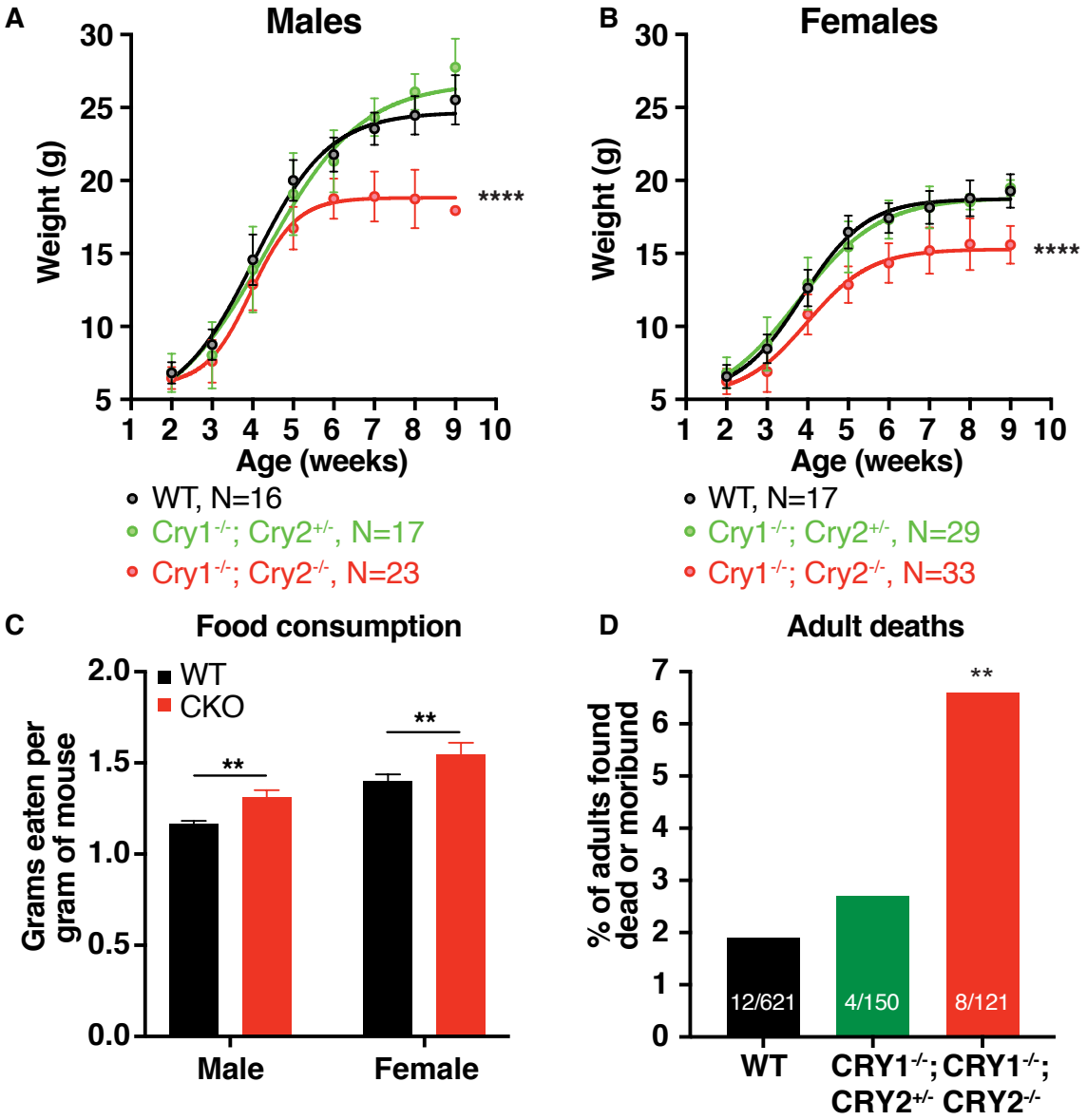

Figure 6.11 CKO mice have health defects. A), B) Growth curves of male and female mice are plotted with weekly weights recorded from mice with the following genotypes: WT, $Cry1^{-/-}$; $Cry2^{+/-}$ and $Cry1^{-/-}$; $Cry2^{-/-}$. Mean±SD. Extra sum-of-squares F test was used to test the null hypothesis that one curve fits all sets. P values annotated as asterisks. **C)** Food consumption measured over 1 week, normalised for mouse weight. Mean±SD, 2-way ANOVA. N=6 per sex for WT, N=4 per sex for CKO. **D)** Spontaneous death rate among the 3 genotypes mentioned in A), expressed as a percentage of the number of mice. The absolute numbers of deaths and total population size are annotated on the bars. Only mice that had been weaned were included, and unnatural causes of death (e.g. cage flooding) were excluded. Asterisk indicates significance from Chi-squared test for trend, p=0.007. Comparing WT and CKO, Fisher's exact test p=0.009. Comparing WT and Het, Fisher's exact test p=0.5.

6.2.9 Pharmacological inhibition of rhythmicity in WT cells

To test the link between CRY and proteostasis further I sought to recapitulate my findings in WT cells by pharmacologically inhibiting CRY1 and CRY2. To do this I treated cells with KS15, a drug designed to inhibit both CRY1 and CRY2 [323, 324].

Measuring PER2::LUC bioluminescence, I found that there was no attenuation of rhythmicity resembling CKO cells, only a small but significant, dose-dependent period shortening (Figure 6.12A, B). This matches findings previously reported using fibroblasts [323]. Hence it is unlikely that KS15 completely inhibits CRY proteins even at the maximum concentration permitted by its solubility. Alternatively, cellular uptake may be low, or the drug may be cleared very efficiently.

I hypothesised that disrupting protein homeostasis should abolish rhythms, since I showed the reverse in Chapter 4, that manipulations that improved protein homeostasis seemed to correlate with the restoration of rhythmicity in CKO cells. In this chapter I showed that CKO cells had reduced proteasome activity, and so I predicted that mimicking this pharmacologically in WT cells may result in a CKO-like phenotype with the PER2::LUC reporter. Proteasome inhibition in WT cells with bortezomib and epoxomicin (within a narrow concentration range) reversibly abolished rhythms (Figure 6.12C, D).

Together with the previous results in this chapter, this provides more evidence to support the hypothesis that in the absence of cryptochromes, proteostasis is disrupted and this in turn attenuates PER2::LUC rhythmicity. To test this in future work, pharmacologically treating WT cells with a CRY activator such as KL001 would be useful – if the hypothesis is correct then both proteostasis and PER2::LUC rhythmicity should be more robust than WT cells treated with control.

6.2.10 Pharmacological inhibition of rhythmicity in WT animals

I sought to take this further and test whether it may be true on the whole organism level. The circadian organisation of mouse behaviour is controlled by the suprachiasmatic nucleus (SCN) in the hypothalamus. However at the cellular level, the same molecular machinery is responsible for generating circadian rhythms in the SCN as the peripheral tissues. Since proteasome inhibition reversibly abolished rhythms in cells, I hypothesised that the same may be true at the whole organism level through effects on the SCN.

Ixazomib is an orally-available analogue of bortezomib [336–338]. As described in Chapter 2, I delivered ixazomib at 35 µg/mL in the drinking water, which was flavoured with blackcurrant squash to mask the taste of the drug. Mouse activity was measured using two methods: a running wheel and an infrared motion sensor.

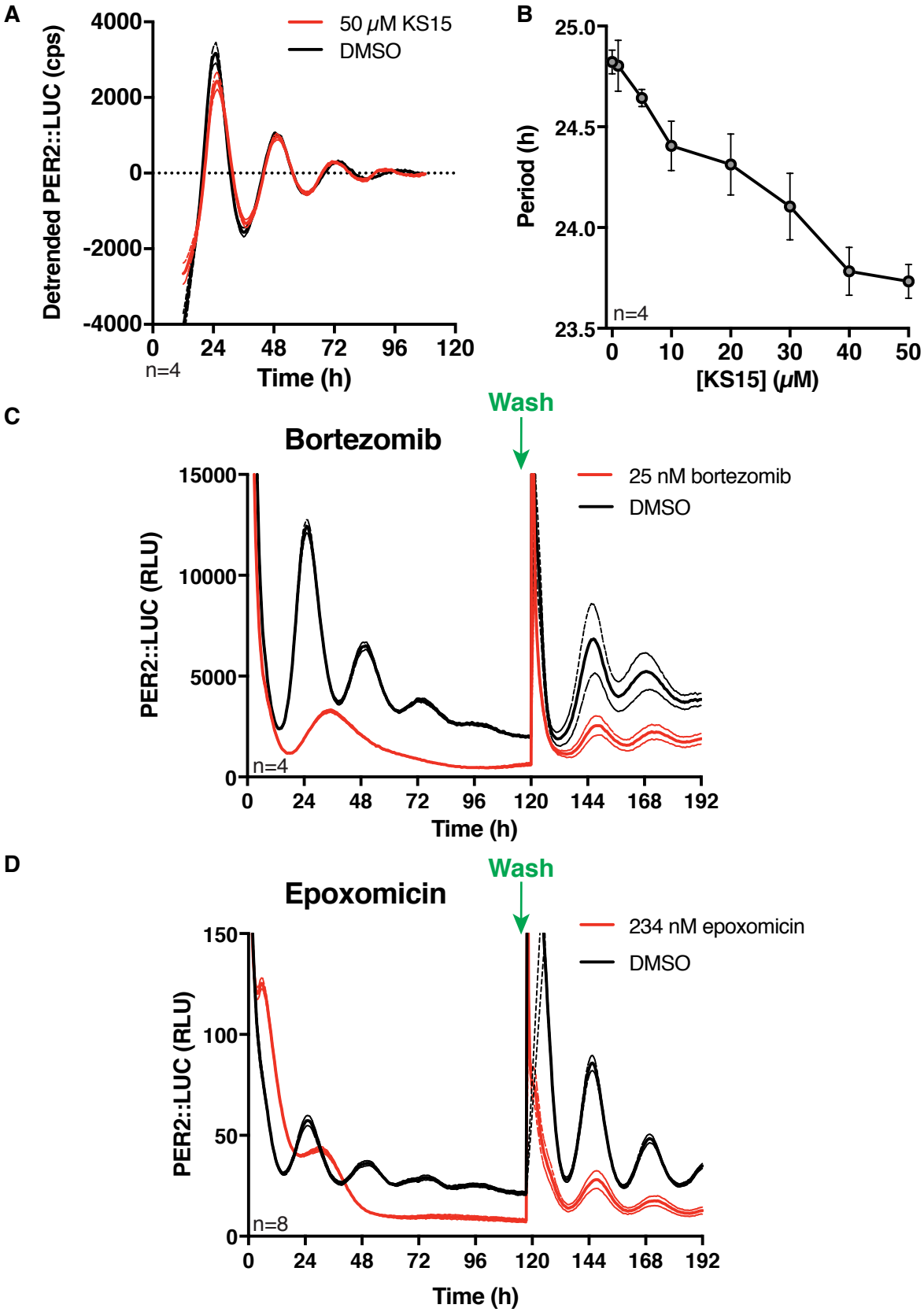

Figure 6.12 WT cells phenocopy CKO cells upon CRY inhibition or proteasome inhibition. **A)** Detrended bioluminescence recordings of WT cells treated with 50 µM KS15 or DMSO control. Mean±SEM. **B)** KS15 treatment results in a dose dependent period shortening. Mean±SEM, one-way ANOVA. **C)** Raw bioluminescence recordings of WT cells treated with 25 nM bortezomib and then washed after 5 days. Mean±SEM. **D)** Raw bioluminescence recordings of WT cells treated with 234 nM epoxomicin and then washed after 5 days. Mean±SEM.

In constant darkness (DD), mice retain their circadian organisation of behaviour – they are more active during the expected dark phase of the cycle (Figure 6.13A, Appendix figure 3). In CKO mice however, they show arrhythmic behaviour in DD despite being able to entrain to LD cycles [230] (Appendix figure 3). I found that mice treated with ixazomib showed lower amplitude rhythms in behaviour, i.e. they were more active during the expected light phase and less active during the dark phase compared to controls (Figure 6.13B, C, D). This reduced consolidation of behaviour to the dark phase is reminiscent of actograms of CKO mice [230] (Appendix figure 3). The effect of ixazomib was reversible when the drug was 'washed out' by changing the drinking water, and there was no effect on period length (Figure 6.13C, D). This is a partial recapitulation of the effect of proteasome inhibition on the cellular level, and fits with the prediction made. However, application of the drug to organotypic SCN slices would be useful to understand the effect on behaviour in more detail, and drug availability to the SCN in an animal must be tested. This is because competing hypotheses include the possibility that ixazomib affects behaviour in a SCN-independent manner, or that circadian organisation of behaviour depends on protein turnover in the SCN. In future, treating CKO mice with a proteasome activator such as PD169316 would be useful as it would test the hypothesis that the reduced proteasome activity ultimately leads to behavioural arrhythmicity.

6.3 Conclusions

6.3.1 Summary of findings

I found that CKO cells have impaired protein degradation and folding as well as disrupted temporal regulation of intrinsically disordered protein abundance. I confirmed that a consequence of this is an increased sensitivity to proteotoxic stress and dysregulated metabolic profile on the cellular level, and reduced growth at the organism level. This could be partially recapitulated in WT cells by pharmacologically targeting CRY proteins, and inducing proteotoxic stress resulted in the reversible attenuation of PER2::LUC rhythmicity *in vitro*, and behavioural rhythmicity *in vivo*.

I hypothesise that CRY proteins are needed to suppress oscillations in IDP abundance and maintain protein homeostasis. Disordered proteins are inherently sensitive to proteasomal degradation [302], and since CKO cells have a reduced proteasome activity they may need to spend more energy on protein quality control in order to maintain proteostasis.

In future studies it will be important to find the precise mechanism behind these findings. As described in section 6.2.2, the reduced proteasome activity in CKO cells relative to WT cannot be fully explained by the small difference in proteasome abundance. Rather, it would be helpful to explore the post-translational regulation of proteasome activity, and whether this is a direct

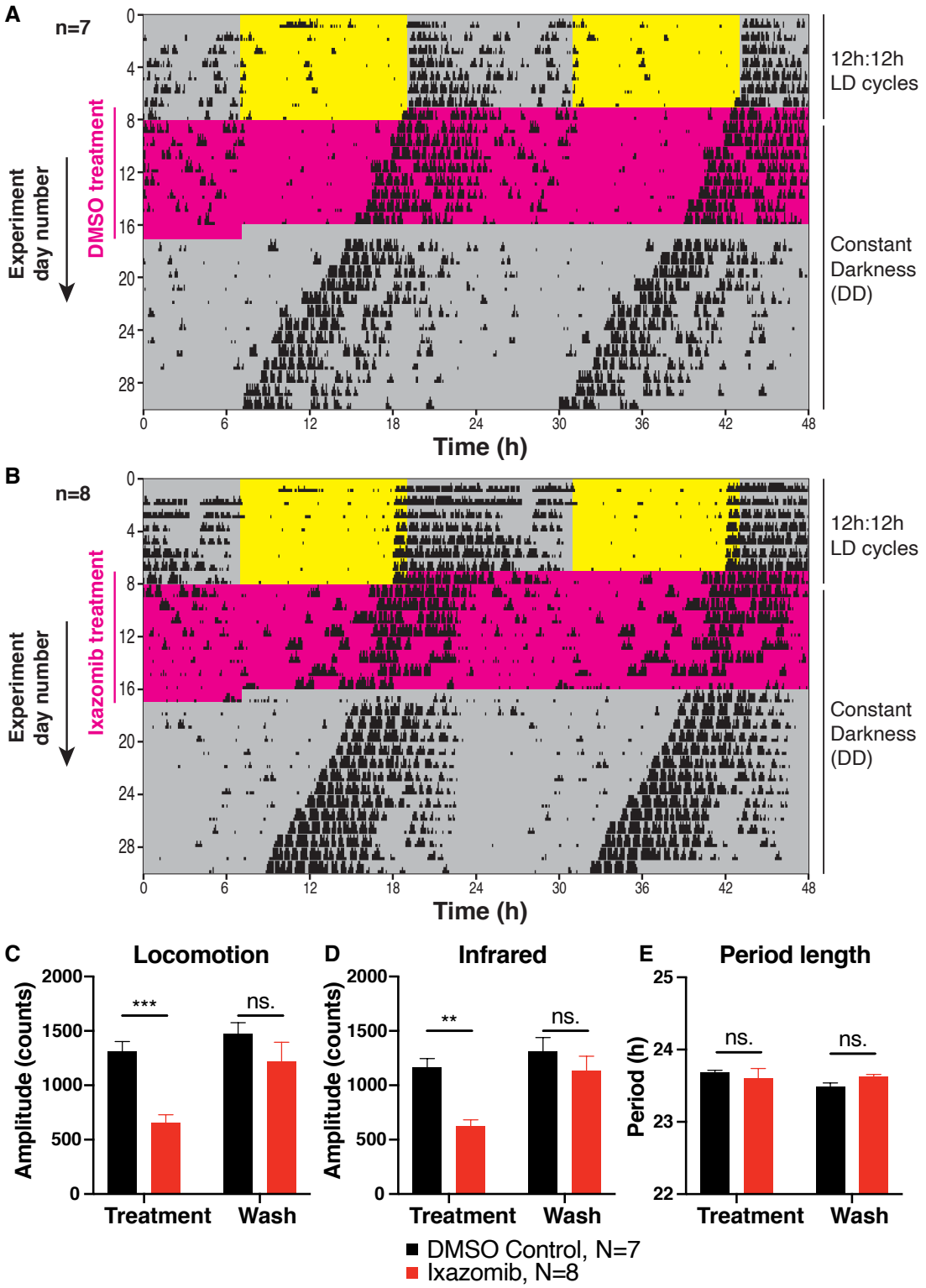

Figure 6.13 WT mice show decreased circadian organisation of activity when treated with proteasome inhibitor ixazomib. A) Representative double-plotted actogram of a WT mouse treated with DMSO control. For the first 7 days the mice were in 12h:12h light-dark cycles, and had drinking water supplemented with blackcurrant squash. The mice then had their drinking water changed to drug-containing blackcurrant squash (or DMSO control), and they were put into constant darkness. After 7 days they were changed back to non-drug-containing blackcurrant squash, but remained in constant darkness until the end of the experiment. **B)** Representative double-plotted actogram of a WT mouse treated with 35 µg/mL ixazomib. **C), D)** Quantification of amplitude of wheel-running activity cycles and infrared-measured total activity cycles during treatment and during the post-drug treatment ('wash') period. Mean±SEM. **E)** Quantification of period length of wheel-running activity cycles during treatment and wash periods. Mean±SEM.

or indirect effect of CRY. Since CRY proteins are promiscuous transcriptional regulators [40] as well as key components of an E3 ligase complex [296, 308], it is feasible that some of its targets are involved in proteasome regulation. Some proteasome regulators were detected in my proteomics and phosphoproteomics data, but experimental validation is needed, along with pharmacological and genetic manipulations to delineate the mechanism.

6.3.2 Proteostasis and TTFL function

In Chapter 5 I described the observation of rhythmic post-translational regulation of PER2::LUC activity, and the sensitivity to experimental conditions that affect protein:ion ratio. The findings in this chapter suggest that CKO cells are less able to regulate protein:ion ratio, and this may result in disrupted proteostasis. There are two possible mechanistic interpretations of this:

1. Loss of the TTFL leads to impaired protein homeostasis
2. Loss of CRY functions that are not related to the TTFL results in impaired protein homeostasis

An experiment to distinguish the two possible mechanisms is to constitutively express CRY1 and CRY2 at their average expression levels. If the first mechanism is correct, there would be defects in proteostasis as described in this chapter. This would not be the case if the second mechanism is correct, since the CRY proteins would be present, maintaining proteostasis independently of the TTFL.

Another useful experiment would be to create an inducible knockout mouse – this would test whether or not the health defects reported in this chapter are due to developmental effects. Such an experiment has been carried out with BMAL1 knockout mice. It was reported in 2006 that BMAL1 knockout mice had a wide range of health problems, including reduced lifespan, premature aging, cataracts and metabolic disorders [339]. At the time it was unclear whether or not this was due to a defect in cellular timekeeping, or another unknown function of BMAL1. 10 years later a conditional knockout was made, and when BMAL1 was knocked out in adult mice, the only health defects remaining were the ocular abnormalities and brain astrogliosis [340]. This indicated that many of the health defects reported in the past were due to problems during development, rather than problems with the clock in adults. However, this does not exclude the possibility that functional rhythms in gene expression are needed during specific developmental windows. To test this, constitutive expression experiments as described above would be decisive. Nevertheless, the fact that BMAL1 knockout mice show health defects lends some credence to the hypothesis that it is the loss of a functioning TTFL that may lead to disrupted protein homeostasis.

Intriguingly, a recent study from the Cao laboratory has reported rhythmic phosphorylation of eIF2α as well as rhythmic activity in GCN2, which is an eIF2α kinase [341]. The authors found that ATF4 binds to a *Per2* promoter (as well as several other clock genes), thus stimulating its transcription. They then propose that there is a significant role of the ISR in circadian physiology, and a possible link between dysregulated ISR and circadian dysfunction in neurodegenerative diseases. I find these results less than convincing, since they were based on data from a timecourse that was carried out over 24 hours only. In addition, samples were taken from mouse tissues so we cannot be certain that any rhythms were cell-autonomous. Finally, they did not directly measure GCN2 activity. Nevertheless, the study does raise the possibility of rhythmic regulation of the ISR, and regulation of the TTFL by the ISR. This means that the TTFL itself may be a key regulator of protein homeostasis through the rhythmic regulation of eIF2α phosphorylation. To confirm the regulation of the ISR by the cell-autonomous clock it would be necessary to test for rhythmic eIF2α phosphorylation in cell culture, using clock gene mutants including CKO cells and BMAL1 knockout cells.

Chapter 7

Perspectives and future work

The goal of this thesis was to improve our understanding of how circadian rhythms are generated. In this work, I characterised the circadian coordination of the proteome and the phosphoproteome at the cell-autonomous level. To my knowledge, this is the second study of circadian proteomics in cell culture, and compared to the first [137], I achieved deeper coverage and drew insights from the parallel use of CRY1$^{-/-}$; CRY2$^{-/-}$ (CKO) cells. Specifically, this work revealed the reciprocal circadian regulation of cellular ion content and cytosolic protein concentration. Surprisingly I found that in the absence of the canonical transcriptional-translational feedback loop (TTFL) a larger proportion of the proteome was under rhythmic control. This provides strong evidence for the post-translational oscillator (PTO) model of circadian rhythm generation as described in Chapter 1, and suggests that the regulation of intracellular protein:ion ratio may be a direct output of the PTO (Figure 7.1).

I went on to explore the elusive rhythms in the PER2::LUC reporter in CKO cells. The PTO model would predict that rhythmic post-translational modification of clock proteins is a direct output of the PTO, and should persist in the absence of the TTFL. I discovered that manipulations of the proteostasis network modulated the robustness of the PER2::LUC rhythms. I hypothesised that because of its disordered structure, the behaviour of PER2 in biomolecular condensates in the cell may be a major source of experimental variation. Few instances of circadian rhythms in absence of CRY have been reported in the past [286, 288, 287], and the experimental variation may be the reason for this. Experiments altering the intracellular protein:ion ratio (for example with media of varying osmolarity) and imaging the localisation and diffusion rate of PER2, for example using the PER2::Venus fluorescent reporter [342], would be helpful in testing this hypothesis.

Aside from the experimental variation, the observations of PER2::LUC rhythms in CKO cells provide evidence for PTO activity. Since PER2 is a key component of the TTFL, PER2 may act as a key temporal signalling node, transmitting timing information from the PTO to the TTFL in order to coordinate gene expression and provide robustness to timekeeping. The discovery

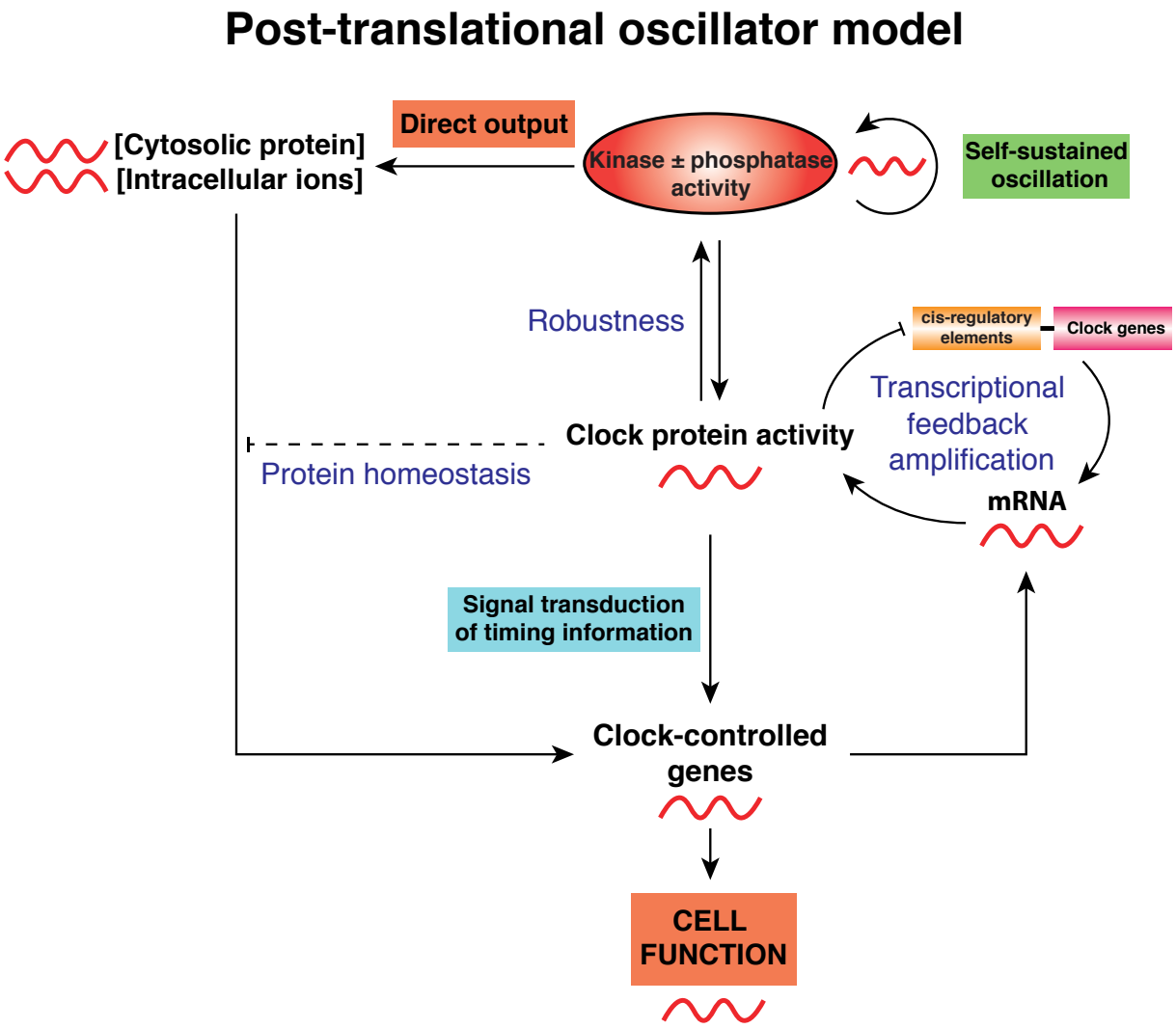

Figure 7.1 An expanded post-translational oscillator model. In light of the findings presented in this thesis, I propose some modifications of the post-translational oscillator (PTO) model shown in Figure 1.3 and Wong and O'Neill (2018) [6]. My phosphoproteomics work revealed that phosphatase as well as kinase activity may be important in the cellular clockwork. The antiphasic rhythms in intracellular ion content and cytosolic protein concentration are direct outputs of the PTO since they are present in cells lacking a functioning TTFL. Cryptochromes are required for protein homeostasis, and indeed the presence of the TTFL is associated with fewer proteins and phosphosites being under rhythmic regulation in abundance. This is depicted with a dashed line because more work is required to distinguish whether this is a direct output of the TTFL, or an indirect output *via* non-timekeeping functions of cryptochrome proteins.

of the strong effects of picrotoxin on PER2::LUC behaviour also suggests that PER2 is a key signalling node. Moreover, the elucidation of its mechanism of action through the functional, structural and mass-spectrometry approaches described in Chapter 3 will provide more insight into how PER2 is regulated, and how it transmits timing information. It is possible that the PTO signals to the TTFL in other ways in addition to PER2. For example, it has been shown that period length may be modulated by a molecular switch that consists of a slow conformational change in the intrinsically disordered C-terminal transactivation domain of BMAL1, and this is regulated by molecular chaperones called cyclophilins [343]. This is critical for permitting the binding of CRY1 to this region [344], resulting in the inhibition of CLOCK/BMAL1 complex activity. This fascinating mechanism suggests that the regulation of BMAL1 protein structure may also be a crucial signalling conduit between the PTO and the TTFL.

This has parallels with previous work in cyanobacteria. As described in Chapter 1, a purely post-translational circadian oscillator in *S. elongatus* was elucidated by reconstitution *in vitro*, using only 3 proteins (KaiA, KaiB and KaiC) with Mg.ATP [115], demonstrating the function of a PTO circadian clock for the first time. More recent work has shown *in silico* and *in vivo* that the PTO in cyanobacteria is elaborated by a TTFL that confers robustness to the timekeeping [121]. Furthermore, it was shown that the histidine kinase SasA interacts with KaiC [345], and subsequently phosphorylates a DNA-binding protein called RpaA [346]. KaiC also regulates RpaA via a negative feedback loop involving a protein called LabA [347]. CikA is another protein important in the cyanobacterial clock, originally discovered as an input pathway [348]. Subsequently it was found that these three major pathways (SasA, LabA and CikA) work in concert to transmit timing information from the KaiA/B/C oscillator to modulate RpaA activity, resulting in the circadian coordination of gene expression [349]. There is no amino acid sequence similarity between any of these cyanobacterial proteins and the mammalian TTFL components, but I hypothesise that this network motif may be conserved. If mammalian PTO components are found, this hypothesis may be tested by genetically altering the interactions between PTO components and putative signal transducers like PER2.

A key remaining question is: what are the components of the mammalian PTO? My proteomics dataset provides a resource that may be used in the search for the minimal set of components required to sustain a circadian oscillation in mammalian cells. As mentioned in Chapter 4, investigation of the activity of kinases including CAMK2, and the activity of phosphatase regulators such as Ppp1 regulatory subunit 12A across the circadian cycle may reveal characteristics or components of the PTO. After this, experiments involving the constitutive activation of putative PTO components at their average activation level pharmacologically or genetically would abolish all circadian rhythms in the cell if the PTO model is correct.

However, with the data that we have so far, I propose that CK1 is likely to be either a component of the PTO itself, or a very important regulator. This is because CK1 inhibition modulates period length in WT cells, CKO cells and red blood cells [100]. In addition, relatively little is known about phosphatases and the relevant adaptors that confer specificity to regulate the

cellular clock. However, kinases and phosphatases need to be balanced to ensure correct protein functions, and also to regulate the biophysical properties of the cell, since most phosphorylation modifications occur in IDRs [334], and this is a key regulator of structure and function of such proteins [335]. Hence I would also like to propose a speculative model for period determination, whereby kinases progressively phosphorylate IDPs, resulting in these proteins gradually coming out of biomolecular condensates. This is a state of net phosphorylation in the cell. Eventually, phosphatases and/or phosphatase adaptors (perhaps including Ppp1 regulatory subunit 12A), are released, and so the balance in the cell gradually tips towards net de-phosphorylation, resulting in re-formation of the biomolecular condensates, and the process starting again. This model would be compatible with the findings about CK1 modulating period length, since it is an abundant and promiscuous kinase in the cell. To explore this model in more depth in future work, it would be valuable to perform proteomic and phosphoproteomic analyses of biomolecular condensates to analyse their components. This in turn could inform the experimenter of appropriate stoichiometry of kinases and phosphatases, to enable an attempt at reconstituting this in vitro using recombinant proteins in a similar manner to how the molecular clock of *Synechococcus elongatus* was elucidated [115]. Such a demonstration would show the minimal components that are necessary and sufficient to generate a circadian rhythm in mammals.

Constitutive expression of the CRY proteins, and of other clock proteins will also help to distinguish between the convergent and divergent models of the evolutionary history of circadian rhythm generation as described in Chapter 1. Constitutive activation of post-translational mechanisms as described above would also help to distinguish between these models. As described above, reconstitution of a PTO *in vitro* akin to the elucidation of the cyanobacterial clock would be supportive of the divergence model, and my proteomics and phosphoproteomics datasets may facilitate this line of experimentation. Moreover, according to the divergence model, PTO components should be conserved amongst many species. Hence it would be valuable to conduct proteomic and phosphoproteomics studies as well constitutive expression experiments in many eukaryotic species to test this model.

Intriguingly, the overlap in rhythmic protein and phosphopeptide identities between genotypes was very small (Figure 4.4). This suggests that in WT cells, the TTFL may be substantially modulating the rhythmic output of the PTO. In addition, my proteomics dataset revealed that a larger number of proteins were rhythmic in CKO cells compared to WT, and that they also had a larger relative amplitude of protein/ion rhythms. These experiments suggest that the TTFL suppresses the oscillations in many proteins (Figure 7.1). This is contrary to the traditional view that the TTFL generates circadian oscillations, and suggests that there may be deleterious consequences for high amplitude rhythms in cellular protein and ion content. I characterised the defects in the proteostasis network of CKO cells, showing the physiological consequences *in vitro* and *in vivo*. I found that CKO cells had a different set point of protein homeostasis compared to wild-type cells, and this renders them more sensitive to proteotoxic stress-inducing stimuli. Given this finding, it would be reasonable to suspect that CKO mice could be more

prone to neurodegenerative diseases and cancer. Clock function is intricately linked to both neurodegenerative diseases [350] and cancer [351], and so it would be worthwhile to investigate if these diseases occur in CKO mice. This disrupted proteostasis could be related to the loss of a functioning TTFL, or it could represent a TTFL-independent function of CRY proteins. As described in Chapter 6, constitutive expression of both CRY1 and CRY2 would help to distinguish these possibilities. In both cases, my work reveals that CRY proteins are major components of the proteostasis network, particularly in the regulation of protein degradation by the proteasome.

Finally, this thesis supports the PTO model for circadian rhythm generation in mammalian cells, and more generally provides evidence for divergent evolution of circadian rhythms in eukaryotes. I propose new roles of the TTFL (Figure 7.1): transmission of timing information from the PTO to gene expression programmes, conferring robustness to cellular timekeeping, and participating in the cellular protein homeostasis network.

References

[1] Eberhard Gwinner. Circadian and circannual programmes in avian migration. *The Journal of experimental biology*, 199(Pt 1):39–48, 1996. ISSN 1477-9145. URL http://www.ncbi.nlm.nih.gov/pubmed/9317295.

[2] Martin Egli. Intricate protein-protein interactions in the cyanobacterial circadian clock. *The Journal of biological chemistry*, 289(31):21267–75, aug 2014. ISSN 1083-351X. doi: 10.1074/jbc.R114.579607. URL http://www.ncbi.nlm.nih.gov/pubmed/24936066http://www.pubmedcentral.nih.gov/articlerender.fcgi?artid=PMC4118088.

[3] Andrew C Liu, Warren G Lewis, and Steve A Kay. Mammalian circadian signaling networks and therapeutic targets. *Nature Chemical Biology*, 3(10):630–639, oct 2007. ISSN 1552-4450. doi: 10.1038/nchembio.2007.37. URL http://www.nature.com/articles/nchembio.2007.37.

[4] C. S. Pittendrigh. Circadian rhythms and the circadian organization of living systems. *Cold Spring Harbor symposia on quantitative biology*, 25:159–184, 1960. ISSN 00917451. doi: 10.1101/SQB.1960.025.01.015. URL http://www.ncbi.nlm.nih.gov/pubmed/13736116.

[5] Colin S Pittendrigh. Temporal organization: reflections of a Darwinian clock-watcher. *Annual Review of Physiology*, 55:16–54, 1993. ISSN 00664278. doi: 10.1146/annurev.physiol.55.1.17.

[6] David CS Wong and John S O'Neill. Non-transcriptional processes in circadian rhythm generation. *Current Opinion in Physiology*, 5:117–132, oct 2018. ISSN 2468-8673. doi: 10.1016/J.COPHYS.2018.10.003. URL https://www.sciencedirect.com/science/article/pii/S2468867318301342?via{%}3Dihub.

[7] I. H. Segel. *Enzyme Kinetics : Behavior and Analysis of Rapid Equilibrium and Steady State Enzyme Systems Horizons in Biochemistry and Biophysics (Volume 1)*, volume 60. 1975.

[8] Jay C. Dunlap, Jennifer J. Loros, and Patricia J. DeCoursey. *Chronobiology : biological timekeeping*. Sinauer Associates, 2004. ISBN 0878933964. URL https://books.google.co.uk/books/about/Chronobiology.html?id=n5SdRwAACAAJ{&}redir{_}esc=y.

[9] David K. Welsh, Seung-Hee Yoo, Andrew C. Liu, Joseph S. Takahashi, and Steve A. Kay. Bioluminescence Imaging of Individual Fibroblasts Reveals Persistent, Independently Phased Circadian Rhythms of Clock Gene Expression. *Current Biology*, 14(24):2289–2295, 2004. ISSN 09609822. doi: 10.1016/j.cub.2004.11.057.

[10] J William Schopf, Kouki Kitajima, Michael J Spicuzza, Anatoliy B Kudryavtsev, and John W Valley. SIMS analyses of the oldest known assemblage of microfossils document their taxon-correlated carbon isotope compositions. *Proceedings of the National Academy of Sciences of the United States of America*, 115(1):53–58, jan 2018. ISSN 1091-6490. doi: 10.1073/pnas.1718063115. URL http://www.ncbi.nlm.nih.gov/pubmed/29255053http://www.pubmedcentral.nih.gov/articlerender.fcgi?artid=PMC5776830.

[11] Antony N Dodd, Neeraj Salathia, Anthony Hall, Eva Kévei, Réka Tóth, Ferenc Nagy, Julian M Hibberd, Andrew J Millar, and Alex A R Webb. Plant circadian clocks increase photosynthesis, growth, survival, and competitive advantage. *Science (New York, N.Y.)*, 309(5734):630–3, jul 2005. ISSN 1095-9203. doi: 10.1126/science.1115581. URL http://www.ncbi.nlm.nih.gov/pubmed/16040710.

[12] André Klarsfeld and François Rouyer. Effects of Circadian Mutations and LD Periodicity on the Life Span of Drosophila melanogaster. *Journal of Biological Rhythms*, 13(6): 471–478, 1998. ISSN 07487304. doi: 10.1177/074873098129000309.

[13] Peijun Ma, Mark A Woelfle, and Carl Hirschie Johnson. An Evolutionary Fitness Enhancement Conferred by the Circadian System in Cyanobacteria. *Chaos, solitons, and fractals*, 50:65–74, may 2013. ISSN 0960-0779. doi: 10.1016/j.chaos.2012.11.006. URL http://www.ncbi.nlm.nih.gov/pubmed/23626410http://www.pubmedcentral.nih.gov/articlerender.fcgi?artid=PMC3633149.

[14] Y Ouyang, C R Andersson, T Kondo, S S Golden, and C H Johnson. Resonating circadian clocks enhance fitness in cyanobacteria. *Proceedings of the National Academy of Sciences of the United States of America*, 95(15):8660–4, jul 1998. ISSN 0027-8424. URL http://www.ncbi.nlm.nih.gov/pubmed/9671734http://www.pubmedcentral.nih.gov/articlerender.fcgi?artid=PMC21132.

[15] Till Roenneberg and Martha Merrow. "What watch?... such much!" Complexity and evolution of circadian clocks. *Cell and Tissue Research*, 309(1):3–9, 2002. ISSN 0302766X. doi: 10.1007/s00441-002-0568-1.

[16] Kamiel Spoelstra, Martin Wikelski, Serge Daan, Andrew S I Loudon, and Michaela Hau. Natural selection against a circadian clock gene mutation in mice. *Proceedings of the National Academy of Sciences of the United States of America*, 113(3):686–91, jan 2016. ISSN 1091-6490. doi: 10.1073/pnas.1516442113. URL http://www.ncbi.nlm.nih.gov/pubmed/26715747http://www.pubmedcentral.nih.gov/articlerender.fcgi?artid=PMC4725470.

[17] Mark A. Woelfle, Yan Ouyang, Kittiporn Phanvijhitsiri, and Carl Hirschie Johnson. The Adaptive Value of Circadian Clocks: An Experimental Assessment in Cyanobacteria. *Current Biology*, 14(16):1481–1486, 2004. ISSN 09609822. doi: 10.1016/j.cub.2004.08.023.

[18] Urs Albrecht. Timing to Perfection: The Biology of Central and Peripheral Circadian Clocks. *Neuron*, 74(2):246–260, 2012. ISSN 08966273. doi: 10.1016/j.neuron.2012.04.006. URL http://dx.doi.org/10.1016/j.neuron.2012.04.006.

[19] Charna Dibner, Ueli Schibler, and Urs Albrecht. The Mammalian Circadian Timing System: Organization and Coordination of Central and Peripheral Clocks. *Annual Review of Physiology*, 72(1):517–549, mar 2010. ISSN 0066-4278. doi: 10.1146/annurev-physiol-021909-135821. URL http://www.annualreviews.org/doi/abs/10.1146/annurev-physiol-021909-135821.

[20] Michael H. Hastings, Akhilesh B. Reddy, and Elizabeth S. Maywood. A clockwork web: circadian timing in brain and periphery, in health and disease. *Nature Reviews Neuroscience*, 4(8):649–661, 2003. ISSN 1471003X. doi: 10.1038/nrn1177. URL http://www.nature.com/doifinder/10.1038/nrn1177.

[21] Jennifer A. Mohawk, Carla B. Green, and Joseph S. Takahashi. Central and Peripheral Circadian Clocks in Mammals. *Annual Review of Neuroscience*, 35(1):445–462, jul 2012. ISSN 0147-006X. doi: 10.1146/annurev-neuro-060909-153128. URL http://www.annualreviews.org/doi/abs/10.1146/annurev-neuro-060909-153128.

[22] Andrew P. Patton and Michael H. Hastings. The suprachiasmatic nucleus. *Current Biology*, 28(15):R816–R822, aug 2018. ISSN 09609822. doi: 10.1016/j.cub.2018.06.052. URL https://linkinghub.elsevier.com/retrieve/pii/S0960982218308431.

[23] Steven M Reppert and David R Weaver. Coordination of circadian timing in mammals. *Nature*, 418(6901):935–41, 2002. ISSN 0028-0836. doi: 10.1038/nature00965.

[24] David K. Welsh, Joseph S. Takahashi, and Steve A. Kay. Suprachiasmatic Nucleus: Cell Autonomy and Network Properties. *Annual Review of Physiology*, 72(1):551–577, mar 2010. ISSN 0066-4278. doi: 10.1146/annurev-physiol-021909-135919. URL http://www.annualreviews.org/doi/abs/10.1146/annurev-physiol-021909-135919.

[25] Aurelio Balsalobre, Francesca Damiola, and Ueli Schibler. A serum shock induces circadian gene expression in mammalian tissue culture cells. *Cell*, 93(6):929–937, 1998. ISSN 00928674. doi: 10.1016/S0092-8674(00)81199-X.

[26] P. Pulimeno, T. Mannic, D. Sage, L. Giovannoni, P. Salmon, S. Lemeille, M. Giry-Laterriere, M. Unser, D. Bosco, C. Bauer, J. Morf, P. Halban, J. Philippe, and C. Dibner. Autonomous and self-sustained circadian oscillators displayed in human islet cells. *Diabetologia*, 56(3):497–507, mar 2013. ISSN 0012-186X. doi: 10.1007/s00125-012-2779-7. URL http://link.springer.com/10.1007/s00125-012-2779-7.

[27] David K. Welsh, Seung-Hee Yoo, Andrew C. Liu, Joseph S. Takahashi, and Steve A. Kay. Bioluminescence Imaging of Individual Fibroblasts Reveals Persistent, Independently Phased Circadian Rhythms of Clock Gene Expression. *Current Biology*, 14(24):2289–2295, 2004. ISSN 09609822. doi: 10.1016/j.cub.2004.11.057.

[28] Seung-Hee Yoo, Shin Yamazaki, Phillip L Lowrey, Kazuhiro Shimomura, Caroline H Ko, Ethan D Buhr, Sandra M Siepka, Hee-Kyung Hong, Won Jun Oh, Ook Joon Yoo, Michael Menaker, and Joseph S Takahashi. PERIOD2::LUCIFERASE real-time reporting of circadian dynamics reveals persistent circadian oscillations in mouse peripheral tissues. *Proceedings of the National Academy of Sciences of the United States of America*, 101(15):5339–46, apr 2004. ISSN 0027-8424. doi: 10.1073/pnas.0308709101. URL http://www.ncbi.nlm.nih.gov/pubmed/14963227http://www.pubmedcentral.nih.gov/articlerender.fcgi?artid=PMC397382.

[29] David Morse, Nicolas Cermakian, Stefano Brancorsini, Martti Parvinen, and Paolo Sassone-Corsi. No circadian rhythms in testis: Period1 expression is Clock independent and developmentally regulated in the mouse. *Molecular Endocrinology*, 17(1):141–151, 2003. ISSN 08888809. doi: 10.1210/me.2002-0184.

[30] Ray Zhang, Nicholas F. Lahens, Heather I. Ballance, Michael E. Hughes, and John B. Hogenesch. A circadian gene expression atlas in mammals: Implications for biology and medicine. *Proceedings of the National Academy of Sciences*, 111(45):16219–16224, nov 2014. ISSN 0027-8424. doi: 10.1073/pnas.1408886111. URL http://www.pnas.org/lookup/doi/10.1073/pnas.1408886111.

[31] Ron C Anafi, Lauren J Francey, John B Hogenesch, and Junhyong Kim. CYCLOPS reveals human transcriptional rhythms in health and disease. *Proceedings of the National Academy of Sciences of the United States of America*, 114(20):5312–5317, may 2017. ISSN 1091-6490. doi: 10.1073/pnas.1619320114. URL http://www.ncbi.nlm.nih.gov/pubmed/28439010http://www.pubmedcentral.nih.gov/articlerender.fcgi?artid=PMC5441789.

[32] Steven A. Brown, Elzbieta Kowalska, and Robert Dallmann. (Re)inventing the Circadian Feedback Loop. *Developmental Cell*, 22(3):477–487, 2012. ISSN 15345807. doi: 10.1016/j.devcel.2012.02.007.

[33] Jay C Dunlap. Molecular Bases for Circadian Clocks. *Cell*, 96(2):271–290, 1999. ISSN 00928674. doi: 10.1016/S0092-8674(00)80566-8.

[34] Joseph S. Takahashi. Transcriptional architecture of the mammalian circadian clock. *Nature Reviews Genetics*, 18(3):164–179, 2016. ISSN 1471-0056. doi: 10.1038/nrg.2016.150. URL http://www.nature.com/doifinder/10.1038/nrg.2016.150.

[35] Jürgen A. Ripperger, Corinne Jud, and Urs Albrecht. The daily rhythm of mice. *FEBS Letters*, 585(10):1384–1392, may 2011. ISSN 00145793. doi: 10.1016/j.febslet.2011.02.027. URL http://doi.wiley.com/10.1016/j.febslet.2011.02.027.

[36] Rajindra P Aryal, Pieter Bas Kwak, Alfred G Tamayo, Michael Gebert, Po-lin Chiu, Thomas Walz, and Charles J Weitz. Macromolecular Assemblies of the Mammalian Circadian Clock. *Molecular Cell*, 67(5):770–782.e6, 2017. ISSN 1097-2765. doi: 10.1016/j.molcel.2017.07.017. URL http://dx.doi.org/10.1016/j.molcel.2017.07.017.

[37] S.A. Brown, Jürgen Ripperger, S Kadener, F. Fleury-Olela, F Vilbois, M. Rosbash, and Ueli Schibler. PERIOD1-Associated Proteins Modulate the Negative Limb of the Mammalian Circadian Oscillator. *Science*, 308(5722):693–696, 2005. ISSN 0036-8075. doi: 10.1126/science.1107373. URL http://www.sciencemag.org/cgi/doi/10.1126/science.1107373.

[38] Jin Young Kim, Pieter Bas Kwak, and Charles J. Weitz. Specificity in Circadian Clock Feedback from Targeted Reconstitution of the NuRD Corepressor. *Molecular Cell*, 56 (6):738–748, dec 2014. ISSN 1097-2765. doi: 10.1016/J.MOLCEL.2014.10.017. URL https://www.sciencedirect.com/science/article/pii/S1097276514008272?via{%}3Dihub.

[39] Jin Young Kim, Pieter Bas Kwak, Michael Gebert, Hao A. Duong, and Charles J. Weitz. Purification and analysis of PERIOD protein complexes of the mammalian circadian clock. *Methods in Enzymology*, 551:197–210, 2015. ISSN 15577988. doi: 10.1016/bs.mie.2014.10.013. URL http://dx.doi.org/10.1016/bs.mie.2014.10.013.

[40] Nobuya Koike, Seung-Hee Yoo, Hung-Chung Huang, Vivek Kumar, Choogon Lee, Tae-Kyung Kim, and Joseph S Takahashi. Transcriptional architecture and chromatin landscape of the core circadian clock in mammals. *Science (New York, N.Y.)*, 338(6105):349–54, oct 2012. ISSN 1095-9203. doi: 10.1126/science.1226339. URL http://www.ncbi.nlm.nih.gov/pubmed/22936566http://www.pubmedcentral.nih.gov/articlerender.fcgi?artid=PMC3694775.

[41] Carrie L. Partch, Carla B. Green, and Joseph S. Takahashi. Molecular architecture of the mammalian circadian clock. *Trends in Cell Biology*, 24(2):90–99, 2014. ISSN 09628924. doi: 10.1016/j.tcb.2013.07.002. URL http://dx.doi.org/10.1016/j.tcb.2013.07.002.

[42] Yong Hoon Kim, Sajid A Marhon, Yuxiang Zhang, David J Steger, Kyoung-Jae Won, and Mitchell A Lazar. Rev-erbα dynamically modulates chromatin looping to control circadian gene transcription. *Science (New York, N.Y.)*, 359(6381):1274–1277, mar 2018. ISSN 1095-9203. doi: 10.1126/science.aao6891. URL http://www.ncbi.nlm.nih.gov/pubmed/29439026.

[43] Jérôme Mermet, Jake Yeung, Clémence Hurni, Daniel Mauvoisin, Kyle Gustafson, Céline Jouffe, Damien Nicolas, Yann Emmenegger, Cédric Gobet, Paul Franken, Frédéric Gachon, and Félix Naef. Clock-dependent chromatin topology modulates circadian transcription and behavior. *Genes & development*, 32(5-6):347–358, mar 2018. ISSN 1549-5477. doi: 10.1101/gad.312397.118. URL http://www.ncbi.nlm.nih.gov/pubmed/29572261http://www.pubmedcentral.nih.gov/articlerender.fcgi?artid=PMC5900709.

[44] Jake Yeung, Jérôme Mermet, Céline Jouffe, Julien Marquis, Aline Charpagne, Frédéric Gachon, and Felix Naef. Transcription factor activity rhythms and tissue-specific chromatin interactions explain circadian gene expression across organs. *Genome research*, 28(2):182–191, feb 2018. ISSN 1549-5469. doi: 10.1101/gr.222430.117. URL http://www.ncbi.nlm.nih.gov/pubmed/29254942http://www.pubmedcentral.nih.gov/articlerender.fcgi?artid=PMC5793782.

[45] Selma Masri, Marlene Cervantes, and Paolo Sassone-Corsi. The circadian clock and cell cycle: Interconnected biological circuits. *Current Opinion in Cell Biology*, 25(6):730–734, 2013. ISSN 09550674. doi: 10.1016/j.ceb.2013.07.013.

[46] Celine Feillet, Gijsbertus T.J. van der Horst, Francis Levi, David A. Rand, and Franck Delaunay. Coupling between the circadian clock and cell cycle oscillators: Implication for healthy cells and malignant growth. *Frontiers in Neurology*, 6(MAY):1–7, 2015. ISSN 16642295. doi: 10.3389/fneur.2015.00096.

[47] Yuichi Kumaki, Maki Ukai-Tadenuma, Ken-ichiro D Uno, Junko Nishio, Koh-hei Masumoto, Mamoru Nagano, Takashi Komori, Yasufumi Shigeyoshi, John B Hogenesch, and Hiroki R Ueda. Analysis and synthesis of high-amplitude Cis-elements in the mammalian circadian clock. *Proceedings of the National Academy of Sciences of the United States of America*, 105(39):14946–51, sep 2008. ISSN 1091-6490. doi: 10.1073/pnas.0802636105. URL http://www.ncbi.nlm.nih.gov/pubmed/18815372http://www.pubmedcentral.nih.gov/articlerender.fcgi?artid=PMC2553039.

[48] Andrew C. Liu, Hien G. Tran, Eric E. Zhang, Aaron A. Priest, David K. Welsh, and Steve A. Kay. Redundant Function of REV-ERBα and β and Non-Essential Role for Bmal1 Cycling in Transcriptional Regulation of Intracellular Circadian Rhythms. *PLoS Genetics*, 4(2):e1000023, feb 2008. ISSN 1553-7404. doi: 10.1371/journal.pgen.1000023. URL http://dx.plos.org/10.1371/journal.pgen.1000023.

[49] Yuxiang Zhang, Bin Fang, Matthew J Emmett, Manashree Damle, Zheng Sun, Dan Feng, Sean M Armour, Jarrett R Remsberg, Jennifer Jager, Raymond E Soccio, David J Steger, and Mitchell A Lazar. Discrete functions of nuclear receptor Rev-erbα couple metabolism to the clock. *Science (New York, N.Y.)*, 348(6242):1488–92, jun 2015. doi: 10.1126/science.aab3021. URL http://www.ncbi.nlm.nih.gov/pubmed/26044300.

[50] Jürgen A Ripperger and Ueli Schibler. Rhythmic CLOCK-BMAL1 binding to multiple E-box motifs drives circadian Dbp transcription and chromatin transitions. *Nature Genetics*, 38(3):369–374, mar 2006. ISSN 1061-4036. doi: 10.1038/ng1738. URL http://www.nature.com/articles/ng1738.

[51] Markus Stratmann, David Michael Suter, Nacho Molina, Felix Naef, and Ueli Schibler. Circadian Dbp Transcription Relies on Highly Dynamic BMAL1-CLOCK Interaction with E Boxes and Requires the Proteasome. *Molecular Cell*, 48(2):277–287, 2012. ISSN 10972765. doi: 10.1016/j.molcel.2012.08.012. URL http://dx.doi.org/10.1016/j.molcel.2012.08.012.

[52] S Mitsui, S Yamaguchi, T Matsuo, Y Ishida, and H Okamura. Antagonistic role of E4BP4 and PAR proteins in the circadian oscillatory mechanism. *Genes & development*, 15(8):995–1006, apr 2001. ISSN 0890-9369. doi: 10.1101/gad.873501. URL http://www.ncbi.nlm.nih.gov/pubmed/11316793http://www.pubmedcentral.nih.gov/articlerender.fcgi?artid=PMC312673.

[53] Hiroki R Ueda, Satoko Hayashi, Wenbin Chen, Motoaki Sano, Masayuki Machida, Yasufumi Shigeyoshi, Masamitsu Iino, and Seiichi Hashimoto. System-level identification of transcriptional circuits underlying mammalian circadian clocks. *Nature Genetics*, 37 (2):187–192, feb 2005. ISSN 1061-4036. doi: 10.1038/ng1504. URL http://www.nature.com/articles/ng1504.

[54] Maki Ukai-Tadenuma, Takeya Kasukawa, and Hiroki R. Ueda. Proof-by-synthesis of the transcriptional logic of mammalian circadian clocks. *Nature Cell Biology*, 10(10): 1154–1163, oct 2008. ISSN 1465-7392. doi: 10.1038/ncb1775. URL http://www.nature.com/articles/ncb1775.

[55] Boris N. Kholodenko, John F. Hancock, and Walter Kolch. Signalling ballet in space and time. *Nature Reviews Molecular Cell Biology*, 11(6):414–426, 2010. ISSN 1471-0072. doi: 10.1038/nrm2901. URL http://www.nature.com/doifinder/10.1038/nrm2901.

[56] Sarah Gibb, Miguel Maroto, and J Kim Dale. The segmentation clock mechanism moves up a notch. *Trends in cell biology*, 20(10):593–600, oct 2010. ISSN 1879-3088. doi: 10.1016/j.tcb.2010.07.001. URL http://www.ncbi.nlm.nih.gov/pubmed/20724159http://www.pubmedcentral.nih.gov/articlerender.fcgi?artid=PMC2954312.

[57] I Palmeirim, D Henrique, D Ish-Horowicz, and O Pourquié. Avian hairy gene expression identifies a molecular clock linked to vertebrate segmentation and somitogenesis. *Cell*, 91 (5):639–48, nov 1997. ISSN 0092-8674. doi: 10.1016/S0092-8674(00)80451-1. URL http://www.ncbi.nlm.nih.gov/pubmed/9393857.

[58] Kei Nakayama, Takayuki Satoh, Aiko Igari, Ryoichiro Kageyama, and Eisuke Nishida. FGF induces oscillations of Hes1 expression and Ras/ERK activation. *Current biology : CB*, 18(8):R332–4, apr 2008. ISSN 0960-9822. doi: 10.1016/j.cub.2008.03.013. URL http://www.ncbi.nlm.nih.gov/pubmed/18430630.

[59] Sung-Young Shin, Oliver Rath, Sang-Mok Choo, Frances Fee, Brian McFerran, Walter Kolch, and Kwang-Hyun Cho. Positive- and negative-feedback regulations coordinate the dynamic behavior of the Ras-Raf-MEK-ERK signal transduction pathway. *Journal of cell science*, 122(Pt 3):425–35, feb 2009. ISSN 0021-9533. doi: 10.1242/jcs.036319. URL http://www.ncbi.nlm.nih.gov/pubmed/19158341.

[60] Louise Ashall, Caroline A Horton, David E Nelson, Pawel Paszek, Claire V Harper, Kate Sillitoe, Sheila Ryan, David G Spiller, John F Unitt, David S Broomhead, Douglas B Kell, David A Rand, Violaine Sée, and Michael R H White. Pulsatile stimulation determines timing and specificity of NF-kappaB-dependent transcription. *Science (New York, N.Y.)*, 324(5924):242–6, apr 2009. ISSN 1095-9203. doi: 10.1126/science.1164860. URL http://www.ncbi.nlm.nih.gov/pubmed/19359585http://www.pubmedcentral.nih.gov/articlerender.fcgi?artid=PMC2785900.

[61] Tanya L. Leise, Connie W. Wang, Paula J. Gitis, and David K. Welsh. Persistent Cell-Autonomous Circadian Oscillations in Fibroblasts Revealed by Six-Week Single-Cell Imaging of PER2::LUC Bioluminescence. *PLoS ONE*, 7(3):e33334, mar 2012. ISSN 1932-6203. doi: 10.1371/journal.pone.0033334. URL http://dx.plos.org/10.1371/journal.pone.0033334.

[62] Helen C. Causton, Kevin A. Feeney, Christine A. Ziegler, and John S. O'Neill. Metabolic Cycles in Yeast Share Features Conserved among Circadian Rhythms. *Current Biology*, 25(8):1056–1062, 2015. ISSN 09609822. doi: 10.1016/j.cub.2015.02.035.

[63] Yanshan Fang, Sriram Sathyanarayanan, and Amita Sehgal. Post-translational regulation of the Drosophila circadian clock requires protein phosphatase 1 (PP1). *Genes & development*, 21(12):1506–18, jun 2007. ISSN 0890-9369. doi: 10.1101/gad.1541607. URL http://www.ncbi.nlm.nih.gov/pubmed/17575052http://www.pubmedcentral.nih.gov/articlerender.fcgi?artid=PMC1891428.

[64] B Kloss, J L Price, L Saez, J Blau, A Rothenfluh, C S Wesley, and M W Young. The Drosophila clock gene double-time encodes a protein closely related to human casein kinase Iepsilon. *Cell*, 94(1):97–107, jul 1998. ISSN 0092-8674. doi: 10.1016/S0092-8674(00)81225-8. URL http://www.ncbi.nlm.nih.gov/pubmed/9674431.

[65] Hyuk Wan Ko, Jin Jiang, and Isaac Edery. Role for Slimb in the degradation of Drosophila Period protein phosphorylated by Doubletime. *Nature*, 420(6916):673–678, dec 2002. ISSN 0028-0836. doi: 10.1038/nature01272. URL http://www.nature.com/articles/nature01272.

[66] P L Lowrey, K Shimomura, M P Antoch, S Yamazaki, P D Zemenides, M R Ralph, M Menaker, and J S Takahashi. Positional syntenic cloning and functional characterization of the mammalian circadian mutation tau. *Science (New York, N.Y.)*, 288(5465):483–92, 2000. ISSN 0036-8075. doi: 10.1126/science.288.5465.483. URL http://www.pubmedcentral.nih.gov/articlerender.fcgi?artid=3869379{&}tool=pmcentrez{&}rendertype=abstract.

[67] Sebastian Martinek, Susan Inonog, Armen S. Manoukian, and Michael W. Young. A Role for the Segment Polarity Gene shaggy/GSK-3 in the Drosophila Circadian Clock. *Cell*, 105(6):769–779, jun 2001. ISSN 00928674. doi: 10.1016/S0092-8674(01)00383-X. URL http://linkinghub.elsevier.com/retrieve/pii/S009286740100383X.

[68] Pipat Nawathean and Michael Rosbash. The doubletime and CKII kinases collaborate to potentiate Drosophila PER transcriptional repressor activity. *Molecular cell*, 13(2):213–23, jan 2004. ISSN 1097-2765. doi: 10.1016/S1097-2765(03)00503-3. URL http://www.ncbi.nlm.nih.gov/pubmed/14759367.

[69] Florian Atger, Cédric Gobet, Julien Marquis, Eva Martin, Jingkui Wang, Benjamin Weger, Grégory Lefebvre, Patrick Descombes, Felix Naef, and Frédéric Gachon. Circadian and feeding rhythms differentially affect rhythmic mRNA transcription and translation in mouse liver. *Proceedings of the National Academy of Sciences*, 112(47):E6579–E6588, 2015. ISSN 0027-8424. doi: 10.1073/pnas.1515308112. URL http://www.pnas.org/lookup/doi/10.1073/pnas.1515308112.

[70] Giorgia Benegiamo, Steven A. Brown, and Satchidananda Panda. RNA Dynamics in the Control of Circadian Rhythm., 2016. ISSN 0065-2598. URL http://link.springer.com/10.1007/978-3-319-29073-7{_}5http://www.ncbi.nlm.nih.gov/pubmed/27256384.

[71] Violeta Castelo-Szekely, Alaaddin Bulak Arpat, Peggy Janich, and David Gatfield. Translational contributions to tissue specificity in rhythmic and constitutive gene expression. *Genome Biology*, 18(1):116, dec 2017. ISSN 1474-760X. doi: 10.1186/s13059-017-1222-2. URL http://genomebiology.biomedcentral.com/articles/10.1186/s13059-017-1222-2.

[72] Jean-Michel Fustin, Masao Doi, Yoshiaki Yamaguchi, Hayashi Hida, Shinichi Nishimura, Minoru Yoshida, Takayuki Isagawa, Masaki Suimye Morioka, Hideaki Kakeya, Ichiro Manabe, and Hitoshi Okamura. RNA-Methylation-Dependent RNA Processing Controls the Speed of the Circadian Clock. *Cell*, 155(4):793–806, 2013. ISSN 00928674. doi: 10.1016/j.cell.2013.10.026.

[73] Carla B. Green. Circadian Post-transcriptional Control of Metabolism. In *A Time for Metabolism and Hormones*. 2016. ISBN 9783319270685. URL http://www.ncbi.nlm.nih.gov/pubmed/28892339.

[74] Carla B Green. Circadian Posttranscriptional Regulatory Mechanisms in Mammals. *Cold Spring Harbor Perspectives in Biology*, page a030692, 2017. ISSN 1943-0264. doi: 10.1101/cshperspect.a030692. URL http://cshperspectives.cshlp.org/lookup/doi/10.1101/cshperspect.a030692.

[75] Christopher Jang, Nicholas F Lahens, John B Hogenesch, and Amita Sehgal. Ribosome profiling reveals an important role for translational control in circadian gene expression. *Genome Research*, pages 1836–1847, 2015. doi: 10.1101/gr.191296.115.4.

[76] Shihoko Kojima, Elaine L Sher-Chen, and Carla B Green. Circadian control of mRNA polyadenylation dynamics regulates rhythmic protein expression. *Genes & development*, 26(24):2724–36, dec 2012. ISSN 1549-5477. doi: 10.1101/gad.208306.112. URL http://www.ncbi.nlm.nih.gov/pubmed/23249735http://www.pubmedcentral.nih.gov/articlerender.fcgi?artid=PMC3533077.

[77] Shihoko Kojima, Kerry L. Gendreau, Elaine L. Sher-Chen, Peng Gao, and Carla B. Green. Changes in poly(A) tail length dynamics from the loss of the circadian deadenylase Nocturnin. *Scientific Reports*, 5(1):17059, dec 2015. ISSN 2045-2322. doi: 10.1038/srep17059. URL http://www.nature.com/articles/srep17059.

[78] Jonathan O. Lipton, Elizabeth D. Yuan, Lara M. Boyle, Darius Ebrahimi-Fakhari, Erica Kwiatkowski, Ashwin Nathan, Thomas Güttler, Fred Davis, John M. Asara, and Mustafa Sahin. The Circadian Protein BMAL1 Regulates Translation in Response to S6K1-Mediated Phosphorylation. *Cell*, 161(5):1138–1151, 2015. ISSN 00928674. doi: 10.1016/j.cell.2015.04.002.

[79] Marco Preußner and Florian Heyd. Post-transcriptional control of the mammalian circadian clock: implications for health and disease. *Pflugers Archiv European Journal of Physiology*, 468(6):983–991, 2016. ISSN 14322013. doi: 10.1007/s00424-016-1820-y. URL http://dx.doi.org/10.1007/s00424-016-1820-y.

[80] Kyung-Chul Woo, Dae-Cheong Ha, Kyung-Ha Lee, Do-Yeon Kim, Tae-Don Kim, and Kyong-Tai Kim. Circadian amplitude of cryptochrome 1 is modulated by mRNA stability regulation via cytoplasmic hnRNP D oscillation. *Molecular and cellular biology*, 30(1):197–205, jan 2010. ISSN 1098-5549. doi: 10.1128/MCB.01154-09. URL http://www.ncbi.nlm.nih.gov/pubmed/19858287http://www.pubmedcentral.nih.gov/articlerender.fcgi?artid=PMC2798294.

[81] Julie E Baggs, Tom S Price, Luciano DiTacchio, Satchidananda Panda, Garret A FitzGerald, and John B Hogenesch. Network Features of the Mammalian Circadian Clock. *PLoS Biology*, 7(3):e1000052, mar 2009. ISSN 1545-7885. doi: 10.1371/journal.pbio.1000052. URL http://dx.plos.org/10.1371/journal.pbio.1000052.

[82] Shuqun Shi, Akiko Hida, Owen P McGuinness, David H Wasserman, Shin Yamazaki, and Carl Hirschie Johnson. Circadian clock gene Bmal1 is not essential; functional replacement with its paralog, Bmal2. *Current biology : CB*, 20(4):316–21, feb 2010. ISSN 1879-0445. doi: 10.1016/j.cub.2009.12.034. URL http://www.ncbi.nlm.nih.gov/pubmed/20153195http://www.pubmedcentral.nih.gov/articlerender.fcgi?artid=PMC2907674.

[83] Dominic Landgraf, Lexie L. Wang, Tanja Diemer, and David K. Welsh. NPAS2 Compensates for Loss of CLOCK in Peripheral Circadian Oscillators. *PLOS Genetics*, 12 (2):e1005882, feb 2016. ISSN 1553-7404. doi: 10.1371/journal.pgen.1005882. URL http://dx.plos.org/10.1371/journal.pgen.1005882.

[84] Matthew D'Alessandro, Stephen Beesley, Jae Kyoung Kim, Rongmin Chen, Estela Abich, Wayne Cheng, Paul Yi, Joseph S. Takahashi, and Choogon Lee. A tunable artificial circadian clock in clock-defective mice. *Nature Communications*, 6:1–11, 2015. ISSN 20411723. doi: 10.1038/ncomms9587.

[85] Yunzhen Fan, Akiko Hida, Daniel A Anderson, Mariko Izumo, and Carl Hirschie Johnson. Cycling of CRYPTOCHROME proteins is not necessary for circadian-clock function in mammalian fibroblasts. *Current biology : CB*, 17(13):1091–100, jul 2007. ISSN 0960-9822. doi: 10.1016/j.cub.2007.05.048. URL http://www.ncbi.nlm.nih.gov/pubmed/17583506http://www.pubmedcentral.nih.gov/articlerender.fcgi?artid=PMC3434691.

[86] Maki Ukai-Tadenuma, Rikuhiro G. Yamada, Haiyan Xu, Jürgen A. Ripperger, Andrew C. Liu, and Hiroki R. Ueda. Delay in feedback repression by cryptochrome 1 Is required for circadian clock function. *Cell*, 144(2):268–281, 2011. ISSN 00928674. doi: 10.1016/j.cell.2010.12.019.

[87] Mathew D Edwards, Marco Brancaccio, Johanna E Chesham, Elizabeth S Maywood, and Michael H Hastings. Rhythmic expression of cryptochrome induces the circadian clock of arrhythmic suprachiasmatic nuclei through arginine vasopressin signal-

ing. *Proceedings of the National Academy of Sciences of the United States of America*, 113(10):2732–7, mar 2016. ISSN 1091-6490. doi: 10.1073/pnas.1519044113. URL http://www.ncbi.nlm.nih.gov/pubmed/26903624http://www.pubmedcentral.nih.gov/articlerender.fcgi?artid=PMC4791030.

[88] Zhaohai Yang and Amita Sehgal. Role of Molecular Oscillations in Generating Behavioral Rhythms in Drosophila. *Neuron*, 29(2):453–467, feb 2001. ISSN 0896-6273. doi: 10.1016/S0896-6273(01)00218-5. URL https://www.sciencedirect.com/science/article/pii/S0896627301002185?via{%}3Dihub.

[89] Luis F Larrondo, Consuelo Olivares-Yañez, Christopher L Baker, Jennifer J Loros, and Jay C Dunlap. Circadian rhythms. Decoupling circadian clock protein turnover from circadian period determination. *Science (New York, N.Y.)*, 347(6221):1257277, 2015. ISSN 1095-9203. doi: 10.1126/science.1257277. URL http://www.pubmedcentral.nih.gov/articlerender.fcgi?artid=4432837{&}tool=pmcentrez{&}rendertype=abstract.

[90] Michael J Deery, Elizabeth S Maywood, Johanna E Chesham, Martin Sládek, Natasha A Karp, Edward W Green, Philip D Charles, Akhilesh B Reddy, Charalambos P Kyriacou, Kathryn S Lilley, and Michael H Hastings. Proteomic analysis reveals the role of synaptic vesicle cycling in sustaining the suprachiasmatic circadian clock. *Current biology : CB*, 19(23):2031–6, dec 2009. ISSN 1879-0445. doi: 10.1016/j.cub.2009.10.024. URL http://www.ncbi.nlm.nih.gov/pubmed/19913422.

[91] Akhilesh B. Reddy, Natasha A. Karp, Elizabeth S. Maywood, Elizabeth A. Sage, Michael Deery, John S. O'Neill, Gabriel K.Y. Wong, Jo Chesham, Mark Odell, Kathryn S. Lilley, Charalambos P. Kyriacou, and Michael H. Hastings. Circadian Orchestration of the Hepatic Proteome. *Current Biology*, 16(11):1107–1115, 2006. ISSN 09609822. doi: 10.1016/j.cub.2006.04.026.

[92] Maria S. Robles, Jürgen Cox, and Matthias Mann. In-Vivo Quantitative Proteomics Reveals a Key Contribution of Post-Transcriptional Mechanisms to the Circadian Regulation of Liver Metabolism. *PLoS Genetics*, 10(1), 2014. ISSN 15537390. doi: 10.1371/journal.pgen.1004047.

[93] Daniel Mauvoisin, Jingkui Wang, Céline Jouffe, Eva Martin, Florian Atger, Patrice Waridel, Manfredo Quadroni, Frédéric Gachon, and Felix Naef. Circadian clock-dependent and -independent rhythmic proteomes implement distinct diurnal functions in mouse liver. *Proceedings of the National Academy of Sciences of the United States of America*, 111(1):167–72, 2014. ISSN 1091-6490. doi: 10.1073/pnas.1314066111. URL http://www.pubmedcentral.nih.gov/articlerender.fcgi?artid=3890886{&}tool=pmcentrez{&}rendertype=abstract.

[94] Guillaume Rey, Nikolay B Milev, Utham K Valekunja, Ratnasekhar Ch, Sandipan Ray, Mariana Silva Dos Santos, Andras D Nagy, Robin Antrobus, James I MacRae, and Akhilesh B Reddy. Metabolic oscillations on the circadian time scale in Drosophila cells lacking clock genes. *Molecular Systems Biology*, 14(8):e8376, aug 2018. ISSN 1744-4292. doi: 10.15252/MSB.20188376. URL http://msb.embopress.org/content/14/8/e8376.

[95] Jennifer M. Hurley, Meaghan S. Jankowski, Hannah De Los Santos, Alexander M. Crowell, Samuel B. Fordyce, Jeremy D. Zucker, Neeraj Kumar, Samuel O. Purvine, Errol W. Robinson, Anil Shukla, Erika Zink, William R. Cannon, Scott E. Baker, Jennifer J. Loros, and Jay C. Dunlap. Circadian Proteomic Analysis Uncovers Mechanisms of Post-Transcriptional Regulation in Metabolic Pathways. *Cell Systems*, 7(6):613–626.e5, dec 2018. ISSN 24054720. doi: 10.1016/j.cels.2018.10.014. URL https://linkinghub.elsevier.com/retrieve/pii/S2405471218304393http://www.ncbi.nlm.nih.gov/pubmed/30553726https://doi.org/10.1016/j.cels.2018.10.014.

[96] Christopher L Baker, Arminja N Kettenbach, Jennifer J Loros, Scott A Gerber, and Jay C Dunlap. Quantitative proteomics reveals a dynamic interactome and phase-specific phosphorylation in the Neurospora circadian clock. *Molecular cell*, 34(3):354–63, may 2009. ISSN 1097-4164. doi: 10.1016/j.molcel.2009.04.023. URL http://www.ncbi.nlm.nih.gov/pubmed/19450533http://www.pubmedcentral.nih.gov/articlerender.fcgi?artid=PMC2711022.

[97] Daniel Mauvoisin, Florian Atger, Loïc Dayon, Antonio Núñez Galindo, Jingkui Wang, Eva Martin, Laetitia Da Silva, Ivan Montoliu, Sebastiano Collino, Francois-Pierre Martin, Joanna Ratajczak, Carles Cantó, Martin Kussmann, Felix Naef, and Frédéric Gachon. Circadian and Feeding Rhythms Orchestrate the Diurnal Liver Acetylome. *Cell reports*, 20(7):1729–1743, aug 2017. ISSN 2211-1247. doi: 10.1016/j.celrep.2017.07.065. URL http://www.ncbi.nlm.nih.gov/pubmed/28813682http://www.pubmedcentral.nih.gov/articlerender.fcgi?artid=PMC5568034.

[98] Maria S. Robles, Sean J. Humphrey, and Matthias Mann. Phosphorylation Is a Central Mechanism for Circadian Control of Metabolism and Physiology. *Cell Metabolism*, 0 (0):35–48, nov 2016. ISSN 15504131. doi: 10.1016/j.cmet.2016.10.004. URL http://linkinghub.elsevier.com/retrieve/pii/S1550413116305356.

[99] Charna Dibner, Daniel Sage, Michael Unser, Christoph Bauer, Thomas D 'eysmond, Felix Naef, and Ueli Schibler. Circadian gene expression is resilient to large fluctuations in overall transcription rates. *The EMBO Journal*, 28262(November 2008):123–134, 2009. ISSN 0261-4189. doi: 10.1038/emboj.2008.262.

[100] Andrew D. Beale, Emily Kruchek, Stephen J. Kitcatt, Erin A. Henslee, Jack S.W. Parry, Gabriella Braun, Rita Jabr, Malcolm von Schantz, John S. O'Neill, and Fatima H. Labeed. Casein Kinase 1 Underlies Temperature Compensation of Circadian Rhythms in Human Red Blood Cells. *Journal of Biological Rhythms*, 34(2):144–153, 2019. ISSN 15524531. doi: 10.1177/0748730419836370.

[101] C.-S. Cho, H. J. Yoon, J. Y. Kim, H. A. Woo, and S. G. Rhee. Circadian rhythm of hyperoxidized peroxiredoxin II is determined by hemoglobin autoxidation and the 20S proteasome in red blood cells. *Proceedings of the National Academy of Sciences*, 111 (33):12043–12048, aug 2014. ISSN 0027-8424. doi: 10.1073/pnas.1401100111. URL http://www.pnas.org/cgi/doi/10.1073/pnas.1401100111.

[102] Erin A. Henslee, Priya Crosby, Stephen J. Kitcatt, Jack S. W. Parry, Andrea Bernardini, Rula G. Abdallat, Gabriella Braun, Henry O. Fatoyinbo, Esther J. Harrison, Rachel S. Edgar, Kai F. Hoettges, Akhilesh B. Reddy, Rita I. Jabr, Malcolm von Schantz, John S. O'Neill, and Fatima H. Labeed. Rhythmic potassium transport regulates the circadian clock in human red blood cells. *Nature Communications*, 8(1):1978, dec 2017. ISSN 2041-1723. doi: 10.1038/s41467-017-02161-4. URL http://www.nature.com/articles/s41467-017-02161-4.

[103] J O'Neill and A Reddy. Circadian clocks in human red blood cells. *Nature*, 469(7331): 498–503, 2011. ISSN 0028-0836. doi: 10.1038/nature09702.Circadian. URL http://www.nature.com/nature/journal/v469/n7331/abs/nature09702.html.

[104] B M Sweeney and F T Haxo. Persistence of a Photosynthetic Rhythm in Enucleated Acetabularia. *Science (New York, N.Y.)*, 134(3):1361–1363, 1961.

[105] John C. Woolum. A Re-Examination of the Role of the Nucleus in Generating the Circadian Rhythm in Acetabularia. *Journal of Biological Rhythms*, 6(2):129–136, 1991. ISSN 15524531. doi: 10.1177/074873049100600203.

[106] Shin-ya Miyagishima, Takayuki Fujiwara, Nobuko Sumiya, Shunsuke Hirooka, Akihiko Nakano, Yukihiro Kabeya, and Mami Nakamura. Translation-independent circadian

control of the cell cycle in a unicellular photosynthetic eukaryote. *Nature Communications*, 5:3807, may 2014. ISSN 2041-1723. doi: 10.1038/ncomms4807. URL http://www.nature.com/doifinder/10.1038/ncomms4807.

[107] Sougata Roy, Mathieu Beauchemin, Steve Dagenais-Bellefeuille, Louis Letourneau, Mario Cappadocia, and David Morse. The Lingulodinium circadian system lacks rhythmic changes in transcript abundance. *BMC Biology*, 12(1):107, dec 2014. ISSN 1741-7007. doi: 10.1186/s12915-014-0107-z. URL http://bmcbiol.biomedcentral.com/articles/10.1186/s12915-014-0107-z.

[108] François-Yves Bouget, Marc Lefranc, Quentin Thommen, Benjamin Pfeuty, Jean-Claude Lozano, Philippe Schatt, Hugo Botebol, and Valérie Vergé. Transcriptional versus non-transcriptional clocks: A case study in Ostreococcus. *Marine Genomics*, 14:17–22, apr 2014. ISSN 1874-7787. doi: 10.1016/J.MARGEN.2014.01.004. URL https://www.sciencedirect.com/science/article/pii/S1874778714000051?via{%}3Dihub.

[109] Kevin A. Feeney, Louise L. Hansen, Marrit Putker, Consuelo Olivares-Yañez, Jason Day, Lorna J. Eades, Luis F. Larrondo, Nathaniel P. Hoyle, John S. O'Neill, and Gerben van Ooijen. Daily magnesium fluxes regulate cellular timekeeping and energy balance. *Nature*, 532(7599):375–379, apr 2016. ISSN 0028-0836. doi: 10.1038/nature17407. URL http://www.nature.com/doifinder/10.1038/nature17407.

[110] John S O'Neill, Gerben van Ooijen, Laura E Dixon, Carl Troein, Florence Corellou, François-Yves Bouget, Akhilesh B Reddy, and Andrew J Millar. Circadian rhythms persist without transcription in a eukaryote. *Nature*, 469(7331):554–8, 2011. ISSN 1476-4687. doi: 10.1038/nature09654. URL http://dx.doi.org/10.1038/nature09654.

[111] Michael H. Hastings, Elizabeth S. Maywood, and John S. O'Neill. Cellular Circadian Pacemaking and the Role of Cytosolic Rhythms. *Current Biology*, 18(17):R805–R815, 2008. ISSN 09609822. doi: 10.1016/j.cub.2008.07.021.

[112] Patricia L. Lakin-Thomas. Transcriptional feedback oscillators: Maybe, maybe not... *Journal of Biological Rhythms*, 21(2):83–92, 2006. ISSN 07487304. doi: 10.1177/0748730405286102.

[113] Martha Merrow, Gabriella Mazzotta, Zheng Chen, and Till Roenneberg. The right place at the right time : regulation of daily timing by phosphorylation. *Genes and Development*, 20:2629–2633, 2006. doi: 10.1101/gad.1479706.GENES.

[114] John S O'Neill, Elizabeth S Maywood, and Michael H Hastings. Cellular mechanisms of circadian pacemaking: beyond transcriptional loops. *Handbook of experimental pharmacology*, (217):67–103, 2013. ISSN 0171-2004. doi: 10.1007/978-3-642-25950-0_4. URL http://www.ncbi.nlm.nih.gov/pubmed/23604476.

[115] Masato Nakajima, Keiko Imai, Hiroshi Ito, Taeko Nishiwaki, Yoriko Murayama, Hideo Iwasaki, Tokitaka Oyama, and Takao Kondo. Reconstitution of circadian oscillation of cyanobacterial KaiC phosphorylation in vitro. *Science (New York, N.Y.)*, 308(5720):414–5, apr 2005. ISSN 1095-9203. doi: 10.1126/science.1108451. URL http://www.ncbi.nlm.nih.gov/pubmed/15831759.

[116] Jun Abe, Takuya B Hiyama, Atsushi Mukaiyama, Seyoung Son, Toshifumi Mori, Shinji Saito, Masato Osako, Julie Wolanin, Eiki Yamashita, Takao Kondo, and Shuji Akiyama. Atomic-scale origins of slowness in the cyanobacterial circadian clock. *Science (New York, N.Y.)*, 349(6245):312–316, 2015.

[117] Koji L. Ode and Hiroki R. Ueda. Design Principles of Phosphorylation-Dependent Timekeeping in Eukaryotic Circadian Clocks. *Cold Spring Harbor Perspectives in Biology*, page a028357, 2017. ISSN 1943-0264. doi: 10.1101/cshperspect.a028357. URL http://cshperspectives.cshlp.org/lookup/doi/10.1101/cshperspect.a028357.

[118] Arren Bar-Even, Elad Noor, Yonatan Savir, Wolfram Liebermeister, Dan Davidi, Dan S. Tawfik, and Ron Milo. The moderately efficient enzyme: Evolutionary and physicochemical trends shaping enzyme parameters. *Biochemistry*, 50(21):4402–4410, may 2011. ISSN 00062960. doi: 10.1021/bi2002289. URL http://pubs.acs.org/doi/abs/10.1021/bi2002289.

[119] S Gandy, A J Czernik, and P Greengard. Phosphorylation of Alzheimer disease amyloid precursor peptide by protein kinase C and Ca2+/calmodulin-dependent protein kinase II. *Proceedings of the National Academy of Sciences of the United States of America*, 85(16):6218–21, aug 1988. ISSN 0027-8424. doi: 10.1073/pnas.85.16.6218. URL http://www.pubmedcentral.nih.gov/articlerender.fcgi?artid=281937{&}tool=pmcentrez{&}rendertype=abstracthttp://www.ncbi.nlm.nih.gov/pubmed/3137567http://www.pubmedcentral.nih.gov/articlerender.fcgi?artid=PMC281937.

[120] Michael J Moore, Joseph A Adams, and Susan S Taylor. Structural basis for peptide binding in protein kinase A. Role of glutamic acid 203 and tyrosine 204 in the peptide-positioning loop. *The Journal of biological chemistry*, 278(12):10613–8, mar 2003. ISSN 0021-9258. doi: 10.1074/jbc.M210807200. URL http://www.ncbi.nlm.nih.gov/pubmed/12499371.

[121] Shu-Wen Teng, Shankar Mukherji, Jeffrey R Moffitt, Sophie de Buyl, and Erin K O'Shea. Robust circadian oscillations in growing cyanobacteria require transcriptional feedback. *Science (New York, N.Y.)*, 340(6133):737–40, may 2013. ISSN 1095-9203. doi: 10.1126/science.1230996. URL http://www.ncbi.nlm.nih.gov/pubmed/23661759http://www.pubmedcentral.nih.gov/articlerender.fcgi?artid=PMC3696982.

[122] Andrian Gutu and Erin K O'Shea. Two antagonistic clock-regulated histidine kinases time the activation of circadian gene expression. *Molecular cell*, 50(2):288–94, apr 2013. ISSN 1097-4164. doi: 10.1016/j.molcel.2013.02.022. URL http://www.ncbi.nlm.nih.gov/pubmed/23541768http://www.pubmedcentral.nih.gov/articlerender.fcgi?artid=PMC3674810.

[123] Martin Egli. Architecture and mechanism of the central gear in an ancient molecular timer. *Journal of the Royal Society, Interface*, 14(128):20161065, mar 2017. ISSN 1742-5662. doi: 10.1098/rsif.2016.1065. URL http://www.ncbi.nlm.nih.gov/pubmed/28330987http://www.pubmedcentral.nih.gov/articlerender.fcgi?artid=PMC5378140.

[124] Yohko Kitayama, Taeko Nishiwaki-Ohkawa, Yukiko Sugisawa, and Takao Kondo. KaiC intersubunit communication facilitates robustness of circadian rhythms in cyanobacteria. *Nature Communications*, 4(1):2897, dec 2013. ISSN 2041-1723. doi: 10.1038/ncomms3897. URL http://www.nature.com/articles/ncomms3897.

[125] Masao Doi, Jun Hirayama, and Paolo Sassone-Corsi. Circadian Regulator CLOCK Is a Histone Acetyltransferase. *Cell*, 125(3):497–508, may 2006. ISSN 0092-8674. doi: 10.1016/J.CELL.2006.03.033. URL https://www.sciencedirect.com/science/article/pii/S0092867406004442?via{%}3Dihub.

[126] David J Durgan, Betty M Pat, Boglarka Laczy, Jerry A Bradley, Ju-Yun Tsai, Maximiliano H Grenett, William F Ratcliffe, Rachel A Brewer, Jeevan Nagendran, Carolina Villegas-Montoya, Chenhang Zou, Luyun Zou, Russell L Johnson, Jason R B Dyck, Molly S Bray, Karen L Gamble, John C Chatham, and Martin E Young. O-GlcNAcylation, novel post-translational modification linking myocardial metabolism and cardiomyocyte circadian clock. *The Journal of biological chemistry*, 286(52):44606–19, dec 2011. ISSN 1083-351X. doi: 10.1074/jbc.M111.278903. URL http://www.ncbi.nlm.nih.gov/pubmed/22069332http://www.pubmedcentral.nih.gov/articlerender.fcgi?artid=PMC3247942.

[127] Nirupama Gupta and Stephen W Ragsdale. Thiol-disulfide redox dependence of heme binding and heme ligand switching in nuclear hormone receptor rev-erb{beta}. *The Journal of biological chemistry*, 286(6):4392–403, feb 2011. ISSN 1083-351X. doi:

10.1074/jbc.M110.193466. URL http://www.ncbi.nlm.nih.gov/pubmed/21123168http://www.pubmedcentral.nih.gov/articlerender.fcgi?artid=PMC3039370.

[128] Choogon Lee, Jean-Pierre Etchegaray, Felino R.A. Cagampang, Andrew S.I. Loudon, and Steven M. Reppert. Posttranslational Mechanisms Regulate the Mammalian Circadian Clock. *Cell*, 107(7):855–867, 2001. ISSN 00928674. doi: 10.1016/S0092-8674(01)00610-9.

[129] Jiwon Lee, Yool Lee, Min Joo Lee, Eonyoung Park, Sung Hwan Kang, Chin Ha Chung, Kun Ho Lee, and Kyungjin Kim. Dual modification of BMAL1 by SUMO2/3 and ubiquitin promotes circadian activation of the CLOCK/BMAL1 complex. *Molecular and cellular biology*, 28(19):6056–65, oct 2008. ISSN 1098-5549. doi: 10.1128/MCB.00583-08. URL http://www.ncbi.nlm.nih.gov/pubmed/18644859http://www.pubmedcentral.nih.gov/articlerender.fcgi?artid=PMC2546997.

[130] Arun Mehra, Christopher L Baker, Jennifer J Loros, and Jay C Dunlap. Post-translational modifications in circadian rhythms. *Trends in biochemical sciences*, 34(10):483–90, oct 2009. ISSN 0968-0004. doi: 10.1016/j.tibs.2009.06.006. URL http://www.ncbi.nlm.nih.gov/pubmed/19740663http://www.pubmedcentral.nih.gov/articlerender.fcgi?artid=PMC2765057.

[131] J. W. Hastings. The Gonyaulax clock at 50: Translational control of circadian expression. *Cold Spring Harbor Symposia on Quantitative Biology*, 72:141–144, 2007. ISSN 00917451. doi: 10.1101/sqb.2007.72.026.

[132] K. A. Feeney, M. Putker, M. Brancaccio, and J. S. ONeill. In-depth Characterization of Firefly Luciferase as a Reporter of Circadian Gene Expression in Mammalian Cells. *Journal of Biological Rhythms*, XX(X):0748730416668898, 2016. ISSN 0748-7304. doi: 10.1177/0748730416668898. URL http://jbr.sagepub.com/cgi/doi/10.1177/0748730416668898.

[133] John S O'Neill, Elizabeth S Maywood, Johanna E Chesham, Joseph S Takahashi, and Michael H Hastings. cAMP-dependent signaling as a core component of the mammalian circadian pacemaker. *Science (New York, N.Y.)*, 320(5878):949–53, may 2008. ISSN 1095-9203. doi: 10.1126/science.1152506. URL http://www.ncbi.nlm.nih.gov/pubmed/18487196http://www.pubmedcentral.nih.gov/articlerender.fcgi?artid=PMC2735813.

[134] Marrit Putker and John Stuart O'Neill. Reciprocal Control of the Circadian Clock and Cellular Redox State - a Critical Appraisal. *Molecules and Cells*, 39(1):6–19, jan 2016. ISSN 1016-8478. doi: 10.14348/molcells.2016.2323. URL http://www.molcells.org/journal/view.html?doi=10.14348/molcells.2016.2323.

[135] Marrit Putker, Priya Crosby, Kevin A Feeney, Nathaniel P. Hoyle, Ana S.H. da Costa, Edoardo Gaude, Christian Frezza, and John Stuart O'Neill. Mammalian circadian period, but not phase and amplitude, is robust against redox and metabolic perturbations. *Antioxidants & Redox Signaling*, 4523:ars.2016.6911, 2017. ISSN 1523-0864. doi: 10.1089/ars.2016.6911. URL http://online.liebertpub.com/doi/10.1089/ars.2016.6911.

[136] Clara Bien Peek, Alison H Affinati, Kathryn Moynihan Ramsey, Hsin-Yu Kuo, Wei Yu, Laura A Sena, Olga Ilkayeva, Biliana Marcheva, Yumiko Kobayashi, Chiaki Omura, Daniel C Levine, David J Bacsik, David Gius, Christopher B Newgard, Eric Goetzman, Navdeep S Chandel, John M Denu, Milan Mrksich, and Joseph Bass. Circadian clock NAD+ cycle drives mitochondrial oxidative metabolism in mice. *Science (New York, N.Y.)*, 342(6158):1243417, nov 2013. ISSN 1095-9203. doi: 10.1126/science.1243417. URL http://www.sciencemag.org/cgi/doi/10.1126/science.1243417http://www.ncbi.nlm.nih.gov/pubmed/24051248http://www.pubmedcentral.nih.gov/articlerender.fcgi?artid=PMC3963134.

[137] Nathaniel P. Hoyle, Estere Seinkmane, Marrit Putker, Kevin A. Feeney, Toke P. Krogager, Johanna E. Chesham, Liam K. Bray, Justyn M. Thomas, Ken Dunn, John Blaikley, and John S. O'Neill. Circadian actin dynamics drive rhythmic fibroblast mobilization during wound healing. *Science Translational Medicine*, 9(415):eaal2774, 2017. ISSN 1946-6234. doi: 10.1126/scitranslmed.aal2774. URL http://stm.sciencemag.org/lookup/doi/10.1126/scitranslmed.aal2774.

[138] Haiyan Xu, Chelsea L. Gustafson, Patrick J. Sammons, Sanjoy K. Khan, Nicole C. Parsley, Chidambaram Ramanathan, Hsiau-Wei Lee, Andrew C. Liu, and Carrie L. Partch. Cryptochrome 1 regulates the circadian clock through dynamic interactions with the BMAL1 C terminus. *Nature Structural & Molecular Biology*, 22(6):476–484, 2015. ISSN 1545-9993. doi: 10.1038/nsmb.3018. URL http://www.nature.com/nsmb/journal/v22/n6/full/nsmb.3018.html.

[139] Sofia I H Godinho, Elizabeth S Maywood, Linda Shaw, Valter Tucci, Alun R Barnard, Luca Busino, Michele Pagano, Rachel Kendall, Mohamed M Quwailid, M Rosario Romero, John O'neill, Johanna E Chesham, Debra Brooker, Zuzanna Lalanne, Michael H Hastings, and Patrick M Nolan. The after-hours mutant reveals a role for Fbxl3 in determining mammalian circadian period. *Science (New York, N.Y.)*, 316(5826):897–900, may 2007. ISSN 1095-9203. doi: 10.1126/science.1141138. URL http://www.ncbi.nlm.nih.gov/pubmed/17463252.

[140] Q He and Y Liu. Degradation of the Neurospora circadian clock protein FREQUENCY through the ubiquitin-proteasome pathway. *Biochemical Society transactions*, 33(Pt 5): 953–6, nov 2005. ISSN 0300-5127. doi: 10.1042/BST20050953. URL http://www.ncbi.nlm.nih.gov/pubmed/16246019.

[141] D P King, Y Zhao, A M Sangoram, L D Wilsbacher, M Tanaka, M P Antoch, T D Steeves, M H Vitaterna, J M Kornhauser, P L Lowrey, F W Turek, and J S Takahashi. Positional cloning of the mouse circadian clock gene. *Cell*, 89(4):641–53, may 1997. ISSN 0092-8674. doi: 10.1016/S0092-8674(00)80245-7. URL http://www.ncbi.nlm.nih.gov/pubmed/9160755http://www.pubmedcentral.nih.gov/articlerender.fcgi?artid=PMC3815553.

[142] Gerben Van Ooijen, Laura E. Dixon, Carl Troein, and Andrew J. Millar. Proteasome function is required for biological timing throughout the twenty-four hour cycle. *Current Biology*, 21(10):869–875, 2011. ISSN 09609822. doi: 10.1016/j.cub.2011.03.060. URL http://dx.doi.org/10.1016/j.cub.2011.03.060.

[143] Sandra M Siepka, Seung-Hee Yoo, Junghea Park, Weimin Song, Vivek Kumar, Yinin Hu, Choogon Lee, and Joseph S Takahashi. Circadian mutant Overtime reveals F-box protein FBXL3 regulation of cryptochrome and period gene expression. *Cell*, 129(5):1011–23, jun 2007. ISSN 0092-8674. doi: 10.1016/j.cell.2007.04.030. URL http://www.ncbi.nlm.nih.gov/pubmed/17462724http://www.pubmedcentral.nih.gov/articlerender.fcgi?artid=PMC3762874.

[144] D. M. Virshup, E. J. Eide, D. B. Forger, M. Gallego, and E. Vielhaber Harnish. Reversible Protein Phosphorylation Regulates Circadian Rhythms. *Cold Spring Harbor Symposia on Quantitative Biology*, 72(1):413–420, jan 2007. ISSN 0091-7451. doi: 10.1101/sqb.2007.72.048. URL http://www.ncbi.nlm.nih.gov/pubmed/18419299http://symposium.cshlp.org/cgi/doi/10.1101/sqb.2007.72.048.

[145] Jean-Pierre Etchegaray, Elizabeth A. Yu, Premananda Indic, Robert Dallmann, and David R. Weaver. Casein Kinase 1 Delta (CK1δ) Regulates Period Length of the Mouse Suprachiasmatic Circadian Clock In Vitro. *PLoS ONE*, 5(4):e10303, apr 2010. ISSN 1932-6203. doi: 10.1371/journal.pone.0010303. URL http://dx.plos.org/10.1371/journal.pone.0010303.

[146] Hyeong-min Lee, Rongmin Chen, Hyukmin Kim, Jean-Pierre Etchegaray, David R Weaver, and Choogon Lee. The period of the circadian oscillator is primarily determined by the balance between casein kinase 1 and protein phosphatase 1. *Proceedings of the National Academy of Sciences of the United States of America*, 108(39):16451–6, sep 2011. ISSN 1091-6490. doi: 10.1073/pnas.1107178108. URL http://www.ncbi.nlm.nih.gov/pubmed/21930935http://www.pubmedcentral.nih.gov/articlerender.fcgi?artid=PMC3182690.

[147] Qing-Jun Meng, Elizabeth S Maywood, David A Bechtold, Wei-Qun Lu, Jian Li, Julie E Gibbs, Sandrine M Dupré, Johanna E Chesham, Francis Rajamohan, John Knafels, Blossom Sneed, Laura E Zawadzke, Jeffrey F Ohren, Kevin M Walton, Travis T Wager, Michael H Hastings, and Andrew S I Loudon. Entrainment of disrupted circadian behavior through inhibition of casein kinase 1 (CK1) enzymes. *Proceedings of the National Academy of Sciences of the United States of America*, 107(34):15240–5, aug 2010. ISSN 1091-6490. doi: 10.1073/pnas.1005101107. URL http://www.ncbi.nlm.nih.gov/pubmed/20696890http://www.pubmedcentral.nih.gov/articlerender.fcgi?artid=PMC2930590.

[148] Bert Maier, Sabrina Wendt, Jens T Vanselow, Thomas Wallach, Silke Reischl, Stefanie Oehmke, Andreas Schlosser, and Achim Kramer. A large-scale functional RNAi screen reveals a role for CK2 in the mammalian circadian clock. *Genes & development*, 23(6):708–18, mar 2009. ISSN 1549-5477. doi: 10.1101/gad.512209. URL http://www.ncbi.nlm.nih.gov/pubmed/19299560http://www.pubmedcentral.nih.gov/articlerender.fcgi?artid=PMC2661607.

[149] Elaine M. Smith, Jui-Ming Lin, Rose-Anne Meissner, and Ravi Allada. Dominant-Negative CK2α Induces Potent Effects on Circadian Rhythmicity. *PLoS Genetics*, 4(1):e12, 2008. ISSN 1553-7390. doi: 10.1371/journal.pgen.0040012. URL http://dx.plos.org/10.1371/journal.pgen.0040012.

[150] Yoshiki Tsuchiya, Makoto Akashi, Mitsuhiro Matsuda, Kyoko Goto, Yoshihiko Miyata, Koichi Node, and Eisuke Nishida. Involvement of the protein kinase CK2 in the regulation of mammalian circadian rhythms. *Science signaling*, 2(73):ra26, jun 2009. ISSN 1937-9145. doi: 10.1126/scisignal.2000305. URL http://www.ncbi.nlm.nih.gov/pubmed/19491384.

[151] Tsuyoshi Hirota, Warren G Lewis, Andrew C Liu, Jae Wook Lee, Peter G Schultz, and Steve A Kay. A chemical biology approach reveals period shortening of the mammalian circadian clock by specific inhibition of GSK-3beta. *Proceedings of the National Academy of Sciences of the United States of America*, 105(52):20746–51, dec 2008. ISSN 1091-6490. doi: 10.1073/pnas.0811410106. URL http://www.ncbi.nlm.nih.gov/pubmed/19104043http://www.pubmedcentral.nih.gov/articlerender.fcgi?artid=PMC2606900.

[152] Chisato Iitaka, Koyomi Miyazaki, Toshihiro Akaike, and Norio Ishida. A role for glycogen synthase kinase-3beta in the mammalian circadian clock. *The Journal of biological chemistry*, 280(33):29397–402, aug 2005. ISSN 0021-9258. doi: 10.1074/jbc.M503526200. URL http://www.ncbi.nlm.nih.gov/pubmed/15972822.

[153] Nobuhiro Kurabayashi, Tsuyoshi Hirota, Mihoko Sakai, Kamon Sanada, and Yoshitaka Fukada. DYRK1A and glycogen synthase kinase 3beta, a dual-kinase mechanism directing proteasomal degradation of CRY2 for circadian timekeeping. *Molecular and cellular biology*, 30(7):1757–1768, 2010. ISSN 0270-7306. doi: 10.1128/MCB.01047-09.

[154] Saurabh Sahar, Loredana Zocchi, Chisato Kinoshita, Emiliana Borrelli, and Paolo Sassone-Corsi. Regulation of BMAL1 Protein Stability and Circadian Function by GSK3β-Mediated Phosphorylation. *PLoS ONE*, 5(1):e8561, jan 2010. ISSN 1932-6203. doi: 10.1371/journal.pone.0008561. URL http://dx.plos.org/10.1371/journal.pone.0008561.

[155] Mary L. Spengler, Karen K. Kuropatwinski, Molly Schumer, and Marina P. Antoch. A serine cluster mediates BMAL1-dependent CLOCK phosphorylation and degradation. *Cell Cycle*, 8(24):4138–4146, 2009. ISSN 15514005. doi: 10.4161/cc.8.24.10273.

[156] Lei Yin, Jing Wang, Peter S Klein, and Mitchell A Lazar. Nuclear receptor Rev-erbalpha is a critical lithium-sensitive component of the circadian clock. *Science (New York, N.Y.)*, 311(5763):1002–5, feb 2006. ISSN 1095-9203. doi: 10.1126/science.1121613. URL http://www.ncbi.nlm.nih.gov/pubmed/16484495.

[157] Monica Gallego, Heeseog Kang, and David M Virshup. Protein phosphatase 1 regulates the stability of the circadian protein PER2. *Biochem. J*, 399:169–175, 2006. ISSN 02646021. doi: 10.1042/BJ20060678.

[158] Isabelle Schmutz, Sabrina Wendt, Anna Schnell, Achim Kramer, Isabelle M. Mansuy, and Urs Albrecht. Protein Phosphatase 1 (PP1) is a post-translational regulator of the Mammalian Circadian Clock. *PLoS ONE*, 6(6), 2011. ISSN 19326203. doi: 10.1371/journal.pone.0021325.

[159] Makoto Akashi, Yoshiki Tsuchiya, Takao Yoshino, and Eisuke Nishida. Control of intracellular dynamics of mammalian period proteins by casein kinase I epsilon (CKIepsilon) and CKIdelta in cultured cells. *Molecular and cellular biology*, 22(6): 1693–703, mar 2002. ISSN 0270-7306. doi: 10.1128/MCB.22.6.1693-1703.2002. URL http://www.ncbi.nlm.nih.gov/pubmed/11865049http://www.pubmedcentral.nih.gov/articlerender.fcgi?artid=PMC135601.

[160] Atsuko Takano, Kimiko Shimizu, Shuichi Kani, Ruud M. Buijs, Masato Okada, and Katsuya Nagai. Cloning and characterization of rat casein kinase 1. *FEBS Letters*, 477 (1-2):106–112, jul 2000. ISSN 00145793. doi: 10.1016/S0014-5793(00)01755-5. URL http://doi.wiley.com/10.1016/S0014-5793{%}2800{%}2901755-5.

[161] E Vielhaber, E Eide, A Rivers, Z H Gao, and D M Virshup. Nuclear entry of the circadian regulator mPER1 is controlled by mammalian casein kinase I epsilon. *Molecular and cellular biology*, 20(13):4888–99, jul 2000. ISSN 0270-7306. doi: 10.1128/MCB.20.13.4888-4899.2000. URL http://www.ncbi.nlm.nih.gov/pubmed/10848614http://www.pubmedcentral.nih.gov/articlerender.fcgi?artid=PMC85940.

[162] Erik J Eide, Erica L Vielhaber, William A Hinz, and David M Virshup. The circadian regulatory proteins BMAL1 and cryptochromes are substrates of casein kinase Iepsilon. *The Journal of biological chemistry*, 277(19):17248–54, may 2002. ISSN 0021-9258. doi: 10.1074/jbc.M111466200. URL http://www.ncbi.nlm.nih.gov/pubmed/11875063http://www.pubmedcentral.nih.gov/articlerender.fcgi?artid=PMC1513548.

[163] Monica Gallego, Erik J Eide, Margaret F Woolf, David M Virshup, and Daniel B Forger. An opposite role for tau in circadian rhythms revealed by mathematical modeling. *Proceedings of the National Academy of Sciences of the United States of America*, 103(28): 10618–10623, 2006. ISSN 0027-8424. doi: 10.1073/pnas.0604511103.

[164] Qun He, Joonseok Cha, Qiyang He, Heng-Chi Lee, Yuhong Yang, and Yi Liu. CKI and CKII mediate the FREQUENCY-dependent phosphorylation of the WHITE COLLAR complex to close the Neurospora circadian negative feedback loop. *Genes & development*, 20(18):2552–65, sep 2006. ISSN 0890-9369. doi: 10.1101/gad.1463506. URL http://www.ncbi.nlm.nih.gov/pubmed/16980584http://www.pubmedcentral.nih.gov/articlerender.fcgi?artid=PMC1578678.

[165] Eun Young Kim and Isaac Edery. Balance between DBT/CKIepsilon kinase and protein phosphatase activities regulate phosphorylation and stability of Drosophila CLOCK protein. *Proceedings of the National Academy of Sciences of the United States of America*, 103(16):6178–83, apr 2006. ISSN 0027-8424. doi: 10.1073/pnas.0511215103.

URL http://www.ncbi.nlm.nih.gov/pubmed/16603629http://www.pubmedcentral.nih.gov/articlerender.fcgi?artid=PMC1458851.

[166] Kamon Sanada, Toshiyuki Okano, and Yoshitaka Fukada. Mitogen-activated protein kinase phosphorylates and negatively regulates basic helix-loop-helix-PAS transcription factor BMAL1. *The Journal of biological chemistry*, 277(1):267–71, jan 2002. ISSN 0021-9258. doi: 10.1074/jbc.M107850200. URL http://www.ncbi.nlm.nih.gov/pubmed/11687575.

[167] Tobias Schafmeier, Andrea Haase, Krisztina Káldi, Johanna Scholz, Marc Fuchs, and Michael Brunner. Transcriptional feedback of Neurospora circadian clock gene by phosphorylation-dependent inactivation of its transcription factor. *Cell*, 122(2): 235–46, jul 2005. ISSN 0092-8674. doi: 10.1016/j.cell.2005.05.032. URL http://www.ncbi.nlm.nih.gov/pubmed/16051148.

[168] Wangjie Yu, Hao Zheng, Jerry H Houl, Brigitte Dauwalder, and Paul E Hardin. PER-dependent rhythms in CLK phosphorylation and E-box binding regulate circadian transcription. *Genes & development*, 20(6):723–33, mar 2006. ISSN 0890-9369. doi: 10.1101/gad.1404406. URL http://www.ncbi.nlm.nih.gov/pubmed/16543224http://www.pubmedcentral.nih.gov/articlerender.fcgi?artid=PMC1434787.

[169] Erik J Eide, Margaret F Woolf, Heeseog Kang, Peter Woolf, William Hurst, Fernando Camacho, Erica L Vielhaber, Andrew Giovanni, and David M Virshup. Control of Mammalian Circadian Rhythm by CKI ε -Regulated Proteasome-Mediated PER2 Degradation. *Molecular and cellular biology*, 25(7):2795 – 2807, 2005. ISSN 0270-7306. doi: 10.1128/MCB.25.7.2795.

[170] Monica Gallego and David M. Virshup. Post-translational modifications regulate the ticking of the circadian clock. *Nature Reviews Molecular Cell Biology*, 8(2):139–148, feb 2007. ISSN 1471-0072. doi: 10.1038/nrm2106. URL http://www.nature.com/articles/nrm2106.

[171] Y. Isojima, M. Nakajima, H. Ukai, H. Fujishima, R. G. Yamada, K.-h. Masumoto, R. Kiuchi, M. Ishida, M. Ukai-Tadenuma, Y. Minami, R. Kito, K. Nakao, W. Kishimoto, S.-H. Yoo, K. Shimomura, T. Takao, A. Takano, T. Kojima, K. Nagai, Y. Sakaki, J. S. Takahashi, and H. R. Ueda. CKIe/d-dependent phosphorylation is a temperature-insensitive, period-determining process in the mammalian circadian clock. *Proceedings of the National Academy of Sciences*, 106(37):15744–15749, sep 2009. ISSN 0027-8424. doi: 10.1073/pnas.0908733106. URL http://www.pnas.org/cgi/doi/10.1073/pnas.0908733106.

[172] Yuta Shinohara, Yohei M Koyama, Maki Ukai-tadenuma, Takatsugu Hirokawa, Masaki Kikuchi, Rikuhiro G. Yamada, Hideki Ukai, Hiroshi Fujishima, Takashi Umehara, Kazuki Tainaka, and Hiroki R. Ueda. Temperature-Sensitive Substrate and Product Binding Underlie Temperature-Compensated Phosphorylation in the Clock. *Molecular Cell*, 67 (5):783–798.e20, 2017. ISSN 1097-2765. doi: 10.1016/j.molcel.2017.08.009. URL http://dx.doi.org/10.1016/j.molcel.2017.08.009.

[173] Leland H. Hartwell, John J. Hopfield, Stanislas Leibler, and Andrew W. Murray. From molecular to modular cell biology. *Nature*, 1999. ISSN 0028-0836. doi: 10.1038/35011540.

[174] Aled M. Edwards, Ruth Isserlin, Gary D. Bader, Stephen V. Frye, Timothy M. Willson, and Frank H. Yu. Too many roads not taken. *Nature*, 470:163–165, 2011. ISSN 0028-0836. doi: 10.1038/470163a.

[175] Marcus Bantscheff, Simone Lemeer, Mikhail M. Savitski, and Bernhard Kuster. Quantitative mass spectrometry in proteomics: Critical review update from 2007 to the present. *Analytical and Bioanalytical Chemistry*, 404(4):939–965, 2012. ISSN 16182642. doi: 10.1007/s00216-012-6203-4.

[176] Nishant Pappireddi, Lance Martin, and Martin Wühr. A Review on Quantitative Multiplexed Proteomics. *ChemBioChem*, 20(10):1210–1224, 2019. ISSN 14397633. doi: 10.1002/cbic.201800650.

[177] Olga T Schubert, Hannes L Röst, Ben C Collins, George Rosenberger, and Ruedi Aebersold. Quantitative proteomics: challenges and opportunities in basic and applied research. *Nature Protocols*, 12(7):1289–1294, jul 2017. ISSN 1754-2189. doi: 10.1038/nprot.2017.040. URL http://www.nature.com/articles/nprot.2017.040.

[178] Ruedi Aebersold and Matthias Mann. Mass spectrometry-based proteomics. *Nature*, 422: 198–207, 2003. ISSN 0028-0836. doi: 10.1038/nature01511.

[179] John B. Fenn, Matthias Mann, Chin Kai Meng, Shek Fu Wong, and Craig M. Whitehouse. Electrospray ionization for mass spectrometry of large biomolecules. *Science*, 246(4926): 64–71, 1989. ISSN 00368075. doi: 10.1126/science.2675315.

[180] Jürgen Cox, Nadin Neuhauser, Annette Michalski, Richard A. Scheltema, Jesper V. Olsen, and Matthias Mann. Andromeda: A peptide search engine integrated into the MaxQuant environment. *Journal of Proteome Research*, 10(4):1794–1805, 2011. ISSN 15353893. doi: 10.1021/pr101065j.

[181] Marcus Bantscheff, Markus Schirle, Gavain Sweetman, Jens Rick, and Bernhard Kuster. Quantitative mass spectrometry in proteomics: A critical review. *Analytical and Bioanalytical Chemistry*, 389(4):1017–1031, 2007. ISSN 16182642. doi: 10.1007/s00216-007-1486-6.

[182] Dirk Chelius and Pavel V Bondarenko. Quantitative profiling of proteins in complex mixtures using liquid chromatography and mass spectrometry. *Journal of Proteome Research*, 1(4):317–323, 2002. ISSN 1535-3893. URL http://www.ncbi.nlm.nih.gov/pubmed/12645887.

[183] Jeffrey C. Silva, Marc V. Gorenstein, Guo-Zhong Li, Johannes P. C. Vissers, and Scott J. Geromanos. Absolute Quantification of Proteins by LCMS E. *Molecular & Cellular Proteomics*, 5(1):144–156, 2006. ISSN 1535-9476. doi: 10.1074/mcp.m500230-mcp200.

[184] Jürgen Cox, Marco Y Hein, Christian A Luber, Igor Paron, Nagarjuna Nagaraj, and Matthias Mann. Accurate proteome-wide label-free quantification by delayed normalization and maximal peptide ratio extraction, termed MaxLFQ. *Molecular & cellular proteomics : MCP*, 13(9):2513–2526, 2014. ISSN 1535-9484. doi: 10.1074/mcp.M113.031591.

[185] Loïc Dayon, Alexandre Hainard, Virginie Licker, Natacha Turck, Karsten Kuhn, Denis F. Hochstrasser, Pierre R. Burkhard, and Jean Charles Sanchez. Relative quantification of proteins in human cerebrospinal fluids by MS/MS using 6-plex isobaric tags. *Analytical Chemistry*, 2008. ISSN 00032700. doi: 10.1021/ac702422x.

[186] Philip L Ross, Yulin N Huang, Jason N Marchese, Brian Williamson, Kenneth Parker, Stephen Hattan, Nikita Khainovski, Sasi Pillai, Subhakar Dey, Scott Daniels, Subhasish Purkayastha, Peter Juhasz, Stephen Martin, Michael Bartlet-Jones, Feng He, Allan Jacobson, and Darryl J Pappin. Multiplexed protein quantitation in Saccharomyces cerevisiae using amine-reactive isobaric tagging reagents. *Molecular & cellular proteomics : MCP*, 3(12):1154–1169, 2004. ISSN 1535-9476. doi: 10.1074/mcp.M400129-MCP200.

[187] Chunaram Choudhary and Matthias Mann. Decoding signalling networks by mass spectrometry-based proteomics. *Nature reviews. Molecular cell biology*, 11(6):427–439, 2010. ISSN 1471-0080. doi: 10.1038/nrm2900.

[188] Silke Reischl and Achim Kramer. Kinases and phosphatases in the mammalian circadian clock. *FEBS Letters*, 585(10):1393–1399, 2011. ISSN 00145793. doi: 10.1016/j.febslet.2011.02.038. URL http://dx.doi.org/10.1016/j.febslet.2011.02.038.

[189] Philip Cohen. The regulation of protein function by multisite phosphorylation - A 25 year update. *Trends in Biochemical Sciences*, 25(12):596–601, 2000. ISSN 09680004. doi: 10.1016/S0968-0004(00)01712-6.

[190] George A Khoury, Richard C Baliban, and Christodoulos A Floudas. Proteome-wide post-translational modification statistics: frequency analysis and curation of the swiss-prot database. *Scientific reports*, 1(90), 2011. ISSN 2045-2322. doi: 10.1038/srep00090.

[191] Simone Lemeer and Albert JR Heck. The phosphoproteomics data explosion. *Current Opinion in Chemical Biology*, 13(4):414–420, 2009. ISSN 13675931. doi: 10.1016/j.cbpa.2009.06.022.

[192] Justine V. Arrington, Chuan Chih Hsu, Sarah G. Elder, and W. Andy Tao. Recent advances in phosphoproteomics and application to neurological diseases. *Analyst*, 142 (23):4373–4387, 2017. ISSN 13645528. doi: 10.1039/c7an00985b.

[193] Lennart Andersson and Jerker Porath. Isolation of phosphoproteins by immobilized metal (Fe3+) affinity chromatography. *Analytical Biochemistry*, 154(1):250–254, 1986. ISSN 10960309. doi: 10.1016/0003-2697(86)90523-3.

[194] Martin R Larsen, Tine E Thingholm, Ole N Jensen, Peter Roepstorff, and Thomas J D Jørgensen. Highly selective enrichment of phosphorylated peptides from peptide mixtures using titanium dioxide microcolumns. *Molecular & cellular proteomics : MCP*, 4(7): 873–886, 2005. ISSN 1535-9476. doi: 10.1074/mcp.T500007-MCP200.

[195] Mark S. Hipp, Prasad Kasturi, and F. Ulrich Hartl. The proteostasis network and its decline in ageing. *Nature Reviews Molecular Cell Biology*, 20(7):421–435, jul 2019. ISSN 1471-0072. doi: 10.1038/s41580-019-0101-y. URL http://www.nature.com/articles/s41580-019-0101-y.

[196] Johnathan Labbadia and Richard I Morimoto. The Biology of Proteostasis in Aging and Disease. *Annual Review of Biochemistry*, 84(1):435–464, jun 2015. ISSN 0066-4154. doi: 10.1146/annurev-biochem-060614-033955. URL http://www.annualreviews.org/doi/10.1146/annurev-biochem-060614-033955.

[197] P Nissen, J Hansen, N Ban, P B Moore, and T A Steitz. The structural basis of ribosome activity in peptide bond synthesis. *Science (New York, N.Y.)*, 289(5481):920–30, aug 2000. ISSN 0036-8075. doi: 10.1126/science.289.5481.920. URL http://www.ncbi.nlm.nih.gov/pubmed/10937990.

[198] Suzanne Wolff, Jonathan S. Weissman, and Andrew Dillin. Differential Scales of Protein Quality Control. *Cell*, 157(1):52–64, mar 2014. ISSN 0092-8674. doi: 10.1016/J.CELL.2014.03.007. URL https://www.sciencedirect.com/science/article/pii/S0092867414003377?via{%}3Dihub.

[199] A Keith Dunker, Israel Silman, Vladimir N Uversky, and Joel L Sussman. Function and structure of inherently disordered proteins. *Current Opinion in Structural Biology*, 18(6): 756–764, dec 2008. ISSN 0959-440X. doi: 10.1016/J.SBI.2008.10.002. URL https://www.sciencedirect.com/science/article/pii/S0959440X08001516?via{%}3Dihub{#}bib28.

[200] A. Keith Dunker, M. Madan Babu, Elisar Barbar, Martin Blackledge, Sarah E. Bondos, Zsuzsanna Dosztányi, H. Jane Dyson, Julie Forman-Kay, Monika Fuxreiter, Jörg Gsponer, Kyou-Hoon Han, David T. Jones, Sonia Longhi, Steven J. Metallo, Ken Nishikawa, Ruth Nussinov, Zoran Obradovic, Rohit V. Pappu, Burkhard Rost, Philipp Selenko, Vinod Subramaniam, Joel L. Sussman, Peter Tompa, and Vladimir N Uversky. What's in a name? Why these proteins are intrinsically disordered. *Intrinsically Disordered Proteins*, 1(1):e24157, jan 2013. ISSN 2169-0707. doi: 10.4161/idp.24157. URL http://www.tandfonline.com/doi/abs/10.4161/idp.24157.

[201] F. Ulrich Hartl. Molecular chaperones in cellular protein folding. *Nature*, 381(6583): 571–580, jun 1996. ISSN 0028-0836. doi: 10.1038/381571a0. URL http://www.nature.com/articles/381571a0.

[202] Arthur L. Horwich. Molecular Chaperones in Cellular Protein Folding: The Birth of a Field. *Cell*, 157(2):285–288, apr 2014. ISSN 0092-8674. doi: 10.1016/J.CELL.2014.03.029. URL https://www.sciencedirect.com/science/article/pii/S0092867414004048?via{%}3Dihub.

[203] Alice B. Fulton. How crowded is the cytoplasm? *Cell*, 30(2):345–347, 1982. ISSN 00928674. doi: 10.1016/0092-8674(82)90231-8.

[204] Rina Rosenzweig, Nadinath B. Nillegoda, Matthias P. Mayer, and Bernd Bukau. The Hsp70 chaperone network. *Nature Reviews Molecular Cell Biology*, pages 1–16, jun 2019. ISSN 1471-0072. doi: 10.1038/s41580-019-0133-3. URL http://www.nature.com/articles/s41580-019-0133-3.

[205] F. Ulrich Hartl, Andreas Bracher, and Manajit Hayer-Hartl. Molecular chaperones in protein folding and proteostasis. *Nature*, 475(7356):324–332, jul 2011. ISSN 0028-0836. doi: 10.1038/nature10317. URL http://www.nature.com/articles/nature10317.

[206] David Balchin, Manajit Hayer-Hartl, and F Ulrich Hartl. In vivo aspects of protein folding and quality control. *Science (New York, N.Y.)*, 353(6294):aac4354, jul 2016. ISSN 1095-9203. doi: 10.1126/science.aac4354. URL http://www.ncbi.nlm.nih.gov/pubmed/27365453.

[207] Yujin E. Kim, Mark S. Hipp, Andreas Bracher, Manajit Hayer-Hartl, and F. Ulrich Hartl. Molecular Chaperone Functions in Protein Folding and Proteostasis. *Annual Review of Biochemistry*, 82(1):323–355, jun 2013. ISSN 0066-4154. doi: 10.1146/annurev-biochem-060208-092442. URL http://www.annualreviews.org/doi/10.1146/annurev-biochem-060208-092442.

[208] Amy R. Wyatt, Justin J. Yerbury, Heath Ecroyd, and Mark R. Wilson. Extracellular Chaperones and Proteostasis. *Annual Review of Biochemistry*, 82(1):295–322, 2013. ISSN 0066-4154. doi: 10.1146/annurev-biochem-072711-163904.

[209] Ivan Dikic. Proteasomal and Autophagic Degradation Systems. *Annual Review of Biochemistry*, 86(1):193–224, 2017. ISSN 0066-4154. doi: 10.1146/annurev-biochem-061516-044908.

[210] Julius Anckar and Lea Sistonen. Regulation of HSF 1 Function in the Heat Stress Response: Implications in Aging and Disease. *Annual Review of Biochemistry*, 80(1):1089–1115, jul 2011. ISSN 0066-4154. doi: 10.1146/annurev-biochem-060809-095203. URL http://www.annualreviews.org/doi/10.1146/annurev-biochem-060809-095203.

[211] Claudio Hetz and Smita Saxena. ER stress and the unfolded protein response in neurodegeneration. *Nature Reviews Neurology*, 13(8):477–491, 2017. ISSN 17594766. doi: 10.1038/nrneurol.2017.99. URL http://dx.doi.org/10.1038/nrneurol.2017.99.

[212] K Sasaki and Y Hiderou. Organelle autoregulation—stress responses in the ER, Golgi,mitochondria and lysosome. *The Journal of Biochemistry*, 157(4):185–195, 2015. doi: 10.1093/jb/mvv010.

[213] Quan Zhao, Jianghui Wang, Ilya V. Levichkin, Stan Stasinopoulos, Michael T. Ryan, and Nicholas J. Hoogenraad. A mitochondrial specific stress response in mammalian cells. *EMBO Journal*, 21(17):4411–4419, 2002. ISSN 02614189. doi: 10.1093/emboj/cdf445.

[214] Karolina Pakos-Zebrucka, Izabela Koryga, Katarzyna Mnich, Mila Ljujic, Afshin Samali, and Adrienne M Gorman. The integrated stress response. *EMBO reports*, 17(10):1374–1395, 2016. ISSN 1469-221X. doi: 10.15252/embr.201642195. URL http://embor.embopress.org/lookup/doi/10.15252/embr.201642195.

[215] Neysan Donnelly, Adrienne M. Gorman, Sanjeev Gupta, and Afshin Samali. The eIF2α kinases: Their structures and functions. *Cellular and Molecular Life Sciences*, 70(19):3493–3511, 2013. ISSN 1420682X. doi: 10.1007/s00018-012-1252-6.

[216] I Novoa, H Zeng, H P Harding, and D Ron. Feedback inhibition of the unfolded protein response by GADD34-mediated dephosphorylation of eIF2alpha. *The Journal of Cell Biology*, 153(5):1011–1022, 2001.

[217] Alan G. Hinnebusch. Molecular Mechanism of Scanning and Start Codon Selection in Eukaryotes. *Microbiology and molecular biology reviews*, 75(3):434–467, 2011. doi: 10.1128/MMBR.00008-11.

[218] Richard J. Jackson, Christopher U.T. Hellen, and Tatyana V. Pestova. The mechanism of eukaryotic translation initiation and principles of its regulation. *Nature Reviews Molecular Cell Biology*, 11(2):113–127, 2010. ISSN 14710072. doi: 10.1038/nrm2838. URL http://dx.doi.org/10.1038/nrm2838.

[219] Ching Ping Chan, Kin Hang Kok, Hei Man Vincent Tang, Chi Ming Wong, and Dong Yan Jin. Internal ribosome entry site-mediated translational regulation of ATF4 splice variant in mammalian unfolded protein response. *Biochimica et Biophysica Acta - Molecular Cell Research*, 1833(10):2165–2175, 2013. ISSN 01674889. doi: 10.1016/j.bbamcr.2013.05.002. URL http://dx.doi.org/10.1016/j.bbamcr.2013.05.002.

[220] Yun Young Lee, Randal C. Cevallos, and Eric Jan. An upstream open reading frame regulates translation of GADD34 during cellular stresses that induce eIF2phosphorylation. *Journal of Biological Chemistry*, 284(11):6661–6673, 2009. ISSN 00219258. doi: 10.1074/jbc.M806735200.

[221] Howard C Masuoka and Tim M Townes. Targeted disruption of the activating transcription factor 4 gene results in severe fetal anemia in mice. *Blood*, 99(3):736–746, 2002. doi: https://doi.org/10.1182/blood.V99.3.736.

[222] Chunxia Wang, Zhiying Huang, Ying Du, Ying Cheng, Shanghai Chen, and Feifan Guo. ATF4 regulates lipid metabolism and thermogenesis. *Cell Research*, 20(2):174–184, 2010. ISSN 10010602. doi: 10.1038/cr.2010.4. URL http://dx.doi.org/10.1038/cr.2010.4.

[223] Chunxia Wang, Tingting Xia, Ying Du, Qingshu Meng, Houkai Li, Bin Liu, Shanghai Chen, and Feifan Guo. Effects of ATF4 on PGC1α expression in brown adipose tissue and metabolic responses to cold stress. *Metabolism: Clinical and Experimental*, 62(2):282–289, 2013. ISSN 00260495. doi: 10.1016/j.metabol.2012.07.017. URL http://dx.doi.org/10.1016/j.metabol.2012.07.017.

[224] Souvik Dey, Thomas D. Baird, Donghui Zhou, Lakshmi Reddy Palam, Dan F. Spandau, and Ronald C. Wek. Both transcriptional regulation and translational control of ATF4 are central to the integrated stress response. *Journal of Biological Chemistry*, 285(43):33165–33174, 2010. ISSN 00219258. doi: 10.1074/jbc.M110.167213.

[225] D. Thomas Rutkowski, Stacey M. Arnold, Corey N. Miller, Jun Wu, Jack Li, Kathryn M. Gunnison, Kazutoshi Mori, Amir A.Sadighi Akha, David Raden, and Randal J. Kaufman. Adaptation to ER stress is mediated by differential stabilities of pro-survival and pro-apoptotic mRNAs and proteins. *PLoS Biology*, 4(11):2024–2041, 2006. ISSN 15457885. doi: 10.1371/journal.pbio.0040374.

[226] Priya Crosby, Ryan Hamnett, Marrit Putker, Nathaniel P. Hoyle, Martin Reed, Carolyn J. Karam, Elizabeth S. Maywood, Alessandra Stangherlin, Johanna E. Chesham, Edward A. Hayter, Lyn Rosenbrier-Ribeiro, Peter Newham, Hans Clevers, David A. Bechtold, and John S. O'Neill. Insulin/IGF-1 Drives PERIOD Synthesis to Entrain Circadian Rhythms with Feeding Time. *Cell*, 177(4):896–909.e20, may 2019. ISSN 0092-8674. doi: 10.1016/J.CELL.2019.02.017. URL https://www.sciencedirect.com/science/article/pii/S0092867419301667?via{%}3Dihub.

[227] Ben J. Greenwell, Alexandra J. Trott, Joshua R. Beytebiere, Shanny Pao, Alexander Bosley, Erin Beach, Patrick Finegan, Christopher Hernandez, and Jerome S. Menet. Rhythmic Food Intake Drives Rhythmic Gene Expression More Potently than the Hepatic Circadian Clock in Mice. *Cell Reports*, 27(3):649–657.e5, apr 2019. ISSN 22111247. doi: 10.1016/j.celrep.2019.03.064. URL https://linkinghub.elsevier.com/retrieve/pii/S2211124719303948.

[228] K. A. Stokkan, S. Yamazaki, H. Tei, Y. Sakaki, and M. Menaker. Entrainment of the circadian clock in the liver by feeding. *Science*, 291(5503):490–493, 2001. ISSN 00368075. doi: 10.1126/science.291.5503.490.

[229] Christopher Vollmers, Shubhroz Gill, Luciano DiTacchio, Sandhya R. Pulivarthy, Hiep D. Le, and Satchidananda Panda. Time of feeding and the intrinsic circadian clock drive rhythms in hepatic gene expression. *Proceedings of the National Academy of Sciences*, 106(50):21453–21458, 2009. ISSN 0027-8424. doi: 10.1073/pnas.0909591106.

[230] G T van der Horst, M Muijtjens, K Kobayashi, R Takano, S Kanno, M Takao, J de Wit, A Verkerk, a P Eker, D van Leenen, R Buijs, D Bootsma, J H Hoeijmakers, and A Yasui. Mammalian Cry1 and Cry2 are essential for maintenance of circadian rhythms. *Nature*, 398(6728):627–30, 1999. ISSN 0028-0836. doi: 10.1038/19323. URL http://www.ncbi.nlm.nih.gov/pubmed/10217146.

[231] Andrei Seluanov, Amita Vaidya, and Vera Gorbunova. Establishing Primary Adult Fibroblast Cultures From Rodents. *Journal of Visualized Experiments*, (44):e2033–e2033, oct 2010. ISSN 1940-087X. doi: 10.3791/2033. URL http://www.jove.com/index/Details.stp?ID=2033.

[232] Deanna L. Plubell, Phillip A. Wilmarth, Yuqi Zhao, Alexandra M. Fenton, Jessica Minnier, Ashok P. Reddy, John Klimek, Xia Yang, Larry L. David, and Nathalie Pamir. Extended Multiplexing of Tandem Mass Tags (TMT) Labeling Reveals Age and High Fat Diet Specific Proteome Changes in Mouse Epididymal Adipose Tissue. *Molecular & Cellular Proteomics*, 16(5):873–890, 2017. ISSN 1535-9476. doi: 10.1074/mcp.M116.065524. URL http://www.mcponline.org/lookup/doi/10.1074/mcp.M116.065524.

[233] Paul F. Thaben and Pål O. Westermark. Detecting rhythms in time series with rain. *Journal of Biological Rhythms*, 29(6):391–400, dec 2014. ISSN 15524531. doi: 10.1177/0748730414553029. URL http://journals.sagepub.com/doi/10.1177/0748730414553029.

[234] Gang Wu, Ron C. Anafi, Michael E. Hughes, Karl Kornacker, and John B. Hogenesch. MetaCycle: an integrated R package to evaluate periodicity in large scale data. *Bioinformatics*, 32(21):3351–3353, nov 2016. ISSN 1367-4803. doi: 10.1093/bioinformatics/btw405. URL https://academic.oup.com/bioinformatics/article-lookup/doi/10.1093/bioinformatics/btw405.

[235] Emerson Giovanelli, Eleonora Muro, Gary Sitbon, Mohamed Hanafi, Thomas Pons, Benoît Dubertret, and Nicolas Lequeux. Highly enhanced affinity of multidentate versus bidentate zwitterionic ligands for long-term quantum dot bioimaging. *Langmuir*, 28(43):15177–15184, 2012. ISSN 07437463. doi: 10.1021/la302896x.

[236] Emmanuel Derivery, Eline Bartolami, Stefan Matile, and Marcos Gonzalez-Gaitan. Efficient Delivery of Quantum Dots into the Cytosol of Cells Using Cell-Penetrating Poly(disulfide)s. *Journal of the American Chemical Society*, 139(30):10172–10175, 2017. ISSN 15205126. doi: 10.1021/jacs.7b02952.

[237] Daniela C Dieterich, A James Link, Johannes Graumann, David A Tirrell, and Erin M Schuman. Selective identification of newly synthesized proteins in mammalian cells using bioorthogonal noncanonical amino acid tagging (BONCAT). *Proceedings of the National Academy of Sciences of the United States of America*, 103(25):9482–7, jun 2006. ISSN 0027-8424. doi: 10.1073/pnas.0601637103. URL http://www.ncbi.nlm.nih.gov/pubmed/16769897http://www.pubmedcentral.nih.gov/articlerender.fcgi?artid=PMC1480433.

[238] Daniela C Dieterich, Jennifer J Lee, A James Link, Johannes Graumann, David A Tirrell, and Erin M Schuman. Labeling, detection and identification of newly synthesized proteomes with bioorthogonal non-canonical amino-acid tagging. *Nature Protocols*, 2(3):532–540, mar 2007. ISSN 1754-2189. doi: 10.1038/nprot.2007.52. URL http://www.nature.com/articles/nprot.2007.52.

[239] Birte Plitzko, Elizabeth N Kaweesa, and Sandra Loesgen. The natural product mensacarcin induces mitochondrial toxicity and apoptosis in melanoma cells. *The Journal of biological chemistry*, 292(51):21102–21116, dec 2017. ISSN 1083-351X. doi: 10.1074/jbc.M116.774836. URL http://www.ncbi.nlm.nih.gov/pubmed/29074620http://www.pubmedcentral.nih.gov/articlerender.fcgi?artid=PMC5743083.

[240] Birte Plitzko and Sandra Loesgen. Measurement of Oxygen Consumption Rate (OCR) and Extracellular Acidification Rate (ECAR) in Culture Cells for Assessment of the Energy Metabolism. *BIO-PROTOCOL*, 8(10), 2018. ISSN 2331-8325. doi: 10.21769/BioProtoc.2850. URL https://bio-protocol.org/e2850.

[241] Tsuyoshi Hirota, Jae Wook Lee, Warren G. Lewis, Eric E. Zhang, Ghislain Breton, Xianzhong Liu, Michael Garcia, Eric C. Peters, Jean-Pierre Etchegaray, David Traver, Peter G. Schultz, and Steve A. Kay. High-Throughput Chemical Screen Identifies a Novel Potent Modulator of Cellular Circadian Rhythms and Reveals CKIα as a Clock Regulatory Kinase. *PLoS Biology*, 8(12):e1000559, dec 2010. ISSN 1545-7885. doi: 10.1371/journal.pbio.1000559. URL http://dx.plos.org/10.1371/journal.pbio.1000559.

[242] D. S. Loose, E. P. Stover, and D. Feldman. Ketoconazole binds to glucocorticoid receptors and exhibits glucocorticoid antagonist activity in cultured cells. *Journal of Clinical Investigation*, 72(1):404–408, 1983. ISSN 00219738.

[243] A. Balsalobre, S. A. Brown, L. Marcacci, F. Tronche, C. Kellendonk, H. M. Reichardt, G. Schutz, and U. Schibler. Resetting of circadian time in peripheral tissues by glucocorticoid signaling. *Science*, 289(5488):2344–2347, 2000. ISSN 00368075. doi: 10.1126/science.289.5488.2344.

[244] Katja A. Lamia, Stephanie J. Papp, Ruth T. Yu, Grant D. Barish, N. Henriette Uhlenhaut, Johan W. Jonker, Michael Downes, and Ronald M. Evans. Cryptochromes mediate rhythmic repression of the glucocorticoid receptor. *Nature*, 480(7378):552–556, 2011. ISSN 0028-0836. doi: 10.1038/nature10700. URL http://www.nature.com/doifinder/10.1038/nature10700.

[245] Zheng Chen and Steven L. McKnight. A conserved DNA damage response pathway responsible for coupling the cell division cycle to the circadian and metabolic cycles. *Cell Cycle*, 6(23):2906–2912, 2007. ISSN 15514005. doi: 10.4161/cc.6.23.5041.

[246] G Mark Freeman, Masato Nakajima, Hiroki R Ueda, and Erik D Herzog. Picrotoxin dramatically speeds the mammalian circadian clock independent of Cys-loop receptors. *Journal of neurophysiology*, 110(1):103–8, jul 2013. ISSN 1522-1598.

doi: 10.1152/jn.00220.2013. URL http://www.ncbi.nlm.nih.gov/pubmed/23576702http://www.pubmedcentral.nih.gov/articlerender.fcgi?artid=PMC3727043.

[247] A. P. Patton, J. E. Chesham, and M. H. Hastings. Combined Pharmacological and Genetic Manipulations Unlock Unprecedented Temporal Elasticity and Reveal Phase-Specific Modulation of the Molecular Circadian Clock of the Mouse Suprachiasmatic Nucleus. *Journal of Neuroscience*, 36(36):9326–9341, 2016. ISSN 0270-6474. doi: 10.1523/JNEUROSCI.0958-16.2016. URL http://www.jneurosci.org/cgi/doi/10.1523/JNEUROSCI.0958-16.2016.

[248] Aurelio Balsalobre, Francesca Damiola, and Ueli Schibler. A serum shock induces circadian gene expression in mammalian tissue culture cells. *Cell*, 93(6):929–937, 1998. ISSN 00928674. doi: 10.1016/S0092-8674(00)81199-X.

[249] D. B. Forger. Signal processing in cellular clocks. *Proceedings of the National Academy of Sciences*, 108(11):4281–4285, 2011. ISSN 0027-8424. doi: 10.1073/pnas.1004720108. URL http://www.pnas.org/cgi/doi/10.1073/pnas.1004720108.

[250] T. Hirota, J. W. Lee, P. C. St. John, M. Sawa, K. Iwaisako, T. Noguchi, P. Y. Pongsawakul, T. Sonntag, D. K. Welsh, D. A. Brenner, F. J. Doyle, P. G. Schultz, and S. A. Kay. Identification of Small Molecule Activators of Cryptochrome. *Science*, 337(6098):1094–1097, 2012. ISSN 0036-8075. doi: 10.1126/science.1223710. URL http://www.sciencemag.org/cgi/doi/10.1126/science.1223710.

[251] Tsuyoshi Oshima, Iori Yamanaka, Anupriya Kumar, Junichiro Yamaguchi, Taeko Nishiwaki-Ohkawa, Kei Muto, Rika Kawamura, Tsuyoshi Hirota, Kazuhiro Yagita, Stephan Irle, Steve A. Kay, Takashi Yoshimura, and Kenichiro Itami. C-H activation generates period-shortening molecules that target cryptochrome in the mammalian circadian clock. *Angewandte Chemie - International Edition*, 54(24):7193–7197, 2015. ISSN 15213773. doi: 10.1002/anie.201502942.

[252] Rajesh Narasimamurthy, Sabrina R Hunt, Yining Lu, Jean-Michel Fustin, Hitoshi Okamura, Carrie L Partch, Daniel B Forger, Jae Kyoung Kim, and David M Virshup. CK1δ/ε protein kinase primes the PER2 circadian phosphoswitch. *Proceedings of the National Academy of Sciences of the United States of America*, 115(23):5986–5991, jun 2018. ISSN 1091-6490. doi: 10.1073/pnas.1721076115. URL http://www.ncbi.nlm.nih.gov/pubmed/29784789.

[253] Min Zhou, Jae Kyoung Kim, Gracie Wee Ling Eng, Daniel B. Forger, and David M. Virshup. A Period2 Phosphoswitch Regulates and Temperature Compensates Circadian Period. *Molecular Cell*, 60(1):77–88, 2015. ISSN 10972765. doi: 10.1016/j.molcel.2015.08.022.

[254] B. Lomenick, R. Hao, N. Jonai, R. M. Chin, M. Aghajan, S. Warburton, J. Wang, R. P. Wu, F. Gomez, J. A. Loo, J. A. Wohlschlegel, T. M. Vondriska, J. Pelletier, H. R. Herschman, J. Clardy, C. F. Clarke, and J. Huang. Target identification using drug affinity responsive target stability (DARTS). *Proceedings of the National Academy of Sciences*, 106(51):21984–21989, 2009. ISSN 0027-8424. doi: 10.1073/pnas.0910040106.

[255] Lindsay B Tulloch, Stefanie K Menzies, Coron P Ross, Matthew D Roberts, Gordon J Florence, and Terry K Smith. Critical Review Direct and Indirect Approaches to Identify Drug Modes of Action. *International Union of Biochemistry and Molecular Biology*, 70(1):9–22, 2017. doi: 10.1002/iub.1697.

[256] Daniel Mauvoisin, Loic Dayon, Frederic Gachon, and Martin Kussmann. Proteomics and circadian rhythms: It's all about signaling! *Proteomics*, 15(2-3):310–317, 2015. ISSN 16159861. doi: 10.1002/pmic.201400187.

[257] Maria S. Robles and Matthias Mann. Proteomic Approaches in Circadian Biology. In *Handbook of experimental pharmacology*, volume 217, pages 29–44. 2013. ISBN 978-3-642-25949-4. doi: 10.1007/978-3-642-25950-0. URL http://www.ncbi.nlm.nih.gov/pubmed/23604474.

[258] Cheng-Kang Chiang, Bo Xu, Neel Mehta, Janice Mayne, Warren Y. L. Sun, Kai Cheng, Zhibin Ning, Jing Dong, Hanfa Zou, Hai-Ying Mary Cheng, and Daniel Figeys. Phosphoproteome Profiling Reveals Circadian Clock Regulation of Posttranslational Modifications in the Murine Hippocampus. *Frontiers in Neurology*, 8:110, mar 2017. ISSN 1664-2295. doi: 10.3389/fneur.2017.00110. URL http://journal.frontiersin.org/article/10.3389/fneur.2017.00110/full.

[259] Mani Kant Choudhary, Yuko Nomura, Lei Wang, Hirofumi Nakagami, and David E Somers. Quantitative Circadian Phosphoproteomic Analysis of Arabidopsis Reveals Extensive Clock Control of Key Components in Physiological, Metabolic, and Signaling Pathways. *Molecular & cellular proteomics : MCP*, 14(8):2243–60, aug 2015. ISSN 1535-9484. doi: 10.1074/mcp.M114.047183. URL http://www.ncbi.nlm.nih.gov/pubmed/26091701http://www.pubmedcentral.nih.gov/articlerender.fcgi?artid=PMC4528250.

[260] Anna H. Chen and Pamela A. Silver. Designing biological compartmentalization. *Trends in Cell Biology*, 22(12):662–670, 2012. ISSN 09628924. doi: 10.1016/j.tcb.2012.07.002.

[261] H. J. Choi, C. J. Lee, A. Schroeder, Y. S. Kim, S. H. Jung, J. S. Kim, D. Y. Kim, E. J. Son, H. C. Han, S. K. Hong, C. S. Colwell, and Y. I. Kim. Excitatory Actions of GABA in the Suprachiasmatic Nucleus. *Journal of Neuroscience*, 28(21):5450–5459, 2008. ISSN 0270-6474. doi: 10.1523/JNEUROSCI.5750-07.2008.

[262] Nathan J. Klett and Charles N. Allen. Intracellular Chloride Regulation in AVP+ and VIP+ Neurons of the Suprachiasmatic Nucleus. *Scientific Reports*, 7(1), 2017. ISSN 20452322. doi: 10.1038/s41598-017-09778-x.

[263] Kerstin Piechotta, Jianming Lu, and Eric Delpire. Cation chloride cotransporters interact with the stress-related kinases Ste20-related proline-alanine-rich kinase (SPAK) and oxidative stress response 1 (OSR1). *Journal of Biological Chemistry*, 277(52):50812–50819, 2002. ISSN 00219258. doi: 10.1074/jbc.M208108200.

[264] Kenneth B E Gagnon, Roger England, and Eric Delpire. Characterization of SPAK and OSR1, regulatory kinases of the Na-K-2Cl cotransporter. *Molecular and cellular biology*, 26(2):689–98, 2006. ISSN 0270-7306. doi: 10.1128/MCB.26.2.689-698.2006.

[265] Anthony N Anselmo, Svetlana Earnest, Wei Chen, Yu-chi Juang, Sung Chan Kim, Yingming Zhao, and Melanie H Cobb. WNK1 and OSR1 regulate the Na+, K+, 2CL- cotransporter in HeLa cells. *Proceedings of the National Academy of Sciences*, 103(29):10883–10888, 2006.

[266] John Danziger and Mark L. Zeidel. Osmotic homeostasis. *Clinical Journal of the American Society of Nephrology*, 10(5):852–62, 2015. ISSN 1555905X. doi: 10.2215/CJN.10741013.

[267] Jonathan O. Lipton, Elizabeth D. Yuan, Lara M. Boyle, Darius Ebrahimi-Fakhari, Erica Kwiatkowski, Ashwin Nathan, Thomas Güttler, Fred Davis, John M. Asara, and Mustafa Sahin. The Circadian Protein BMAL1 Regulates Translation in Response to S6K1-Mediated Phosphorylation. *Cell*, 161(5):1138–1151, 2015. ISSN 00928674. doi: 10.1016/j.cell.2015.04.002.

[268] Christopher Jang, Nicholas F Lahens, John B Hogenesch, and Amita Sehgal. Ribosome profiling reveals an important role for translational control in circadian gene expression. *Genome Research*, pages 1836–1847, 2015. doi: 10.1101/gr.191296.115.4.

[269] Celine Jouffe, Gaspard Cretenet, Laura Symul, Eva Martin, Florian Atger, Felix Naef, and Fr??d??ric Gachon. The Circadian Clock Coordinates Ribosome Biogenesis. *PLoS Biology*, 11(1), 2013. ISSN 15449173. doi: 10.1371/journal.pbio.1001455.

[270] Samarpita Sengupta, Andres Lorente-Rodriguez, Svetlana Earnest, Steve Stippec, Xiaofeng Guo, David C. Trudgian, Hamid Mirzaei, and Melanie H. Cobb. Regulation of OSR1 and the sodium, potassium, two chloride cotransporter by convergent signals. *Proceedings of the National Academy of Sciences of the United States of America*, 110 (47):18826–18831, 2013. ISSN 00278424. doi: 10.1073/pnas.1318676110.

[271] Won Jun Oh and Estela Jacinto. mTOR complex 2 signaling and functions. *Cell Cycle*, 10(14):2305–2316, 2011. ISSN 15514005. doi: 10.4161/cc.10.14.16586.

[272] A. Colbeau, J. Nachbaur, and P. M. Vignais. Enzymac characterization and lipid composition of rat liver subcellular membranes. *Biochimica et biophysica acta*, 249(2):462–92, 1971. ISSN 00052736. doi: 10.1016/0005-2736(71)90123-4.

[273] Gary Fiskum. Intracellular levels and distribution of Ca2+ in digitonin-permeabilized cells. *Cell Calcium*, 6(1):25–37, 1985. ISSN 01434160. doi: 10.1016/0143-4160(85)90032-6.

[274] Irene Schulz. Permeabilizing cells: Some methods and applications for the study of intracellular processes. *Methods in Enzymology*, 192(C):280–300, 1990. ISSN 15577988. doi: 10.1016/0076-6879(90)92077-Q.

[275] Paul H. Weigel, Darryl A. Ray, and Janet A. Oka. Quantitation of intracellular membrane-bound enzymes and receptors in digitonin-permeabilized cells. *Analytical Biochemistry*, 1983. ISSN 10960309. doi: 10.1016/0003-2697(83)90106-9.

[276] Math J.H. Geelen. The use of digitonin-permeabilized mammalian cells for measuring enzyme activities in the course of studies on lipid metabolism. *Analytical Biochemistry*, 347(1):1–9, 2005. ISSN 00032697. doi: 10.1016/j.ab.2005.03.032.

[277] M Delarue, G P Brittingham, S Pfeffer, I V Surovtsev, S Pinglay, K J Kennedy, M Schaffer, J I Gutierrez, D Sang, G Poterewicz, J K Chung, J M Plitzko, J T Groves, C Jacobs-Wagner, B D Engel, and L J Holt. mTORC1 Controls Phase Separation and the Biophysical Properties of the Cytoplasm by Tuning Crowding. *Cell*, 0(174):1–12, jun 2018. ISSN 1097-4172. doi: 10.1016/j.cell.2018.05.042. URL http://www.ncbi.nlm.nih.gov/pubmed/29937223.

[278] JC Freedman. *Cell Physiology Source Book*. Academic Press, 4th edition, 2012. ISBN 9780123877383. doi: https://doi.org/10.1016/B978-0-12-387738-3.00001-9.

[279] Bryan T. MacDonald, Keiko Tamai, and Xi He. Wnt/β-Catenin Signaling: Components, Mechanisms, and Diseases. *Developmental Cell*, 17(1):9–26, 2009. ISSN 15345807. doi: 10.1016/j.devcel.2009.06.016. URL http://dx.doi.org/10.1016/j.devcel.2009.06.016.

[280] Else K. Hoffmann, Ian H. Lambert, and Stine F. Pedersen. Physiology of Cell Volume Regulation in Vertebrates. *Physiological Reviews*, 89(1):193–277, 2009. ISSN 0031-9333. doi: 10.1152/physrev.00037.2007.

[281] Kazuhiko Kume, Mark J. Zylka, Sathyanarayanan Sriram, Lauren P. Shearman, David R. Weaver, Xiaowei Jin, Elizabeth S. Maywood, Michael H. Hastings, and Steven M. Reppert. mCRY1 and mCRY2 are essential components of the negative limb of the circadian clock feedback loop. *Cell*, 98(2):193–205, 1999. ISSN 00928674. doi: 10.1016/S0092-8674(00)81014-4.

[282] Trey K Sato, Rikuhiro G Yamada, Hideki Ukai, Julie E Baggs, Loren J Miraglia, Tetsuya J Kobayashi, David K Welsh, Steve A Kay, Hiroki R Ueda, and John B Hogenesch. Feedback repression is required for mammalian circadian clock function. *Nature Genetics*, 38(3):312–319, 2006. ISSN 1061-4036. doi: 10.1038/ng1745. URL http://www.nature.com/doifinder/10.1038/ng1745.

[283] Rui Ye, Cristopher P Selby, Yi-Ying Chiou, Irem Ozkan-Dagliyan, Shobhan Gaddameedhi, and Aziz Sancar. Dual modes of CLOCK:BMAL1 inhibition mediated by Cryptochrome and Period proteins in the mammalian circadian clock. *Genes & development*, 28(18):1989–98, sep 2014. ISSN 1549-5477. doi: 10.1101/gad.249417.114. URL http://www.ncbi.nlm.nih.gov/pubmed/25228643http://www.pubmedcentral.nih.gov/articlerender.fcgi?artid=PMC4173159.

[284] Andrew C Liu, David K Welsh, Caroline H Ko, Hien G Tran, Eric E Zhang, Aaron A Priest, Ethan D Buhr, Oded Singer, Kirsten Meeker, Inder M Verma, Francis J Doyle, Joseph S Takahashi, and Steve A Kay. Intercellular coupling confers robustness against mutations in the SCN circadian clock network. *Cell*, 129(3):605–16, may 2007. ISSN 0092-8674. doi: 10.1016/j.cell.2007.02.047. URL http://www.ncbi.nlm.nih.gov/pubmed/17482552http://www.pubmedcentral.nih.gov/articlerender.fcgi?artid=PMC3749832.

[285] Rajat Gupta, Prasad Kasturi, Andreas Bracher, Christian Loew, Min Zheng, Adriana Villella, Dan Garza, F Ulrich Hartl, and Swasti Raychaudhuri. Firefly luciferase mutants as sensors of proteome stress. *Nature Methods*, 8(10):879–884, 2011. ISSN 1548-7091. doi: 10.1038/nmeth.1697. URL http://www.nature.com/doifinder/10.1038/nmeth.1697.

[286] E. S. Maywood, J. E. Chesham, J. A. O'Brien, and M. H. Hastings. A diversity of paracrine signals sustains molecular circadian cycling in suprachiasmatic nucleus circuits. *Proceedings of the National Academy of Sciences*, 108(34):14306–14311, aug 2011. ISSN 0027-8424. doi: 10.1073/pnas.1101767108. URL http://www.pnas.org/cgi/doi/10.1073/pnas.1101767108.

[287] Daisuke Ono, Sato Honma, and Ken-ichi Honma. Cryptochromes are critical for the development of coherent circadian rhythms in the mouse suprachiasmatic nucleus. *Nature Communications*, 4:1666, 2013. ISSN 2041-1723. doi: 10.1038/ncomms2670. URL http://www.nature.com/doifinder/10.1038/ncomms2670.

[288] Daisuke Ono, Sato Honma, and Ken Ichi Honma. Postnatal constant light compensates Cryptochrome1 and 2 double deficiency for disruption of circadian behavioral rhythms in mice under constant dark. *PLoS ONE*, 8(11), 2013. ISSN 19326203. doi: 10.1371/journal.pone.0080615.

[289] Jay C. Dunlap and Jennifer J. Loros. Just-So Stories and Origin Myths: Phosphorylation and Structural Disorder in Circadian Clock Proteins. *Molecular Cell*, (2017):1–4, 2017. ISSN 10972765. doi: 10.1016/j.molcel.2017.11.028. URL http://linkinghub.elsevier.com/retrieve/pii/S1097276517308870.

[290] Jack Hanson, Kuldip Paliwal, and Yaoqi Zhou. Accurate Single-Sequence Prediction of Protein Intrinsic Disorder by an Ensemble of Deep Recurrent and Convolutional Architectures. *Journal of Chemical Information and Modeling*, 58(11):2369–2376, nov 2018. ISSN 15205142. doi: 10.1021/acs.jcim.8b00636. URL http://pubs.acs.org/doi/10.1021/acs.jcim.8b00636.

[291] Bálint Mészáros, Gábor Erdős, and Zsuzsanna Dosztányi. IUPred2A: context-dependent prediction of protein disorder as a function of redox state and protein binding. *Nucleic Acids Research*, 46(W1):W329–W337, jul 2018. ISSN 0305-1048. doi: 10.1093/nar/gky384. URL https://academic.oup.com/nar/article/46/W1/W329/5026265.

[292] Salman F Banani, Hyun O Lee, Anthony A Hyman, and Michael K Rosen. Biomolecular condensates: organizers of cellular biochemistry. *Nature Reviews Molecular Cell Biology*, 18(5):285–298, 2017. ISSN 1471-0072. doi: 10.1038/nrm.2017.7. URL http://dx.doi.org/10.1038/nrm.2017.7.

[293] Domenico Ribatti. A revisited concept: Contact inhibition of growth. From cell biology to malignancy. *Experimental Cell Research*, 359(1):17–19, 2017. ISSN 10902422. doi: 10.1016/j.yexcr.2017.06.012. URL http://dx.doi.org/10.1016/j.yexcr.2017.06.012.

[294] Tian Zhang, Clara Wolfe, Andrew Pierle, Kevin A. Welle, Jennifer R. Hryhorenko, and Sina Ghaemmaghami. Proteome-wide modulation of degradation dynamics in response to growth arrest. *Proceedings of the National Academy of Sciences*, 114(48):10329–10338, 2017. ISSN 0027-8424. doi: 10.1073/pnas.1710238114.

[295] John S O'Neill and Michael H Hastings. Increased coherence of circadian rhythms in mature fibroblast cultures. *Journal of biological rhythms*, 23(6):483–8, 2008. ISSN 0748-7304. doi: 10.1177/0748730408326682. URL http://www.pubmedcentral.nih.gov/articlerender.fcgi?artid=2735814{&}tool=pmcentrez{&}rendertype=abstract.

[296] Anne Laure Huber, Stephanie J. Papp, Alanna B. Chan, Emma Henriksson, Sabine D. Jordan, Anna Kriebs, Madelena Nguyen, Martina Wallace, Zhizhong Li, Christian M. Metallo, and Katja A. Lamia. CRY2 and FBXL3 Cooperatively Degrade c-MYC. *Molecular Cell*, 64(4):774–789, 2016. ISSN 10974164. doi: 10.1016/j.molcel.2016.10.012. URL http://dx.doi.org/10.1016/j.molcel.2016.10.012.

[297] U Klueh, Z Liu, B Cho, T Ouyang, B Feldman, TP Henning, M Kaur, and D Kreutzer. Continuous glucose monitoring in normal mice and mice with prediabetes and diabetes. *Diabetes Technology & Therapeutics*, 8(3):402–412, 2006.

[298] Lisa M. Lindqvist, Kristofferson Tandoc, Ivan Topisirovic, and Luc Furic. Cross-talk between protein synthesis, energy metabolism and autophagy in cancer. *Current Opinion in Genetics and Development*, 48:104–111, 2018. ISSN 18790380. doi: 10.1016/j.gde.2017.11.003. URL http://dx.doi.org/10.1016/j.gde.2017.11.003.

[299] Kyoko Kubota, Yoshifumi Niinuma, Masayuki Kaneko, Yasunobu Okuma, Mami Sugai, Tomohiro Omura, Mai Uesugi, Takashi Uehara, Toru Hosoi, and Yasuyuki Nomura. Suppressive effects of 4-phenylbutyrate on the aggregation of Pael receptors and endoplasmic reticulum stress. *Journal of Neurochemistry*, 97(5):1259–1268, 2006. ISSN 00223042. doi: 10.1111/j.1471-4159.2006.03782.x.

[300] Adam Pickard, Joan Chang, Nissrin Alachkar, Ben Calverley, Richa Garva, Peter Arvan, Qing-Jun Meng, and Karl E. Kadler. Preservation of circadian rhythms by the protein folding chaperone, BiP. *The FASEB Journal*, page fj.201802366RR, mar 2019. ISSN 0892-6638. doi: 10.1096/fj.201802366RR. URL https://www.fasebj.org/doi/10.1096/fj.201802366RR.

[301] Amila Suraweera, Christian Münch, Ariane Hanssum, and Anne Bertolotti. Failure of amino acid homeostasis causes cell death following proteasome inhibition. *Molecular Cell*, 48(2):242–253, 2012. ISSN 10972765. doi: 10.1016/j.molcel.2012.08.003.

[302] Marcin J. Suskiewicz, Joel L. Sussman, Israel Silman, and Yosef Shaul. Context-dependent resistance to proteolysis of intrinsically disordered proteins. *Protein Science*, 20(8):1285–1297, aug 2011. ISSN 09618368. doi: 10.1002/pro.657. URL http://doi.wiley.com/10.1002/pro.657.

[303] Kiyomichi Imamura, Hikari Yoshitane, Kazuki Hattori, Mitsuo Yamaguchi, Kento Yoshida, Takenori Okubo, Isao Naguro, Hidenori Ichijo, and Yoshitaka Fukada. ASK family kinases mediate cellular stress and redox signaling to circadian clock. *Proceedings of the National Academy of Sciences of the United States of America*, 115(14):3646–3651, 2018. ISSN 10916490. doi: 10.1073/pnas.1719298115.

[304] Jennifer M. Hurley, Luis F. Larrondo, Jennifer J. Loros, and Jay C. Dunlap. Conserved RNA Helicase FRH Acts Nonenzymatically to Support the Intrinsically Disordered Neurospora Clock Protein FRQ. *Molecular Cell*, 52(6):832–843, dec 2013. ISSN 1097-2765. doi: 10.1016/J.MOLCEL.2013.11.005. URL https://www.sciencedirect.com/science/article/pii/S1097276513008307.

[305] Peter Tsvetkov, Nina Reuven, and Yosef Shaul. The nanny model for IDPs. *Nature Chemical Biology*, 5(11):778–781, nov 2009. ISSN 1552-4450. doi: 10.1038/nchembio.233. URL http://www.nature.com/articles/nchembio.233.

[306] Chelsea L. Gustafson, Nicole C. Parsley, Hande Asimgil, Hsiau-Wei Lee, Christopher Ahlbach, Alicia K. Michael, Haiyan Xu, Owen L. Williams, Tara L. Davis, Andrew C. Liu, and Carrie L. Partch. A Slow Conformational Switch in the BMAL1 Transactivation Domain Modulates Circadian Rhythms. *Molecular Cell*, pages 1–11, 2017. ISSN 10972765. doi: 10.1016/j.molcel.2017.04.011. URL http://linkinghub.elsevier.com/retrieve/pii/S1097276517302678.

[307] Amy S Farrell and Rosalie C Sears. MYC degradation. *Cold Spring Harbor perspectives in medicine*, 4(3):a014365, mar 2014. ISSN 2157-1422. doi: 10.1101/cshperspect.a014365. URL http://www.ncbi.nlm.nih.gov/pubmed/24591536http://www.pubmedcentral.nih.gov/articlerender.fcgi?artid=PMC3935390.

[308] Stephanie Papp Correia, Alanna B. Chan, Megan Vaughan, Norjin Zolboot, Valerie Perea, Anne-Laure Huber, Anna Kriebs, James J. Moresco, John R. Yates, and Katja A. Lamia. The circadian E3 ligase complex SCFFBXL3+CRY targets TLK2. *Scientific Reports*, 9(1):198, dec 2019. ISSN 2045-2322. doi: 10.1038/s41598-018-36618-3. URL http://www.nature.com/articles/s41598-018-36618-3.

[309] Anna Kriebs, Sabine D. Jordan, Erin Soto, Emma Henriksson, Colby R. Sandate, Megan E. Vaughan, Alanna B. Chan, Drew Duglan, Stephanie J. Papp, Anne-Laure Huber, Megan E. Afetian, Ruth T. Yu, Xuan Zhao, Michael Downes, Ronald M. Evans, and Katja A. Lamia. Circadian repressors CRY1 and CRY2 broadly interact with nuclear receptors and modulate transcriptional activity. *Proceedings of the National Academy of Sciences*, page 201704955, 2017. ISSN 0027-8424. doi: 10.1073/pnas.1704955114. URL http://www.pnas.org/lookup/doi/10.1073/pnas.1704955114.

[310] Katja A Lamia, Stephanie J Papp, Ruth T Yu, Grant D Barish, N Henriette Uhlenhaut, Johan W Jonker, Michael Downes, and Ronald M Evans. Cryptochromes mediate rhythmic repression of the glucocorticoid receptor. *Nature*, 480(7378):552–6, 2011. ISSN 1476-4687. doi: 10.1038/nature10700. URL http://www.ncbi.nlm.nih.gov/pubmed/25300886{%}5Cnhttp://www.pubmedcentral.nih.gov/articlerender.fcgi?artid=PMC4188370{%}5Cnhttp://www.ncbi.nlm.nih.gov/pubmed/22170608{%}5Cnhttp://www.pubmedcentral.nih.gov/articlerender.fcgi?artid=PMC3245818.

[311] Isabelle M. Bur, Anne M. Cohen-Solal, Danielle Carmignac, Pierre Yves Abecassis, Norbert Chauvet, Agnès O. Martin, Gijsbertus T.J. van der Horst, Iain C.A.F. Robinson, Patrick Maurel, Patrice Mollard, and Xavier Bonnefont. The circadian clock components CRY1 and CRY2 are necessary to sustain sex dimorphism in mouse liver metabolism. *Journal of Biological Chemistry*, 284(14):9066–73, 2009. ISSN 00219258. doi: 10.1074/jbc.M808360200.

[312] Shizue Masuki, Takeshi Todo, Yasushi Nakano, Hitoshi Okamura, and Hiroshi Nose. Reduced α-adrenoceptor responsiveness and enhanced baroreflex sensitivity in Cry-deficient mice lacking a biological clock. *Journal of Physiology*, 566:213–224, 2005. ISSN 00223751. doi: 10.1113/jphysiol.2005.086728.

[313] J L Barclay, A Shostak, A Leliavski, A H Tsang, O Johren, H Muller-Fielitz, D Landgraf, N Naujokat, G T J van der Horst, and H Oster. High-fat diet-induced hyperinsulinemia and tissue-specific insulin resistance in Cry-deficient mice. *AJP: Endocrinology and Metabolism*, 304(10):E1053–E1063, 2013. ISSN 0193-1849. doi: 10.1152/ajpendo.00512.2012. URL http://ajpendo.physiology.org/cgi/doi/10.1152/ajpendo.00512.2012{%}0Apapers2://publication/doi/10.1152/ajpendo.00512.2012.

[314] Nana N. Takasu, Takahiro J. Nakamura, Isao T. Tokuda, Takeshi Todo, Gene D. Block, and Wataru Nakamura. Recovery from Age-Related Infertility under Environmental Light-Dark Cycles Adjusted to the Intrinsic Circadian Period. *Cell Reports*, 12(9): 1407–1413, sep 2015. ISSN 2211-1247. doi: 10.1016/J.CELREP.2015.07.049. URL https://www.sciencedirect.com/science/article/pii/S221112471500827X.

[315] Robert A. Saxton and David M. Sabatini. mTOR Signaling in Growth, Metabolism, and Disease. *Cell*, 168(6):960–976, 2017. ISSN 10974172. doi: 10.1016/j.cell.2017.02.004. URL http://dx.doi.org/10.1016/j.cell.2017.02.004.

[316] Carson C. Thoreen, Seong A. Kang, Jae Won Chang, Qingsong Liu, Jianming Zhang, Yi Gao, Laurie J. Reichling, Taebo Sim, David M. Sabatini, and Nathaniel S. Gray. An ATP-competitive mammalian target of rapamycin inhibitor reveals rapamycin-resistant functions of mTORC1. *Journal of Biological Chemistry*, 284(12):8023–8032, 2009. ISSN 00219258. doi: 10.1074/jbc.M900301200.

[317] V Thulasiraman and R L Matts. Luciferase renaturation assays of chaperones and chaperone antagonists. *Methods in molecular biology (Clifton, N.J.)*, 102(6):129–141, 1998. ISSN 1064-3745. doi: 10.1385/0-89603-520-4:129.

[318] Robert J. Schumacher, Robin Hurst, William P. Sullivan, Nancy J. McMahon, David O. Toft, and Robert L. Matts. ATP-dependent chaperoning activity of reticulocyte lysate. *Journal of Biological Chemistry*, 269(13):9493–9499, 1994. ISSN 00219258.

[319] Vanitha Thulasiraman and Robert L. Matts. Effect of geldanamycin on the kinetics of chaperone-mediated renaturation of firefly luciferase in rabbit reticulocyte lysate. *Biochemistry*, 35(41):13443–13450, 1996. ISSN 00062960. doi: 10.1021/bi9615396.

[320] Phoebe D. Lu, Heather P. Harding, and David Ron. Translation reinitiation at alternative open reading frames regulates gene expression in an integrated stress response. *Journal of Cell Biology*, 167(1):27–33, 2004. ISSN 00219525. doi: 10.1083/jcb.200408003.

[321] Aaron Heifetz, Roy W. Keenan, and Alan D. Elbein. Mechanism of action of tunicamycin on the UDP-GlcNAc:dolichyl-phosphate GlcNAc-1-phosphate transferase. *Biochemistry*, 18(11):2186–2192, may 1979. ISSN 0006-2960. doi: 10.1021/bi00578a008. URL http://pubs.acs.org/doi/abs/10.1021/bi00578a008.

[322] Christine M Oslowski and Fumihiko Urano. Measuring ER stress and the unfolded protein response using mammalian tissue culture system. *Methods in enzymology*, 490:71–92, 2011. ISSN 1557-7988. doi: 10.1016/B978-0-12-385114-7.00004-0. URL http://www.ncbi.nlm.nih.gov/pubmed/21266244http://www.pubmedcentral.nih.gov/articlerender.fcgi?artid=PMC3701721.

[323] Sung Kook Chun, Jaebong Jang, Sooyoung Chung, Hwayoung Yun, Nam Jung Kim, Jong Wha Jung, Gi Hoon Son, Young Ger Suh, and Kyungjin Kim. Identification and validation of cryptochrome inhibitors that modulate the molecular circadian clock. *ACS Chemical Biology*, 9(3):703–710, 2014. ISSN 15548937. doi: 10.1021/cb400752k.

[324] Sung Kook Chun, Sooyoung Chung, Hee Dae Kim, Ju Hyung Lee, Jaebong Jang, Jeongah Kim, Doyeon Kim, Gi Hoon Son, Young J. Oh, Young Ger Suh, Cheol Soon Lee, and Kyungjin Kim. A synthetic cryptochrome inhibitor induces anti-proliferative effects and

increases chemosensitivity in human breast cancer cells. *Biochemical and Biophysical Research Communications*, 467(2):441–446, 2015. ISSN 10902104. doi: 10.1016/j.bbrc.2015.09.103. URL http://dx.doi.org/10.1016/j.bbrc.2015.09.103.

[325] Pavel Tsaytler, Heather P. Harding, David Ron, and Anne Bertolotti. Selective inhibition of a regulatory subunit of protein phosphatase 1 restores proteostasis. *Science*, 332(6025): 91–94, 2011. ISSN 00368075. doi: 10.1126/science.1201396.

[326] Indrajit Das, Agnieszka Krzyzosiak, Kim Schneider, Lawrence Wrabetz, Maurizio D'Antonio, Nicholas Barry, Anna Sigurdardottir, and Anne Bertolotti. Preventing proteostasis diseases by selective inhibition of a phosphatase regulatory subunit. *Science*, 348 (6231):239–242, 2015. ISSN 10959203. doi: 10.1126/science.aaa4484.

[327] Ana Crespillo-Casado, Joseph E. Chambers, Peter M. Fischer, Stefan J. Marciniak, and David Ron. PPP1R15A-mediated dephosphorylation of eIF2a is unaffected by sephin1 or guanabenz. *eLife*, 6:1–29, 2017. ISSN 2050084X. doi: 10.7554/eLife.26109.

[328] Robin van der Lee, Marija Buljan, Benjamin Lang, Robert J. Weatheritt, Gary W. Daughdrill, A. Keith Dunker, Monika Fuxreiter, Julian Gough, Joerg Gsponer, David T. Jones, Philip M. Kim, Richard W. Kriwacki, Christopher J. Oldfield, Rohit V. Pappu, Peter Tompa, Vladimir N. Uversky, Peter E. Wright, and M. Madan Babu. Classification of Intrinsically Disordered Regions and Proteins. *Chemical Reviews*, 114(13):6589–6631, jul 2014. ISSN 0009-2665. doi: 10.1021/cr400525m. URL http://pubs.acs.org/doi/10.1021/cr400525m.

[329] M Madan Babu, Robin van der Lee, Natalia Sanchez de Groot, and Jörg Gsponer. Intrinsically disordered proteins: regulation and disease. *Current Opinion in Structural Biology*, 21(3):432–440, jun 2011. ISSN 0959-440X. doi: 10.1016/J.SBI.2011.03.011. URL https://www.sciencedirect.com/science/article/pii/S0959440X11000637?via{%}3Dihub.

[330] Zachary A Levine, Luca Larini, Nichole E LaPointe, Stuart C Feinstein, and Joan-Emma Shea. Regulation and aggregation of intrinsically disordered peptides. *Proceedings of the National Academy of Sciences of the United States of America*, 112(9):2758–63, mar 2015. ISSN 1091-6490. doi: 10.1073/pnas.1418155112. URL http://www.ncbi.nlm.nih.gov/pubmed/25691742http://www.pubmedcentral.nih.gov/articlerender.fcgi?artid=PMC4352815.

[331] Eri Uemura, Tatsuya Niwa, Shintaro Minami, Kazuhiro Takemoto, Satoshi Fukuchi, Kodai Machida, Hiroaki Imataka, Takuya Ueda, Motonori Ota, and Hideki Taguchi. Large-scale aggregation analysis of eukaryotic proteins reveals an involvement of intrinsically disordered regions in protein folding. *Scientific Reports*, 8(1):678, dec 2018. ISSN 2045-2322. doi: 10.1038/s41598-017-18977-5. URL http://www.nature.com/articles/s41598-017-18977-5.

[332] R.John Ellis. Macromolecular crowding: obvious but underappreciated. *Trends in Biochemical Sciences*, 26(10):597–604, oct 2001. ISSN 0968-0004. doi: 10.1016/S0968-0004(01)01938-7. URL https://www.sciencedirect.com/science/article/pii/S0968000401019387?via{%}3Dihub.

[333] Matt E. Oates, Pedro Romero, Takashi Ishida, Mohamed Ghalwash, Marcin J. Mizianty, Bin Xue, Zsuzsanna Dosztányi, Vladimir N. Uversky, Zoran Obradovic, Lukasz Kurgan, A. Keith Dunker, and Julian Gough. D2P2: database of disordered protein predictions. *Nucleic Acids Research*, 41(D1):D508–D516, nov 2012. ISSN 0305-1048. doi: 10.1093/nar/gks1226. URL http://academic.oup.com/nar/article/41/D1/D508/1069637/D2P2-database-of-disordered-protein-predictions.

[334] Lilia M. Iakoucheva, Predrag Radivojac, Celeste J. Brown, Timothy R. O'Connor, Jason G. Sikes, Zoran Obradovic, and A. Keith Dunker. The importance of intrinsic disorder for protein phosphorylation. *Nucleic Acids Research*, 32(3):1039–49, 2004. ISSN 03051048. doi: 10.1093/nar/gkh253.

[335] Alaji Bah and Julie D. Forman-Kay. Modulation of intrinsically disordered protein function by post-translational modifications. *Journal of Biological Chemistry*, 291(13): 6696–705, 2016. ISSN 1083351X. doi: 10.1074/jbc.R115.695056.

[336] Jason Brayer and Rachid Baz. The potential of ixazomib, a second-generation proteasome inhibitor, in the treatment of multiple myeloma. *Therapeutic advances in hematology*, 8(7):209–220, jul 2017. ISSN 2040-6207. doi: 10.1177/2040620717710171. URL http://www.ncbi.nlm.nih.gov/pubmed/28694935http://www.pubmedcentral.nih.gov/articlerender.fcgi?artid=PMC5495505.

[337] Lenka Kubiczkova, Ludek Pour, Lenka Sedlarikova, Roman Hajek, and Sabina Sevcikova. Proteasome inhibitors - molecular basis and current perspectives in multiple myeloma. *Journal of Cellular and Molecular Medicine*, 18(6):947–961, 2014. ISSN 15824934. doi: 10.1111/jcmm.12279.

[338] Wei Liu, Juan Chen, Archito T. Tamayo, Changgeng Ruan, Li Li, Shouhao Zhou, Chan Shen, Ken H. Young, Jason Westin, Richard E. Davis, Shimin Hu, Leonard J. Medeiros, Richard J. Ford, Lan V. Pham, Wei Liu, Juan Chen, Archito T. Tamayo, Changgeng Ruan, Li Li, Shouhao Zhou, Chan Shen, Ken H. Young, Jason Westin, Richard E. Davis, Shimin Hu, Leonard J. Medeiros, Richard J. Ford, and Lan V. Pham. Preclinical efficacy and biological effects of the oral proteasome inhibitor ixazomib in diffuse large B-cell lymphoma. *Oncotarget*, 9(1):346–360, jan 2018. ISSN 1949-2553. doi: 10.18632/oncotarget.20378. URL http://www.oncotarget.com/fulltext/20378.

[339] Roman V Kondratov, Anna A Kondratova, Victoria Y Gorbacheva, Olena V Vykhovanets, and Marina P Antoch. Early aging and age-related pathologies in mice deficient in BMAL1, the core componentof the circadian clock. *Genes & development*, 20(14):1868–73, jul 2006. ISSN 0890-9369. doi: 10.1101/gad.1432206. URL http://www.ncbi.nlm.nih.gov/pubmed/16847346http://www.pubmedcentral.nih.gov/articlerender.fcgi?artid=PMC1522083.

[340] G. Yang, L. Chen, G. R. Grant, G. Paschos, W.-L. Song, E. S. Musiek, V. Lee, S. C. McLoughlin, T. Grosser, G. Cotsarelis, and G. A. FitzGerald. Timing of expression of the core clock gene Bmal1 influences its effects on aging and survival. *Science Translational Medicine*, 8(324):324ra16–324ra16, 2016. ISSN 1946-6234. doi: 10.1126/scitranslmed.aad3305. URL http://stm.sciencemag.org/cgi/doi/10.1126/scitranslmed.aad3305.

[341] Salil Saurav Pathak, Dong Liu, Tianbao Li, Nuria de Zavalia, Lei Zhu, Jin Li, Ramanujam Karthikeyan, Tommy Alain, Andrew C. Liu, Kai-Florian Storch, Randal J. Kaufman, Victor X. Jin, Shimon Amir, Nahum Sonenberg, and Ruifeng Cao. The eIF2α Kinase GCN2 Modulates Period and Rhythmicity of the Circadian Clock by Translational Control of Atf4. *Neuron*, 104:1–12, 2019. ISSN 08966273. doi: 10.1016/j.neuron.2019.08.007. URL https://doi.org/10.1016/j.neuron.2019.08.007.

[342] Nicola J. Smyllie, Violetta Pilorz, James Boyd, Qing-Jun Meng, Ben Saer, Johanna E. Chesham, Elizabeth S. Maywood, Toke P. Krogager, David G. Spiller, Raymond Boot-Handford, Michael R.H. White, Michael H. Hastings, and Andrew S.I. Loudon. Visualizing and Quantifying Intracellular Behavior and Abundance of the Core Circadian Clock Protein PERIOD2. 2016.

[343] Chelsea L. Gustafson, Nicole C. Parsley, Hande Asimgil, Hsiau-Wei Lee, Christopher Ahlbach, Alicia K. Michael, Haiyan Xu, Owen L. Williams, Tara L. Davis, Andrew C. Liu, and Carrie L. Partch. A Slow Conformational Switch in the BMAL1 Transactivation Domain Modulates Circadian Rhythms. *Molecular Cell*, pages 1–11, 2017. ISSN 10972765. doi: 10.1016/j.molcel.2017.04.011. URL http://linkinghub.elsevier.com/retrieve/pii/S1097276517302678.

[344] Haiyan Xu, Chelsea L. Gustafson, Patrick J. Sammons, Sanjoy K. Khan, Nicole C. Parsley, Chidambaram Ramanathan, Hsiau-Wei Lee, Andrew C. Liu, and Carrie L. Partch. Cryptochrome 1 regulates the circadian clock through dynamic interactions with the BMAL1 C terminus. *Nature Structural & Molecular Biology*, 22(6):476–484, 2015. ISSN 1545-9993. doi: 10.1038/nsmb.3018. URL http://www.nature.com/nsmb/journal/v22/n6/full/nsmb.3018.html.

[345] Hideo Iwasaki, Stanly B. Williams, Yohko Kitayama, Masahiro Ishiura, Susan S. Golden, and Takao Kondo. A KaiC-interacting sensory histidine kinase, SasA, necessary to sustain robust circadian oscillation in cyanobacteria. *Cell*, 101(2):223–233, 2000. ISSN 00928674. doi: 10.1016/S0092-8674(00)80832-6.

[346] N. Takai, M. Nakajima, T. Oyama, R. Kito, C. Sugita, M. Sugita, T. Kondo, and H. Iwasaki. A KaiC-associating SasA-RpaA two-component regulatory system as a major circadian timing mediator in cyanobacteria. *Proceedings of the National Academy of Sciences*, 103 (32):12109–12114, aug 2006. ISSN 0027-8424. doi: 10.1073/pnas.0602955103. URL http://www.pnas.org/cgi/doi/10.1073/pnas.0602955103.

[347] Yasuhito Taniguchi, Mitsunori Katayama, Rie Ito, Naoki Takai, Takao Kondo, and Tokitaka Oyama. labA: A novel gene required for negative feedback regulation of the cyanobacterial circadian clock protein KaiC. *Genes and Development*, 21(1):60–70, 2007. ISSN 08909369. doi: 10.1101/gad.1488107.

[348] O. Schmitz, M. Katayama, S. B. Williams, T. Kondo, and S. S. Golden. CikA, a bacteriophytochrome that resets the cyanobacterial circadian clock. *Science*, 289(5480):765–768, 2000. ISSN 00368075. doi: 10.1126/science.289.5480.765.

[349] Y. Taniguchi, N. Takai, M. Katayama, T. Kondo, and T. Oyama. Three major output pathways from the KaiABC-based oscillator cooperate to generate robust circadian kaiBC expression in cyanobacteria. *Proceedings of the National Academy of Sciences*, 107 (7):3263–3268, feb 2010. ISSN 0027-8424. doi: 10.1073/pnas.0909924107. URL http://www.pnas.org/cgi/doi/10.1073/pnas.0909924107.

[350] Erik S. Musiek and David M. Holtzman. Mechanisms linking circadian clocks, sleep, and neurodegeneration. *Science*, 354(6315), 2016. ISSN 0036-8075. doi: 10.1126/science.aah4968.

[351] Zandra E. Walton, Brian J. Altman, Rebekah C. Brooks, and Chi V. Dang. Circadian Clock's Cancer Connections. *Annual Review of Cancer Biology*, 2(1):133–153, 2018. ISSN 2472-3428. doi: 10.1146/annurev-cancerbio-030617-050216.

Appendix A

Appendix Tables and Figures

Table A.1 Proteomics data: Proteins rhythmic in both WT and CKO cells.

Uniprot ID	Gene name	WT pVal	CKO pVal	WT Relative Amplitude	CKO Relative Amplitude
Q9CYZ6	2810428I15Rik	0.03827552	0.036692444	0.231094538	0.184061457
Q8K449	Abca9	0.01783095	0.016589697	0.292209383	0.194747797
Q61102	Abcb7	0.01142425	0.011836272	0.272633212	0.299357135
A5D6P3	Abcc1	0.0258595	0.000276886	0.14520119	0.142331345
Q3U645	Abcd3	0.02836791	0.000133547	0.19886745	0.30797014
Q9Z1Q2	Abhd16a	0.00065554	0.006312679	0.157743149	0.218023605
Q7M759	Abhd17b	0.0049913	0.033206837	0.104889556	0.191078386
E9QMV2	Abracl	0.03786309	0.027758531	0.199639222	0.221840428
D3Z041	Acsl1	0.03473324	0.016475332	0.119429467	0.121360338
Q3UC67	Acsl5	0.03166854	0.000136517	0.22951726	0.199756061
Q8JZQ2	Afg3l2	0.01925344	0.011836272	0.185449802	0.19232578
O08715	Akap1	0.00570066	0.001955667	0.223806675	0.162286104
P45377	Akr1b8	0.00707723	0.014049397	0.113865643	0.153439304
Q9CTE8	Alg5	0.02361011	0.001027592	0.184276193	0.239197396
Q8VDI9	Alg9	0.03832596	0.003954018	0.317497554	0.272509255
Q8BH79	Ano10	0.0301981	0.000142758	0.239919491	0.252754141
Q6P9J9	Ano6	0.00189258	0.030368323	0.206247743	0.119169996
Q9CZ52	Antxr1	0.00753382	0.033215354	0.188732022	0.183344301
Q78IK4	Apool	0.01470966	0.002307443	0.174247354	0.195331128
A2AL85	Asph;ASPH	0.01774832	0.001363455	0.169996211	0.235398893
Q6PA06	Atl2	0.02318151	0.000904116	0.203750758	0.222931844

Continued on next page

Table A.1 – continued from previous page

Uniprot ID	Gene name	WT pVal	CKO pVal	WT Relative Amplitude	CKO Relative Amplitude
Q91YH5	Atl3	0.0455385	0.00212129	0.188759136	0.188921678
Q9EPE9	Atp13a1;mKIAA1825	0.00392479	0.003383938	0.178155456	0.214400081
O55143	Atp2a2	0.01398533	0.00130592	0.195413576	0.269399072
G5E829	Atp2b1	0.04214819	8.19E-05	0.108781275	0.14783681
P56135	Atp5j2	0.03797319	0.001398173	0.310115125	0.311066534
Q9CPQ8	Atp5l	0.03981225	0.000143518	0.223006903	0.249718939
Q8CJ69	Bmper	0.03291128	0.009557936	0.192771106	0.104503969
E9PZJ6	Casc4	0.00367158	0.009806438	0.219475673	0.339525313
Q8K1A6	Cc2d1a	0.00030754	0.005868324	0.127980678	0.110707539
D3Z7R9	Ccpg1	0.0099826	0.038077524	0.274966193	0.547351231
Q920X8	CD14;Cd14	0.00451192	2.17E-05	0.121380856	0.153807103
A0A0R4J090	Cd1d1;Cd1d2	0.03166854	0.002644792	0.185002579	0.229854938
Q9DCG2	Cd302	0.01613317	0.006269802	0.214558408	0.150413982
P60766	Cdc42	0.00028677	0.000194561	0.146053973	0.165246088
Q8BSI9	Cdh2	0.00530323	0.008756278	0.13755918	0.101626685
Q14AX8	Cemip	0.00909988	0.003892676	0.243592472	0.224228077
Q8BMK4	Ckap4	0.00255649	0.000513796	0.184189269	0.224611882
B1AWE0	Clta	0.00012894	0.042097534	0.109536263	0.142478736
O88587-2	Comt	0.00268266	0.009816873	0.123239269	0.100955733
Q8BGD5	Cpt1c	0.03166854	0.003541078	0.180109872	0.247982647
A8C1T7	Creld1	0.041956	0.035878562	0.167478663	0.224005253
A0A0G2JEK2	Crip1	0.0354387	0.022848494	0.325521982	0.158790444

Continued on next page

Table A.1 – continued from previous page

Uniprot ID	Gene name	WT pVal	CKO pVal	WT Relative Amplitude	CKO Relative Amplitude
Q9CQX2	Cyb5b	0.03036832	0.000128942	0.329136171	0.20398406
Q3UGB8	Derl1	0.03622183	0.030368323	0.195191889	0.207246485
Q61712	Dnajc1	0.02247904	0.002980432	0.189105353	0.252628022
Q8C7X2-2	Emc1	0.03416436	0.001297197	0.129301276	0.191425785
Q99KI3	Emc3	0.01941308	0.000655544	0.178882441	0.238250455
Q99K41	Emilin1	0.00123918	0.022966188	0.354379768	0.278845654
Q3TDP9	Emilin2	0.00366318	0.035754802	0.371862876	0.298775194
Q9D379	Ephx1	0.00184006	0.005851816	0.296346464	0.232107866
Q4FK22	Ergic1	0.02463624	0.019678126	0.260578793	0.338250757
Q3U7R1	Esyt1	0.00134193	0.002023083	0.134936812	0.163267266
Q3TZZ7	Esyt2	0.00699348	0.000942518	0.18256939	0.165750978
Q9D6U8	Fam162a	0.01251043	0.027836815	0.171055379	0.221043067
F8VPU2	Farp1	7.56E-05	2.85E-05	0.120722698	0.120961957
Q9DC36	Flot2	0.01880642	0.00700442	0.127885347	0.162222911
Q6P551	Fzd7	0.00012894	0.049392657	0.137926059	0.197417612
Q3U6L3	Glrx	0.02173786	0.000210635	0.104240547	0.112451414
G3X9L6	Gm10250;Atp5h	0.04261058	0.000944105	0.163637975	0.256711756
F7BGR7	Gm21992;Rbm4	0.00845342	0.0338516	0.101845659	0.174186404
P27601	Gna13	0.041956	0.00045555	0.12018219	0.118593032
Q9D8V0	Hm13	0.00190351	0.000436315	0.306511873	0.269153234
Q0VGQ1	Hsd17b12	0.01639096	0.000542238	0.240827286	0.266167464
E9PZ16	Hspg2	0.03532	0.02361011	0.16793524	0.136135804

Continued on next page

Table A.1 – continued from previous page

Uniprot ID	Gene name	WT pVal	CKO pVal	WT Relative Amplitude	CKO Relative Amplitude
Q9DCE9	Igtp;Ifggd1	0.04209753	0.003892676	0.222711271	0.185629108
P43406	Itgav	0.00042773	0.006993482	0.136455546	0.146353824
Q6PE70	Itgb5	0.04415854	0.000633693	0.194129233	0.206784878
P70227	Itpr3	0.04495807	0.00058999	0.179588859	0.188099768
Q8C1D8	Iws1	0.0416378	0.016464467	0.142142825	0.245443031
Q9CX60	Lbh	0.041956	0.000920029	0.156398704	0.206706837
B0V2Q7	Lclat1	0.03402657	0.024997518	0.249192166	0.325062696
Q9Z2I0	Letm1	0.0072875	0.000938932	0.184647657	0.202918709
Q8C3X8	Lmf2	0.00684893	0.003310315	0.200085814	0.239100658
Q91V01	Lpcat3	0.04033662	0.005851816	0.219336669	0.223084202
Q8CG19	Ltbp1	0.01819977	0.005241449	0.363115575	0.290459208
Q3TCS3	Lyn	0.03284821	0.016464219	0.191542158	0.201136261
Q8BW75	Maob	0.02391164	0.02246245	0.344397887	0.323548452
Q9WVS7	Map2k5	0.04495807	0.04936	0.271120757	0.219281714
Q8CIC9	Mgat1	0.04129501	0.003310315	0.167536897	0.205464538
Q8VEK8	Mgp	0.03427274	0.026023623	0.244889104	0.191604527
Q3U026	Mogs	0.00195567	0.000914748	0.151695536	0.263309272
Q3TNL9	mt-Nd1;ND1;Mtnd1	0.01475859	0.016919691	0.198830038	0.23834468
Q791T5-2	Mtch1	0.04490404	0.030660766	0.183910219	0.183901421
Q80WJ7	Mtdh	0.03294338	0.000180172	0.182267613	0.194325566
Q69ZN7	Myof	0.00243292	0.000374716	0.125449714	0.134776501
D3YU17	Ncln	0.00493313	0.005571215	0.190404362	0.282748394

Continued on next page

Table A.1 – continued from previous page

Uniprot ID	Gene name	WT pVal	CKO pVal	WT Relative Amplitude	CKO Relative Amplitude
I1E4X7	Nudt3	0.00264479	0.012805751	0.100891467	0.499287321
Q78XF5	Ostc	0.02602362	0.016919691	0.219313119	0.259618247
Q9DBN4	P33monox;4833439L19Rik	0.00477897	0.032943379	0.255992814	0.28933408
Q3TFP8	Pgrmc1	0.01131361	0.001888211	0.16238676	0.206833938
Q80UU9	Pgrmc2	0.01254481	0.00440628	0.2203438	0.192421818
A0A140LI54	Pnpla6	0.00249565	0.01366647	0.216132107	0.293411343
P37040	Por	0.0342497	0.000287037	0.179887705	0.199763553
Q3UYK2	Psen1	0.01812287	0.008751564	0.392265561	0.266748618
G3UXZ5	Psme1	0.04976531	0.01070303	0.129699666	0.106730756
O35074	Ptgis	0.0027019	0.001027592	0.20221821	0.205596294
P35831	Ptpn12	0.02674643	0.024636235	0.117657897	0.105027965
Q8BVI4	Qdpr	0.019127	2.25E-05	0.109646895	0.143136631
Q0PD34	Rab22a	0.044424	0.028594776	0.176528942	0.189229188
Q3TW01	Rab32	0.00453072	0.002556633	0.196456466	0.103909566
Q0PD50	Rab8a	0.01123123	0.005289286	0.122852626	0.185384733
P63321	Rala	2.90E-05	9.67E-05	0.13766813	0.161320311
Q8BHS3	Rbm22	0.00188821	0.029493439	0.104450752	0.147043261
Q3UDZ1	Rhog	0.04033662	0.013836182	0.121212721	0.192717169
Q9EPK2-3	Rp2	0.0217331	0.015993946	0.170209113	0.165858629
Q642K1	Rpl18	0.03131733	0.005365325	0.217663209	0.198929602
P62717	Rpl18a	0.00063369	0.017748324	0.189273436	0.356597343
Q9D823	Rpl37	0.01202064	0.014889348	0.406589945	0.386814263

Continued on next page

Table A.1 – continued from previous page

Uniprot ID	Gene name	WT pVal	CKO pVal	WT Relative Amplitude	CKO Relative Amplitude
Q5RKP4	Rpn1	0.04026344	0.003931613	0.164095583	0.235535223
Q61833	Rpn2	0.00742829	0.004694659	0.200630101	0.238279008
P62071	Rras2	0.02549298	0.00130592	0.12391819	0.158421317
A2AVJ7	Rrbp1	0.00332753	2.48E-08	0.139166624	0.177469213
Q8R127	Sccpdh	0.00047126	0.000870614	0.114663159	0.273586568
Q3V1F2	Sdc1	0.00917376	0.031048975	0.208648188	0.284918516
O08547	Sec22b	0.00924962	0.001685058	0.189305903	0.223668974
Q8BU14	Sec62	0.00955794	0.000513796	0.255273515	0.323881271
Q8VHE0	Sec63	0.04129501	0.001448108	0.199134604	0.205326463
Q8BUH8	Senp7	0.0390597	0.021587192	0.671074401	0.13443294
Q543J5	Serpinc1	0.01372641	0.000848266	0.302731284	0.636318795
E9QM38	Slc12a2	0.04860164	0.001863418	0.132246852	0.173947295
Q99MR3	Slc12a9	0.02318151	0.007305522	0.136124566	0.163539783
Q80UP8	Slc20a2	0.03402657	0.000117451	0.284575987	0.311177029
Q8BH59	Slc25a12	0.01565867	0.004853271	0.125145218	0.166226373
Q8C140	Slc25a13	0.00332753	0.002980432	0.134287677	0.203716957
P48962	Slc25a4	0.00014627	0.000195304	0.195432698	0.240276025
Q545A2	Slc25a5	0.01358108	0.001485251	0.170236649	0.24843706
Q8C145	Slc39a6	0.038254	9.00E-06	0.2087089	0.241841835
Q3TN39	Slc3a2	0.00059508	2.17E-05	0.154051448	0.169593748
A0A0R4J2A1	Slc8a1	0.01702451	0.000389121	0.199804723	0.312537654
Q923B6	Spcs1	0.00223532	0.000699247	0.140620071	0.141026811

Continued on next page

Table A.1 – continued from previous page

Uniprot ID	Gene name	WT pVal	CKO pVal	WT Relative Amplitude	CKO Relative Amplitude
P70452	Steap4	0.00415161	0.028418643	0.182083461	0.137304786
Q4VBD2	Stx4	0.00730552	0.000633693	0.389308843	0.347579554
Q9R099	Tapt1	0.02327732	0.002531526	0.129399037	0.176900622
Q3TR40	Tbl2	0.04785872	0.037463767	0.107867104	0.19868341
Q8C7F9	Thbs1	0.03138856	0.031939111	0.175487761	0.174598845
Q571B0	Tm9sf2	0.0116671	0.000617118	0.171449846	0.229967184
Q6PDC2	Tm9sf3	0.02391164	0.003438451	0.173753705	0.173414936
Q91W52	Tmed9	0.01886713	0.000888304	0.156787056	0.298176028
Q8CIV2	Tmem19	0.01583427	0.016328269	0.46368206	0.365944906
Q9DBS1	Tmem259	0.01086893	0.000852211	0.23423959	0.257068531
Q4VAE3	Tmem43	0.00502999	0.004614887	0.261737699	0.286118391
Q8VBT0	Tmem65	0.00489102	0.003490476	0.315701289	0.278888435
Q8BXZ1	Tmx1	0.01467195	0.001215581	0.143000366	0.225677095
Q80YX1	Tmx3	0.00012971	0.023664432	0.199574987	0.183750086
Q4FK50	Tnc	0.01599395	0.00753382	0.185803904	0.266138299
Q924Z5	Tpst1	0.00184006	8.19E-05	0.294960848	0.422069286
P70697	Tram2	0.019127	0.006402875	0.110150653	0.114660281
Q3UN04	Urod	0.00042127	0.000611841	0.267636594	0.412657926
Q3TX38	Usp30	0.04215855	0.011928667	0.165451328	0.274820128
Q6DID7	Vdac3	0.01197957	0.000193467	0.184929528	0.25405945
Q9CQW1	Wls	0.01114243	4.34E-06	0.148005624	0.136509328
O88967	Ykt6	0.02949344	0.000436315	0.20696017	0.227120429

Continued on next page

Table A.1 – continued from previous page

Uniprot ID	Gene name	WT pVal	CKO pVal	WT Relative Amplitude	CKO Relative Amplitude
B2KGA7	Yme1l1	0.0390597	0.021737855	0.173790221	0.182846954
B9EHY2	Zbtb8os	0.00684893	0.011441537	0.213857271	0.321843964
Q80X32	Zmpste24	0.00255663	0.012135419	0.19712535	0.178396901

Table A.2 Phosphoproteomics data: Phosphosites rhythmic in both WT and CKO cells. Phosphosites are presented as Uniprot ID, serine/threonine, residue number and multiplicity. Multiplicity refers to the number of phosphates present on the phosphopeptide quantified.

Phosphosite	Gene name	WT pVal	CKO pVal	WT Relative Amplitude	CKO Relative Amplitude
E9Q616_S1321___1	Ahnak	0.001840057	0.003527738	0.342095065	0.264229562
P31750_S124___3	Akt1	0.015310792	0.005197659	0.133596893	0.151000908
P31750_S126___3	Akt1	0.015310792	0.005197659	0.133596893	0.151000908
P31750_S129___3	Akt1	0.015310792	0.005197659	0.133596893	0.151000908
Q9CZ52_S360___1	Antxr1	0.014045017	0.046892	0.286925766	0.392478216
G5E829_T1165___2	Atp2b1	0.043500786	8.49E-05	0.506311307	0.476498649
G5E829_S1155___2	Atp2b1	0.007117576	8.49E-05	0.499151748	0.476498674
Q02248_S552___1	Ctnnb1	0.010868927	0.008941295	0.310087593	0.258773323
G3X9V2_S914___1	Ctnnd1	0.047546073	0.01583427	0.286225378	0.274867172
Q60598_S405___2	Cttn	0.032266344	0.000307539	0.208800291	0.270564365
Q61712_S478___2	Dnajc1	0.014235152	0.004308406	0.373325966	0.448192237
E9PWE8_S635___1	Dpysl3	0.002732952	0.028470303	0.253120255	0.149946464
A0A1D5RLL3_S719___1	Efr3a	0.001899092	0.025667153	0.339429693	0.318679092
Q01279_S1166___1	Egfr	0.001829495	0.005619759	0.466178069	0.466220973
Q544H0_T41___1	Eif3g	0.003541078	0.000852211	0.144176679	0.216321763
B2RUK2_S1324___1	Erbb2ip	0.005029992	0.021074095	0.220098365	0.235539894
B2RUK2_T485___1	Erbb2ip	0.000944105	0.013162667	0.403696017	0.421760031
Q3TZZ7_S685___2	Esyt2	0.005989559	0.015310792	0.416362987	0.425784397
F8VPU2_S427___1	Farp1	0.000263591	0.000218515	0.274286368	0.237291021
F8VPU2_T24___1	Farp1	0.000131795	0.000403018	0.438954615	0.36143499

Continued on next page

Table A.2 – continued from previous page

Phosphosite	Gene name	WT pVal	CKO pVal	WT Relative Amplitude	CKO Relative Amplitude
A0A0R4J0H8_S208___1	Fndc3b	0.003327533	0.002732952	0.281914414	0.372533302
P97825_S79___1	Hn1	0.029625408	0.01851	0.320070576	1.456407557
Q9CX86_S84___1	Hnrnpa0	0.029149989	0.003610838	0.737826576	1.132287522
E9PX30_S433___1	Map4k5	0.007055476	0.000942518	0.362204992	0.221373588
Q80WJ7_S423___1	Mtdh	0.013084578	8.07E-06	0.412481878	0.456231572
Q80WJ7_S565___1	Mtdh	0.01851	0.022966188	0.354631089	0.761299353
Q80WJ7_S454___1	Mtdh	0.032065782	0.000266997	0.327635086	0.456760294
Q9CWE0_S235___1	Mtfr1l	0.007404	0.00045136	0.161389785	0.188317954
Q7TPW1_S16___1	Nexn	0.007219078	0.049392657	0.209825202	0.135475508
Q9D6Z1_S513___1	Nop56	0.047546073	0.048895756	0.434005913	0.506653054
Q3B7Z2_S191___2	Osbp	0.046307288	0.005694061	0.224104429	0.258607353
Q6P9R2_S339___1	Oxsr1;mKIAA1101	0.001005353	0.034026565	0.259535753	0.215565222
Q9Z0P4_T145___1	Palm	0.001252466	0.005324053	0.165953005	0.336783929
Q3UFJ3_S295___2	Pdha1	0.001831592	0.001840057	0.346543764	0.317761089
Q5EBQ2_S52___1	Pebp1	0.03341363	0.000460014	0.171154698	0.219815154
Q3TFP8_S161___1	Pgrmc1	0.0206264	0.000632881	0.437193251	0.469835407
Q80UU9_T205___1	Pgrmc2	0.014297388	0.000977661	0.408008332	0.445038259
E9Q9J4_S38___1	Ppip5k2	0.018199765	0.04554134	0.387264941	0.244473112
Q9DBR7_S994___1	Ppp1r12a	0.004361526	3.55E-05	0.305413618	0.344303942
Q3UYK2_S329___1	Psen1	0.011667095	0.018672043	0.509009132	0.413908698
Q99P72_S105___1	Rtn4	0.019522002	0.000588803	0.339919284	0.288254596
Q6GQT6_S934___1	Scap	0.005674837	0.005197659	0.383233348	0.553775685

Continued on next page

Table A.2 – continued from previous page

Phosphosite	Gene name	WT pVal	CKO pVal	WT Relative Amplitude	CKO Relative Amplitude
Q80U72_S1566___2	Scrib	0.049172889	0.016589697	0.317585305	0.227805962
O08547_S137___1	Sec22b	0.014049397	0.000203112	0.468208475	0.49245273
Q8BU14_T375___1	Sec62	0.021484499	4.40E-05	0.519546812	0.625263303
Q9DBG7_S295___3	Srpr	0.0095635	0.015184162	0.33088762	0.418600989
Q9DBG7_S296___3	Srpr	0.0095635	0.015184162	0.33088762	0.418600989
Q9DBG7_S297___3	Srpr	0.0095635	0.015184162	0.33088762	0.418600989
E9PUK6_S655___2	Srrm1	0.028367909	0.003817673	0.26885876	0.748893731
E9PUK6_S591___2	Srrm1	0.042778588	8.80E-05	0.342849713	0.350138151
E9PUK6_T593___2	Srrm1	0.042778588	8.80E-05	0.342849713	0.350138151
Q8BTI8_S333___1	Srrm2	0.01451771	0.046918451	0.320928701	0.911132252
Q8BTI8_S1269___1	Srrm2	0.016891313	0.031362013	0.190452486	0.123221776
Q8BTI8_T1428___1	Srrm2	0.003538612	0.007908036	0.335808304	0.807266218
Q8BTI8_S1400___1	Srrm2	0.04319	0.023770516	0.478623024	0.542797374
Q3THA6_S233___1	Srsf7	0.001903508	0.032911278	0.459413393	0.304851094
P70452_S15___1	Stx4;Stx4a	0.017573688	0.037973186	0.243283594	0.317580548
A0A1B0GS91_S1098___1	Svil	0.008877204	0.005157676	0.495618012	0.361554252
H3BL37_S1339___1	Tcof1	0.009403222	0.000580969	0.352411299	0.34592718
B9EHJ3_S617___1	Tjp1	0.010174577	0.020319576	0.176495862	0.209668421
Q8VBT0_S245___1	Tmx1	0.000633693	0.00130592	0.597274629	0.48453256
A0A0N4SVC2_S96___3	Tra2a	0.014738132	0.018670004	0.312060411	0.908173313
A0A0N4SVC2_S98___3	Tra2a	0.014738132	0.018670004	0.312060411	0.908173313
A0A0N4SVC2_S94___3	Tra2a	0.014738132	0.018670004	0.312060411	0.908173313

Continued on next page

Table A.2 – continued from previous page

Phosphosite	Gene name	WT pVal	CKO pVal	WT Relative Amplitude	CKO Relative Amplitude
Q924Z5_S332___1	Tram2	0.001327694	1.71E-05	0.490573928	0.699568452

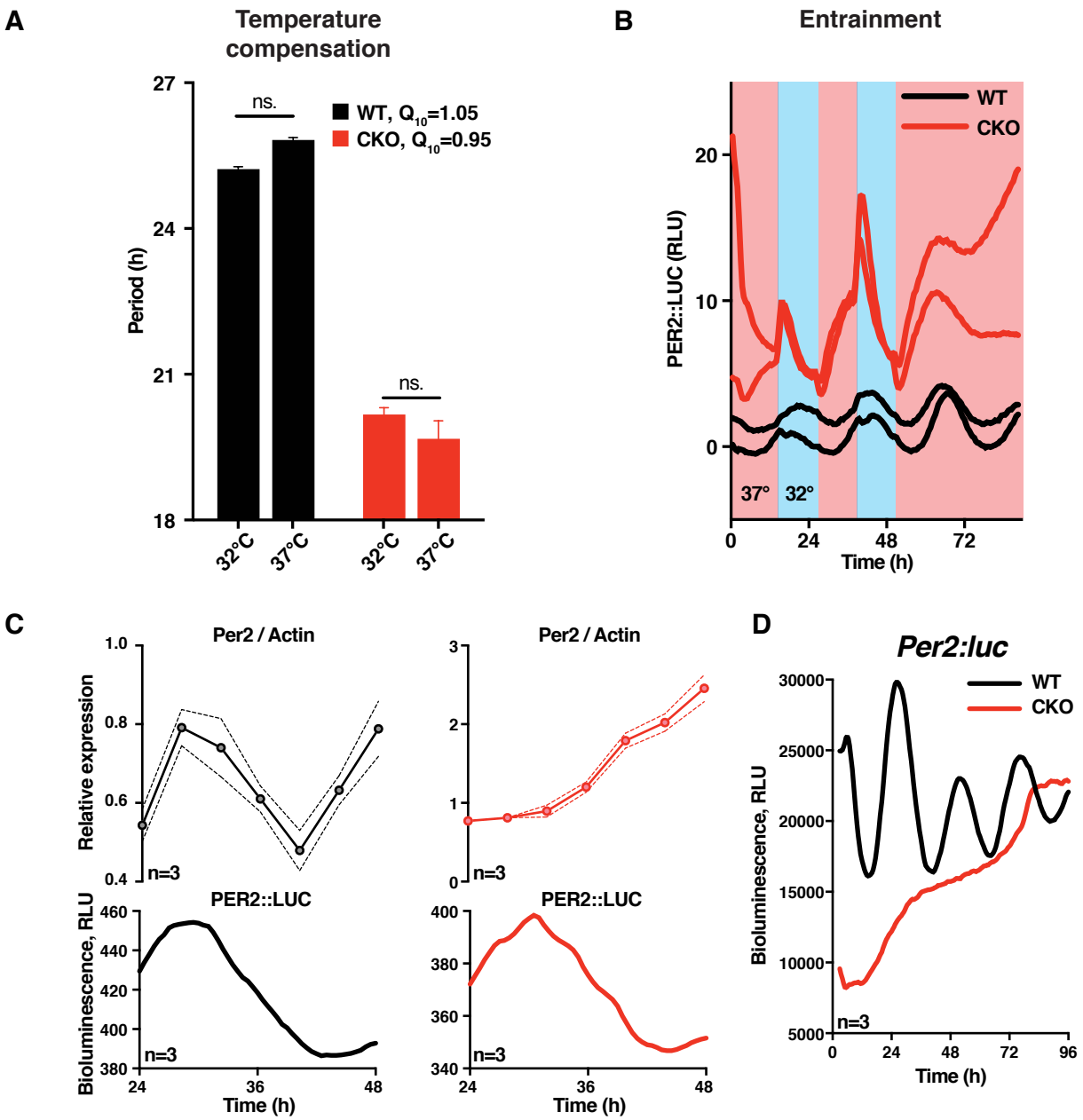

Figure A.1 Circadian features of PER2::LUC rhythms in CKO cells. **A)** PER2::LUC rhythms in CKO cells are temperature-compensated. Mean±SEM, n=4, 2-way ANOVA, p=0.8 for temperature effect. Q_{10} values are annotated. **B)** PER2::LUC rhythms in CKO cells can be entrained by temperature cycles. **C)** Per2 mRNA abundance measured using qPCR. Mean±SEM. Representative parallel PER2::LUC recordings are shown below, n=3. **D)** Per2:Luciferase transcriptional reporter stably expressed in WT and CKO mouse embryonic fibroblasts. Representative recordings shown, n=3.

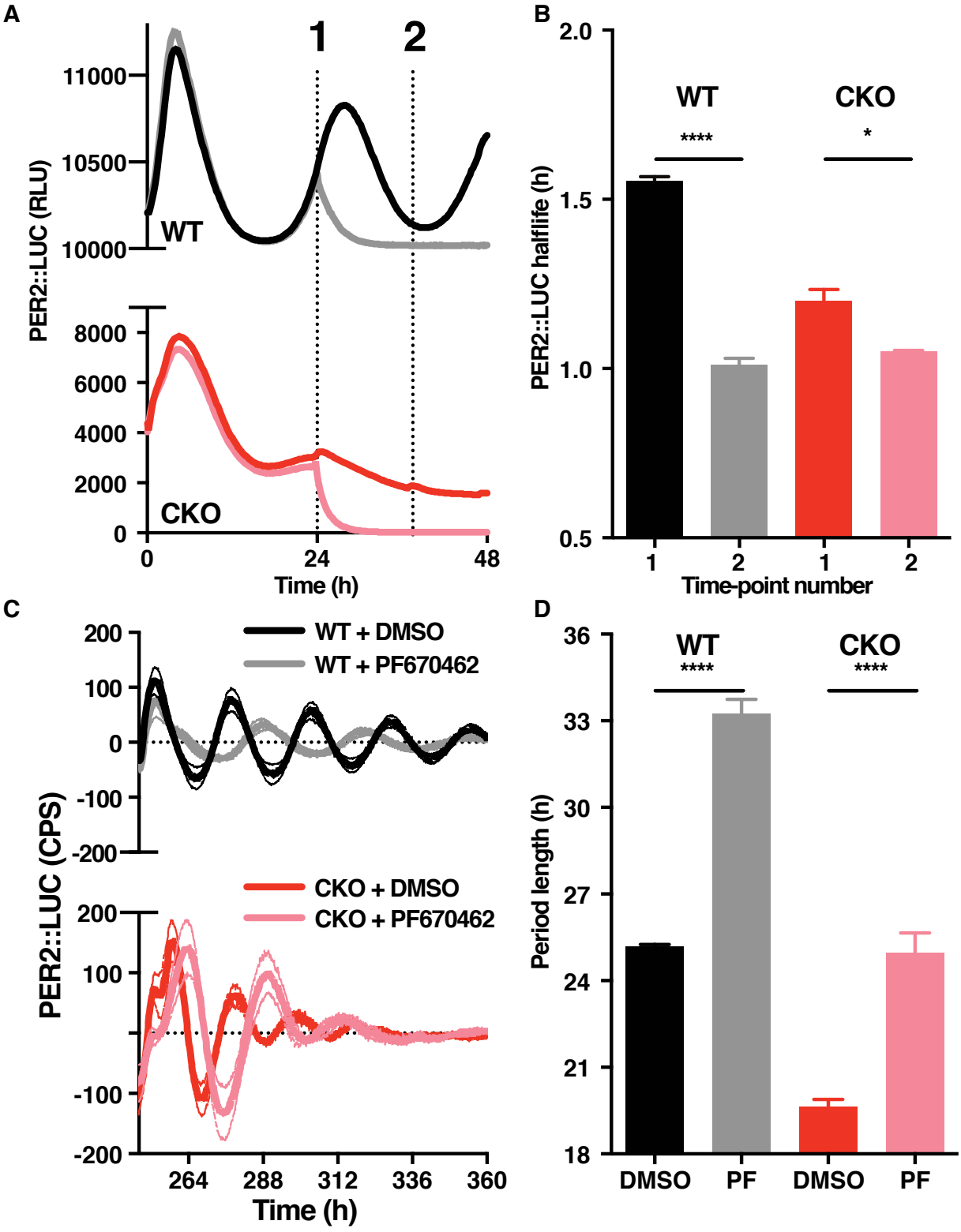

Figure A.2 Post-translational modification of PER2 in CKO cells. A) PER2::LUC recordings as a reference, illustrating time points 1 and 2, occurring at the rising and falling of PER2::LUC respectively. **B)** PER2::LUC half-life measured by fitting an exponential decay curve to the traces in A) that have been treated with cycloheximide (CHX), n=4, t test. **C)** PER2::LUC recordings of cells treated with 0.3 μM PF670462 (CK1 inhibitor) or DMSO control. Mean±SEM, n=4. **D)** Quantification of period length from C). Mean±SEM, n=4, t-test.

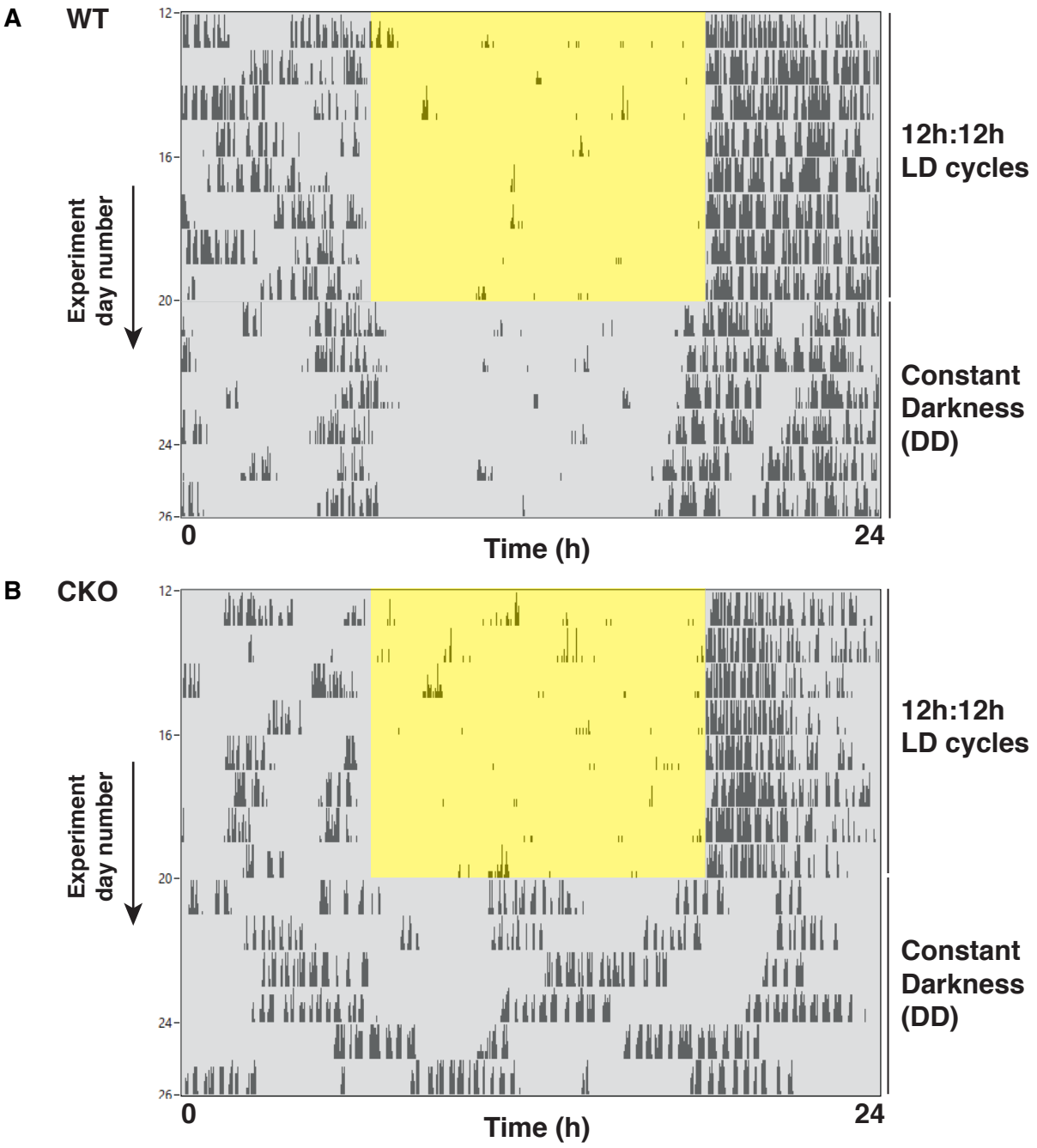

Figure A.3 Examples of WT and CKO mouse behavioural recordings. A) Single-plotted actogram of a wild-type mouse, showing 14 days of recording over the transition between 12h:12h light:dark (LD) cycles and constant darkness (DD). During LD, most wheel running occurs during the dark phase (entrainment). During DD, behaviour is temporally organised in a circadian fashion, to occur at the predicted dark phase. **B)** Single-plotted actogram of a CRY1$^{-/-}$; CRY2$^{-/-}$ mouse under the same conditions. This demonstrates normal entrainment to LD cycles, but arrhythmic behaviour in DD.